

**Characterizing the dominant role of interferon-
lambda (IFN- λ) signaling in the intestinal epithelium**

By

Jacob A. Van Winkle

A DISSERTATION

Presented to the Department of Molecular Microbiology and Immunology

and Oregon Health & Science University

School of Medicine

in partial fulfillment of

the requirements for the degree of

Doctor of Philosophy

April 2022

TABLE OF CONTENTS

List of Figures	iv
List of Abbreviations	vi
Acknowledgements	viii
Abstract	x

CHAPTER 1: Introduction

The Murine Intestine - A Brief Primer	1
Intestinal Epithelial Cells	3
Intestinal Epithelial Cell Development and Differentiation	3
Diverse Functions and Features of Intestinal Epithelial Cells	4
Intestinal Epithelial Cell Death and Extrusion	7
Intestinal Organoid Model System	9
Interferon Signaling	13
Interferon Signaling Pathways	13
The Antiviral Function of Interferon Stimulated Genes	16
Non-Canonical IFN Signaling and Differences in IFN- α/β and IFN- λ Responses	17
Induction of Interferon Expression	20
Interferon Responsiveness in the Intestine	23
The Rotavirus Model System	26
Rotavirus Structure, Life Cycle, and Pathogenicity	26
Rotavirus and Interferon Signaling	28
Intestinal Bacterial Microbiota	31
Development and Composition of the Intestinal Bacterial Microbiota	31
Manipulation of Bacterial Microbiota	32
Physiological Effects of the Intestinal Bacterial Microbiota	34
The Enteric Immune Environment	39
Immune cells of the enteric niche	39

Interactions Between the Immune System and Bacterial Microbiota	43
Impacts of Bacterial Microbiota on Viral Infection	46
The Impact of Rewilding the Bacterial Microbiota in the Laboratory Mouse Model	50

CHAPTER 2: Selective Interferon Responses of Intestinal Epithelial Cells Minimize Tumor Necrosis Factor Alpha Cytotoxicity

Authors, Affiliations, Contributions, and Acknowledgements	52
Introduction	54
Results	56
IECs in the neonatal intestine are minimally response to IFN- β	56
IEC organoids are dually response to IFN- β and IFN- λ	59
Global ISG expression in response to IFN- β is suppressed <i>in vivo</i>	61
Apoptosis genes are among IFN- β -specific ISGs	64
IFN- β potentiates TNF α -triggered apoptosis	68
The strength of the canonical ISRE differentiates ISG categories	70
IFN- β -specific apoptosis ISGs are dependent on the canonical transcription factor STAT1	73
Discussion	75

CHAPTER 3: A Homeostatic Interferon-lambda Response to Bacterial Microbiota Stimulates Preemptive Antiviral Defense in Discrete Pockets of Intestinal Epithelium

Authors, Affiliations, Contributions, and Acknowledgements	78
Introduction	81
Results	84
Bacterial microbiota stimulate IFN- λ response genes in the ileum at homeostasis	84
Homeostatic, microbiota- and <i>Ifnlr1</i> -dependent ISGs are primarily expressed in intestinal tissues	90

Homeostatic ISG expression is independent of type I IFN	94
Homeostatic ISG expression in the intestine is restricted to epithelial cells	97
Bacterial microbiota stimulate expression of <i>Ifn12/3</i> by CD45-positive cells	99
Homeostatic ISG expression in the small intestine is highly localized	102
Mature enterocytes express homeostatic ISGs in public single-cell datasets from mouse and human	107
Assessing the effect of peroral bacterial products on localized homeostatic ISGs in ABX-treated mice	110
The homeostatic IFN- λ response preemptively protects IECs from murine rotavirus infection	114
Discussion	121

CHAPTER 4: Conclusions, Implications, and Future Directions

Conclusions and Implications	126
Future Directions	131
Final Thoughts	141

CHAPTER 5: Materials and Methods

References

ADDENDUM

Curriculum Vitae

List of Figures

1.1 The regions of the gastrointestinal tract	2
1.2 A diagram of intestinal epithelial cells in the small intestine and colon	4
1.3 TNF signaling outcomes	9
1.4 Intestinal organoids	11
1.5 IFN- α/β and IFN- λ induction and signaling	15
2.1 IECs in the neonatal intestine are minimally response to IFN- β	58
2.2 IEC organoids are dually responsive to IFN- β and IFN- λ	60
2.3 Global ISG expression in response to IFN- β is suppressed <i>in vivo</i>	63
2.4 Common ISGs in IEC organoids are highly stimulated and consist of canonical antiviral genes	66
2.5 IFN- β -specific ISGs include apoptosis pathway genes	67
2.6 IFN- β potentiates TNF α -triggered apoptosis	69
2.7 The strength of the canonical ISRE differentiates ISG categories	72
2.8 IFN- β -specific apoptosis ISGs are dependent on the canonical transcription factor STAT1	74
3.1 Bacterial microbiota stimulate IFN- λ response genes in the ileum at homeostasis	87
3.2 <i>Ifnlr1</i> -deficiency does not alter intestinal bacterial microbiota	88
3.3 Gene set enrichment analysis of hallmark gene sets	89
3.4 Treatment with antibiotics reduces enteric 16S gene copies to below the limit of detection	89
3.5 Homeostatic, microbiota- and <i>Ifnlr1</i> -dependent ISGs are primarily expressed in intestinal tissues	92
3.6 Homeostatic ISGs are more abundantly expressed in the ileum than in the colon ...	93
3.7 Treatment with antibiotics does not ablate responsiveness to IFN- λ	93
3.8 Homeostatic ISG expression is independent of type I IFN	96
3.9 Homeostatic ISG expression in the intestine is restricted to epithelial cells	98
3.10 Bacterial microbiota stimulate expression of <i>Ifnl2/3</i> by CD45-positive cells	101

3.11 Enrichment of EpCAM+ and CD45+ cells from the intestinal epithelium and lamina propria	101
3.12 Homeostatic ISG expression in the small intestine is highly localized	104
3.13 The entire intestinal epithelium is responsive to IFN- λ	105
3.14 Homeostatic ISG expression is also highly localized in the colon	106
3.15 Mature enterocytes express homeostatic ISGs in public single-cell datasets from mouse and human	109
3.16 Assessing the effect of peroral bacterial products on localized homeostatic ISGs in ABX-treated mice	112
3.17 Assessing the effect of peroral bacterial products on homeostatic ISGs in ABX-treated mice	113
3.18 The homeostatic IFN- λ response preemptively protects IECs from murine rotavirus infection	117
3.19 The homeostatic IFN- λ response preemptively protects IECs from murine rotavirus infection (12hr)	118
3.20 Murine rotavirus and <i>Ifit1</i> co-incidence	119
3.21 Murine rotavirus infection increases the distribution of <i>Ifit1</i> expression at late times post-inoculation	120
4.1 IFN regulatory genes are repressed in organoids relative to <i>in vivo</i>	132
4.2 Combined IFN treatment potentiates TNF α cytotoxicity in human IEC organoids ...	134
4.3 Epithelial-associated CD11c+/CD11b-/MHC-II+ myeloid cells produce <i>Ifn12/3</i> at homeostasis	136
4.4 Transcriptional pathway analysis of ISG-positive and ISG-negative regions of the ileum	140

List of Abbreviations

ABX: antibiotics
AMP: antimicrobial peptide
APRIL: a proliferation-inducing ligand
ASF: altered Schaedler's flora
BAFF: B cell activating factor
CA: cholic acid
CARD: caspase-recruitment domain
CDCA: chenodeoxycholic acid
cGAMP: cyclic GMP-AMP
cGAS: cGAMP synthase
ChIP: chromatin immunoprecipitation
CLA: conjugated linoleic acid
CM: conditioned media
CVB: coxsackievirus B
DAI: DNA-dependent activator of IRFs
DC: Dendritic cell
DCA: deoxycholic acid
DTR: diphtheria toxin receptor
DEG: differentially expressed gene
EGF: epidermal growth factor
EPCAM: epithelial cell adhesion molecule
ER: endoplasmic reticulum
ESCRT: endosomal sorting complex required for transport
FADD: fas-associating death domain-containing protein
FXR: farnesoid X receptor
GAP: goblet cell associated passages
GSEA: gene set enrichment analysis
HBGA: histone blood group antigens
HOMER: hypergeometric optimization of motif enrichment
IBD: inflammatory bowel disease
IEC: intestinal epithelial cell
IEL: intraepithelial lymphocyte
IFIT: induced protein with tetratricopeptide repeats
IFITM: interferon-induced transmembrane protein
IFN: interferon
IFNAR: interferon alpha receptor
IFNGR: interferon gamma receptor
IFNLR: interferon lambda receptor
IgA: immunoglobulin A
IL: interleukin
ILC: innate lymphoid cells
IRF: interferon regulatory factor
ISG: interferon stimulated gene
ISGF3: interferon stimulated gene factor 3
ISRE: interferon stimulated response element
JAK: Janus kinase
LCA: lithocholic acid
LCM: laser capture microdissection

LCMV: lymphatic choriomeningitis virus
LPS: lipopolysaccharide
MAIT: mucosal associated invariant T cell
MAMP: microbe associated molecular pattern
MAPK: mitogen activated protein kinase
MAVS: mitochondrial antiviral signaling protein
MEF: mouse embryonic fibroblast
MHC: major histocompatibility complex
MLKL: mixed lineage kinase domain-like
MLN: mesenteric lymph node
MMTV: mouse mammary tumor virus
MNV: murine norovirus
MX: myxovirus resistance
NF- κ B: nuclear factor kappa-light-chain-enhancer of activated B cells
NSP: non-structural protein
OAS: oligoadenylate synthetase
PAMP: pathogen associated molecular pattern
PCA: principle component analysis
pDC: plasmacytoid dendritic cell
pIgR: polymeric immunoglobulin A receptor
PP: peyer's patch
PPAR: peroxisome proliferator-activated receptor
PRR: pattern recognition receptor
RIPK: receptor-interacting protein kinase
SCFA: short-chain fatty acid
SFB: segmented filamentous bacteria
slgA: secretory immunoglobulin A
SOCS: suppressor of cytokine signaling
STAT: signal transducer and activator of transcription
STING: stimulator of interferon genes
S1P: sphingosine-1-phosphate
TA: transit amplifying
TAM: *Tyro3*, *Axl*, and *Mertk*
TBK1: TANK binding kinase 1
TCR: T cell receptor
TED: transepithelial dendrites
TGF: transforming growth factor
TLR: toll-like receptor
TNF: tumor necrosis factor
TNFR: tumor necrosis factor receptor
TRIM: tripartite motif
TSS: transcription start site
TYK: tyrosine kinase
U-ISGF3: unphosphorylated interferon stimulated gene factor 3
VP: viral protein
WT: wild-type
ZAP: zinc-finger antiviral proteins

Acknowledgements

I knew pursuing a PhD would be a challenging experience – it has certainly been quite a wild ride. Looking back at the past several years, I can only say that I've found the whole experience exceptionally fulfilling – a phrase that is a true testament to the amazingness of my personal support structure and work colleagues.

To my mentor, boss, and PI-extraordinaire – Tim. I owe you one for the wonderful graduate school experience. For some reason you let me join your lab as a woefully underprepared and unexperienced recent undergraduate student. You have delicately balanced your guidance to instill scientific rigor while never being overbearing. You've allowed me to mature as a researcher at my own pace, while grounding me in the realities of our projects. You've been so understanding of my personal circumstances and have extended so much grace and patience throughout the pandemic and beyond. I don't think I could have asked for a better mentor. It's been an incredible honor to work with you for the past several years. If academia were made for it, I would have gladly spent many more years working with you on all of the amazing projects we have in the pipeline. I can't wait to see where they go!

To my collaborators out at Wash U – thank you for all of your contributions to chapter 3 of this dissertation. You have all been so helpful and gracious with your time, energy, and data. I can firmly say this dissertation wouldn't be nearly the same without your contributions.

To my DAC – Drs. Bill Messer, Missy Wong, Dave Lewinsohn, and Vic Defilippis. Thank you all for being so willing to commit time and energy to being on my advisory committee. Your feedback at meetings and constant support has always been

appreciated. To the newest defense committee member, Dr. Bella Rauch – thank you for being willing to take part in my dissertation defense – I appreciate it!

To all the past and present Nice Lab members – it's been great working with all of you. Though it's been a few years since some of you have been in lab, all of you have contributed to my graduate school experience. I appreciate the banter, the scientific discussion, and commiseration when things don't go as planned.

To my family, (Van Winkles and Downes, alike!) – thank you for being a centering and grounding force in my life. The love and support that you show for me is extraordinary. In particular, mom and dad, thank you for all of the unconditional support that you've had. I'm sure it's been a strange decade and a half watching me go from a meandering high school student with a skateboard and no college plans to a grad student on the cusp of a PhD. Also, a very special thank you to you, mom – from the beginning you've nurtured my curiosity and taught me to learn independently (a highly relevant skill in grad school!). You've also shown me the importance of perseverance, not just in the in the face of insurmountable odds the past few years, but throughout my entire life.

To my amazing wife, April – thank you for everything! If I had to list all the ways that you've supported me throughout our relationship and graduate school this dissertation would be twice as long. You've been incredibly gracious and understanding throughout all of the ways that graduate school tests a relationship. You've brought an immeasurable happiness to my life and graduate school tenure. Above everything else, I'm absolutely certain that I would never have gotten to where I am without your unwavering support. Thank you.

Abstract

Interferon (IFN) family cytokines stimulate a broad group of genes known as interferon stimulated genes (ISGs). The primary function of ISGs is to provide antiviral host defense. IFN- α and IFN- β signal through IFN- α receptor (IFNAR) whereas IFN- λ signals through IFN- λ receptor (IFNLR). IFNAR is expressed by many cell types, but IFNLR is primarily expressed by epithelial cells in barrier tissues. However, unlike most epithelial barriers that respond to both IFN- λ and IFN- α/β , intestinal epithelial cells (IECs) preferentially respond to IFN- λ and are hyporesponsive to IFN- α/β . As such, IFN- λ has a dominant role in protecting IECs from enteric viruses. The physiological rationale for this selective responsiveness by IECs is poorly understood. Furthermore, the interactions of IFN- λ signaling in IECs with the environmental context of bacterial microbiota have not been determined. In this dissertation, I describe the consequences and contexts surrounding the IFN- λ response by IECs.

To assess the rationale for IFN- α/β hyporesponsiveness by IECs, I interrogated the capabilities of IFN- α/β and IFN- λ responses. First, I confirmed that IFN- λ treatment elicits robust and uniform ISG expression in neonatal mouse IECs and inhibits replication of IEC-tropic rotavirus. In contrast, IFN- β elicits a marginal ISG response in neonatal mouse IECs and does not inhibit rotavirus replication. *In vitro* treatment of IEC organoids with IFN- λ results in ISG expression that mirrors the *in vivo* IFN- λ response. However, IEC organoids have increased expression of IFNAR relative to neonate IECs, and the response of IEC organoids to IFN- β is strikingly increased in magnitude and scope. The expanded IFN- β -specific response includes pro-apoptotic genes and potentiates toxicity triggered by tumor necrosis factor alpha (TNF α). The ISGs stimulated in common by IFN- β and IFN- λ have strong interferon-stimulated response element (ISRE) promoter motifs, whereas the expanded set of IFN- β -specific ISGs, including pro-apoptotic genes, have

weak ISRE motifs. Thus, preferential responsiveness of IECs to IFN- λ *in vivo* enables selective ISG expression during infection that confers antiviral protection but minimizes disruption of intestinal homeostasis.

The dominant role of IFN- λ signaling in the intestinal epithelium is accompanied by the context of abundant stimuli in the form of the intestinal bacterial microbiota. I sought to determine whether the presence of bacterial microbiota in the enteric environment stimulates IFN- λ signaling. I found that bacterial microbiota stimulate a homeostatic ISG signature in the intestine of specific pathogen-free mice. This homeostatic ISG expression is restricted to IECs, depends on IEC-intrinsic expression of IFNLR, and is associated with IFN- λ production by leukocytes. Strikingly, imaging of these homeostatic ISGs reveals localization to pockets of the epithelium and concentration in mature IECs. Correspondingly, a minority of mature IECs express these ISGs in public single-cell RNA sequencing datasets from mice and humans. Furthermore, I assessed the ability of orally-administered bacterial components to restore localized ISGs in mice lacking bacterial microbiota. Lastly, I found that IECs lacking IFNLR are hyper-susceptible to initiation of murine rotavirus infection. These observations indicate that bacterial microbiota stimulate ISGs in localized regions of the intestinal epithelium at homeostasis, thereby preemptively activating antiviral defenses in vulnerable IECs to improve host defense against enteric viruses.

Here, I describe the consequences and contexts surrounding the IFN- λ response by IECs. I found that the IFN- λ response is preferentially used by IECs because IFN- α/β signaling potentiates epithelial cytotoxicity. I also found that the intestinal microbiota stimulate a localized, homeostatic ISG response in the intestinal epithelium. Together these findings highlight the unique role that IFN- λ plays in the intestinal epithelium.

CHAPTER 1: Introduction

The Murine Intestine – A Brief Primer

The intestine is a mixed endodermal and mesodermal tissue compartment composed of two distinct regions: the small intestine and the colon (1). These mucosal tissues are an essential interface between host and the non-host environment. Knowledge of the mucosal interface gained through basic research is highly relevant to organismal health and resistance to disease. Given the difficulties associated with acquiring healthy human tissues, the mouse model system is commonly used to assess basic biology prior to confirmation in humans. Use of mouse models are especially essential to study tissues that are difficult to access in humans, such as the intestine.

In the intestine the host absorbs nutrients, repels pathogens, and balances its homeostasis with commensal microbes. The intestine composes a highly circuitous mucosal barrier tissue that is often multiple times longer than the organism. The small intestine is the largest segment of the intestine, making up roughly 80% of its total length. The small intestine is organized into the duodenum, jejunum, and ileum in anterior to posterior order (**Figure 1.1**). Given the length of the small intestine, its most general role is absorption of nutrients required for host survival. To this end, the small intestine has structures called villi – “projections” of the epithelium and underlying cells (lamina propria). The initial formation of small intestinal villi occurs during fetal development and serves to increase the surface area of the intestine (2). However, given the length and surface area of the small intestine, it is also the site of infection by many enteric pathogens and boasts a high density of immune cells that reinforce host-immunity against pathogens and exclusion of commensal microbiota (3). Unlike the small intestine, the colon does not have distinct villi structures and is composed of a much more regular, undulating epithelial

surface. The colon is home to the greatest density of commensal bacterial microbiota in the gastrointestinal tract (3), but has a much sparser density of immune cells than the small intestine (3). This is partially due to the decreases in surface area relative to the small intestine and also because the colon is covered in a dense layer of mucus that helps prevent interactions between commensal microbes and pathogens with the host (4). The intestine is lined with a single-cell layer of simple columnar cells called intestinal epithelial cells (IECs). These cells are the primary barrier between the non-host space (intestinal lumen) and the host lamina propria.

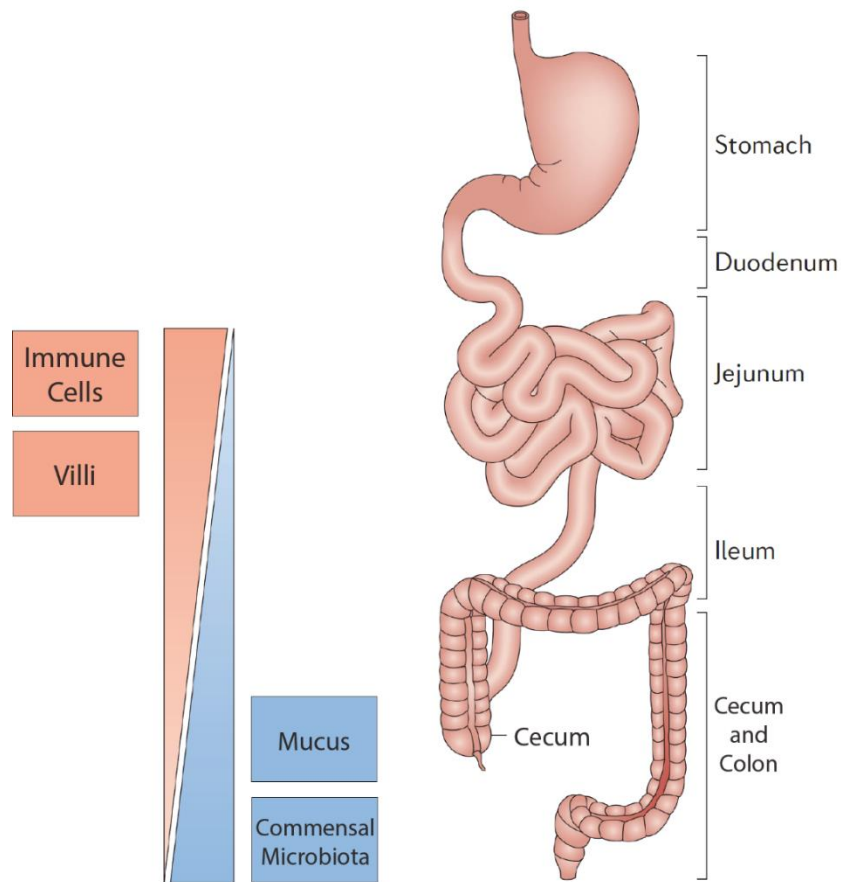


Figure 1.1. The regions of the gastrointestinal tract. The small intestine, composed of the duodenum, jejunum, and ileum. The cecum and colon. Gradient indicating increased density of immune cells and the presence of villi structures in the small intestine and increased mucus and commensal microbiota in the colon.

Adapted with permission from Springer Nature: Nature Reviews Immunology. Regional specialization within the intestinal immune system, Allan M. Mowat and William W. Agace, 2014.

Intestinal Epithelial Cells

Intestinal Epithelial Cell Development and Differentiation

IECs are derived from the intestinal crypts – small invaginations of the epithelial layer that make up the stem cell niche (5–7). From these crypts, the intestinal epithelium proliferates and migrates to fill the space between crypts (8, 9). In the small intestine, these IECs migrate up the villi and develop into mature, differentiated cells prior to shedding at the villus tip. The intestinal crypts harbor long-lived, continually-proliferating intestinal stem cells (ISCs). Active epithelial renewal is driven by ISCs that have robust expression of *Lgr5*, an essential growth factor receptor that complexes with Frizzled receptors to mediate ISC self-renewal (10, 11). In addition to containing proliferating ISCs, small intestinal crypts also host Paneth cells, a relatively quiescent population of ISCs called +4 cells, and transit amplifying (TA) cells that give rise to intestinal epithelial progenitor cells (12). These Paneth cells lie interspersed with ISCs at the bottom of the intestinal crypt and produce essential growth factors required for TA cell proliferation and ISC self-renewal (13). The growth factors secreted by Paneth cells include both Wnt and Notch family ligands such as Wnt-3, Wnt-11, and Dll4 that are essential for the maintenance of the ISC niche (14–17). An additional growth factor that plays an outsized role in maintaining the ISC niche is R-spondin, a growth factor produced by stromal cells near intestinal crypts (18, 19). In fact, R-spondin signals through *Lgr5*, the hallmark receptor of ISCs, to potentiate Wnt signaling in these cells (20). Although *Lgr5* is the canonical marker of ISCs, a more widely expressed homologue, *Lgr4* is also stimulated by R-spondin. However, combined deletion of both *Lgr4* and *Lgr5* is sufficient to abolish ISC self-renewal, highlighting the importance of robust Wnt signaling for the maintenance of the ISC population (21). In cases where primary proliferating ISCs are damaged or destroyed, slower-cycling +4 cells are capable of reconstituting the ISC niche as well as

differentiating to repopulate diverse epithelial cell types (22–24). The preservation and proliferative potential of these +4 cells under adverse conditions underscores the many necessary functions of the intestinal epithelium.

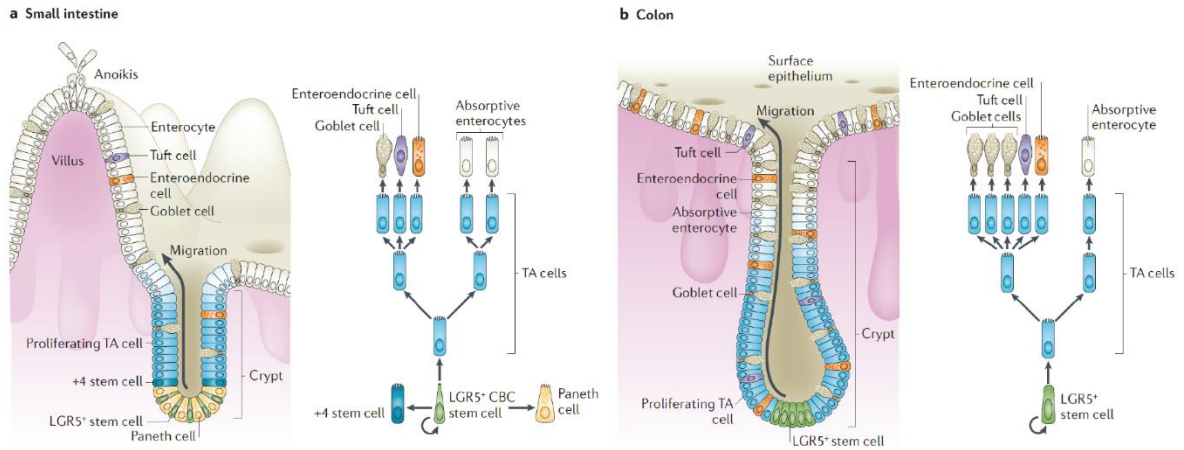


Figure 1.2. A diagram of intestinal epithelial cells in the small intestine and colon. Intestinal crypts with LGR5⁺ intestinal stem cells. Paneth cells and +4 stem cells are present in the small intestine (A). Differences in epithelial cell arrangement with a lack of villi in the colon (B). Proliferation of intestinal stem cells into TA cell intermediates. Differentiation of IECs into secretory lineage cells (goblet cell, tuft cell, enteroendocrine cell) or absorptive lineage cells occurs in both tissues.

Adapted with permission from Springer Nature: Nature Reviews Molecular Cell Biology. Adult intestinal stem cells: critical drivers of epithelial homeostasis and regeneration, Nick Barker, 2014.

Diverse Functions and Features of Intestinal Epithelial Cells

Differentiated IECs have many functions but are developmentally grouped into two distinct types: secretory or absorptive. Secretory IECs include Paneth cells, enteroendocrine cells, goblet cells, and tuft cells whereas absorptive cells are enterocytes (6). IECs arise from epithelial lineage progenitor cells through different balances of transcription factor usage informed by a complex signaling milieu and intrinsic proliferation cues (25). In particular, the differentiation of progenitor cells into a secretory or an absorptive IEC has been largely attributed to transcriptional programs mediated by the transcription factor ATOH1 (also known as MATH1) (26). Deletion of *Atoh1* in the majority

of IECs dramatically decreases the proportion of secretory cells: paneth, enteroendocrine, and goblet cells, suggesting ATOH1 is the dominant regulator of secretory IEC differentiation. Full deletion of *Atoh1* in all IECs is embryonic lethal, suggesting secretory IEC function may be necessary for viability (27). Conversely, constitutively-expressed ATOH1 is sufficient to direct differentiation of TA cells into secretory cells, and expands secretory cell types to the detriment of absorptive cell populations (28). In fact, the relationship between secretory and absorptive IEC differentiation is directly antagonistic and is mediated by Notch signaling. HES1, a downstream effector of Notch has been shown to repress ATOH1 function and, therefore, decrease the proportion of secretory IECs (29). Likewise, inhibition of the Notch pathway relieves ATOH1 repression and increases the proportion of secretory IECs (30, 31)

Secretory IECs play diverse roles that are absolutely essential for maintenance of homeostasis in the intestine, consistent with loss of secretory IECs correlating with embryonic lethality (27). In addition to their role supplying intestinal crypts with growth factors, Paneth cells also perform essential immune functions. In particular, Paneth cells prolifically secrete antimicrobial effector molecules such as antimicrobial peptides, defensins, lysozymes, and phospholipases that are functional against a variety of microbes (32, 33). Although Paneth cells secrete a wide variety of effector molecules, the range of hormones secreted by enteroendocrine cells are even more astounding. Enteroendocrine cells can be subclassified into a dizzying array of cell types that each produce signaling molecules ranging from established hormones to neurotransmitters. These effectors include serotonin, glucagon-like and insulin-like digestive hormones, and even satiety hormones like ghrelin (34). Unlike enteroendocrine cells, goblet cells have relatively limited effector output, but still play an essential role in intestinal homeostasis. Goblet cells are most well-known for their production of mucins, the key component of

mucus (35). The primary mucin goblet cells produce is mucin-2 in additions to mucins that range from freely secreted to cell-membrane-anchored. The aggregation of these mucins leads to the formation of a protective mucus barrier. Interestingly, in addition to actively contributing to host mucus barrier formation, goblet cells also are sites for passage of luminal antigen across the intestinal epithelial barrier (36, 37). Additionally, goblet cells have been observed interacting with underlying phagocytes, firmly placing them at the intersection between luminal antigen and host immunity (38). Lastly, intestinal tuft cells are a relatively new and understudied secretory cell that are defined by a striking “tufted” appearance and a number of other puzzling characteristics (39). These unique cells express a variety of proteins associated with chemosensory “taste” functionality, neuron-associated cell-markers, and even a kinase that is canonically associated with immune signaling by hematopoietic cells (40). Consistent with a role in immunity, tuft cells play an essential role in anti-helminth immunity by secreting IL-25 and TSLP to activate innate lymphoid cells and skew T cell responses in the intestine (41–43). Unlike secretory IECs, absorptive enterocytes have a more unified role and regulate the uptake of nutrients and solutes from the luminal space (44). The vast majority of cellular absorption occurs through these enterocytes, including direct transcytosis of up to μm -sized particles (45, 46). Absorption of solutes and ions can also be mediated around the boundaries of IECs in a paracellular manner, with enterocytes contributing to the restriction and permissiveness of paracellular trafficking by modulating tight junctions (47). Ultimately, enterocytes express a plethora of transport machinery to allow for absorption of all macromolecular groups, including: carbohydrates, lipids, peptides, and amino acids – an essential function for host survival (48, 49).

Intestinal Epithelial Cell Death and Extrusion

Normal function of IECs requires their constant turnover through controlled cell death pathways and a lack of controlled IEC turnover can manifest in outgrowth of malignant cells (50). As such, IEC turnover occurs rapidly, at a rate of 3-5 days in mice and 5-7 days in humans with essentially all turnover in the small intestine occurring at the tips of villi (5, 7). The pace with which IECs are replaced is corroborated with histological observations noting that over 5% of villi contain an IEC that is in the process of being extruded from the epithelial layer (51). This suggests widespread remodeling of the intestinal epithelium occurs continually. Nearly all of the IECs that are extruded from the intestinal epithelium are positive for activated caspase-3, an essential executioner caspase that is canonically associated with apoptosis (51–53). It is clear that individual, dissociated IECs undergo apoptosis, but it remains unclear whether apoptosis is the cause or the consequence of cellular extrusion under homeostatic conditions (54). A recent study noted that there was no lack of epithelial shedding in mice with IEC-specific deletion of caspase-3 and caspase-7, suggesting that canonical apoptosis is not required for homeostatic extrusion from the epithelial barrier (55). Extrusion of IECs is a complex process that leads to the formation of a contractile actin and myosin ring. In the case of apoptotic cells, increases in the concentration of sphingosine 1-phosphate (S1P) are associated with signaling to S1P receptor 2 on neighboring cells to initiate cellular extrusion (56). However, live cell extrusion has also been studied. In zebrafish models, crowding of non-apoptotic cells can also increase S1P through mechanosensing by Piezo1, a stretch-activated ion channel (57). The actual formation of this contractile ring is mediated by Rho kinases, presumably through regulators like P115 RhoGEF (53). Ultimately, Rho coordinates with myosin kinases to directionally squeeze the IEC from its place in the epithelial layer (58, 59).

Under inflammatory conditions, IEC shedding occurs more regularly than under homeostatic conditions, often in response to dead and dying cells. The hallmark inflammatory cytokine studied in the intestine is tumor necrosis factor α (TNF α), which has strong genetic links to inflammatory bowel disease (60–62). TNF α has pleiotropic effects on intestinal permeability and wound-healing, and cell death (63). At homeostasis, IECs express both components of the tumor necrosis factor receptor (TNFR), TNFR1 and TNFR2. These receptors are not downregulated during intestinal inflammation which allows robust signaling in IECs (64). The detailed pathways that lead to cell death following TNF α signaling are regulated by magnitude of signaling stimuli and the current cell state, and TNF α signaling leads to a variety of death outcomes (65). In mouse models, robust signaling through TNFR1/2 leads to dramatic shedding and apoptosis of IECs (66, 67). In simple terms, this apoptotic TNFR signaling is mediated by interactions with fas-associated death domain-containing protein (FADD), which associates with TNFR and complexes with pro-caspase-8 to lead to self-cleavage and activation (65). The activation of caspase-8 leads to cleavage of executioner caspases-3/7 and cellular apoptosis. Caspase-8 can also cleave a pro-apoptotic protein, BID, to activate a cascade of BCL-2 family proteins that leads to mitochondrial outer membrane permeabilization and apoptosis. Despite TNF α 's moniker as a “necrosis factor”, necroptosis of IECs following TNF α stimulation generally only occurs under certain circumstances, such as when caspase-8 is inhibited (68, 69). In these cases, the TNF signaling pathway is shunted towards activation of receptor-interacting protein kinase 3 (RIPK3) which can subsequently activate mixed lineage kinase domain-like (MLKL) (70). Upon activation, MLKL complexes with ion channels and leads to rapid destabilization of cellular gradients and cell death.

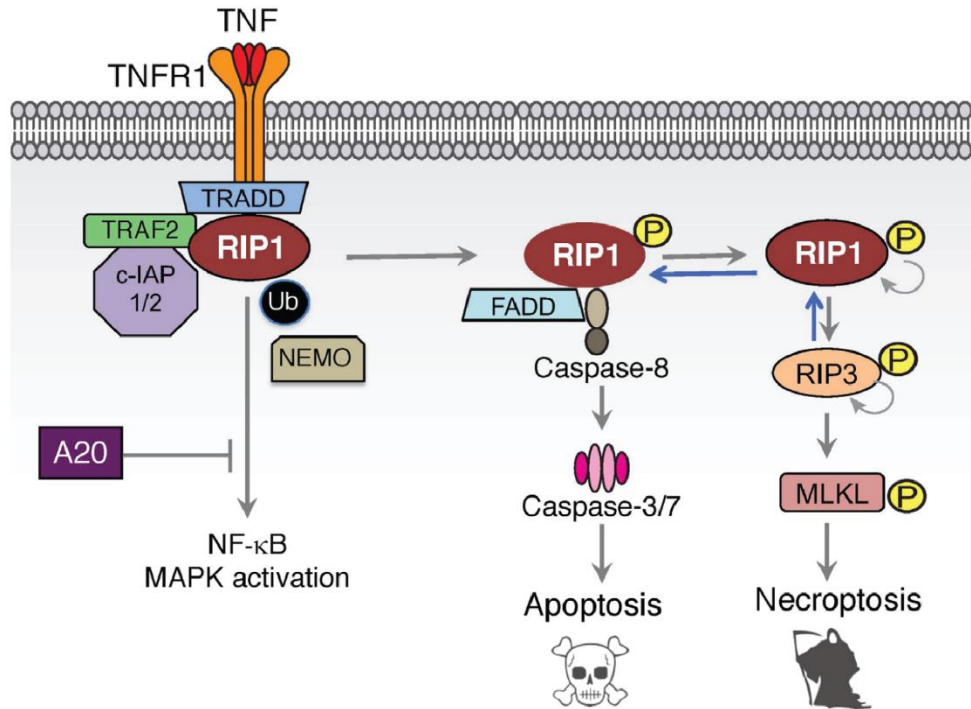


Figure 1.3. TNF signaling outcomes. Signaling through TNFR1 can lead to NF-κB activation, apoptosis, or necroptosis. Apoptosis requires association with FADD and activation of caspase-8 and caspases-3/7.

Adapted from Frontiers Media: Frontiers in Cell and Developmental Biology. The Balance of TNF Mediated Pathways Regulates Inflammatory Cell Death Signaling in Healthy and Diseased Tissues, Joshua Webster and Domagoj Vucic, 2020.

Intestinal Organoid Model System

Investigation of IECs was catalyzed by the development of the intestinal organoid model system. Intestinal organoids are a three-dimensional cell culture and were pioneered by the Clevers Group in 2009 (71). The development of these organoids enabled the long-term maintenance of primary intestinal epithelium and dramatically increased the ease of studying IECs. For example, organoids now can be derived from human patients as well as agricultural animals such as pigs, rabbits, chickens, and cows (72). These organoids also enable direct isolation and growth of genetically modified primary cells and they are also amenable to genetic engineering with CRISPR technology

(73). At their basis, organoid cultures were developed to recapitulate the ISC niche and allow for the constant proliferation of ISCs *in vitro*. To this end, organoids originated by isolating intestinal crypts, suspending them in a laminin-rich extracellular matrix (ECM), and culturing them with recombinant R-spondin, epidermal growth factor (EGF), and Noggin to stimulate their proliferation (71). Since that time additional IEC organoid culture media has been developed, including conditioned media (CM) that replaces EGF with Wnt-3a (74). The development of CM-producing L-WRN cells has disseminated the ability to culture organoids with relatively high-reproducibility, fueling the use of the organoid model system (75).

IEC organoids have been derived from nearly the entire gastrointestinal tract ranging from the stomach to the colon (74). These organoids readily polarize with the apical side facing away from the ECM in which they are suspended, towards the interior of the 3D organoid. However, removal of ECM from established organoids results in a dynamic repolarization of the apical surface of the IECs to the exterior of the 3D organoid (76). The ease with which organoids develop from intestinal tissues is largely attributed to intrinsic interactions between IECs and stochastic gradients of Notch and Dll1 in hyper-localized areas of the organoid (77). These gradients lead to symmetry breaking and the self-assembled budding of crypt-like structures. The degree to which organoids are retained in a spherical organization or spontaneously bud leads to their classification as either spheroids (spherical with no obvious crypt-like buds) or enteroids (multiple lobules of crypt-like buds) (78). The factors that determine spheroid or enteroid formation are not fully understood, but replacing of EGF with Wnt-3a is associated with spheroid formation (74). Perhaps the abundance of Wnt ligand in CM overrides the local cues required for crypt-like bud formation or maybe Wnt increases proliferation rate of amplifying cells in the organoid, which can reduce the differentiation of secretory cells (25). Despite these

differences between enteroids and spheroids, both types of structures retain their intrinsic tissue-specific programming during long-term culture, allowing for nuanced interrogation of differences in the intestinal epithelium along the length of the gastrointestinal tract (79, 80).

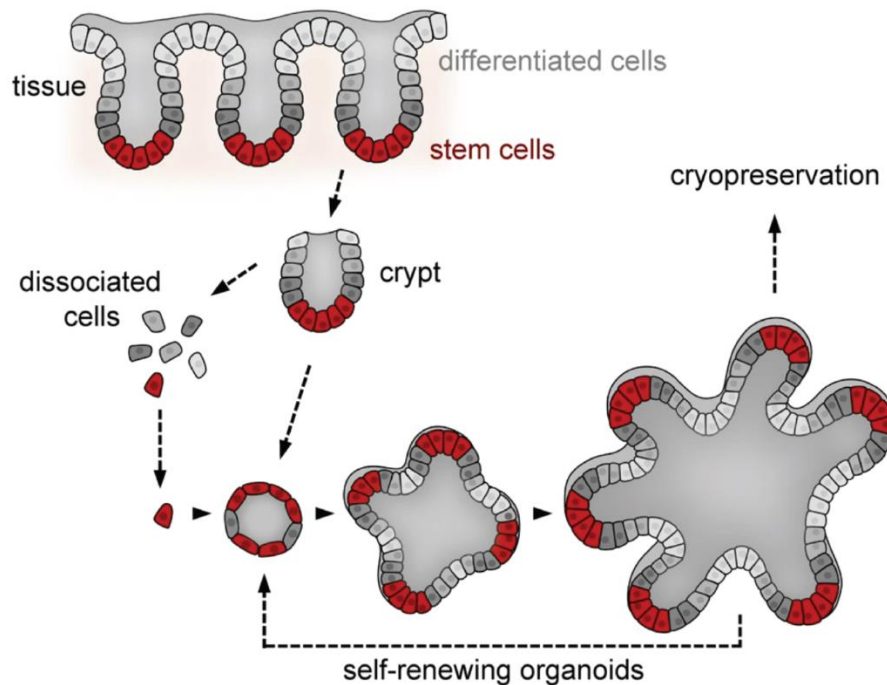


Figure 1.4. Intestinal organoids. Intestinal crypts with LGR5+ intestinal stem cells are isolated from fresh intestinal tissue. Incubation with stem cell factor media results in self-organization of proliferating organoids that can be maintained in culture long-term or cryopreserved.

Adapted with permission from Springer Nature: Cell Death & Differentiation. Organoid-based modeling of intestinal development, regeneration, and repair, Joep Sprangers, Irene C. Zaalberg, & Madelon M. Maurice, 2021.

Since organoids readily recapitulate the intestinal epithelium and are primary cells, they are well suited to model enteric infection (81). A number of human and simian viruses have been found to infect organoid cultures including infection of human organoids with lab-grown rhesus rotavirus and patient-derived rotavirus strains (82–84). Human organoids can also be infected with other enteric viruses like encephalomyocarditis virus,

echovirus 11, coxsackievirus B, enterovirus 71, and even SARS-CoV-2 (85–89). Similarly, organoids can be infected with pathogenic bacteria by direct microinjection of the pathogen into the apical-facing center of individual organoids (81). While this may sound straightforward, cell culture media must be carefully formulated to allow balanced growth of both IECs and bacteria (90). With these approaches, a number of bacterial infections have been established in organoids models, including *Salmonella*, *Helicobacter*, and *Clostridium* (91–94). Even protozoan parasites such as *Cryptosporidium* can be microinjected into organoids to model infection *in vitro* (95). Although these infections are relatively rudimentary at present, future advances in co-culturing organoids with pathogenic or commensal microbes will provide increasingly complex models to simulate the role of IECs *in vivo*. Currently, the standard organoid model system restricts analysis to the intestinal epithelium. However, very simple co-culture models exist to assess interactions between host immune cells and the intestinal epithelium. To investigate macrophage-epithelial interactions, co-culture models require seeding organoid cells in a two-dimensional monolayer (96). However, T cell co-culture models allow for direct addition of T cells to three-dimensional organoid culture (97, 98). The continued development of these models will soon allow for simplified reconstructions of *in vivo* microbe and immune interactions with the intestinal epithelium.

Interferon Signaling

Interferon Signaling Pathways

Interferons (IFNs) are a family of cytokines that provide antiviral defense by inducing the expression of interferon stimulated genes (ISGs), a large group of genes that include direct-acting antiviral genes (99, 100). Members of the IFN family are divided into three major types. IFN- α s and IFN- β (hereafter IFN- α/β) are the most commonly studied type I IFNs, but other less-characterized type I IFNs include IFN- ϵ , IFN- ω , IFN- κ , IFN- δ , IFN- τ and IFN- ζ (101). These other forms of type I IFNs are highly species- and cell-type specific and will therefore not be discussed here. The other major types of interferon are IFN- γ (type II IFN) and IFN- λ s (type III IFNs) (102, 103). Signaling by IFN- α/β , IFN- γ , and IFN- λ s are differentiated by their use of different cognate receptors. IFN- α/β signals through a heterodimeric receptor composed of *Ifnar1* and *Ifnar2* (IFNAR) (104), whereas IFN- γ signals through a complex of heterodimeric *Ifngr1* and *Ifngr2* (IFNGR) (105). IFN- λ s signal through a heterodimeric receptor (IFNLR) composed of a specific chain, *Ifnlr1*, and a non-specific chain that is shared with IL-10 family cytokines, *Il10rb* (106, 107). Indeed, although IFN- λ shares cytokine function with IFN- α/β , it is structurally much more similar to IL-10 family cytokines than type I IFNs (108). IFN- λ 's structural similarity to IL-10 family cytokines is consistent with its ability to bind to the common IL-10 family receptor, IL10R β (109).

Canonical signaling by all three types of IFN occur through the Janus-kinase (JAK) and signal transducer and activator of transcription (STAT) pathway, with IFNAR and IFNLR signaling using the same set of signaling factors, unlike IFNGR (110). Specifically, IFNAR and IFNLR both use the same canonical signaling kinases, JAK1 and tyrosine kinase 2 (TYK2), whereas IFNGR signals through JAK1 and JAK2 (111). Subsequently, these kinases phosphorylate STAT transcription factors that mediate induction of ISG

expression. In the case of IFNAR and IFNLR signaling, JAK1 and TYK2 lead to phosphorylation of STAT1 and STAT2 which allows them to bind to interferon regulatory factor 9 (IRF9) (**Figure 1.4**). This heterotrimeric complex, termed interferon stimulated gene factor 3 (ISGF3), translocates to the nucleus and binds interferon-stimulated response element (ISRE) motifs in the promoter region of ISGs (99, 106, 107, 112). Alternatively, in the case of canonical IFNGR signaling, JAK1 and JAK2 phosphorylate STAT1 which dimerizes and translocates to the nucleus to bind gamma-activated sequence (GAS) motifs in the promoter region of some ISGs (111). Signaling through all of the IFN pathways leads to the expression of a broad group of ISGs, however, the best characterized of the ISGs are those with antiviral activity.

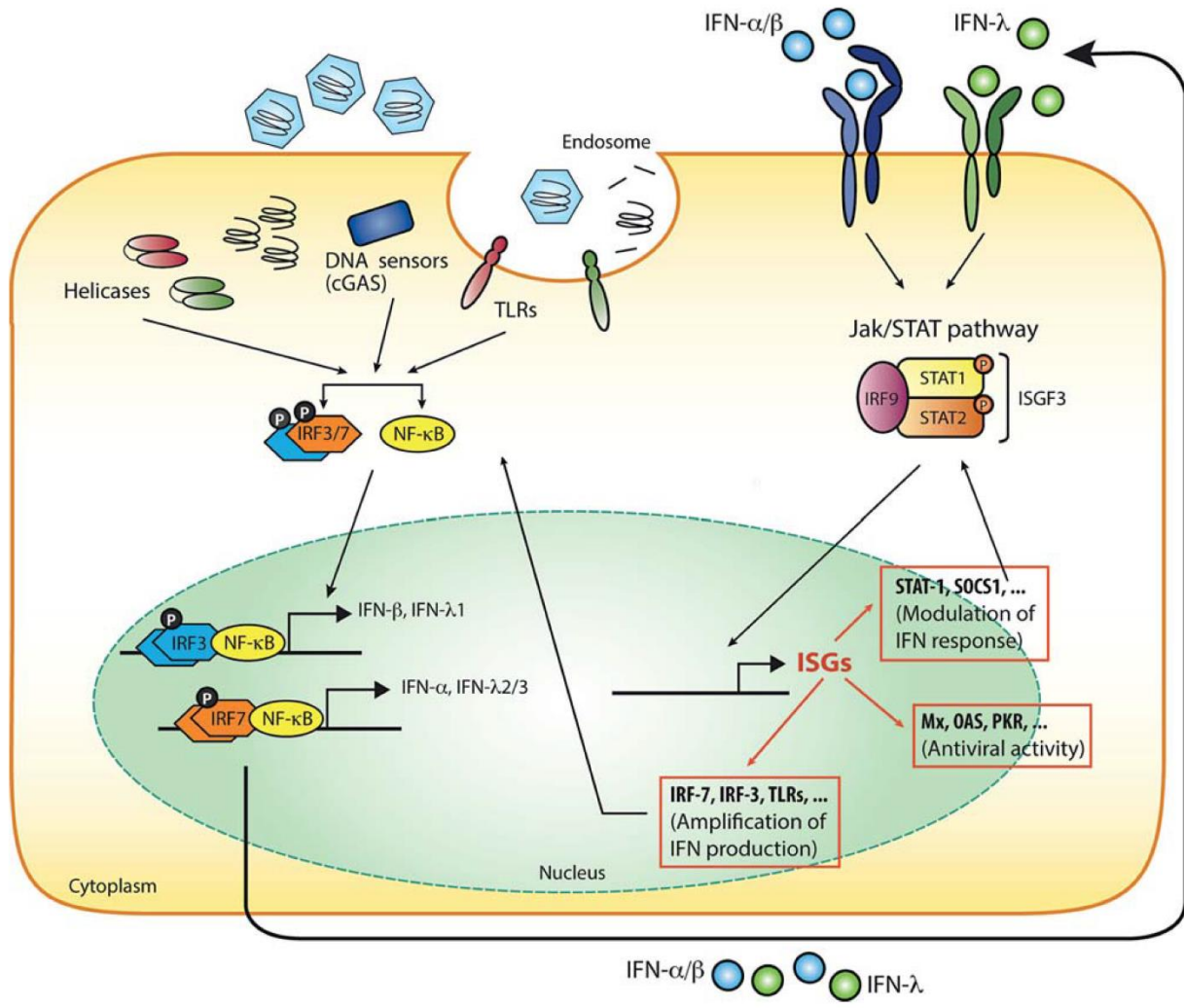


Figure 1.5. IFN- α/β and IFN- λ induction and signaling. Detections of MAMPs and PAMPs occurs through a variety of sensors including helicases like RIG-I and MDA, DNA sensors such as cGAS, and membrane-localized receptors such as TLRs. Sensing leads to activation of IRF3/7 and NF- κ B to stimulate expression of IFN- α/β and IFN- λ . Binding of IFN- α/β and IFN- λ to their cognate receptors leads to activation of ISGF3, composed of STAT1, STAT2, and IRF9. ISGF3 binds to the promoter of ISGs and activates a broad group of genes, including genes with antiviral activity.

Used with permission from S. Karger AG, Basel: Journal of Innate Immunity, Interferon- λ in the Context of Viral Infections: Production, Response and Therapeutic Implications, Pascale Hermant and Thomas Michiels, 2014.

The Antiviral Function of Interferon Stimulated Genes

Given the shared canonical transcription factor usage by IFNAR and IFNLR signaling, the transcriptional responses of IFN- λ and IFN- α/β largely overlap. In fact, IFN- λ does not stimulate expression of unique ISGs that are not stimulated by IFN- α/β (113–115). The overlapping core transcriptional response between IFNAR and IFNLR contains a number of well-characterized anti-viral ISGs that can target specific steps of certain viral lifecycles (110). Some of the primary viral processes that ISGs antagonize are entry, nuclear import, transcription, translation, viral RNA and protein stability, and egress (116). Following virion binding, viral internalization requires bypassing the cellular membrane of the host cell. One family of ISGs that classically antagonize viral entry are the interferon-induced transmembrane (IFITM) proteins such as IFITM1, IFITM2, and IFITM3 (117). Consistent with their role in preventing viral entry, IFITMs are primarily localized to the plasma membrane and endocytic vesicles where they inhibit membrane fusion and endosomal processes through incompletely characterized mechanisms. As such, IFITMs primarily inhibit entry of enveloped viruses, though IFITM3 has also been shown to inhibit entry of non-enveloped reovirus through an endosomal mechanism (118). Another set of ISGs is the myxovirus resistance (MX) family which can target multiple steps of various viral lifecycles. Some MX family members such Mouse Mx1 and human MxB both localize to nuclear membranes and may antagonize nuclear import of viral components (119). In cases where initiation of viral replication cannot be blocked, the oligoadenylate synthetase (OAS) family of ISGs recognizes dsRNA and activates RNaseL to mediate the degradation of viral RNAs (120). Another unique group of ISGs are the ISG15 family that contain proteins with ubiquitin-like function. This family facilitates the conjugative addition of ISG15 to both host and viral proteins to alter their function (114). In the case of altering viral proteins, ISG15 typically prevents oligomerization and assembly of viral components.

ISG15 can also dampen host IFN signaling to prevent runaway positive feedback loops. In a regulatory mechanism analogous to de-ubiquitination, USP18 is a de-ISGylating enzyme that removes ISG15 modifications and increases the antiviral ISG response (121). Another expansive family of ISGs is the tripartite motif (TRIM) proteins, consisting of dozens of members that can target nearly every step of the viral lifecycle (122). These TRIM proteins have a variety of abilities ranging from ubiquitin-ligase activity, to immune signaling modulation, and even the ability of TRIM21 to function as an antibody receptor. Some TRIM proteins suppress viral transcription, like TRIM22, whereas TRIM25 can regulate zinc-finger antiviral proteins (ZAP) to mediate translational suppression of viruses (123). Another group of ISGs that suppress viral translation are IFN-induced protein with tetratricopeptide repeats (IFIT) family members (124). These IFITs inhibit viral translation by binding triphosphorylated viral RNA as well as by suppressing the general translational activity of the host cell by binding to the eukaryotic initiation factor 3 (eIF3) translational complex (125). Lastly, antiviral ISGs such as tetherin and viperin can inhibit budding of specific viruses to prevent viral dissemination (116). Together, the canonical IFN response induces the broad expression antiviral proteins that can target many steps of the viral lifecycle.

Non-Canonical IFN Signaling and Differences in IFN- α/β and IFN- λ Responses

In addition to the canonical mediators of ISG transcription, ISGF3 and STAT1-homodimers, slightly altered transcription factor complexes can also play a role in the ISG expression under highly-specific circumstances (126–129). The primary non-canonical, JAK-STAT pathways that are present in IFN- α/β signaling are unphosphorylated ISGF3 (U-ISGF3) signaling and STAT1-independent signaling. Although IFN- α/β and IFN- λ

signal through the same canonical pathway, it remains unclear whether IFN- λ can elicit U-ISGF3 and STAT1-independent signaling. At its simplest, U-ISGF3 signaling is an extension of traditional ISGF3-mediated transcription. U-ISGF3 signaling is thought to occur due to either nuclear retention of ISGF3 that is subsequently dephosphorylated or nuclear accumulation of unphosphorylated components of ISGF3. For example, following IFN- β stimulation, dephosphorylation of ISGF3 can occur and nuclear U-ISGF3 can contribute to lingering expression of some antiviral ISGs (130). Components of ISGF3 are reported to accumulate in the nuclei of many cell lines through unknown mechanisms. The formation of nuclear U-ISGF3 in the absence of IFN stimulation appears sufficient to induce basal expression of antiviral ISGs that are dramatically reduced upon deletion of any U-ISGF3 components (131). In contrast to U-ISGF3, STAT1-independent transcription utilizes an incomplete ISGF3 signaling complex consisting of just STAT2 and IRF9. These STAT1-independent were first characterized during overexpression experiments in miscellaneous cell lines (132, 133) and ultimately STAT1-independent complexes do not bind DNA with high stability (134). STAT1-independent protection against dengue virus infection has been suggested in mice because deletion of both STAT1 and STAT2 increases susceptibility to infection to a greater extent than just STAT1 deletion (135). However, single deletion of STAT2 alone does not increase susceptibility, indicating that more research is required to confirm these phenotypes.

It has also been suggested that IFN- γ can signal through non-canonical pathways. Examples include STAT1-homodimer association with IRF9 or by using an ISGF3 complex with an unphosphorylated STAT2 protein (ISGF3-II). The most well-characterized IRF9 interactions with STAT1-homodimer were noted in immortalized cell lines following stimulation with IFN- γ and they were required for expression of the chemokine CXCL10 (136). These findings were repeated in bone-marrow macrophages

and showed that macrophages lacking IRF9 express less *Cxcl10* than WT macrophages following stimulation with IFN- γ (137). This increased CXCL10 production was then suggested to play a role in a dextran sulfate sodium model of colitis. Lastly, IFN- γ is capable of inducing the formation of ISGF3 that lacks phosphorylated STAT2 in mouse embryonic fibroblast cell lines (138). This ISGF3-II complex was also observed in A549 cells and was independent from IFN- α/β and IFN- λ signaling (139). Ultimately, it is unclear how broadly IFN- α/β and IFN- γ use these altered forms of canonical IFN signaling complexes. Extending their impacts to multiple cell lines and controlling for inadvertent activation of the IFN signaling pathway are necessary to confirm some of these non-canonical processes.

Despite the implication that IFN- α/β can use these non-canonical signaling complexes, there are very few noted differences in the use of signaling pathways between IFN- α/β and IFN- λ . However, there are several intriguing differences in the transcriptional responses to IFN- λ and IFN- α/β . For example, distinct differences in the kinetics of ISG transcriptional responses have been noted between IFN- λ and IFN- α/β , with IFN- λ stimulated a slower, but more sustained ISG response than IFN- α/β (140, 141). These kinetic differences were found to be independent of receptor abundance since overexpression of IFNAR or IFNLR did not alter the timing of transcriptional responses (142). Although it is unclear why the kinetics of IFN- λ and IFN- α/β responses vary, there is evidence that IFN- λ displays more reliance on mitogen-activated protein kinase (MAPK) signaling than IFN- α/β for optimal induction of ISGs by IFN- λ (143–145). In particular, inhibition of p38, ERK, or JNK all selectively decreased ISG responses elicited by IFN- λ . Furthermore, inflammatory gene expression is differentially regulated between IFN- α/β and IFN- λ . IFN- α/β is capable of inducing inflammatory cytokine expression by myeloid cells such as dendritic cells, macrophages, and neutrophils – unlike IFN- λ (146, 147). This

difference in inflammatory cytokine expression is due to selective induction of IRF1 by IFN- α/β which subsequently facilitates the induction of inflammatory cytokines (148).

Induction of Interferon Expression

Interferons (IFNs) are commonly induced in response to detection of pathogen- and microbe-associated molecular patterns (PAMPs and MAMPs) via a suite of cytoplasmic and membrane-associated sensors (**Figure 1.4**) (149–151). There are numerous cytoplasmic sensors that detect nucleic acids during viral infection, but many of the nucleic acid sensing pathways signal through stimulator of interferon genes (STING) or mitochondrial antiviral-signaling protein (MAVS) (152). One hallmark mechanism for activating the STING pathway is by sensing of cytosolic DNA by cGAMP synthase (cGAS). cGAS sensing results in cyclization of ATP and GTP into a secondary messenger molecule, cyclic GMP-AMP (cGAMP). Following its synthesis, cGAMP can bind to STING in the endoplasmic reticulum (ER) and induce expression of IFNs through TANK-binding kinase 1 (TBK1) (153, 154). Subsequently, activation of TBK1 leads to phosphorylation of interferon regulatory factor 3 (IRF3) and induction of IFN expression (152). Other cytosolic DNA sensors have been reported to signal through TBK1, including DNA-dependent activator of IRFs (DAI), IFI16, and DDX41, but play minor roles relative to cGAS-STING. Two sensors upstream of MAVS are RIG-I and MDA5. Both sense dsRNA with their helical domains and activate caspase-recruitment (CARD) domains to initiate IFN responses (155). Activation of CARD domains results in CARD oligomerization which is sufficient to drive induction of IFNs by binding to the CARD-like domain of MAVS (156, 157). Signaling through MAVS subsequently activates TBK1 and induces expression of IFNs.

Although cytosolic sensing plays a prominent role in IFN induction, stimulation of membrane-associated toll-like receptors (TLR) can also induce IFN responses. There are

thirteen TLRs in mice, however only nine (TLR1-TLR9) are shared with humans and are commonly studied (150). TLR1, TLR2, TLR4, TLR5, and TLR6 recognizing bacterial components such as lipopolysaccharide (TLR4), flagellin (TLR5), and lipopeptides (TLR1/2 and TLR 2/6). On the other hand, TLR3, TLR7, TLR8, and TLR9 recognize distinct classes of nucleic acid such as dsRNA (TLR3), unmethylated double-stranded DNA (TLR9), and ssRNAs or specific quinolone compounds and nucleoside analogs (TLR7 and TLR8) (149). Coincidentally, the localization of these TLRs correlates with the type of ligand recognized, as bacterial-sensing TLRs localize to the plasma membrane and nucleic acid sensing TLRs signal from the endosome (149). TLR-dependent pathways primarily signal through two separate adaptor proteins: myeloid differentiation primary response 88 (MYD88) and TIR-domain-containing adapter-inducing interferon- β (TRIF) (158). Of the nine common TLRs, only TLR3 is unable to recruit MYD88 and depends solely on TRIF as its signaling adapter (159). TLR4 can signal through both MYD88 and TRIF, although TRIF usage is restricted to endosomal compartments following endocytosis of receptor after ligand binding (159, 160).

Signaling through cytoplasmic sensing pathways and TLRs leads to induction of many genes that play roles in inflammation, survival, and proliferation. However, these pathways can also stimulate the expression of IFNs. Expression of IFNs is largely controlled transcriptionally by interferon regulatory factors (IRFs) and nuclear factor kappa-light-chain-enhancer of activated B cells (NF- κ B). Of these factors, IRF3 and IRF7 in IFN regulation have been particularly well-studied and both play essential roles in the induction of IFNs. IRF3 is constitutively expressed in many cell types at steady-state. On the other hand, IRF7 expression is induced by sensing of viral infection, LPS, or by IFN itself in most non-lymphoid cells (161–163). As such, IRF7 is essential for maximal expression of all IFNs, due to the positive feedback loop induced by autocrine exposure

to IFNs (164–166). One feature of IRF7 is its ability to directly interact with MyD88 and subsequently induce IFN expression (167, 168). As such, cells with constitutive expression of IRF7, such as plasmacytoid dendritic cells (pDCs), are primed for robust IFN production (169). IRF3 and IRF7 bind to ISRE sites in the promoter regions of IFN- λ and IFN- α/β , however each IFN relies on specific combinations of IRFs and NF- κ B for expression (103, 151, 170). IFN- λ and IFN- α s are preferentially driven by IRF7 as opposed to IFN- β which is productively stimulated by both IRF3 and IRF7 (164, 166, 171–173). However, IFN- λ and IFN- β also use NF- κ B family members for efficient induction, unlike IFN- α s (174). These findings show that induction of IFN- λ is unique compared to IFN- α/β . IFN- λ exhibits robust expression in response to stimuli due to primary dependence on IRF7, but this response is slightly delayed due to less dependence on the constitutively expressed IRF3. However, IFN- λ is also reported to be highly dependent on NF- κ B for robust expression compared to IFN- α/β (175), suggesting that the specific contexts for IFN- λ expression may be heavily regulated by NF- κ B.

Since IFN responses are most well-characterized as antiviral, virus-induced IFN expression has been extensively studied (103, 151, 164, 166, 170–173). However, bacteria can also stimulate expression of IFN through both TLRs and cytosolic sensors (176). In bone-marrow derived dendritic cells, essentially every bacterial TLR ligand is sufficient to induce IFN- λ and IFN- β expression (76). Likewise many bacterial components such as LPS, flagellin, and lipoproteins are capable of inducing IFN in specific *in vivo* contexts (161, 177–180). Similarly, bacterial-mediated stimulation of nucleic-acid sensing TLRs is associated with increased IFN- β expression in certain *in vivo* contexts (181–183). Two commonly studied intracellular bacterial pathogens, *Listeria monocytogenes* and *Mycobacterium tuberculosis*, induce expression of IFN- α/β and IFN- γ . These bacterial infections highlight some of the differences between bacterial and viral responses to

individual types of IFN (179, 180, 184, 185). Upon infection with *L. monocytogenes* and *M. tuberculosis*, IFN- γ is essential for bacterial clearance and resistance to infection, however IFN- α/β increases susceptibility to *M. tuberculosis* (186, 187). IFN- α/β does not universally increase susceptibility to intracellular bacteria though. For example, IFN- α/β signaling has mixed effects on *L. monocytogenes* infection (188). The impact of IFN- α/β on *L. monocytogenes* infection is linked to the timing IFN signaling and the route of infection (189, 190). In particular, IFN- α/β signaling is detrimental to the host following intraperitoneal injection of *Listeria* infection, but is protective during intragastric infection. These findings suggest that the role of IFNs and the responsiveness of the host may vary by location.

Interferon Responsiveness in the Intestine

IFNAR is almost ubiquitously expressed and, as such, nearly all cells and tissues respond to IFN- α/β . On the other hand, *Ifnlr1* is predominantly expressed in the gastrointestinal tract, with skin and lung tissues also having abundant *Ifnlr1* transcripts (191). Consistent with these findings, mice with a *LacZ* reporter gene inserted into the *Ifnlr1* gene locus had the most prominent expression of *Ifnlr1* in the gastrointestinal tract at homeostasis (192). *Ifnlr1* expression is limited to specific cell types and is largely restricted to epithelial cells and neutrophils (103, 191, 193). By comparison, IFNAR is almost ubiquitously expressed in every type of cell. Consistent with the tissue-specific and cell type-specific expression of *Ifnlr1*, the gastrointestinal epithelium robustly responds to IFN- λ stimulation (194–196). Intriguingly however, IEC responsiveness to IFN- λ is accompanied by hyporesponsiveness to IFN- α/β . Imaging of mouse small intestines following injection of IFN- λ or IFN- α indicated distinct compartmentalization of IFN responsiveness (195, 197). Injection with IFN- λ increased phosphorylation of STAT1 and reporter ISG activation in IECs, but not underlying lamina propria cells. However,

stimulation with IFN- α displayed an inverse phenotype with increased phosphorylation of STAT1 and reporter ISG activation in lamina propria cells, but not IECs. These findings were further corroborated by transcriptional analysis of sorted IECs and lamina propria cells (194). Some of this compartmentalized response may be due to less expression of *Ifnar1* and *Ifnar2* transcripts in IECs as compared to non-epithelial cells in the intestine (194). However, there is some evidence suggesting that signaling through IFNAR is possible in IECs. For example, disruption of IFNAR1 endocytosis in IECs increases IEC proliferation and apoptosis (198). These findings suggest that IFNAR is translated in IECs *in vivo* and may support limited signaling but be unable to robustly respond to IFN- α/β (198). Consistent with the hyporesponsiveness of IECs to IFN- α/β , IFN- λ plays a dominant role in protection of IECs against epithelial-tropic enteric viruses like murine rotavirus and murine norovirus (MNV) (195, 196, 199, 200). This hyporesponsiveness to IFN- α/β in the intestinal epithelium is unique and not observed in epithelial cells at other barrier tissues that respond to both IFN- α/β and IFN- λ . For example, the lung is a highly analogous mucosal barrier tissue to the gastrointestinal tract and yet lung epithelial cells respond to both IFN- α/β and IFN- λ *in vivo* (147, 201). Similarly, the vaginal epithelium also responds to both IFN- α/β and IFN- λ (175, 202). Even reproductive tissues like the placenta can respond to both IFN- α/β and IFN- λ (203, 204). Thus, downregulation of epithelial response to IFN- α/β seen in the intestine is not observed in other barrier tissues, suggesting that dependence on IFN- λ signaling in IECs is due to unique, tissue-specific context.

Interestingly, culturing primary intestinal epithelial cells as organoids does not fully recapitulate the compartmentalized IFN responses observed *in vivo*. In fact, instead of hyporesponsiveness to IFN- α/β , organoids display robust responses to both IFN- λ and IFN- α/β (205). In fact, IFN- α/β more potently stimulates ISGs than IFN- λ in organoid cultures. Accordingly, stimulation of organoids with both IFN- λ and IFN- α/β elicits robust

antiviral responses and protection against mammalian reovirus, human rotavirus, and human astrovirus infections (143, 206, 207). It remains unclear why organoids respond to IFN- α/β . The mechanism of *in vivo* IFN- α/β hyporesponsiveness has not been established, but increased IFN- α/β responsiveness may be due to loss of regulatory repression of signaling *in vivo*. Alternatively there may be tissue-specific cues *in vivo* that are lost in organoid cultures. Administration of IFN- λ to mice results in robust ISG expression in differentiated intestinal epithelium (194–196), however, the ISG response in organoids appears much more heterogeneous (205). It remains to be seen how closely these differences in IFN responsiveness are related to organoid-specific biology. Regardless, the suppression of IFN- α/β responses *in vivo* suggests that there are unique physiological advantages for preferential responsiveness to IFN- λ by the intestinal epithelium *in vivo*.

The Rotavirus Model System

Rotavirus Structure, Life Cycle, and Pathogenicity

Rotaviruses (RV) are genus of the *Reoviridae* family and predominantly infect the gastrointestinal tract of a variety of mammalian species. There are currently 8 groups of rotavirus (Group A – Group H) that are differentiated by antigenic properties and sequence, but group A rotaviruses are responsible for more than 90% of infections in humans (208). Currently, rotavirus is the dominant cause of diarrheal mortality across all age groups (209). In the past 15 years, two rotavirus vaccines have been licensed for use in the United States and provide near complete protection from severe rotavirus-induced gastroenteritis (210, 211). Since their introduction, rotavirus vaccines have gradually reduced mortality in children, however, there are still over 200,000 estimated deaths, globally, largely concentrated in developing countries (212).

As a member of *Reoviridae*, rotaviruses have double-stranded RNA genomes organized into 11 segments. Cumulatively, these segments encode 6 structural proteins (VP1, VP2, VP3, VP4, VP6, VP7) and 6 non-structural proteins (NSP1, NSP2, NSP3, NSP4, NSP5, NSP6) that facilitate replicative function of the virus (213). Structurally, rotavirus virions are non-enveloped and consist of triple-layered particles (TLPs) that are wrapped in a layer of VP7 proteins interspersed with VP4 spike proteins. In combination, these VP4 and VP7 facilitate binding and viral entry into host cells through complex, combinatorial interactions with integrins and glycans such as sialic acid and histone-blood group antigens (HBGAs) (214). The role of sialic acid for viral binding is particularly well-defined, with strain-dependent requirements for the presence of sialic acid (215, 216). Likewise, it has been speculated that age-dependent variation of HBGAs may contribute to increased incidence of rotavirus infection in neonates and children (217). Unlike binding of virion, rotavirus internalization remains relatively under characterized. Currently,

endocytosis is thought to be required for virion internalization with requirements for the Endosomal Sorting Complex Required for Transport (ESCRT) pathway and species-specific interactions with Rab proteins (218, 219). Ultimately, internalization of rotavirus leads to formation of viral replicative complexes in the cytoplasm of the host cell. These 'viroplasms' produce double-layered viral particles which mature to TLPs in the endoplasmic reticulum (ER) of the host. Following maturation, virions can be released from the ER through both lytic and non-lytic mechanisms (220, 221).

The study of rotavirus pathogenesis has led to the isolation of patient-derived strains as well as the development of animal rotavirus models, including: rhesus rotavirus, bovine rotavirus, porcine rotavirus, and murine rotavirus (222–224). In particular, infection of laboratory mice with rotavirus has provided unique insights into the mechanisms of pathogenicity and immunity. Infection of mice with both murine and rhesus rotavirus results in peak shedding of viral antigen in stool between days 3 and 5 with full clearance of infection by day 10 (225–227). Consistent with the timing of viral clearance, resolution of rotavirus infection largely depends on mobilization of the adaptive immune response. In particular, robust B cell responses and production of antibody facilitate resolution of infection (228). This B cell response is bolstered by CD4 T cell activity, but neither CD4, nor CD8 T cell activity is required for clearance of murine rotavirus infection (229).

Intriguingly, murine rotavirus infection in mice recapitulates age-dependent diarrheal symptoms with adult mice not developing diarrhea that is present in neonatal mice (230). One possible reason why adult mice are not susceptible to diarrheal disease may be due to the mechanism of diarrheal-induction. Previously, the non-structural protein 4 (NSP4) of rotavirus was found to be a potent enterotoxin which is singularly capable of inducing diarrhea, likely through activation of calcium signaling (231, 232). Although

calcium signaling is implicated in rotavirus-induced diarrhea, infection appears to predominantly increase intestinal motility, rather than having acute effects on intestinal permeability (233). Additionally, diarrheal symptoms in neonatal mice may also be linked to age-dependent effects on TLR expression by IECs. In particular, IECs exhibit higher expression of *Tlr3* in adult mice than neonatal mice and therefore adult mice have increased IFN- β expression in response to murine rotavirus than neonatal mice (234). These differences correlate with increased viral load in neonatal mice compared to adult mice, suggesting that the immature IFN responses in neonatal mice may exacerbate murine rotavirus infection and lead to increased diarrheal symptoms.

Rotaviruses are predominantly considered enteric pathogens, although there are reports that mice can acquire systemic infection of both murine and rhesus rotavirus (235, 236). In the gastrointestinal tract, murine rotavirus most readily infects the ileum region of the small intestine over the cecum, colon, or other regions of the small intestine. In the small intestine, murine rotavirus robustly infects enterocytes, with preferential infection of enterocytes distally located at the tips of villi (227, 237, 238). Following infection, histological perturbations occur within the intestinal epithelium, including the blunting or shortening of intestinal villi and the formation of vacuoles within infected IECs (239). On a cellular level, these acute changes include contraction of crypt-associated stem cells and paneth cells, and a decrease in the maturity of differentiating enterocytes (240).

Rotavirus and Interferon Signaling

The ability of rotavirus to combat the expression of IFNs and a subsequent IFN response has been characterized in cell lines and infections of laboratory mice (241). *In vitro* characterization of the interactions between rotavirus and IFN signaling has primarily been performed with human rotaviruses and rhesus rotavirus. Reports indicate that

multiple species of rotavirus NSP1, including human and simian rotaviruses, can antagonize induction of IFN by targeting IRFs for degradation (242, 243). Both human and rhesus rotavirus strains are also able to inhibit IFN responses by directly antagonizing STAT1 and STAT2 (244, 245). Additionally, rhesus rotavirus can target type I and type II IFN receptors for degradation *in vitro* (246).

Characterization of rotavirus infection in mice has consolidated around distinct differences in the pathogenicity of rhesus and murine rotavirus. Generally, rhesus rotavirus induces more IFNs than murine rotavirus during *in vivo* infection of neonatal mice, correlating with less efficient infection by rhesus rotavirus than murine rotavirus (247, 248). These findings suggest that IFN controls heterologous rotavirus infection of mice to a greater extent than homologous rotavirus infection. This control of rhesus rotavirus by IFNs extends to systemic tissues, as knockout of both type I and type II IFN signaling increases systemic replication of rhesus rotavirus, but not murine rotavirus (236). Even in the intestine where IFN- λ responses are dominant, the protective capacity of endogenous IFN- λ against homologous murine rotavirus remains enigmatic. Direct sensing of murine rotavirus by TLR3 in IECs can induce IFN- λ responses during the peak of homologous infections, but cytosolic signaling through MAVS is dispensable for protection against murine rotavirus (234, 248). Despite the induction of IFN- λ responses, murine rotavirus is highly adapted to its murine host and efficiently replicates *in vivo*, unlike rhesus rotavirus (248). This is largely due to immune evasion provided by combinatorial action of murine rotavirus NSP1, NSP2, and NSP3 (249) and the ability of murine rotavirus to downregulate IFN receptors in infected cells (246).

Ultimately, consensus on the ability of endogenously-produced IFN- λ to control murine rotavirus infection throughout the course of infection has not been reached and

there are conflicting reports on the susceptibility of *Ifnlr1*^{-/-} mice to murine rotavirus infection. For instance, the Kotenko lab did not find differences in murine rotavirus antigen shedding from WT or *Ifnlr1*^{-/-} neonatal mice (197). Likewise, two other lab groups that assessed murine rotavirus titers and viral RNA found no role for endogenous IFN signaling in controlling infection using neonatal *Stat1*^{-/-} mice that lack all IFN signaling (247, 249, 250). However, one of these studies found increased murine rotavirus antigen shedding in the stool of neonatal *Stat1*^{-/-} mice, despite no evidence of increased antigen in intestinal tissue (250). In contrast to the study by Kotenko group, the Staeheli lab and colleagues determined that deleting *Ifnlr1* dramatically increases murine rotavirus antigen shedding in neonatal mice and in intestinal tissue (195, 251). Ultimately, these discrepant findings suggest that the ability of endogenous IFN to control murine rotavirus may be more nuanced than initially appreciated.

The protective capacity of the endogenous IFN- λ response to murine rotavirus infection is unclear, perhaps reflecting the success of murine rotaviruses immune evasion mechanisms. However, despite the unsettled nature of endogenous protection by IFNs, the capacity of prophylactic and therapeutic administration of IFN- λ to reduce murine rotavirus infection remains unequivocal. Two studies convincingly show that administration of IFN- λ to neonatal mice 8 hours prior to inoculation significantly reduces murine rotavirus antigen in intestinal tissue (195, 251). The differences in protective capacity of endogenous and prophylactic IFN- λ has also been modeled in rotavirus infection of organoids, with prophylactic initiation of antiviral defenses appearing to be essential to control rotavirus infection (206).

Intestinal Bacterial Microbiota

Development and Composition of the Intestinal Bacterial Microbiota

The gastrointestinal tract is home to the greatest diversity and density of bacterial species out of any host tissue. In the case of humans, it is estimated that tens of trillions of bacteria from up to 500 species colonize the gastrointestinal tract as intestinal microbiota (252, 253). These bacteria are present in increasing density as the gastrointestinal tract progresses, with relatively sparse bacterial presence in the highly acidic stomach and incredibly dense bacterial presence in the colon (254). This density gradient is also partially reinforced by bile acids that are secreted into the duodenum and can have antibacterial, detergent-like properties (255). Despite this species diversity and density, most of the bacterial microbiome consists of four specific Phyla of bacteria: Bacteroidetes, Firmicutes, Actinobacteria, and Proteobacteria. In fact, up to 90% of the bacterial microbiota are either Bacteroidetes or Firmicutes (254, 256, 257). Both the small intestine and the colon house populations of Bacteroidetes, whereas the colon also has large populations of Firmicutes (252, 258, 259). There are several features that makes the colon more amenable to bacterial growth than the small intestine including: more neutral pH, a larger volume, and less concentration of bile acids (254). These factors allow two other prevalent bacterial phyla to expand in the colon, Actinobacteria and Proteobacteria (257)

The composition of a host's bacterial microbiota is always changing in response to the introduction of new species and specific nutrient availability acquired through ingestion. However, the most rapid changes to the bacterial microbiota occur during birth with the primary seeding of maternal microbiota (260). Prior to delivery, the fetal microbiome is thought to be completely undeveloped, as amniotic fluid does not contain

detectable microbial sequences (261). Upon delivery newborns acquire maternal associated microbiota; in fact, the newborn microbiome recapitulates the route of their delivery with vaginal-delivered newborns harboring their mother's vaginal-associated microbial communities and cesarean-delivered newborns harboring their mother's skin-associated microbiota (262). After initial maternal seeding, the second largest developmental changes to the bacterial microbiota occur during weaning and upon ingestion of microbe-replete solid food (263–265). Accordingly, microbiota diversity strongly correlates with dietary diversity across mammals (266).

Given the variability in the seeding and development of the intestinal microbiota, each host has a highly individual microbiota. This is evident even in genetically uniform mice housed in controlled laboratory environments. Variation in the composition of the intestinal microbiota has been readily noted on a facility-by-facility basis (267), most infamously in the case of vendor-specific differences in the presence of segmented-filamentous bacteria (SFB) (268). Even intra-institutional differences in intestinal microbiota have been noted, with the most prominent differences being dependent on different caging and maternal sources (269). These microbial differences illustrate the need for littermate controls when performing rigorous experimentation as the simplest method of standardizing the bacterial microbiota (270).

Manipulation of Bacterial Microbiota

Given the complex diversity of bacterial microbiota, techniques have been developed to interrogate the role of the bacterial microbiota in host-processes. One of the simplest methods to determine the role of the bacterial microbiota is by depletion. Techniques to raise germ-free animals began as early as the late 19th century and development of gnotobiotic rodent models soon followed the mid-20th century (271). These

models have been refined over the past seventy years and now represent the gold-standard of microbiota research as they consist of meticulously controlled sterilization procedures to deliver material to mice living in isolators (272). Increasingly, less stringent approaches to deplete bacterial microbiota have been developed, including persistent administration of multiple antibiotics (ABX). These cocktails of ABX are formulated to target broad species of bacteria and first consisted of vancomycin, neomycin, ampicillin, and metronidazole (273). Additional antibiotic regimens include treatment with streptomycin and amoxicillin/clavulanic acid (274), likely in an attempt to stave off dehydration-induced weight loss induced by the bitterness of metronidazole (275, 276). In some cases, limited administration of antibiotics are sufficient to perturb the communal dynamics of the intestinal microbiota and are used in specific experiments (277, 278).

Combinatorial use of several antibiotic classes must be used to effectively target the entirety of the intestinal bacterial microbiota. Ampicillin and amoxicillin are β -lactam antibiotics that bind penicillin-binding proteins to terminate bacterial cell wall formation and are broadly bactericidal (279). Vancomycin is a glycopeptide antibiotic that binds to bacterial lipid II, a peptidoglycan precursor used to form the cell wall of gram-positive bacteria (280). Neomycin and streptomycin are aminoglycoside antibiotics that inhibit bacterial protein synthesis by binding bacterial ribosomes (281, 282). To be effective aminoglycosides must be taken up by bacteria which requires active electron transport; therefore, although aminoglycosides are broadly antibacterial, they are ineffective against anaerobic bacteria (283). On the other hand, metronidazole is a nitrogenous antibiotic that disrupts DNA but requires a partially reduced state that is most prevalent in anaerobic bacteria (284). Given their broad coverage and diverse mechanisms, these antibiotic regimens are sufficient to ablate nearly all intestinal bacteria. Following treatment with

these cocktails, essentially the only detectable source of bacterial sequences are a small amount sourced from plant-associated dietary intake (274, 285).

In addition to depletion of bacterial microbiota, targeted studies perform defined microbial colonization of germ-free mice with either single bacterial species or a limited diversity of bacterial species (274). Among the most well-known of these monocolonization experiments was performed with SFB in germ-free mice to show sufficiency of SFB to skew enteric immune responses (268, 286). Similar experiments have been performed with *Bacteroides fragilis* (287, 288) and with *Escherichia coli* mutants (289) to assess their impacts on the enteric immune system, highlighting the tractability of single-species microbiota models. More complex colonization models also exist, most prominently being a cocktail of microbes called altered Schaedler's flora (ASF) (290). This formulation consists of specific *Clostridium*, *Lacobacillus*, *Mucispirillum*, *Eubacterium*, *Firmicutes*, and *Parabacteroides* species that stably colonize the length of the gastrointestinal tract and recapitulate a minimal microbiome (291). Similar to monocolonization, colonization with ASF has been used to study enteric immunology with great effect (292). Continued use of minimally microbial-colonized animals will reveal further functions of the intestinal bacterial microbiota.

Physiological Effects of the Intestinal Bacterial Microbiota

The intestinal bacterial microbiota perform many essential homeostatic functions and one of the primary ways that intestinal bacterial microbiota perform these functions is through the production of bacterial metabolites. These metabolites include lipid species, carbohydrate species, and bile acids made by lipid and amino acid precursors. The presence or absence of these metabolites can have dramatic and systemic effects on the host, including on host metabolism (293). For example, the sera of germ-free mice has

reduced concentrations of “energy-associated” metabolites like pyruvate, citrate, fumarate and increased concentrations of certain lipid species like linoleic acid (294). These global alterations in the metabolism of germ-free mice are suggested to be partially responsible for the development of undersized hearts, lungs, and livers in the absence of bacterial microbiota (295). The bacterial microbiota can also play complex roles in predisposing the host to metabolic disease. For example, germ-free mice are protected from development of obesity when fed a high-fat diet (296). This protection is partially because loss of microbiota reduces suppression of Fiaf, a lipoprotein lipase inhibitor. Germ-free mice that lack microbiota exhibit decreased LPL activity and decreased storage of triglycerides. Bacterial microbiota can also shape susceptibility to heart-disease through production of specific metabolites. For example, bacterial catabolism of phosphatidylcholine has been linked to increased risk of atherosclerosis due to increased uptake of metabolic byproducts by macrophages (297). However, phosphatidylcholine can also bind to peroxisome proliferator-activated receptor α (PPAR α) in the liver to dramatically alter the metabolic landscape of the host (298). Some of the many functions of PPAR α include modulating fatty acid oxidation and lipid transport (299), therefore bacterial microbiota can also indirectly regulate host metabolism through hepatic mechanisms. Likewise, some bacterial species like *Lactococcus* can process linoleic acid into different conjugated linoleic acid (CLA) species. These CLAs can play modulate host metabolism depending on their conjugated forms. c9,t11-CLA and t9,t11-CLA decreases risk of atherosclerosis, whereas t10,c12-CLA can exacerbate atherosclerosis through PPAR-dependent mechanisms (293).

Intestinal bacteria are also well-known to metabolize dietary carbohydrates into multiple metabolites, as germ-free mice develop grossly distended cecums due to increased concentration of undigested, complex carbohydrates which contributes to

increased water retention (295). One well-characterized group of carbohydrate-derived metabolites are the short chain fatty acids (SCFAs): acetate, propionate, and butyrate (300). Following their production, these SCFAs play an outsized role in host functions including energy metabolism, gut-brain neurology, and immunomodulation (301). The role of SCFAs in host metabolism is mediated by both direct uptake as well as by signaling. For example, IECs directly absorb SCFA along the length of the gastrointestinal tract, providing them with direct access to these metabolites (302). It has been suggested that SCFAs may provide direct contributions to host metabolism, with SCFAs estimated to contribute up to 10% of the caloric requirement in humans (303). SCFAs also signal through two G protein coupled receptors, GPR41 and GPR43, that use Pertussis toxin-sensitive G protein intermediates to stimulate host responses (304). Much of the way that SCFA alter host energy metabolism is by indirect mechanisms following signaling through GPR41 and GPR43. GPR41 and GPR43 are expressed by enteroendocrine cells which are known to secrete a variety of hormones (305, 306). Stimulation with SCFAs is thought to increase secretion of glucagon-like proteins, Glp-1 and Glp-2, to modulate blood glucose levels and peptide YY (PYY) to suppress intestinal motility (307, 308). Signaling by SCFAs also affects the proliferation of the intestinal epithelium, perhaps reflecting its role as a proxy for abundant metabolic energy in the intestine (309). In addition to IEC-specific roles, SCFAs also signal to non-epithelial cells. For example, GPR41 is expressed by certain sensory ganglia, suggesting SCFA can impact neural function (310). Recent studies suggest that SCFAs can modulate neural processes in the intestine with effects on brainstem sensory neurons and premotor neurons (311). Other roles for SCFA signaling are prominent in the enteric immune system as neutrophils express abundant amounts of GPR43 and use SCFAs as a chemoattractant to induce inflammation (312).

Inflammatory roles for bacterial-derived SCFAs are implicated in models of colitis and graft-versus-host disease (313).

In addition to SCFAs, bile acids can be produced by the intestinal bacterial microbiota and have effects on intestinal immunity and inflammatory responses (314). Primary bile acids such as chenodeoxycholic acid (CDCA) and cholic acid (CA) are conjugated in the liver and are then secreted by the gall bladder into the intestine to aid in digestion (315). However, certain members of the bacterial microbiota can metabolize primary bile acids into secondary bile acids using bile acid inducible (bai) genes (316). These bai genes can convert primary bile acids like CDCA and CA into the secondary bile acids such deoxycholic acid (DCA) and lithocholic acid (LCA) by removing a $7\alpha/\beta$ -hydroxy group. All four of these bile acids are known to bind Farnesoid X receptor (FXR), a nuclear receptor that is abundantly expressed in the intestine (317). Stimulation of FXR with bile acids is associated with homeostatic functions such as tight junction maintenance, cellular proliferation, and immunomodulatory effects (318).

Independent of SCFAs and bile acids, there are many other homeostatic functions performed by the bacterial microbiota. For example, members of the intestinal bacterial microbiota have been purported to aid in the synthesis of vitamins (319). In particular, it is most commonly suggested that microbiota aid the synthesis of B family vitamins such as B12, riboflavin, and folate (320, 321). The bacterial microbiota can also directly provide colonization resistance against bacterial pathogens usually by nature of complex, incompletely understood community dynamics (322). Disruption of these ecosystems with limited antibiotic use can increase susceptibility to enteric pathogens (323). Inversely, colonization of germ-free animals with limited bacterial species can be sufficient to mediate defense against enteric pathogens like *Listeria monocytogenes*, *Enterococcus faecium*, and *Clostridium difficile* (324–326). Other effects of the bacterial microbiota are

observed in enteric tissue with depletion of bacterial microbiota (327); these changes include reduced proliferation of IECs (276), alterations in the attachment of mucins in the small intestine and colon (328), and decreased integrity of tight junctions (329–331). Lastly, the intestinal bacterial microbiota directly interact with the enteric immune system in a myriad of ways, which will be covered more fully below in “The Enteric Immune Environment”.

The Enteric Immune Environment

Immune Cells of the Enteric Niche

The gastrointestinal tract is the largest physical compartment of the immune system and houses large numbers of both lymphoid and myeloid cells (3). T cells, B cells and plasma cells, and innate lymphoid cells (ILCs) compose the majority of the lymphoid compartment. The myeloid compartment includes enteric macrophages and dendritic cells (DCs) (332). Generally, these immune cells reside in the lamina propria underlying the intestinal epithelium or in association with IECs. In the lamina propria of the small intestine, accumulations of enteric immune cells develop into secondary lymphoid organs *in utero* (333). These regions are maintained through adulthood, are known as Peyer's patches (PP), and generally recapitulate lymph node architecture by housing lymphoid cells and antigen-presenting DCs. Additional immune infrastructure such as lymphatic vessels also develop *in utero* and link these PP to regional lymph nodes in the mesentery (MLNs).

One of the most prevalent types of immune cell in the intestine are T cells. These cells can reside in PPs and the lamina propria, but they also can stably interact with IECs, in which case they are called intraepithelial lymphocytes (IELs). Estimates indicate that there is nearly one IEL for every ten epithelial cells in the intestine, suggesting that they play a large role in the enteric immune system (334). IELs are a highly heterogeneous group, consisting of "natural" and "induced" subsets, each being an umbrella for more niche IEL types that are distinguished by comparison of cell markers and signaling machinery (335, 336). A common cell marker of IELs is the constitutive expression of CD103, an integrin that binds to E-cadherin on IECs, which allows IELs to patrol the intestinal epithelial layer (337). Natural populations of IELs are more prevalent early in life and undergo alternative maturation in the thymus that uses a positive-selection process on self-antigen (338). One group of well-known natural IELs are $\gamma\delta$ T cells, delineated by

their usage of specific $\gamma\delta$ T cell receptors (TCR $\gamma\delta$) (339). These natural $\gamma\delta$ T cells are appreciated to surveil the IEC space, by probing and infiltrating the intestinal epithelial layer (340, 341). The primary role of these cells is to maintain the integrity of the epithelium and modulate intestinal inflammation. As such, natural $\gamma\delta$ IELs can secrete antimicrobial peptides (AMPs) and transforming growth factor- β (TGF- β), an immunomodulatory cytokine (342, 343). Depletion of $\gamma\delta$ T cells is detrimental in animal models of IBD, suggesting that these cells are essential for controlling intestinal inflammation (344, 345). As opposed to “natural” IELs, many “induced” IELs are predominantly CD8+, cytotoxic, TCR $\alpha\beta$ T cells (335). These $\alpha\beta$ T cells also surveil the intestinal epithelium and can help clear many types of infection, including: lymphocytic choriomeningitis virus (LCMV), rotavirus, *Salmonella*, *Toxoplasma*, and *Giardia* (346–350). Interestingly, IELs are capable of secreting IFNs in response to TCR stimulation, suggesting that they may play a protective role in enteric viral infection (351).

Unlike T cells which are nearly ubiquitous throughout the gastrointestinal tract, B cells are largely restricted to lymphoid structures such as Peyer’s patches and isolated lymphoid follicles (352). In these locations B cells interact with antigen presenting cells, become activated, and undergo class switch recombination to express immunoglobulin A (IgA) (353, 354). This class switching can occur through canonical T cell-dependent mechanisms and T cell-independent mechanisms that depends on microbial-stimulated signaling factors like B-cell activating factor (BAFF) and a proliferation-inducing ligand (APRIL) (354). IgA is the dominant form of immunoglobulin present in the intestine and over 80% of plasma cells secrete IgA rather than IgG or IgM (355). After class-switching, plasmablasts hone to the lamina propria of the small intestine or colon they become long-lived plasma cells that secrete IgA as their primary effector function. This IgA is dimeric and linked with a J-chain domain that facilitates transcytosis of IgA across the intestinal

epithelial barrier by the polymeric immunoglobulin receptor (pIgR) (356). During transcytosis to the luminal space, part of the J-chain of IgA is cleaved resulting in free dimeric, secretory IgA (sIgA) which can neutralize pathogens and prevent commensal microbe penetration of the epithelium (357).

The last common type of lymphoid cell in the intestine are ILCs. There are three types of ILCs (ILC1, ILC2, and ILC3) that all derive from a common ILC precursor (358). In simplest terms these ILCs are analogous to CD4 T cell subtypes and utilize the same canonical transcription factors as Th1, Th2, and Th17 cells. ILC1s require T-bet like Th1 cells, ILC2s require GATA-3 like Th2 cells, and ILC3s are influenced by the transcription factor ROR γ t like Th17 cells (359–361). Similarly, ILC function also recapitulates features of their helper T cell cousins (362). Upon activation by Th1 cytokines ILC1s can secrete IFN- γ and TNF- α to potentiate responses against intracellular pathogens (363). Likewise, upon activation, ILC2s express Th2 effector cytokines like IL-4 and IL-10 which can play a role in anti-helminth and allergy-associated immune responses (364). Lastly, ILC3s produce a similar cytokine profile as Th17 cells and secrete IL-17 and IL-22 which can boost anti-fungal immunity and condition the intestinal epithelium in response to intestinal microbiota (365, 366).

Myeloid cells of the intestine are largely comprised of macrophages and dendritic cells (DCs). Enteric macrophages are seeded by monocytes that are recruited to the intestine through the chemokine receptor CCR2 (367). On the other hand, enteric DCs are derived from precursor DCs that express the classical DC transcription factor, *Zbtb46* (368). Characterization of these cell types in the intestine is complicated because some intestinal macrophages express surface markers canonically associated with DCs (332). In particular, co-expression of CD11c and major histocompatibility complex II (MHCII) is a

hallmark of DCs; however, in the intestine nearly all mononuclear phagocytic cells are positive for CD11c (369, 370). Furthermore, intestinal macrophages can also express high levels of MHCII, preventing the use of CD11c+/MHCII+ phenotyping for discrimination of enteric macrophages and DCs (371). Even relying on labeling or depleting cells that utilize Zbtb46 may not fully differentiate enteric macrophages and DCs, since depletion of CCR2+ cells can reduce Zbtb46-expressing cells in the intestine (372). One suggested mechanism to differentiate between enteric macrophages and DCs is by staining for CD64, the immunoglobulin binding protein FcγRI, in combination with a pan myeloid staining panel (373).

At homeostasis, enteric macrophages help maintain the intestinal epithelial barrier and non-inflammatory states. Consistent with their phagocytic ability, enteric macrophages sample apoptotic cells and phagocytose stray apoptotic material (374). Despite the proximity of enteric macrophages to the intestinal epithelium and avid phagocytic ability, the majority of these cells poorly initiate inflammatory responses (375). In fact, most resident macrophages that robustly express the chemokine receptor CX3CR1 (CX3CR1^{hi}) constitutively produce IL-10 (376). A minority of macrophages in the intestine express more modest levels of CX3CR1 (CX3CR1^{int}), expand dramatically during inflammatory conditions, and express pro-inflammatory cytokines like TNF-α (372). Similar to enteric macrophages, intestinal DCs play a large role reinforcing immune tolerance. In particular, a subset of DCs that are CD103+ induce regulatory T cells differentiation by secreting retinoic acid and TGF-β (377, 378). However, unlike CX3CR1^{hi} macrophages, intestinal DCs are able to flip from a tolerogenic to inflammatory state upon TLR stimuli. Following stimulation these intestinal DCs produce IL-23 to stimulate IFN-γ production by T cells and IL-6 to activate a general inflammatory state (379, 380).

Interactions Between the Immune System and Intestinal Bacterial Microbiota

The presence of the intestinal bacterial microbiota influences essentially every cell in the enteric niche. Immune responses to bacterial microbiota are present within IECs, macrophages and DCs, adaptive immune cells, and others (381–386). As the predominant barrier cell-type, IEC interactions with the intestinal microbiota primarily involve direct sensing of microbial products and subsequent responses. The most well-defined mechanism of microbiota-sensing by IECs occurs through TLR signaling (387). In mice, IECs express TLR2, TLR4, and TLR5 in the small intestine and colon (388). All three of these TLRs are expressed in proximal colonocytes, but in the small intestine TLR4 is primarily localized to the distal regions of villi and TLR5 is largely restricted to paneth cells in the crypts. Signaling through these TLRs is sufficient to drive multiple processes in IECs ranging from proliferation, to antimicrobial peptide secretion, to mucus production, and upregulation of IgA transcytosis proteins. Coincident with the observation that intestinal microbiota are required for intestinal homeostasis, it was shown that deletion of *Myd88* reduce IEC proliferation (273), suggesting that signaling by MAMPs promotes the proliferative potential of IECs. Later, it was shown that TLR1/TLR2 expression by IECs is dependent on the bacterial microbiota by comparing germ-free or ABX-treated mice with conventionally raised mice (389). Furthermore, deletion of *Tlr2* reduced phosphorylation of essential signaling mediators required for IEC proliferation, ERK1/2 and AKT (390). As such, *Tlr2* deletion also phenocopied the decreased proliferation of IECs observed in both *Myd88* deletion and absence of bacterial microbiota.

The effects of this TLR signaling are not restricted to IEC-intrinsic responses, as stimulation of IECs also leads to alterations in the secretion of effector molecules. One

example is the antimicrobial peptides secreted from the intestinal crypts by paneth cells. Previously it was shown that treatment with antibiotics decreases the expression of antimicrobial peptides (AMPs) by paneth cells, including peptidoglycan-binding proteins RegIII γ and RegIII β (391–393). Furthermore, sensing of bacterial microbiota by PRRs upstream of Myd88 is required for induction of paneth AMPs, as deletion of *Myd88* reduces expression of RegIII γ and RegIII β (392, 394). Secretion of these AMPs leads to sequestration of intestinal microbiota to the lumen and reductions in mucus-associated bacteria (32). Additionally some of these AMPs such as RegIII γ are protective during infection with bacterial pathogens like *Listeria monocytogenes* (395). Sensing of microbiota via TLRs is present in goblet cells as well. IEC-specific deletion of *Myd88* is associated with decreases in secretion of mucin-2 by goblet cells (394). Furthermore, specific “sentinel” populations of goblet cells in the colon respond to TLR2, TLR4, and TLR5 stimuli with increased secretion of mucin-2 (396). Lastly, IEC-specific deletion of *Myd88* decreases pIgR and decreases the transcytosis of IgA across the intestinal epithelial barrier. These secretory and transcytosis functions of IECs in response to sensing of bacterial microbiota decrease incursions by bacterial microbiota and maintain intestinal homeostasis. Interestingly, the effects of the intestinal microbiota on IECs appear to be partially-regulated by circadian rhythms (397). In this case the expression of epithelial TLRs correlated with circadian rhythms controlled by ROR α , a protein directly upstream of the master circadian genes *Bmal1* and *Clock*. This circadian regulation also extended to AMP genes like *Reg3g*, the transcytosis gene *Pigr*, and can drive circadian variations in resistance to *Salmonella* infection (398).

Intestinal macrophages and DCs play an essential role in conditioning the enteric immune system that was briefly described in the previous section. However, consistent with their role as phagocytic cells and antigen processing cells, a major role of

macrophages and DCs is also the acquisition of commensal, dietary, and pathogenic antigen and subsequent priming of immune responses. Acquisition of luminal antigen by macrophages and dendritic cells occurs in either Peyer's patches (PPs) or in discrete locations scattered under the intestinal epithelium. In the PPs, specialized epithelial cells known as M cells transcytose luminal antigen and deliver it directly to DCs and B cells (399, 400). However, in non-lymphoid intestinal tissue, early literature suggested that enteric CX3CR1⁺ macrophages actively survey the lumen of the small intestine by extending transepithelial dendrites (TEDs) to sample luminal antigen (401, 402). These initial observations incorrectly attributed this sampling to intestinal DCs. Since that time these CX3CR1⁺ cells have been classified as macrophages and essentially all TEDs are considered artifacts of tissue preservation, rather than homeostatic events. In fact, with the introduction of live-animal imaging, TEDs in intestinal villi decreased from over one per villus observed by *ex vivo* tissue imaging experiments to one in every few hundred villi observed within living tissue (36). Another way that macrophages and dendritic cells acquire luminal antigen is through goblet cell associated passages (GAPs). These GAPs are passages formed in goblet cells following stimulation by acetylcholine (403, 404). Although mucin secretion by goblet cells is also regulated by acetylcholine sensing, GAP formation is not required for mucus secretion and not every goblet cell forms GAPs. Intriguingly, these GAPs form in a Myd88-dependent manner as conditional deletion of *Myd88* in *Atoh1* expressing secretory cells ablates GAP formation. Following the formation of a GAP, a mixture of nearby CD103⁺ and CD103⁻ myeloid cells acquire antigens passed from the lumen (36, 38). Following their acquisition of antigen CD103⁺ DCs traffic to MLN to present antigen to adaptive immune cells (405). However enteric macrophages exhibit different activities delineated by their expression of CX3CR1. CX3CR1^{hi} macrophages upregulate CCR7 and traffic to MLN like dendritic cells, but CX3CR1^{int} macrophages

remain in the lamina propria to form tertiary lymphoid structures (406). The formation of these lymphoid structures plays a large role in the maturation of IgA responses in the intestine. It is in these locations that myeloid secretion of BAFF and APRIL enhances T cell independent class switch recombination in local populations of B cells (354).

Direct interactions between conventional T cells and the intestinal bacterial microbiota have not been well characterized; however, $\gamma\delta$ IELs express RegIII γ in response to detection of intestinal microbiota. The vast majority of $\gamma\delta$ IELs express RegIII γ in conventional mice, but there is no expression in germ-free and ABX-treated mice (343). Interestingly, these IELs require *Myd88* expression by IECs to express RegIII γ , suggesting that interactions with microbiota may be mediated by IECs. One set of T cells that is suggested to respond to bacterial microbiota are mucosal-associated invariant T (MAIT) cells. These T cells have an invariant T cell receptor that recognizes ligands displayed by MHC Class I (MHC I)-related protein 1 (MR1) (407, 408). MR1 is expressed in the majority of tissues and is appreciated to bind to several bacterial-derived metabolites (409). These MR1 ligands include a metabolite of vitamin B9, 6-formyl pterin, and some intermediates from the vitamin B2 biosynthesis pathway (410, 411). As such, these cells require the presence of bacterial microbiota for development in the host as well as the presence of abundant metabolite ligands (412). These MAIT cells are much more abundant in humans than laboratory mice (413), suggesting that dense seeding of MAIT cells during development requires additional interactions with bacterial microbiota that are not currently present in laboratory mice.

Impacts of Bacterial Microbiota on Viral Infection

The intestinal bacterial microbiota exhibit complex interactions with viral pathogens, ranging from upregulating or antagonizing antiviral IFN signaling, to more

general immunomodulatory effects, and even direct interactions with virions (414, 415). One mechanism by which the bacterial microbiota interact with enteric viruses is through bile acid intermediates. Secondary bile acids are metabolic products of the intestinal microbiota and can have diverse effects on host immunity, including direct interactions with IFN signaling (314). *In vitro* studies on hepatitis C virus and a porcine enteric calicivirus suggest that bile acids may antagonize IFN signaling possibly by antagonizing phosphorylation of STAT1 (416, 417). However, it remains unclear how well these *in vitro* models recapitulate *in vivo* biology since sensing of bile acids also increases resistance to rotavirus and murine norovirus (MNV) in mouse models (418, 419). In particular, both the host-derived bile acid CDCA and the microbe-derived bile acid DCA appeared to prime induction of IFN- λ (418). However, sufficient engagement of the bile acid receptor FXR ablated the ability of CDCA and DCA to prime IFN- λ induction, indicating that more research is required into the distinct effects of bile acid signaling on the intestinal IFN response *in vivo*.

There is a growing body of work showing that the bacterial microbiota induces systemic IFN responses. In fact, there is stronger evidence that bile acids impact IFN signaling in systemic tissues than they do in the intestine. For example, deletion of FXR in mice decreases hepatic IFN induction in response to LCMV (420). Most convincingly, depletion of microbiota was shown to reduce induction of IFN- α s in splenic pDCs which led to increased susceptibility to chikungunya virus injected into the footpad of mice (421). These effects in pDCs were rescued upon administration of the bile acid DCA in drinking water, providing a link between enteric secondary bile acids and systemic IFN signaling. Similarly, germ-free mice have reduced IFN- β expression in splenic pDCs at homeostasis (422), though the mechanism of bile acid responses was not assessed. These systemic IFN effects are not strictly mediated by bile acids as the presence of microbiota was

correlated with an IFNAR-dependent homeostatic ISG signature that was protective against influenza infection (423, 424). Furthermore, the microbial metabolite, desaminotyrosine, enhances IFNAR signaling in pulmonary macrophages leading to protective amplification of the IFN response (424). Commensal microbiota also have been shown to induce IFN- α/β responses in non-enteric macrophages and DCs that provide protection against LCMV, vesicular stomatitis virus, and encephalomyocarditis virus (425–427).

The bacterial microbiota also provide protection against viral infection through IFN-independent mechanisms. In the case of rotavirus, antibiotic-treatment dramatically increased susceptibility of mice to murine rotavirus infection and correlated with reduced interleukin-22 (IL-22) expression; however, exogenous administration of IL-22 restored protection. Although the mechanism of IL-22-mediated protection against murine rotavirus was not determined, it was found to be independent of IFN-signaling since IL-22 provided protection in *Stat1*^{-/-} mice (428). This study corroborated a previous observation that an IL-22 and IL-18 can mediate IFN-independent protection against murine rotavirus and provided evidence that the intestinal microbiota may reinforce this pathway at homeostasis (429). Additionally, colonization of mice with SFB has been shown to prevent and cure murine rotavirus infection in mice independent of both IL-22 and IFN signaling (430). These IFN-independent mechanisms also extend to alterations in adaptive immune cells. For example, treatment with ABX was found to reduce mouse mammary tumor virus (MMTV) infection (431). This reduction was due to loss of IL-10 signaling which is required for MMTV persistence in the mouse host (432). Similarly, ABX-treatment of mice increased the severity of infection with three flaviviruses: West Nile virus, Dengue virus, and Zika virus (433). This increased susceptibility to flavivirus infection was found to be

due to inefficient priming of T cell responses, consistent with the ability of the intestinal microbiota to induce global alterations to adaptive immunity.

The presence or absence of the intestinal bacterial microbiota can have dramatic effects on the enteric immune system, as covered above. However, in some cases intestinal bacterial microbiota physically interact with enteric viruses to impact viral replication, independent of immune mechanisms. For this reason, care must be taken when attributing the role of the bacterial microbiota in altering viral pathogenesis to immunomodulatory mechanisms. For example, treatment with a cocktail of ABX was correlated with decreased infection by poliovirus and reovirus in mice (434). However, in the case of poliovirus, bacterial-derived LPS was determined to stabilize poliovirus virions and binding to the poliovirus receptor (435). Similarly, bacterial components such as LPS and peptidoglycan can increase the thermostability of reovirus virions and, subsequently, increase enteric viral infection independent of altering binding or internalization kinetics (436). These stabilizing interactions are not restricted to poliovirus and reovirus, as additional viruses such as coxsackievirus B3, Aichi virus, and mengovirus also exhibit increased stability when associated with LPS (437, 438).

The bacterial microbiota can also mediate non-immune alterations in the host that can impact enteric viral infection. Norovirus infections are a keen example of these effects. As mentioned previously, secondary bile acids are metabolic products of the intestinal microbiota with wide-ranging effects on the host immune system (314), including interactions with IFN- λ signaling (418). However, both host-derived and microbiota-derived bile acids were also shown to bind to the norovirus receptor, CD300lf (439). These bile acids are consistent with the report of a heat-resistant co-factor that enhanced norovirus infection (440). Similar bile-acid dependent enhancements have also been

modeled with human norovirus infections in organoids (441, 442). Separate from bile acid effects, it was shown that ABX-treatment reduced MNV infection in an *Ifnl1*-dependent manner (443). However, reduced MNV infection with ABX-treatment was later determined to be partially due to ABX-dependent decreases in the presence of tuft cells that are the obligate epithelial host of MNV (444). Furthermore, direct antibiotic-dependent effects have even been observed *in vitro*. For example, neomycin can increase the size of plaque formation when titering CVB3 (445). These effects were attributed to electrostatic interactions that arise upon addition of positively-charged antibiotics to culture media, highlighting that care must be taken when assessing the role of the intestinal microbiota in viral infections, especially in context of antibiotic-treatment.

The Impact of Rewilding on the Laboratory Mouse Model

Recent studies described above have shed light on the importance of the intestinal bacterial microbiota in conditioning the immune system. However, one major advance in the field is the use of “wild” intestinal microbiota to study the immune system (446). In 2016, the Masopust and Jameson groups assessed the T cell responses of feral, pet store, and cleanly-housed laboratory mice to determine the impacts of “wild” microbes on adaptive immune status (447). They found that laboratory mice have highly naïve T cell immunity compared to mice from stores or the wild. Furthermore, they found that co-housing laboratory mice with these wild mice increased the number of memory T cells and concentrations of antibody in the 78% of laboratory mice that survived co-housing. This microbial challenge appeared to dramatically mature the immune status of these mice such that they more closely resembled the transcriptional profile of an adult human rather than newborn humans, like naïve laboratory mice. Following this study, the Rehermann group performed controlled transplantation of wild microbiota to selectively study the role

of microbiota in defining immune status (448). To do this they transplanted the microbiota from wild-caught mice into pregnant laboratory mice and raised successive generations of laboratory mice with a true “wild-type” microbiota (wildR). The microbiota of these wildR mice had dramatic expansion of *Proteobacteria* and contraction of *Firmicutes* compared to control mice and very few major microbial discrepancies from wild-caught mice. Intriguingly, wildR mice exhibited enhanced protection against influenza infection and inflammatory tumorigenesis challenge compared to their lab controls. These differences correlated with decreased inflammatory cytokine expression, suggesting that this wild microbiota more efficiently balances inflammatory responses and pathogen challenge. The Rehermann group continued their studies and profiled immune cells of systemic and barrier tissues to determine the cellular differences between laboratory and wildR mice (449). Perhaps unsurprisingly, they found the most robust and consistent cellular alterations in the intestine, where wildR mice had expansion of dendritic cells and many T cell types compared to controls. These stable alterations suggest that wild-microbiota mice may be especially robust models for enteric infection. Accordingly, wild-microbiota mice exhibited severe susceptibility to gastrointestinal helminth infection compared to laboratory controls (450), largely due to reductions of Th2 responses in wild-microbiota mice. Continued research in co-housed laboratory and pet store mice has revealed novel *Coronaviridae*, *Astroviridae*, *Picornaviridae*, and *Narnaviridae* enteric pathogens (451). These findings confirm that wild-microbiota models are broadly applicable to many classes of enteric pathogens and will continue to expand into a broadly-utilized model in the field.

CHAPTER 2: Selective Interferon Responses of Intestinal Epithelial Cells Minimize Tumor Necrosis Factor Alpha Cytotoxicity

Authors, Affiliations, Contributions, Acknowledgements, and Citation

Authors

Jacob A. Van Winkle¹, David A. Constant¹, Lena Li¹, and Timothy J Nice¹

Affiliations

¹ Department of Molecular Microbiology and Immunology, Oregon Health & Science University, Portland, OR, USA

Correspondence to: nice@ohsu.edu (T.J.N.)

Contributions

Conceptualization, T.J.N.; Methodology, J.A.V.W., D.A.C., L.L., and T.J.N.; Investigation, J.A.V.W., D.A.C., L.L., and T.J.N.; Writing – Original Draft, T.J.N.; Writing – Review & Editing, J.A.V.W. and D.A.C.; Visualization, T.J.N.; Supervision, T.J.N.; Project Administration, L.L. and T.J.N.; Funding Acquisition, T.J.N.

J.A.V.W. directly contributed to figures 2.1, 2.2, 2.3, and 2.6. J.A.V.W. contributed the source data analyzed in figures 2.4, 2.5, and 2.7.

Acknowledgements

We thank the following OHSU core facilities for technical support: the Integrated Genomics Laboratory, the Advanced Light Microscopy Core, the Flow Cytometry Core, and the Histopathology Core.

T.J.N. was supported by NIH grant R01-AI130055 and by a faculty development award from the Sunlin and Priscilla Chou Foundation. J.A.V.W. was supported by NIH grants T32-GM071338 and T32-AI007472. D.A.C. was supported by NIH grant T32AI007472.

The funders had no role in study design, data collection and interpretation, or the decision to submit the work for publication.

Citation

Van Winkle JA, Constant DA, Li L, and Nice TJ. Selective interferon responses of intestinal epithelial cells minimize TNF α cytotoxicity. *Journal of Virology* 2020; 94(21): e00603-20. PMID: 32847859

Introduction

Interferon (IFN) family cytokines provide antiviral defense through stimulation of a broad transcriptional response that includes direct-acting antiviral genes (99, 100). Members of the IFN family are divided into three types based on receptor usage: multiple type I IFN genes (many IFN- α s, IFN- β , others; hereafter IFN- α/β), a single type II IFN gene (IFN- γ), and multiple type III IFN genes (up to four IFN- λ s) (102, 103). IFN- α/β and IFN- λ are produced upon detection of viral nucleic acids and are primary components of the early response to infection. The heterodimeric receptor for IFN- α/β (IFNAR) is expressed by most cell types, but the distinct heterodimeric receptor for IFN- λ (IFNLR) is preferentially expressed by neutrophils and epithelial cells (103, 191, 193). Prior studies from us and others in mouse models of gastrointestinal virus infection have used receptor-deficient animals to show that IFN- λ is particularly important for protection of intestinal epithelial cells (IECs) (195, 199, 200, 452). Additional mouse studies suggest that IECs require IFN- λ for antiviral protection because they are less responsive to IFN- α/β in comparison to other epithelial cell types (194, 195, 197), which may result from downregulated IFNAR expression *in vivo* (194, 195). However, the physiological benefit of this preferential IEC responsiveness to IFN- λ has remained unclear.

Activation of IFNAR or IFNLR results in phosphorylation of signal transducer and activator of transcription (STAT) transcription factors and upregulation of IFN-stimulated genes (ISGs). More specifically, STAT1 and STAT2 are phosphorylated, bind interferon response factor 9 (IRF9), and form a hetero-trimeric complex called interferon stimulated gene factor 3 (ISGF-3). ISGF-3 translocates to the nucleus and binds interferon-stimulated response element (ISRE) motifs in ISG promoters (99, 106, 107). Additionally, STAT1 homodimers, other STAT family members, and non-canonical factors also play a role in the transcription of some ISGs (126, 453). Prior comparisons of ISG induction by IFN- λ or

IFN- α/β in cultured hepatocytes revealed largely overlapping responses consisting of canonical antiviral ISGs (113–115, 140, 141, 144). However, other in-depth studies of neutrophils and hepatocytes have indicated that IFN- α/β is generally more potent than IFN- λ and results in greater chemokine and cytokine production (109, 145–148). Additionally, studies of IECs cultured *in vitro* as 3D organoids have found that they are highly responsive to IFN- α/β , unlike IECs *in vivo* (143, 205–207, 454, 455). Thus, the physiological basis of preferential IEC responsiveness to IFN- λ *in vivo* remains unclear.

Herein, we directly and quantitatively compare the IEC response to IFN- β and IFN- λ *in vivo* and *in vitro*. We find that the *in vivo* IEC response to IFN- β is minimal and does not inhibit replication of IEC-tropic rotavirus. In contrast, *in vitro* IFN- β treatment of IEC organoids elicits hundreds of ISGs, including pro-apoptotic genes, and potently blocks rotavirus infection. *In vitro* and *in vivo* IECs are equally responsive to IFN- λ and upregulate known antiviral genes but not pro-apoptotic genes. Consistent with differing pro-apoptotic gene expression, we show that cytotoxicity triggered by tumor necrosis factor alpha (TNF α) is increased in IEC organoids pre-treated with IFN- β relative to IFN- λ . Finally, bioinformatic scoring of promoter motifs indicates that IFN- β -specific ISGs, including pro-apoptotic genes, have low-scoring, weak ISREs. Antiviral ISGs stimulated in common by IFN- λ and IFN- β have high-scoring, strong ISREs. Together, these findings suggest that preferential responsiveness of IECs to IFN- λ *in vivo* ensures that antiviral ISGs are minimally accompanied by pro-apoptotic genes to promote epithelial homeostasis during clearance of enteric infection.

Results

IECs in the neonatal intestine are minimally response to IFN- β

To extend our understanding of the transcriptional response to IFN in the intestine, we performed ISG *in situ* hybridization on intestinal tissues following IFN treatment *in vivo*. We injected PBS, IFN- β , or IFN- λ 3 into seven-day-old neonatal mice, which have low baseline ISG expression, and detected transcripts for a canonical ISG (*Usp18*) four hours later. IFN- λ stimulated a robust increase in expression within the epithelial layer with no visible stimulation of cells in the underlying lamina propria tissue (**Figure 2.1A**). In contrast, IFN- β injection resulted in a modest increase of *Usp18* in dispersed cells of the epithelium and lamina propria (**Figure 2.1A**).

To more quantitatively compare transcript abundance in IECs and intra-epithelial hematopoietic cells, we FACS sorted EpCAM-positive/CD45-negative epithelial (EpCAM+) and CD45-positive/EpCAM-negative hematopoietic (CD45+) cells from dissociated epithelium. Consistent with *in situ* hybridization results, qPCR analysis showed that *Usp18* was stimulated more than 20-fold in EpCAM+ cells following IFN- λ injection but less than two-fold following IFN- β injection (**Figure 2.1B**). Conversely, *Usp18* was stimulated less than two-fold in intra-epithelial CD45+ cells following IFN- λ injection but stimulated five-fold following IFN- β injection (**Figure 2.1B**).

To determine whether *Usp18* transcripts were indicative of a broader ISG program that conferred antiviral protection upon IECs, we challenged neonatal mice treated as above with IEC-tropic murine rotavirus and quantitated viral genomes in the intestine 20 hours later. IFN- λ injection resulted in three- to ten-fold lower viral genomes compared to PBS injection, but IFN- β injection provided no significant protection (**Figure 2.1C**). These data align with previous reports of the preferential IEC response to IFN- λ in adult mice,

and suggest that hypo-responsiveness of IECs to IFN- α/β *in vivo* arises in early neonatal life.

To determine if IFN receptor gene expression correlated with responsiveness to cognate ligands, we performed qPCR for IFN receptor gene components in CD45+ and EpCAM+ cells sorted from neonatal intestine (**Figure 2.1B**). Transcripts encoding the IFNAR heterodimer (*Ifnar1* and *Ifnar2*) were relatively abundant in all cells, but were two-fold lower in EpCAM+ IECs compared to IFN- β -responsive CD45+ cells (**Figure 2.1D**). Transcripts for the specific subunit of the IFNLR heterodimer (*Ifnlr1*) were significantly more abundant in IFN- λ -responsive IECs compared to CD45+ intra-epithelial cells, but were less abundant overall than IFNAR gene transcripts. Transcript abundance of the other IFNLR1 subunit (*Il10rb*) was not significantly different between these cell types.

IFNAR abundance at the cell surface is regulated by both transcriptional and post-transcriptional mechanisms (456, 457). Therefore, we compared surface expression of IFNAR1 and IFNAR2 subunits on CD45+ and EpCAM+ intestinal cells by flow cytometry. Staining for IFNAR1 was 4-fold above background for CD45+ cells and less than 2-fold above background for EpCAM+ cells; staining for IFNAR2 was 2-fold above background for CD45+ cells and 4-fold above background for EpCAM+ cells (**Figure 2.1E**). Thus, IFNAR1/IFNAR2 ratio is lower on IECs relative to CD45+ cells. These data suggest that relatively low expression of IFNAR1 on IECs of the neonatal intestine underlies IEC hypo-responsiveness to IFN- β *in vivo*, consistent with prior studies of IFNAR1 staining in adult mice (194).

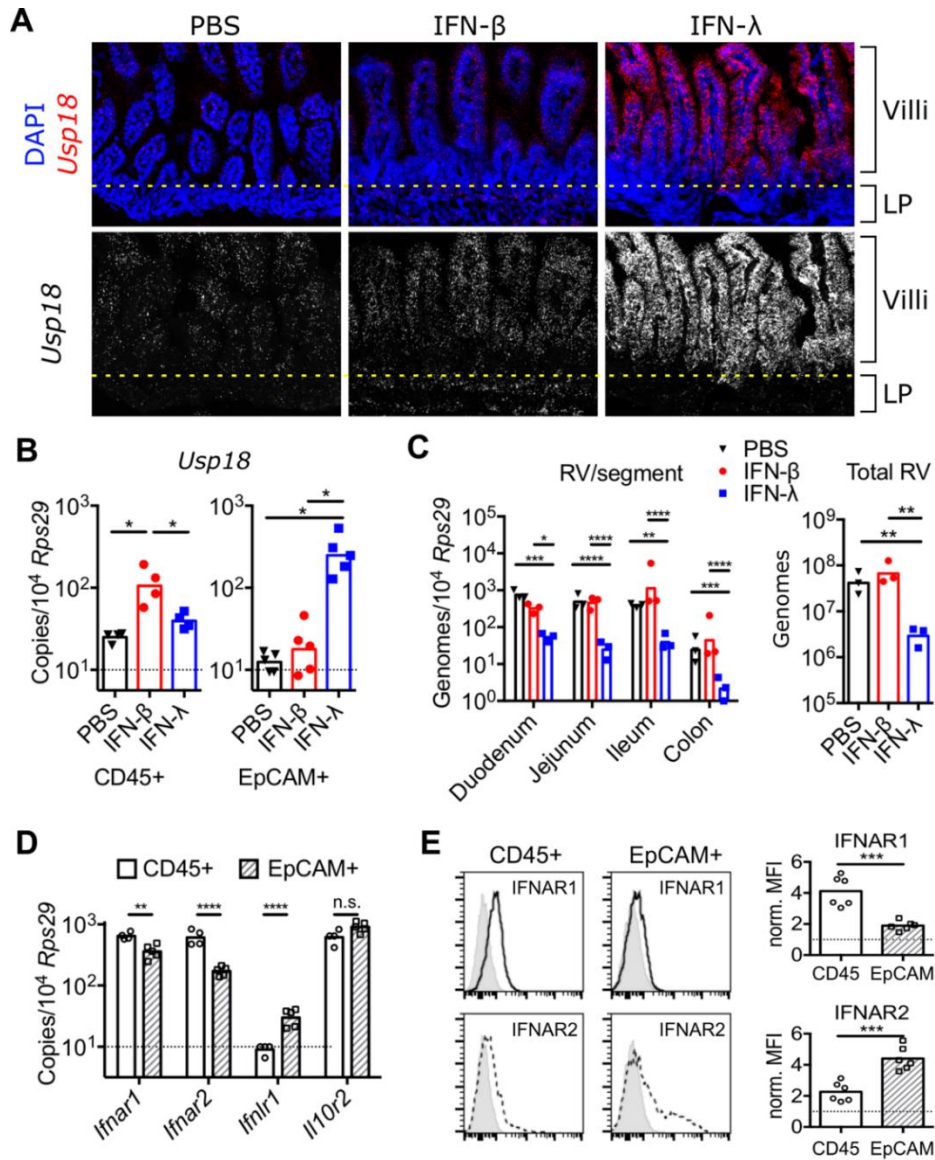


Figure 2.1. IECs in the neonatal intestine are minimally responsive to IFN- β . Neonatal mice were injected with either IFN- β or IFN- λ 3 for four hours. **A.** Small intestinal tissue was isolated and stained with DAPI and *Usp18* antisense probes. Dashed line indicates the approximate boundary between villi and lamina propria. **B.** *Usp18* abundance in sorted IECs (EpCAM-positive/CD45-negative) and hematopoietic cells (CD45-positive/EpCAM-negative) was determined by qPCR. **C.** mice were inoculated with rotavirus and viral genomes were quantitated in intestines 20 hours later. **D.** Comparison of IFN receptor gene abundance by qPCR in sorted EpCAM+ IECs and CD45+ hematopoietic cells. **E.** Flow cytometry staining of IFNAR1 and IFNAR2 on EpCAM+ IECs and CD45+ hematopoietic cells. Grey histograms are control stains (no IFNAR antibody), and bar graphs show geometric mean-fluorescence intensity (MFI) of IFNAR fluorescence normalized to control for each replicate. Data are combined from at least two experiments with a total of three to five mice per experimental condition; data points indicate individual animals with bars indicating the mean. Significance determined by one-way or two-way ANOVA (**B-D**) or t-test (**E**); *, $p < 0.05$; **, $p < 0.01$; ***, $p < 0.001$, ****, $p < 0.0001$.

IEC organoids are dually response to IFN- β and IFN- λ

To determine whether IFN- α/β hypo-responsiveness was intrinsic to IECs, we generated *in vitro* IEC organoids from isolated epithelial stem cells (**Figure 2.2A**). We stimulated these IEC organoids with 0, 0.1, 1, 10, or 100 ng/mL of mouse IFN- β or IFN- λ 2 for 2, 4, 8, or 16 hours and quantitated the abundance of three canonical ISGs (*Isg15*, *Usp18*, and *Cxcl10*). All three ISGs were increased by IFN- β and IFN- λ 2 treatments with a maximal upregulation between 100 and 1000-fold (**Figure 2.2B**). The expression kinetics were similar for all three ISGs following IFN- λ stimulation, with maximal upregulation four to eight hours post-treatment and sustained expression at 16 hours. Similar expression kinetics were observed for *Isg15* and *Usp18* following IFN- β stimulation. However, at the highest doses of IFN- β , *Cxcl10* reached a peak of induction at four hours and decreased thereafter (**Figure 2.2B**). Comparison of the dose-response for IFN- β or IFN- λ at four hours post-treatment indicated that early ISG upregulation was between two- and ten-fold greater for IFN- β compared to IFN- λ (**Figure 2.2C**). These data indicate that IEC organoids upregulate canonical ISGs in response to IFN- β and IFN- λ , with minimal differences in expression kinetics, but higher maximum response to IFN- β . Therefore, IFN- α/β hypo-responsiveness observed *in vivo* is not an intrinsic property of IECs

To confirm that the above ISG expression was indicative of the overall antiviral program stimulated by IFN treatments, we challenged IEC organoids with murine rotavirus and quantitated viral genomes 0, 8, and 16 hours later. IFN- λ treatment resulted in modest reductions in viral genomes relative to PBS treatment, but IFN- β treatment resulted in three- to ten-fold reduction in viral genomes (**Figure 2.2D**). Therefore, IFN- β stimulates a stronger antiviral response than IFN- λ in cultured IEC organoids. These data indicate that the antiviral ISG response of IECs *in vivo* is regulated by factors not recapitulated in organoid culture.

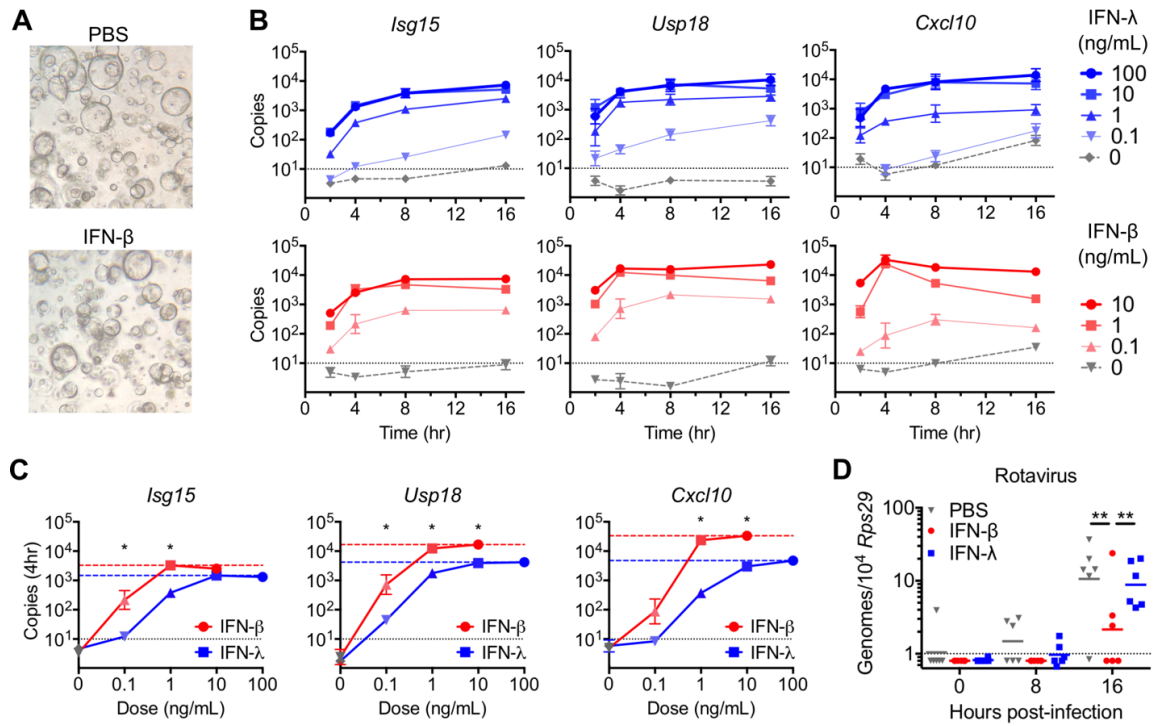


Figure 2.2. IEC organoids are dually responsive to IFN-β and IFN-λ. **A.** Representative images of IEC organoids. **B.** IEC organoids were treated with the indicated concentrations of recombinant IFN-β or IFN-λ for the indicated times and RNA was isolated for quantitation of *Isg15*, *Usp18*, and *Cxcl10* transcripts by qPCR. The dotted line indicates the limit of detection. **C.** Transcript abundance of the indicated genes four-hours after IFN treatment across the range of IFN doses tested. Dashed lines indicate maximal responses for IFN-β (red) or IFN-λ (blue). **D.** IEC organoids pre-treated with PBS, IFN-β or IFN-λ for eight hours were infected with rotavirus. Viral genomes were quantified at the indicated time post-infection. Data is from two (**B-C**) or three (**D**) experiments with duplicate treatment/infection wells; error bars show SEM. Statistical significance determined by t-test (**C**) or one-way ANOVA (**D**); *, $p < 0.05$; **, $p < 0.01$.

Global ISG expression in response to IFN- β is suppressed *in vivo*

To more comprehensively compare the *in vivo* and *in vitro* IEC response to IFN, we performed RNA sequencing on sorted EpCAM+ cells from neonatal mice treated with PBS, IFN- β , or IFN- λ 3 and compared to RNAseq of IEC organoids treated with PBS, IFN- β , or IFN- λ 2 for four hours. Normalized read counts for *Usp18* were increased between 5- and 1000-fold by IFN treatment, with a greater increase in IEC organoids by IFN- β treatment relative to IFN- λ treatment and a greater increase in neonatal IECs by IFN- λ treatment relative to IFN- β treatment (**Figure 2.3A**). These differences are reflective of qPCR results from **figures 2.1-2.2**, validating the RNAseq dataset. PCA analysis indicated that the primary component differentiating these samples (PC1, 95% of variance) was their organoid or neonate origin and included differential expression of metabolism and cell cycle genes (**Figure 2.3B**). The secondary PCA component (PC2, 2% variance) separated IFN treatment groups from matched PBS controls (**Figure 2.3B**).

We identified differentially expressed genes among IFN treatment groups relative to their corresponding PBS controls using liberal inclusion criteria (fold-change > 1.5, adjusted p-value < 0.1). Few genes were downregulated by IFN treatments, consistent with the known transcriptional activation downstream of IFN receptors. Identification of ISGs in neonatal IECs revealed 210 IFN- λ -stimulated genes but only 64 IFN- β -stimulated genes (**Figure 2.3C**). Furthermore, all IFN- β -stimulated genes but one (63/64) were present among the 210 IFN- λ -stimulated genes (**Figure 2.3C**). Therefore, the global early response of neonatal IECs to IFN- λ is substantially larger than to IFN- β .

IEC organoids had a comparable number of IFN- λ -stimulated genes (190) as neonatal IECs (210), with the majority of genes (134) present in both (**Figure 2.3D-E**). However, in striking contrast to neonatal IECs, IEC organoids had a greater number (527)

of IFN- β -stimulated genes (**Figure 2.3E**). Among IEC organoid treatment groups, there were zero genes unique to IFN- λ , with all 190 IFN- λ -stimulated genes present among the 527 IFN- β -stimulated genes (**Figure 2.3E**). Therefore, the early responses of IEC organoids to IFN- β and IFN- λ are highly overlapping with IFN- λ -stimulated genes comprising a subset of IFN- β -stimulated genes.

To more comprehensively analyze the relationship between IFN responses of neonate and organoid IECs, we normalized the log₂ fold-change of all 527 organoid ISGs to matching PBS controls and plotted these changes on a heatmap with hierarchical clustering (**Figure 2.3F**). IFN- λ -stimulated neonate and organoid IECs clustered closer to each other than to other treatment groups, supporting the conclusion that IFN- λ responses are similar between neonate and organoid. In contrast, IFN- β -stimulated neonatal IECs clustered closer to PBS controls than to other IFN treatment groups (**Figure 2.3F**). These comparisons indicate that the *in vivo* hypo-responsiveness of IECs to IFN- α/β applies globally to all ISGs, whereas responsiveness to IFN- λ is a relatively stable IEC-intrinsic property.

To determine if expression of IFNAR genes was correlated with responsiveness of IECs to IFN- β , we compared the abundance of receptor genes in neonatal and organoid IECs. *Ifnar1*, *Ifnar2*, *Ifnlr1*, and *Il10rb* were not differentially expressed between these IEC types (**Figure 2.3G**). However, additional comparisons of 30 previously-identified IFNAR regulatory genes curated from the literature (456–458) indicated that 11/30 of these genes were significantly more abundant in neonatal IECs relative to organoid IECs, but only 1/30 was modestly more abundant in organoid IECs (**Figure 2.3H**). The increased abundance of 11/30 known IFNAR negative regulatory genes with minimal differences in IFNAR receptor genes suggested the potential for post-transcriptional suppression of IFNAR in

neonatal IECs. Indeed, we found that surface staining of IFNAR1 and IFNAR2 were significantly increased on organoid IECs relative to neonatal IECs (**Figure 2.3I**). Together, these data are consistent with a post-transcriptional mechanism of IEC hypo-responsiveness to IFN- β *in vivo*.

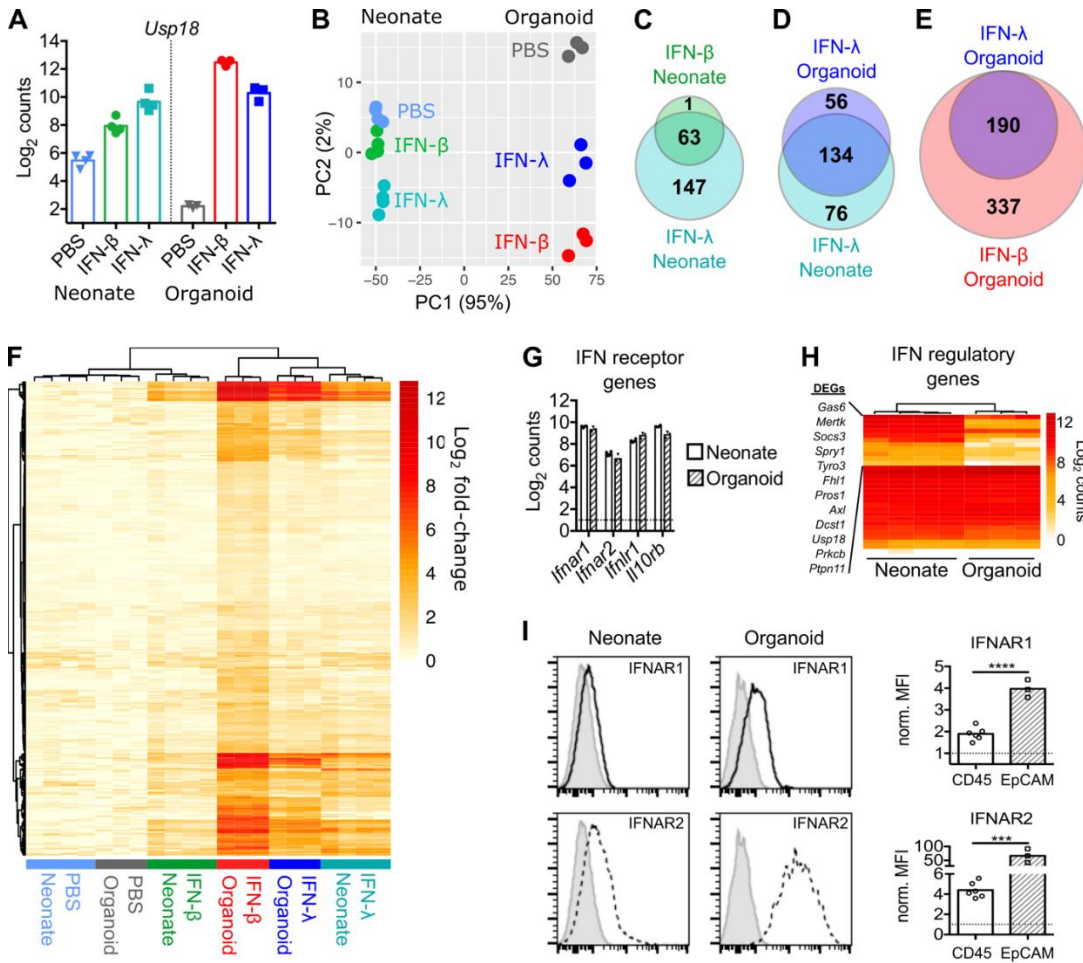


Figure 2.3. Global ISG expression in response to IFN- β is suppressed *in vivo*. IEC organoids or neonatal mice were treated for four hours with PBS or IFN as in **figures 2.1-2.2** and isolated IECs were analyzed by RNAseq. **A.** Normalized read counts for *Usp18*. **B.** PCA analysis of the top 500 differentially expressed genes. **C-E.** Venn diagrams showing the overlap in genes stimulated by the indicated IFN treatment relative to their matched PBS treated controls. **F.** Heatmap comparing log2 fold-change of 527 ISGs among organoid and neonate IFN treatment groups relative to matched PBS controls. **G-H.** Log2 normalized counts of the indicated IFN receptor genes (**G**) and heatmap of IFN regulatory genes (**H**) from PBS treated neonate and organoid IECs. DEGs listed in (**H**) are significantly different between neonate and organoid. **I.** Flow cytometry staining of IFNAR1 and IFNAR2 on neonate IECs (from **Figure 2.1E**) and organoid IECs. Grey histograms are control stains (no IFNAR antibody), and bar graphs show geometric mean-fluorescence intensity (MFI) of IFNAR fluorescence normalized to controls. Data points represent replicate treatments (**A, B, G**) or replicate experiments (**I**). Significance determined by t-test (**I**); *, $p < 0.05$; **, $p < 0.01$.

Apoptosis genes are among IFN- β -specific ISGs

The preceding data from neonatal mice, together with prior studies of adult mice, strongly suggest that hypo-responsiveness of IECs to IFN- α/β *in vivo* is physiologically advantageous. To gain insight into the potential advantages of selective IFN- λ responsiveness, we further analyzed the transcriptomes of IFN- β -responsive IEC organoids. The 337 “IFN- β -specific ISGs” of IEC organoids represented a subset of the overall IFN response that is not present *in vivo* whereas the 190 genes stimulated by IFN- λ and IFN- β represented a “common ISG” module. Notably, the “common ISGs” were stimulated to a significantly greater extent by IFN- β treatment than the “IFN- β -specific ISGs” (**Figure 2.4A**), and the 190 common ISGs were stimulated to a significantly greater extent by IFN- β than by IFN- λ treatment (**Figure 2.4B**). Therefore, common ISGs consist almost entirely of the most highly responsive genes. To identify differential pathway associations, we compared the 337 IFN- β -specific ISGs with the 190 common ISGs using g:Profiler (459). Comparison of curated pathways from gene ontology (GO), KEGG, and Reactome databases indicated that 1) common ISGs were more significantly associated with antiviral effector pathways, 2) common ISGs and IFN- β -specific ISGs were similarly associated with antigen processing and presentation pathways, and 3) IFN- β -specific ISGs were significantly associated with apoptosis pathways (**Figure 2.4C**). A heatmap of all apoptosis pathway genes (KEGG:04210) confirmed that IFN- β treated IEC organoids clustered separately from other treatment groups and controls (**Figure 2.5A**). Specifically, IFN- β treatment of organoids uniquely stimulated 19/130 apoptosis pathway genes including pro-apoptotic genes *Bid*, *Bcl2l11*, and *Casp8* (**Figure 2.5A-B**). Together, these analyses indicate that IFN- β and IFN- λ are similarly capable of eliciting antiviral effectors, but IFN- β uniquely stimulates expression of apoptosis-pathway genes.

Prior studies in other cell types have indicated that inflammatory cytokines are a gene set that distinguishes IFN- α/β from IFN- λ (147, 148). To determine whether these genes were also differentially regulated in our IEC organoid studies, we performed focused analysis of 37 inflammatory cytokines, including IL-6, IL-1 β , and TNF α , shown by Galani et al. to be differentially regulated in neutrophils. Unlike neutrophils, the majority of these inflammatory cytokines were not stimulated in IEC organoids, with the notable exception of the pro-inflammatory chemokine *Cxcl10* (**Figure 2.5C**). This suggests that neutrophils and IECs differ in their capacity for ISG expression. To determine whether this difference extended to the set of IFN- β -specific apoptosis ISGs identified here, we analyzed expression of these genes in the RNAseq data from Galani et al. Similar to our results in IECs, neutrophils upregulated apoptosis pathway genes following treatment with IFN- α but not IFN- λ (**Figure 2.5D**). These comparisons suggest that some IFN- α/β -specific ISGs (i.e. inflammatory cytokines) are cell-type specific and others (i.e. pro-apoptotic genes) are similar across cell types.

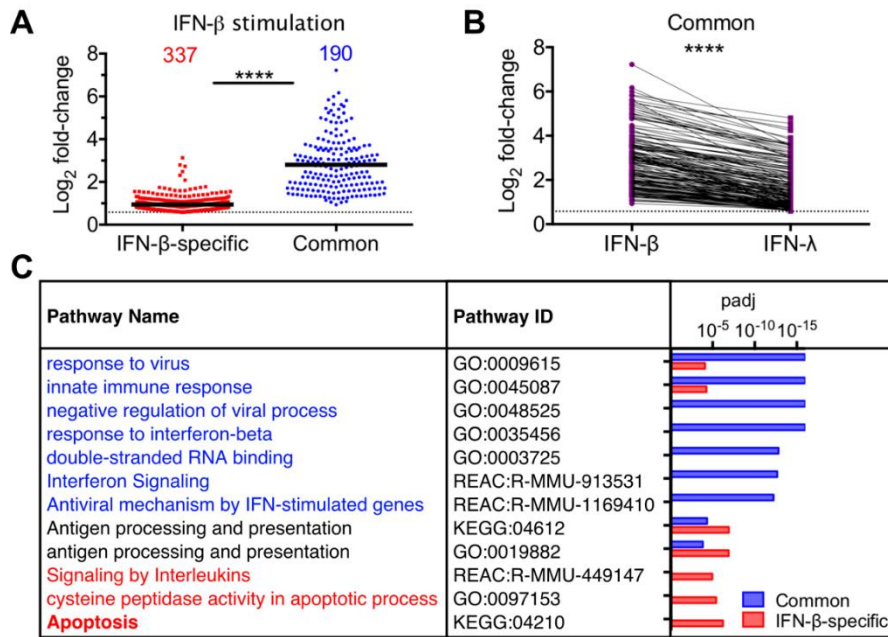


Figure 2.4. Common ISGs in IEC organoids are highly stimulated and consist of canonical antiviral genes. **A.** Log₂ fold-change from RNAseq of genes stimulated by IFN- β but not IFN- λ (337, IFN- β -specific), or genes stimulated by both IFN- β and IFN- λ (190, Common). **B.** Comparison of log₂ fold-change for common ISGs following stimulation by IFN- β or IFN- λ . Lines indicated gene identity across treatment groups. **C.** Selected pathways differentiating the indicated ISG categories; “padj” is the p-value adjusted for multiple comparisons. Statistical significance determined by Mann-Whitney test; ****, $p < 0.0001$.

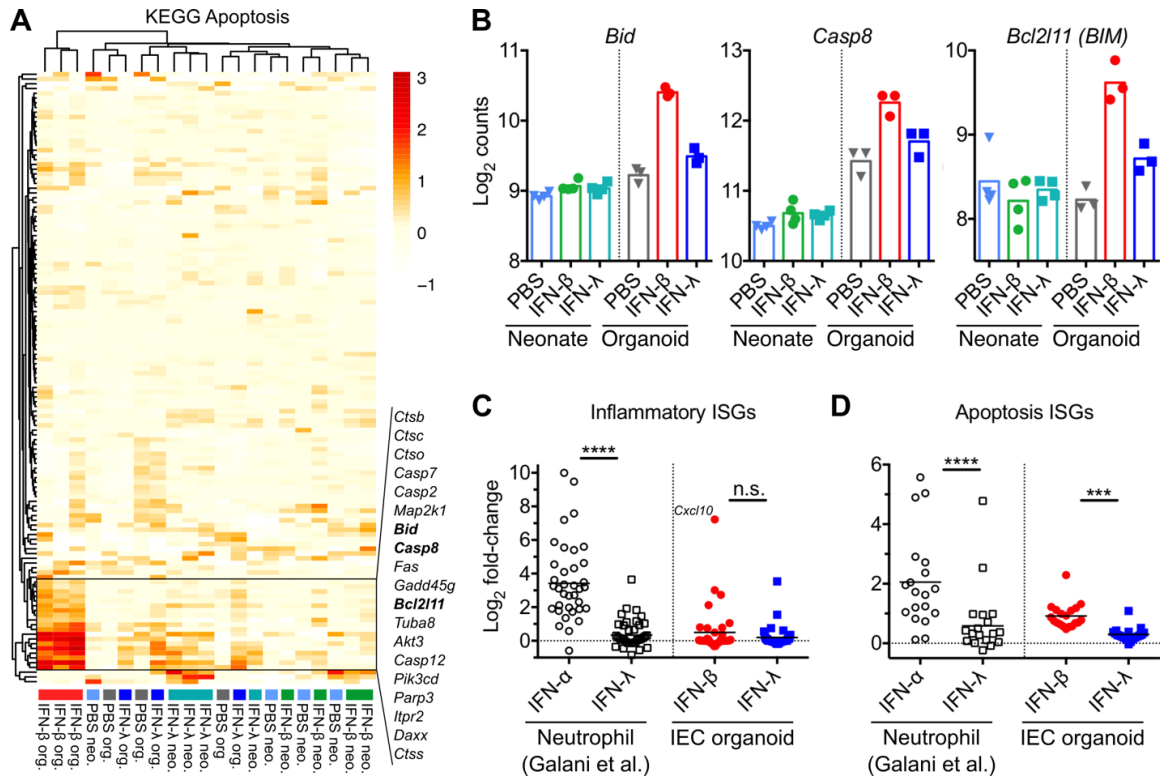


Figure 2.5. IFN-β-specific ISGs include apoptosis pathway genes. **A.** Heatmap comparing log₂ fold change of all KEGG apoptosis pathway genes among organoid and neonate IFN treatment groups relative to their corresponding PBS controls. Names are shown for the cluster of “apoptosis ISGs” stimulated by IFN-β treatment of organoids. **B.** Normalized RNAseq counts for three apoptosis ISGs. **C-D.** Log₂ fold change of inflammatory ISGs (**C**) or apoptosis ISGs (**D**) from IFN-treated neutrophils (147) (open circles = IFN-α, open squares = IFN-λ) or IEC organoids (filled circles = IFN-β, filled squares = IFN-λ) relative to their corresponding PBS controls. Statistical significance determined by Kruskal-Wallis test. ***, p < 0.001; ****, p < 0.0001; n.s., p > 0.05.

IFN- β potentiates TNF α -triggered apoptosis

Among apoptosis pathway genes identified in **Figure 2.5A**, *Bid* and *Casp8* gene products are integral effectors in the extrinsic apoptosis pathway triggered by the inflammatory cytokine TNF α (460). To determine whether IFN- β treatment potentiates TNF α -triggered apoptosis, we pre-treated IEC organoid cultures with IFN- β , IFN- λ , or PBS followed by treatment with TNF α and measured cell viability using the MTT assay (**Figure 2.6A**). Treatment with TNF α , IFN- β or IFN- λ alone resulted in minimal loss of IEC viability (<10%) suggesting that our IEC organoids are resistant to the cytotoxic effects of TNF α at baseline. However, IFN- β treatment synergized with TNF α and resulted in an average 30% loss in viability. In contrast, IFN- λ followed by TNF α treatment resulted in significantly less (average 18%) loss of viability (**Figure 2.6A**). To confirm that death in these IEC organoid cultures was related to apoptosis, we examined cleaved (active) executioner caspase 3 by immunofluorescence. IFN- β treatment followed by TNF α resulted in a significant increase in the percentage of cleaved caspase 3 in IEC organoids whereas IFN- λ treatment did not (**Figure 2.6B-C**). These data indicate that IFN- β stimulation results in greater sensitivity of IECs to TNF α -triggered apoptosis, and suggest that hypo-responsiveness of IECs to IFN- α/β *in vivo* favors epithelial viability.

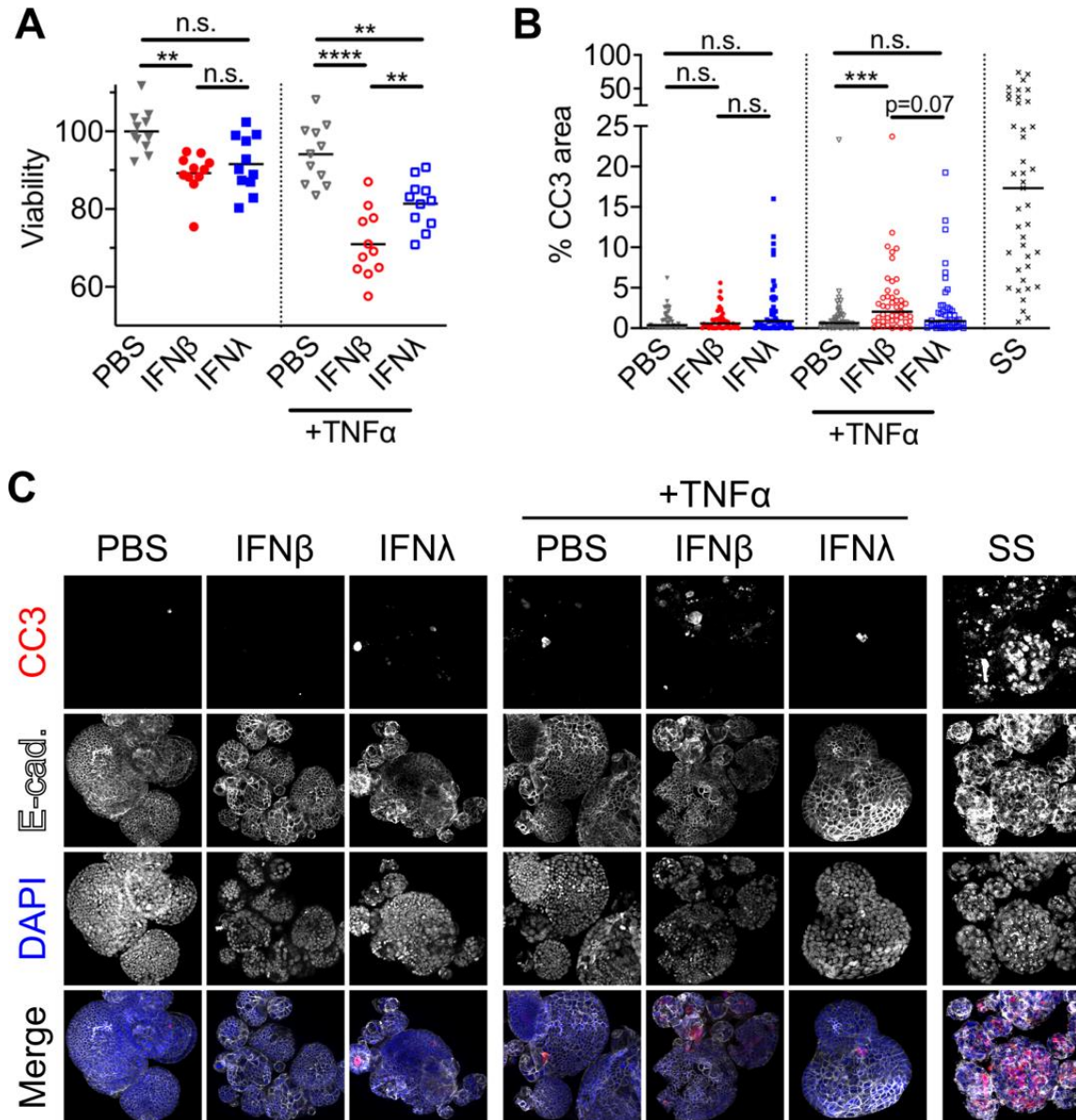


Figure 2.6. IFN-β potentiates TNFα-triggered apoptosis. **A.** MTT viability assay of IEC organoids treated with 10ng/mL IFN-λ3, IFN-β, or PBS for four hours followed by treatment with 100 ng/mL TNFα for 20 hours. **B-C.** Cleaved-caspase 3 (CC3) in IEC organoids was assessed by immunofluorescence following pre-treatment with 10ng/mL IFN-λ3, IFN-β, or PBS for 4-8 hours and subsequent treatment with media or 100ng/mL TNFα for 16-20 hours. The positive apoptosis control, staurosporine (SS), was administered to PBS organoids for 16-20 hours. Data are pooled from three independent experiments with statistical significance determined by one-way ANOVA in **A** and statistical significance determined by Kruskal-Wallis test with Dunn's multiple comparisons in **B**. Solid line depicts the mean in **A** and the median in **B** with **, $p < 0.01$; ***, $p < 0.001$; ****, $p < 0.0001$; n.s., $p > 0.05$.

The strength of the canonical ISRE differentiates ISG categories

To globally define distinguishing promoter motifs of common and IFN- β -specific ISG categories, we used the Hypergeometric Optimization of Motif EnRichment (HOMER) software package (461). We searched for motifs enriched in IFN- β -specific ISG promoters relative to a “background” of common ISG promoters or *vice versa*. This comparison resulted in no statistically significant promoter motifs that distinguished IFN- β -specific ISGs from common ISGs. However, a *de novo* motif was significantly enriched in common ISG promoters relative to IFN- β -specific ISG promoters (**Figure 2.7A**). This “common ISG motif” was clustered near the transcription start site (TSS) of these genes, consistent with a direct role in initiating transcription (**Figure 2.7B**). The *de novo* common ISG motif had a high degree of similarity to previously described ISRE and IRF motifs, suggesting that it reflected stronger canonical promoter motifs among common ISGs. Indeed, previously defined (canonical) ISRE and IRF motifs were present with significantly higher frequency among common ISGs than among IFN- β -specific ISGs (**Figure 2.7A**). Further comparison of common ISGs and IFN- β -specific ISGs to a “background” of other genes within the mouse genome revealed that ISRE and IRF motifs were significantly enriched in both ISG sets, and a STAT1 motif was specifically enriched among common ISGs (**Figure 2.7A-B**). As a control for these comparisons, the GC-rich basal promoter motif of specificity protein 1 (Sp1) was found at a similar frequency near TSS of all gene categories (**Figure 2.7A-B**).

We were interested in determining how well the global analysis of IFN- β -specific ISG promoters reflected properties of apoptosis ISGs and neutrophil inflammatory ISGs. Additionally, we sought to perform more quantitative motif comparisons beyond a simple presence/absence determination. So, we determined the ISRE score for each gene, which is higher for promoter sequences that more closely match the ideal ISRE (**Figure 2.7A**).

ISRE motif scores were similarly low among apoptosis ISGs, inflammatory ISGs, or IFN- β -specific ISGs, all of which were significantly lower than common ISGs (**Figure 2.7C**). These data indicate that promotor characteristics of IFN- β -specific ISGs as a whole are reflected in apoptosis and inflammatory gene subsets.

Prior studies in other cell types have indicated that IFN- λ stimulates less robust STAT1 phosphorylation and ISRE transactivation than IFN- α/β (114, 115). Consistent with these findings, we observed a lower fold-increase of common ISGs by IFN- λ than by IFN- β (**Figure 2.4B**). To explore the relationship among ISRE score and fold-increase, we performed correlation analyses of these two variables for all ISGs. We observed a significant positive correlation between IFN- β -stimulated fold-change and ISRE score, confirming the relevance of this promoter motif (**Figure 2.7D**). IFN- λ -stimulated fold-change was also significantly correlated with ISRE score, but had a significantly shallower slope ($p = 0.0293$) (**Figure 2.7E**). Together, these data indicated ISGs with low-scoring ISRE motifs were less likely to be stimulated by IFN- λ and correspondingly more likely to be IFN- β -specific.

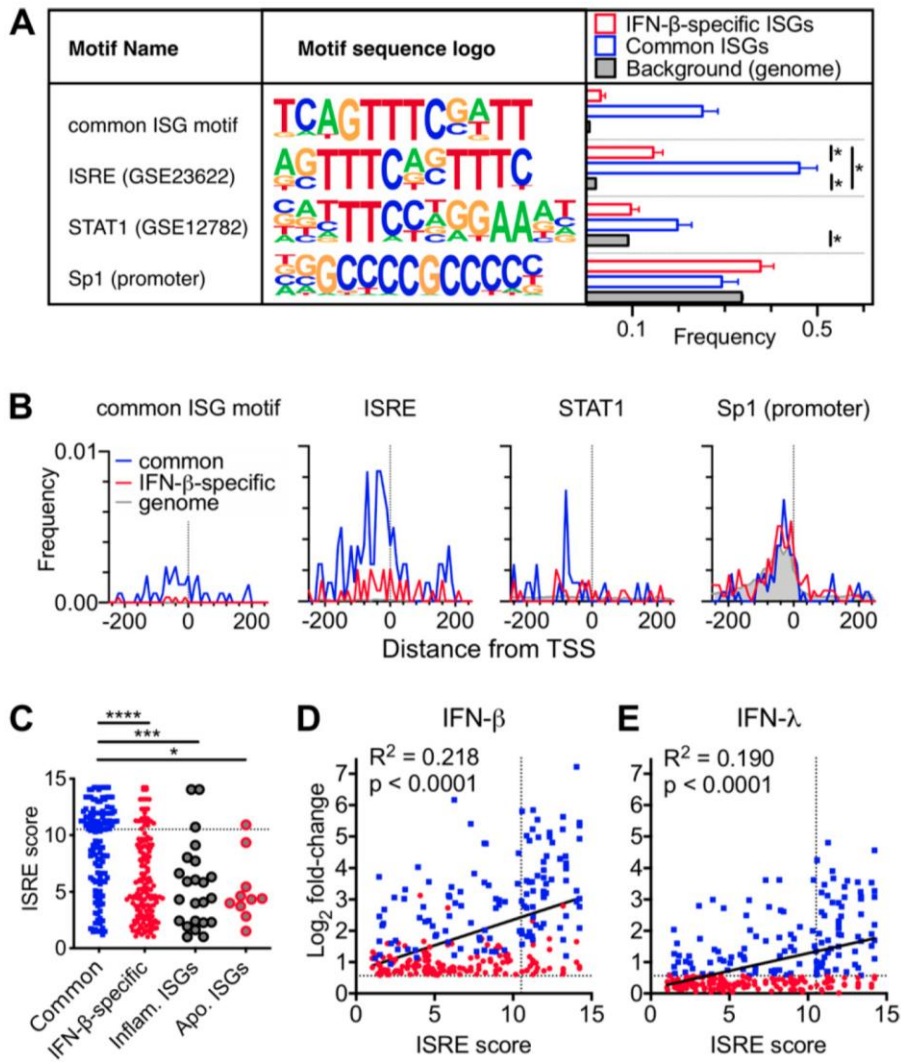


Figure 2.7. Strength of canonical ISRE differentiates ISG categories. Motifs were identified in genomic sequences 500 bp upstream to 250 bp downstream of annotated transcriptional start sites (TSS) for gene sets. **A.** Motif sequence logos for *de novo* “common ISG motif” and known motifs from the HOMER database. Height of bases are proportional to their preference at that position. Frequency graph depicts the proportion of genes in each category with at least one instance of the indicated motif scoring above threshold, with * indicating q-value < 0.05. **B.** Histograms of motif location relative to TSS. **C.** Comparison of ISRE (GSE23622) motif score among previously defined common, IFN- β specific, apoptosis, and inflammatory ISGs. Dashed line indicates threshold score from analysis in **(A)**; highest scoring motif is shown for each gene with at least one motif score > 1. **D-E.** Correlation of ISRE score with log₂ fold-change following treatment with IFN- β **(D)** or IFN- λ **(E)**. Vertical dashed line indicates threshold score from analysis in **(A)**, horizontal dashed line indicates 1.5-fold differential expression cutoff.

IFN- β -specific apoptosis ISGs are dependent on the canonical transcription factor STAT1

The preceding bioinformatic analyses suggested that promoters of IFN- β -specific ISGs would be less effective in recruitment of ISGF-3 components (STAT1, STAT2, and IRF9). To determine whether binding of these canonical transcription factors to promoters of common ISGs differed from binding to promoters of IFN- β -specific ISGs, we re-analyzed a previously published dataset (GSE115433) that sequenced DNA following chromatin immunoprecipitation (ChIP-seq) of STAT1, STAT2, and IRF9 from macrophages. In these data, promoters of common ISGs were significantly more likely than promoters of IFN- β -specific ISGs to be precipitated with any ISGF-3 component from untreated or IFN- β -treated cells (**Figure 2.8A**). These data are consistent with our bioinformatic analyses (**Figure 2.7**), and suggest that lower-scoring ISRE motifs in promoters of IFN- β -specific ISGs result in less robust binding of STAT1, STAT2, and IRF9.

Despite the low-scoring ISRE motifs of IFN- β -specific ISGs, we hypothesized that their stimulation by IFN- β would remain dependent on canonical usage of STAT1. To test this hypothesis, we generated IEC organoids from *Stat1*^{-/-} mice that are unable to generate active STAT1 homodimers, or heterotrimeric ISGF-3. We treated WT and *Stat1*^{-/-} organoids with 10ng/mL IFN- β or IFN- λ 3 for four hours followed by qPCR to measure induction of common ISGs (*Isg15*, *Cxcl10*) and IFN- β -specific, apoptosis ISGs (*Casp8*, *Bid*, *Bcl2l11*). Common ISGs were induced greater than 1000-fold by IFN- β and greater than 100-fold by IFN- λ in WT IECs. We confirmed that common ISGs were not induced by either IFN type in *Stat1*^{-/-} IECs, consistent with an absolute requirement of STAT1 for their stimulation (**Figure 2.8A-B**). Pro-apoptotic ISGs were induced two- to three-fold by IFN- β in WT IECs, but were not induced by IFN- λ in WT IECs or by either treatment in *Stat1*^{-/-} IECs (**Figure 2.8A-B**). These data indicate that the IFN- β -specific ISGs *Casp8*, *Bid*, and

Bcl2l11 are dependent on canonical ISG transcription factors. Taken together, our findings support the conclusion that IFN- β -specific ISGs are largely distinguished by low-scoring ISRE promoter motifs rather than a unique non-canonical motif. In conclusion, we propose a straightforward model in which a stronger transcriptional response downstream of IFN- β results in an expanded array of ISGs with low-scoring ISRE motifs. This expanded set of ISGs includes pro-apoptotic genes that have the potential to disrupt epithelial homeostasis and are therefore physiologically disadvantageous *in vivo*.

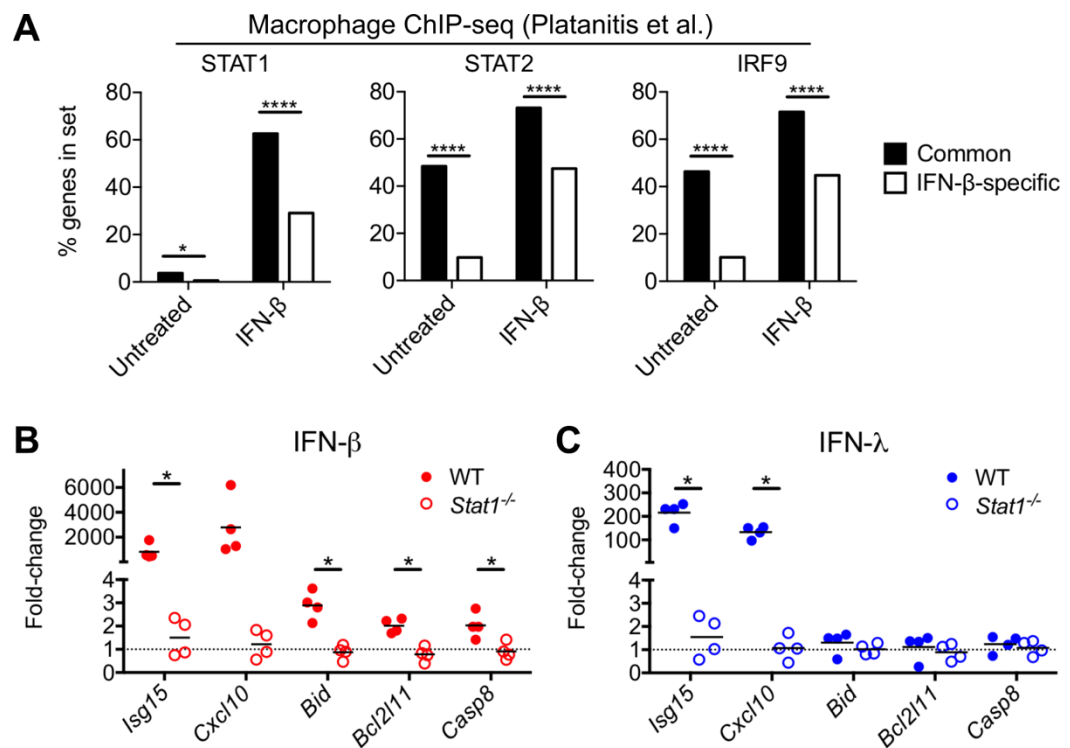


Figure 2.8. IFN- β -specific apoptosis ISGs are dependent on canonical transcription factor STAT1. **A.** Re-analysis of ChIP-seq data from GSE115433 (462). Percentage of genes in common ISG and IFN- β -specific ISG sets that had significant ChIP-seq peaks for STAT1, STAT2, or IRF9 within 500 bp of the transcription start site. Statistical significance determined by chi-square of contingency tables of genes with or without peaks. *, $p < 0.05$; ****, $p < 0.0001$. **B-C.** Quantitative PCR analysis of genes indicated on the x-axis following treatment of WT (filled symbol) or *Stat1*^{-/-} (open symbol) IEC organoids with 10ng/mL IFN- β (**B**) or IFN- λ 3 (**C**) for four hours; normalized to PBS-treated controls. Data are combined from four experiments, with * indicating p -value < 0.05 by one-way ANOVA.

Discussion

Here, we find that *in vivo* IECs are hypo-responsive to IFN- α/β beginning in early neonatal life (**Figure 2.1**), thereby elevating the importance of IFN- λ in epithelial antiviral immunity. Prophylactic IFN- λ , but not IFN- β , reduces early replication of the IEC-tropic mouse rotavirus, consistent with prior studies of Pott et al. (195). This ineffective IFN- β response of neonatal IECs was somewhat unanticipated based on the prior study from Lin et al., which found that IFN- α/β stimulated phospho-STAT1 in IECs of neonatal but not adult mice (197). Our transcriptomic comparison of ISG responses indicates that phospho-STAT1 may underlie a modest transcriptional response to IFN- β in neonatal IECs, but it is significantly diminished relative to the *in vivo* response of neonatal IECs to IFN- λ or the *in vitro* response of IEC organoids to IFN- β (**Figure 2.3**). In fact, we find that IEC organoids expanded *in vitro* from intestinal stem cells are highly responsive to IFN- β , with more robust ISG induction relative to IFN- λ (**Figure 2.2**). This IFN response profile of mouse IEC organoids is consistent with recent human IEC organoid studies, which found that IFN- α/β provides more potent antiviral protection from rotavirus (143, 206). We suggest that, similar to mouse IECs, human IECs in their natural context *in vivo* may become hypo-responsive to IFN- α/β .

Our studies of viral infection in mouse IEC organoids here together with prior studies of others in human IEC organoids present a paradox: IFN- λ is the dominant effector in mouse models of gastrointestinal virus infection whereas IFN- α/β elicits superior antiviral defense *in vitro* (206). Our work here shows that IFN- β treatment of IEC organoids, in addition to stimulating significantly greater production of antiviral ISGs than IFN- λ , stimulates an expanded set of ISGs with low-scoring ISRE motifs (**Figure 2.7**). This expanded ISG profile includes pro-apoptotic genes that potentiate TNF α -triggered cytotoxicity (**Figure 2.6**). These findings in IECs are reminiscent of recent studies in

neutrophils that identified a set of inflammatory cytokine genes, including TNF α , triggered by IFN- β but not IFN- λ (147). We find here that IECs are not capable of readily producing most of these inflammatory ISGs in response to IFN- β , emphasizing the importance of cell-lineage-specific studies (**Figure 2.5C**). However, when considered in the context of preceding neutrophil studies, our findings here suggest that a neutrophilic, inflamed intestine is a scenario in which IEC hypo-responsiveness to IFN- α/β would be particularly beneficial. If IECs were not hypo-responsive in this inflammatory scenario, IFN- α/β would synergistically elicit TNF α production by neutrophils and potentiate TNF α -triggered cytotoxicity of IECs. Indeed, such a synergistic response may explain observations of epithelial apoptosis in the IFN- α/β -responsive lung epithelium during influenza infection, where IFN α but not IFN- λ treatment amplifies apoptosis of lung epithelial cells (146). In addition to the less damaging ISG profile of IFN- λ , Broggi et al. showed that IFN- λ can actively suppress inflammatory responses of neutrophils by a post-transcriptional mechanism, providing further homeostatic benefits (145). Thus, hypo-responsiveness of IECs to IFN- α/β *in vivo* may be moderately dis-advantageous for antiviral protection, but reduces the risk of inflammatory response amplification loops that result in epithelial damage.

Previous work has suggested apical trafficking of IFNAR and reduced *Ifnar1/Ifnar2* transcript expression as mechanisms for IEC hypo-responsive to IFN- α/β *in vivo* (194, 195). Our study supports a role for post-transcriptional regulation of IFNAR1 and IFNAR2 in determining IEC responsiveness to IFN- α/β . IEC organoids have increased surface staining for both IFNAR subunits and reduced expression of several known negative regulators of IFNAR signaling. These mechanisms may relate to post-natal changes in intestinal exposure to nutrients and the microbiome, which elicit corresponding changes in IEC metabolism and immunity. Neil et al. recently showed that when the microbiome is

depleted from adult mice with antibiotics and the epithelium is exposed to damaging dextran sodium sulfate, an IFN- α/β response in IECs can promote beneficial recruitment of IL-22-producing leukocytes (463, 464). This role of IFN- α/β in IECs suggests the following possibilities: 1) depletion of the microbiome together with epithelial damage could increase IFN- α/β responsiveness of IECs, or 2) under certain types of epithelial damage the modest responsiveness of IECs to IFN- α/β *in vivo* may be beneficial. Further studies are needed to determine the effect of the microbiome and inflammatory triggers on IFN- α/β responsiveness of IECs and to understand the signals that regulate IEC-intrinsic IFNAR responses *in vivo*. Our work here emphasizes the important pleiotropic roles of the IFN response and provides a physiological basis for regulating the ISG expression capacity of IECs to maintain intestinal homeostasis.

CHAPTER 3: A Homeostatic Interferon-lambda Response to Bacterial Microbiota Stimulates Preemptive Antiviral Defense in Discrete Pockets of Intestinal Epithelium

Authors, Affiliations, Contributions, Acknowledgements, and Citations

Authors

Jacob A. Van Winkle¹, Stefan T Peterson², Elizabeth A Kennedy², Michael J Wheadon², Harshad Ingle², Chandni Desai³, Rachel Rodgers², David A. Constant¹, Austin P Wright¹, Lena Li¹, Maxim N Artyomov⁴, Sanghyun Lee², Megan T Baldrige^{5*}, and Timothy J Nice^{1*}

Affiliations

¹ Department of Molecular Microbiology and Immunology, Oregon Health & Science University, Portland, OR, USA

² Division of Infectious Diseases, Department of Medicine, Edison Family Center for Genome Sciences & Systems Biology, Washington University School of Medicine, St. Louis, MO, USA

³ Division of Immunobiology, Department of Pathology and Immunology, Washington University School of Medicine, St. Louis, MO, USA

⁴ Department of Pediatrics, Washington University School of Medicine, St. Louis, MO, USA

⁵ Department of Molecular Microbiology, Washington University School of Medicine, St. Louis, MO, USA

* Correspondence to: nice@ohsu.edu (T.J.N.), mbaldrige@wustl.edu (M.T.B.)

Contributions

Conceptualization, J.A.V.W., M.T.B., and T.J.N.; Methodology, J.A.V.W., M.T.B., and T.J.N.; Investigation, J.A.V.W., S.T.P., E.A.K., M.W., H.I., R.R., C.D., D.C., A.W., M.A., S.L., and T.J.N.; Writing – Original Draft, J.A.V.W.; Writing – Review & Editing, J.A.V.W., M.T.B., and T.J.N.; Visualization, J.A.V.W.; Supervision, M.T.B. and T.J.N.; Project Administration, L.L., M.T.B., and T.J.N.; Funding Acquisition, M.T.B. and T.J.N.

J.A.V.W. directly contributed to figures 3.4, 3.10, 3.11, 3.12, 3.13, 3.14, 3.16, 3.18, 3.19, 3.20, 3.21. J.A.V.W. performed analysis of previously generated RNA sequencing datasets in figures 3.3 and 3.15.

Acknowledgements

The authors would like to thank the following OHSU core facilities: Integrated Genomics Laboratory, Advanced Light Microscopy Core, and Histopathology Core; and the following WUSTL core facilities: Genome Technology Access Center. TJN was supported by NIH grant R01-AI130055 and by a faculty development award from the Sunlin & Priscilla Chou Foundation. JAV was supported by NIH grants T32-GM071338 and T32-AI007472. MTB was supported by NIH grants R01-AI139314, R01-AI141716, and R01-AI141478, the Pew Biomedical Scholars Program of the Pew Charitable Trusts, and a Children's Discovery Institute of Washington University and St Louis Children's Hospital Interdisciplinary Research Initiative grant (MI-II-2019–790). The funders had no role in study design, data collection, and interpretation, or the decision to submit the work for publication.

Citation

Van Winkle JA, Peterson ST, Kennedy EA, Wheadon MJ, Ingle H, Desai C, Rodgers R, Constant DA, Wright AP, Li L, Artyomov M, Lee S, Baldrige MT, and Nice TJ. A homeostatic interferon-lambda response to bacterial microbiota stimulates preemptive antiviral defense within discrete pockets of intestinal epithelium. *eLife* 2022; 11:e74072. PMID: 35137688

Introduction

Interferons (IFNs) are a family of cytokines produced in response to infection that signal IFN receptor-bearing cells to induce transcription of hundreds of interferon-stimulated genes (ISGs). These ISGs perform diverse functions, but many cooperate to induce an antiviral state (99, 465). There are three types of IFNs: type I IFNs (IFN- α s, IFN- β , others), type II IFN (IFN- γ), and type III IFNs (IFN- λ s). These three types are differentiated by receptor usage (type I IFN receptor: *Ifnar1/Ifnar2*; type II IFN receptor: *Ifngr1/Ifngr2*; type III IFN receptor: *Ifnlr1/Il10rb*), but all three receptor complexes signal through Janus-kinase (JAK) and signal transducer and activator of transcription (STAT) factors to stimulate ISG transcription (110, 466). Type I and III IFNs are directly stimulated by host detection of microbe-associated molecular patterns (MAMPs) such as viral nucleic acids, and the prominent contribution of these IFN types to antiviral defense is reflected by the breadth of evasion strategies used by diverse viral families to prevent their production or action (467–469). The type I IFN receptor is expressed broadly across most cell types, whereas the type III IFN receptor, *Ifnlr1*, is primarily restricted to epithelial cells (191, 470). Accordingly, IFN- λ is of particular importance in effective antiviral defense of barrier tissues.

Interestingly, previous studies in mice have noted that intestinal epithelial cells (IECs) are hyporesponsive to type I IFN (194, 195, 197, 471). The responsiveness of IECs to type I IFN appears to be developmentally regulated because the IECs of adult mice exhibit weaker type I responses than IECs of neonatal mice (197). Additionally, infection of mice deficient in IFN receptors (*Ifnar1*, *Ifngr1*, *Ifnlr1*; single or double knockouts) with enteric viruses indicates that IFN- λ is the predominant antiviral IFN type that controls viral replication in the gastrointestinal epithelium (194, 195, 199). IECs can robustly respond to IFN- λ with upregulation of canonical antiviral ISGs and increased resistance to infection

by enteric viruses, such as rotaviruses and noroviruses (195, 199, 200). Murine rotavirus is a natural pathogen of mice that infects enterocytes located at the tips of villi in the small intestine (227). Rotaviruses have developed mechanisms to antagonize the induction of IFN by infected cells, suggesting that evasion of the IFN response is necessary for efficient epithelial infection (241). Indeed, prophylactic administration of IFN- λ significantly reduces the burden of murine rotavirus infection, demonstrating its potential for mediating epithelial antiviral immunity to this pathogen (195, 197, 471, 472). However, a protective role of the endogenous IFN- λ response to murine rotavirus infection is less clear, perhaps reflecting the success of murine rotavirus evasion mechanisms.

Epithelial immunity in the gut must be appropriately balanced to protect the intestinal epithelium while preventing loss of barrier integrity and intrusion by microbes that are abundant within the gastrointestinal tract. The bacterial microbiota in the intestine perform critical functions by aiding in host metabolism (473), providing a competitive environment to defend against pathogens (322), and initiating and maintaining host immune function during homeostasis (300, 384). In this complex environment host epithelial and immune cells detect bacteria and viruses using a suite of pattern recognition receptors (PRRs) that sense the presence of MAMPs. Stimulation of PRRs, such as the toll-like receptor (TLR) family, activates antimicrobial and antiviral defenses providing local protection in many tissues (150, 474, 475). TLR-dependent pathways induce production of IFNs, primarily by signaling through TIR-domain-containing adapter-inducing interferon- β (TRIF) and myeloid differentiation primary response 88 (MYD88) adapter proteins (176, 476), providing a mechanism by which bacterial MAMPs can initiate IFN responses.

Signals from the bacterial microbiota have been shown to elicit a steady-state type I IFN response in systemic tissues and cell types that can prime antiviral immunity by several independent studies (421, 423–426, 477). Additionally, a steady-state ISG signal

has been observed in the intestine of uninfected mice (197, 443, 478), but this intestinal response remained poorly characterized. Together with the observed hypo-responsiveness of IECs to type I IFN, these findings suggested that bacterial microbiota may stimulate an IFN- λ response in the gut. To explore this interaction, we undertook the present study to assess the role of bacterial microbiota in induction of enteric ISGs at homeostasis using a combination of broad-spectrum antibiotics (ABX) and genetically modified mice.

In this study, we uncovered an ISG signature in IECs that was dependent on the presence of bacteria and IFN- λ signaling (hereafter referred to as 'homeostatic ISGs'). This panel of genes was present in WT mice with conventional microbiota and was reduced in WT mice treated with ABX and in mice lacking *Ifnlr1*. We revealed that homeostatic ISG expression is i) restricted to the intestinal epithelium across both the ileum and colon, ii) independent of type I IFN signaling, and iii) associated with IFN- λ transcript expression by epithelium-associated CD45+ leukocytes. Surprisingly, we found that homeostatic ISGs are not expressed uniformly by all IECs; rather, expression is concentrated in localized pockets of IECs and in differentiated IECs relative to crypt-resident progenitors. These patterns of localized ISG expression are corroborated by independently-generated single-cell RNA sequencing data from mouse and human IECs. We also found that ISG expression can be increased in ABX-treated mice by reconstitution of bacterial microbiota or administration of bacterial lipopolysaccharide (LPS). Finally, we found that this microbiota-stimulated ISG signature provides protection from initiation of murine rotavirus infection. Cumulatively, this study found that bacteria initiate preemptive IFN- λ signaling in localized areas to protect IECs from enteric viruses.

Results

Bacterial microbiota stimulate IFN- λ response genes in the ileum at homeostasis

To determine the effect of bacterial microbiota on homeostatic IFN- λ responses, we compared gene expression in whole ileum tissue for the following experimental groups: i) wild-type C57BL/6J (WT) mice intraperitoneally-injected with IFN- λ as compared to unstimulated WT mice, ii) WT mice with conventional microbiota as compared to WT mice treated with an antibiotic cocktail (ABX) to deplete bacteria, iii) WT mice with conventional microbiota as compared to *Ifnlr1*^{-/-} mice with conventional microbiota, and iv) *Ifnlr1*^{-/-} mice with conventional microbiota compared to *Ifnlr1*^{-/-} mice treated with ABX (**Figure 3.1A**). To rule out contributions of *Ifnlr1* toward an altered intestinal bacterial microbiota, we performed 16S rRNA sequencing on stool from *Ifnlr1*^{+/+}, *Ifnlr1*^{+/-}, and *Ifnlr1*^{-/-} mice and did not find statistically significant differences in alpha-diversity and beta-diversity measurements with the statistical power available from 12 mice per group (**Figure 3.2**). For each comparison of ileum gene expression shown in **Figure 3.1A**, we performed gene-set-enrichment-analysis (GSEA) to determine enrichment or depletion of hallmark gene sets (479). The hallmark gene set that was most enriched in IFN- λ -treated WT mice compared to unstimulated WT mice was INTERFERON_ALPHA_RESPONSE (**Figure 3.1B** and **Figure 3.3**). Therefore, this gene set reflects differences in IFN- λ responses between experimental conditions.

To deplete bacterial microbiota, we administered a cocktail of broad-spectrum antibiotics, and demonstrated that this treatment reduced bacterial 16S gene copies in stool to below the limit of detection (**Figure 3.4**). GSEA of WT mice treated with ABX showed a significant depletion (negative enrichment score) of INTERFERON_ALPHA_RESPONSE hallmark genes in the ileum relative to WT mice with

conventional microbiota (**Figure 3.1C**). These data indicate that ISGs are present at steady-state in the ileum of specific-pathogen-free mice with conventional microbiota and suggest that microbiota stimulate expression of these genes in the ileum at homeostasis.

Type I, II, and III IFN responses have substantial gene expression overlap; therefore, to prove that the IFN- λ receptor was necessary for expression of ISGs at homeostasis, we analyzed gene expression in the ileum of *Ifnlr1*^{-/-} mice. Indeed, GSEA showed significant reduction of INTERFERON_ALPHA_RESPONSE hallmark genes in the ileum of *Ifnlr1*^{-/-} mice compared to WT mice (**Figure 3.1D**). Furthermore, expression of INTERFERON_ALPHA_RESPONSE hallmark genes was not significantly decreased in *Ifnlr1*^{-/-} mice treated with ABX compared to *Ifnlr1*^{-/-} mice with conventional microbiota (**Figure 3.1E**). In contrast to INTERFERON_ALPHA_RESPONSE, other hallmark gene sets such as INFLAMMATORY_RESPONSE and IL6_JAK_STAT3_SIGNALING were significantly decreased by ABX treatment in both WT mice and *Ifnlr1*^{-/-} mice (**Figure 3.3**), which indicates a selective requirement for *Ifnlr1* to elicit ISGs and a minimal effect of *Ifnlr1*-deficiency on other microbiota-dependent genes. Together, these findings suggest that *Ifnlr1* is necessary for the bacterial microbiota-dependent expression of ISGs in the ileum at homeostasis. Since ISGs are enriched in mice upon IFN- λ stimulation and are decreased in *Ifnlr1*^{-/-} and ABX-treated mice, we conclude that the bacterial microbiota stimulates IFN- λ responses in the ileum at homeostasis.

To define a core set of bacterial microbiota-dependent, *Ifnlr1*-dependent 'homeostatic ISGs', we determined the overlap of differentially expressed genes (DEGs) by defining genes with: i) increased expression upon IFN- λ stimulation in WT mice, ii) decreased expression upon ABX treatment in WT mice, and iii) decreased expression in *Ifnlr1*^{-/-} mice relative to WT mice. The DEGs shared by each of these comparisons comprised a set of 21 genes that are decreased upon treatment with ABX and loss of

Ifnlr1, and are induced in response to IFN- λ (**Figure 3.1F**). This set of homeostatic ISGs includes antiviral genes that are dependent on bacterial microbiota and the IFN- λ pathway. Comparison of homeostatic ISG transcript counts between experimental treatments revealed similar insights as prior GSEA analysis. WT mice treated with IFN- λ had higher expression of all homeostatic ISGs than untreated mice, whereas WT mice with a conventional microbiota had higher expression of homeostatic ISGs than *Ifnlr1*^{-/-} mice and ABX-treated mice of both genotypes (**Figure 3.1G**). We did not detect additional decreases in these homeostatic ISGs in ABX-treated *Ifnlr1*^{-/-} mice relative to conventional *Ifnlr1*^{-/-} mice, suggesting that *Ifnlr1* is necessary for expression of homeostatic ISGs (**Figure 3.1G**). These results indicate that there is modest but significant expression of ISGs at homeostasis that is lost with *Ifnlr1* deficiency or ABX treatment. Together, these analyses revealed a homeostatic signature of ISGs in the ileum that depends upon the presence of bacterial microbiota and on intact IFN- λ signaling.

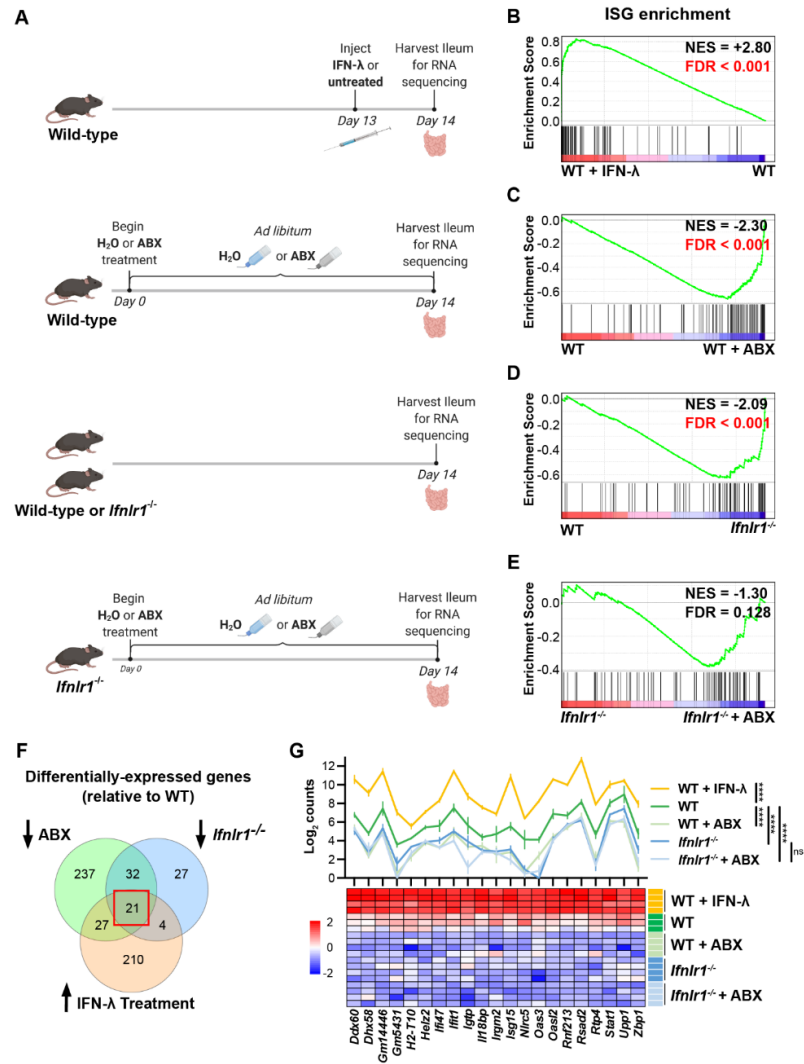


Figure 3.1. Bacterial microbiota stimulate IFN-λ response genes in the ileum at homeostasis.

A. Depiction of experimental treatments and comparison groups. Following the indicated treatments, a segment of whole ileum tissue was harvested and analyzed by RNA sequencing for differentially expressed genes between paired conditions. **B-E.** Gene-set enrichment analysis of INTERFERON_ALPHA_RESPONSE hallmark genes (ISGs) was performed with the following comparisons: WT mice treated with 25μg of IFN-λ relative to WT mice treated with PBS (**B**), WT mice treated with ABX relative to untreated WT mice (**C**), *Ifnlr1*^{-/-} mice relative to WT mice (**D**), and *Ifnlr1*^{-/-} mice treated with ABX relative to untreated *Ifnlr1*^{-/-} mice (**E**). Normalized enrichment score (NES) and false-discovery rate (FDR) are overlaid for each comparison with significant FDR's highlighted (red). **F.** A Venn diagram depicting the total number of differentially expressed genes that are i) increased with IFN-λ stimulation (orange), ii) decreased with ABX treatment (green), or iii) decreased in *Ifnlr1*^{-/-} mice relative to WT (blue). An overlapping subset of 21 genes was shared among all three comparisons (red box). **G.** A graph and heatmap of the relative expression of the 21 genes that overlap in all experimental groups in (**F**) ('homeostatic ISGs'). Statistical significance in (**G**) was determined by one-way ANOVA with Tukey's multiple comparisons where ns = p > 0.05, and **** = p < 0.0001.

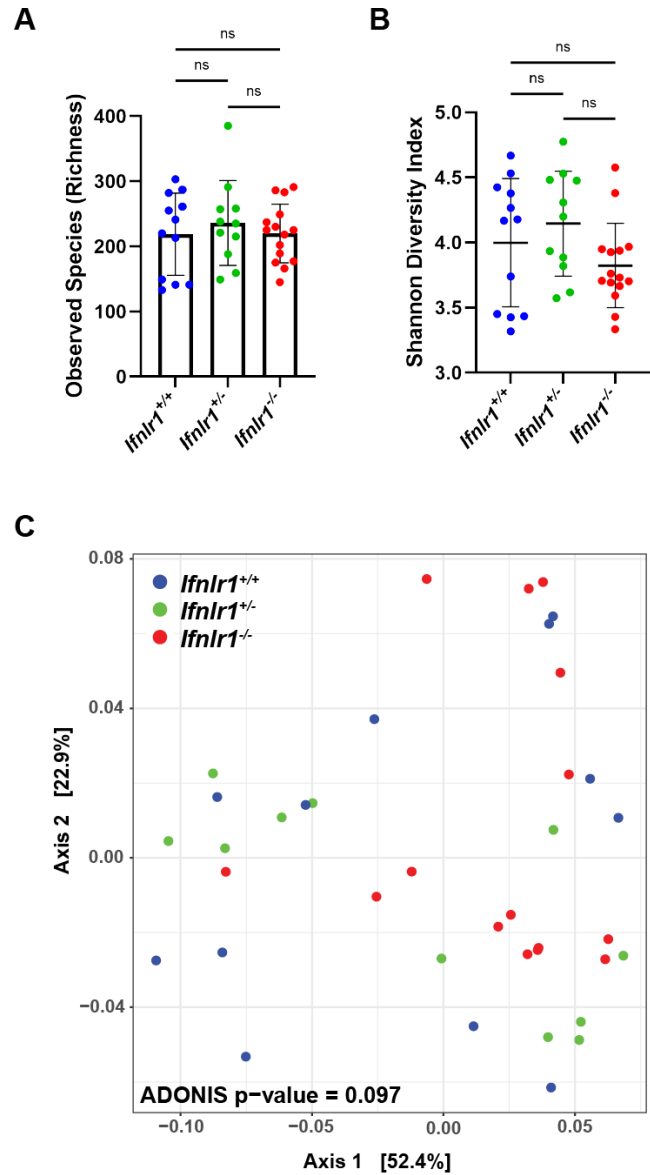


Figure 3.2. *Ifnlr1*-deficiency does not alter intestinal bacterial microbiota. Stool was harvested from *Ifnlr1*^{+/+}, *Ifnlr1*^{+/-}, and *Ifnlr1*^{-/-} mice and 16S rRNA genes were sequenced. Alpha-diversity metrics of observed bacterial species (**A**) and Shannon Diversity Index (**B**). **C**. Principle component analysis of beta-diversity UniFrac distances. Statistical significance was determined one-way ANOVA with Tukey's multiple comparisons, where ns = p > 0.05.

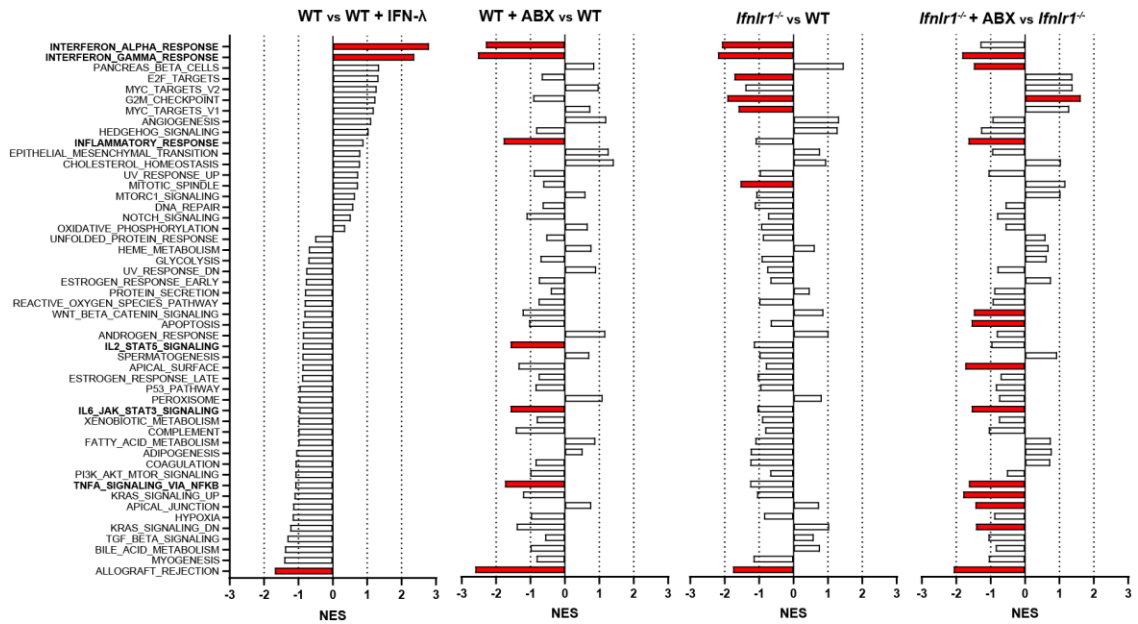


Figure 3.3. Gene set enrichment analysis of hallmark gene sets. Log₂ counts from RNA sequencing output were assessed for enrichment and depletion of hallmark gene sets by gene set enrichment analysis. Graphs of normalized enrichment score (NES) are displayed for each hallmark gene set and each comparison. Gene sets in red are statistically significantly altered in their given comparison.

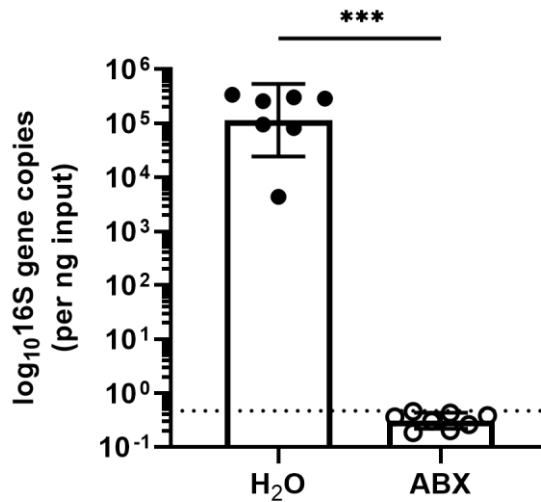


Figure 3.4. Treatment with antibiotics reduces enteric 16S gene copies to below the limit of detection. rDNA was isolated from luminal contents of mice after 14 days of ABX-treatment. 16S gene copies were assessed by qPCR and normalized to input. Limit of detection: dashed line. Data points represent individual mice and are pooled from 2 independent experiments. Statistical significance was determined by Mann Whitney, where *** = $p < 0.001$.

Homeostatic, microbiota- and *Ifnlr1*-dependent ISGs are primarily expressed in intestinal tissues

To complement the results of the RNA-sequencing and extend this analysis to other tissue sites, we quantified tissue-level expression of a panel of three ISGs by qPCR: *Ifit1*, *Oas1a*, and *Stat1*. *Ifit1* and *Stat1* were present among the 21 homeostatic ISGs in the preceding analysis and *Oas1a* was included as a representative canonical ISG that we hypothesized would be present in the homeostatic signature, but did not meet the statistical criteria used to define the core set of 21 homeostatic ISGs (**Figure 3.1F-G**). We assessed absolute abundance of these ISG transcripts in the ileum, colon, mesenteric lymph nodes (MLN), and spleen tissue of WT and *Ifnlr1*^{-/-} mice with or without ABX treatment (**Figure 3.5A-C**). Consistent with our RNA-seq data, these ISGs were reduced in the ilea of *Ifnlr1*^{-/-} mice and ABX-treated WT mice compared to WT mice with conventional microbiota (**Figure 3.5A**). Secondly, homeostatic ISGs were expressed in WT colonic tissue and were significantly decreased in colonic tissue of *Ifnlr1*^{-/-} mice and ABX-treated WT mice (**Figure 3.5B**). These data indicate that homeostatic ISGs in both the ileum and colon were dependent on *Ifnlr1* and the bacterial microbiota; however, these homeostatic ISGs were more abundantly expressed in ileal tissue than colonic tissue (**Figure 3.6**). To confirm that treatment with ABX does not ablate the ability of the intestine to respond to IFN- λ , we stimulated ABX-treated mice with intraperitoneal IFN- λ and harvested ileum tissue. Stimulation with small amounts of IFN- λ rescued ISG expression in whole tissue (**Figure 3.7**), indicating that that reduction of homeostatic ISG expression upon treatment with ABX is not due to an inability of the intestine to respond to IFN- λ .

Enteric colonization by bacteria was shown to stimulate systemic type I IFN responses (421, 423–426, 477), so we assessed whether the decreases in ISGs upon ABX treatment or loss of *Ifnlr1* in the ileum were recapitulated in systemic immune tissues.

We quantified *Ifit1*, *Stat1*, and *Oas1a* expression in the MLN and the spleen and found that ABX treatment and *Ifnlr1* deletion did not reduce ISGs in these tissues (**Figure 3.5C**). Although we observe increases in *Ifit1* expression in MLN upon treatment with ABX, these results are not recapitulated by *Stat1* and *Oas1a* expression, and no significant changes in ISG expression were detected in the spleen. Cumulatively, these data indicate that homeostatic ISGs include genes beyond the core signature identified in **Figure 3.1** (e.g. *Oas1a*), that homeostatic ISGs are present in colonic tissue, and that homeostatic IFN- λ stimulated genes are most prominent in enteric tissues.

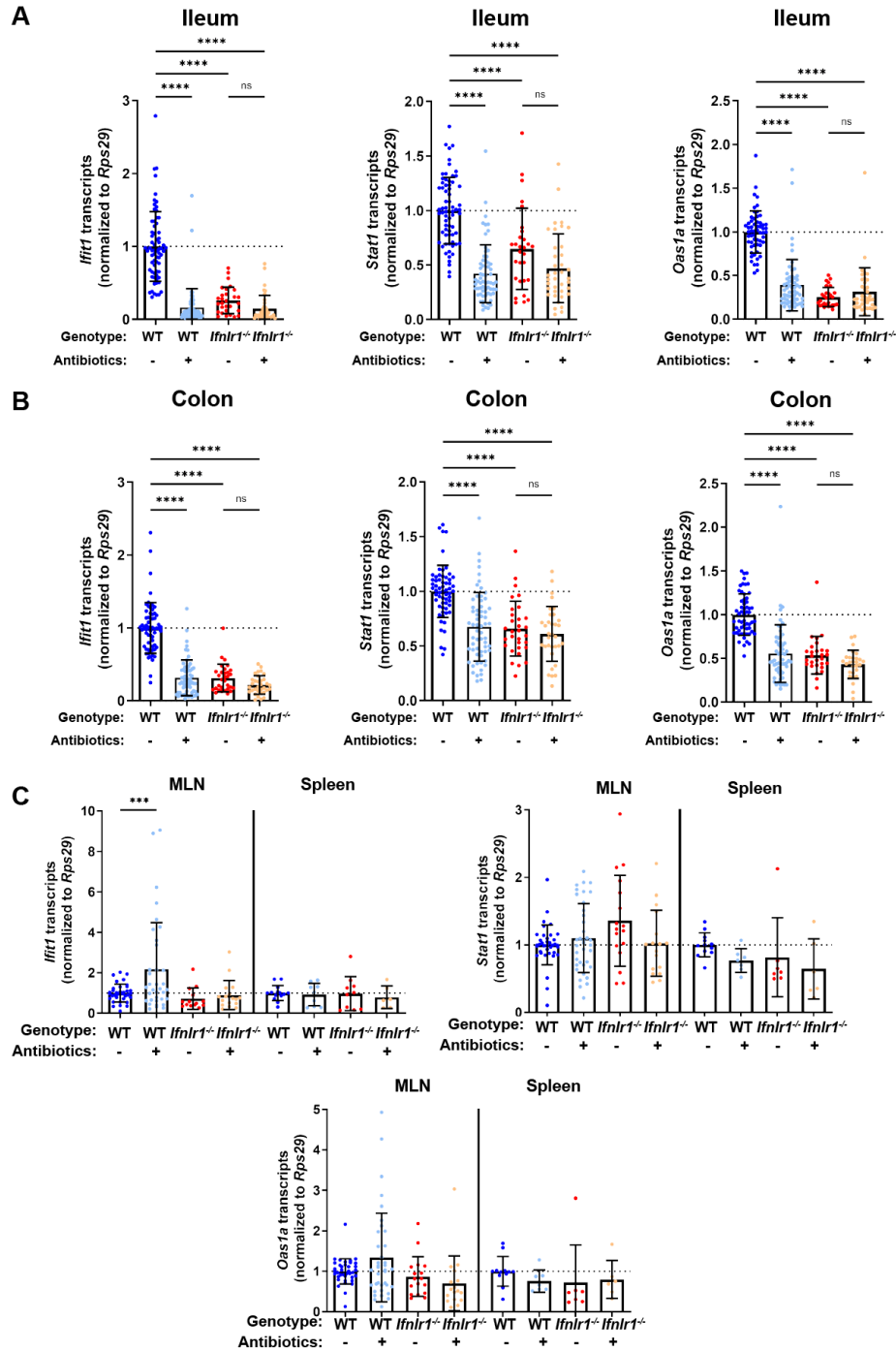


Figure 3.5. Homeostatic, microbiota- and *Ifnlr1*-dependent ISGs are primarily expressed in intestinal tissues. A segment of ileum or colon tissue from WT or *Ifnlr1*^{-/-} mice was harvested following H₂O or ABX treatment and the ISGs *Ifit1*, *Stat1*, and *Oas1a* were analyzed by qPCR. Transcripts were quantified in ileum (A), colon (B), or MLN and spleen (C) with normalization to untreated WT mice. Data points represent individual mice and data are pooled from 10-20 independent experiments in A-B and 15 independent experiments in C. Statistical significance was determined by one-way ANOVA with Tukey's multiple comparisons in A-B and Dunnett's multiple comparisons in C. * = p < 0.05, ** = p < 0.01, *** = p < 0.001, **** = p < 0.0001.

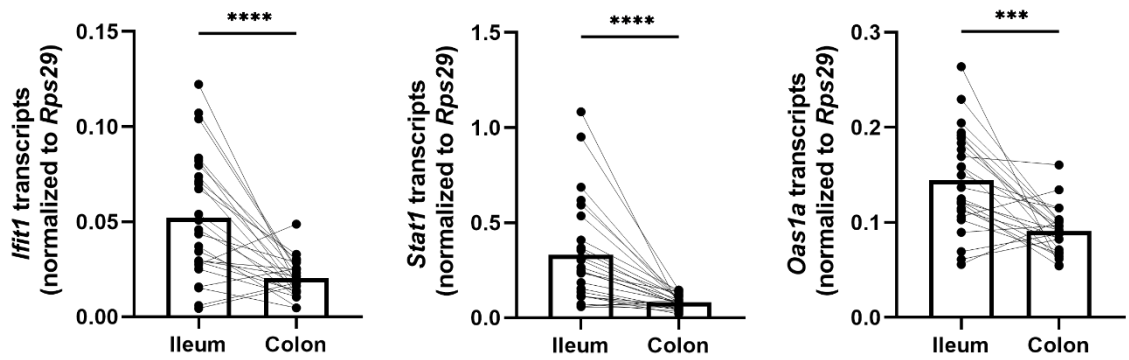


Figure 3.6. Homeostatic ISGs are more abundantly expressed in the ileum than in the colon. *Ifit1*, *Stat1*, and *Oas1a* expression was quantified from the ileum and colon tissue of WT mice. Data points represent individual mice and are pooled from 5 independent experiments. Statistical significance was determined by paired t-test where *** = $p < 0.001$ and **** = $p < 0.0001$.

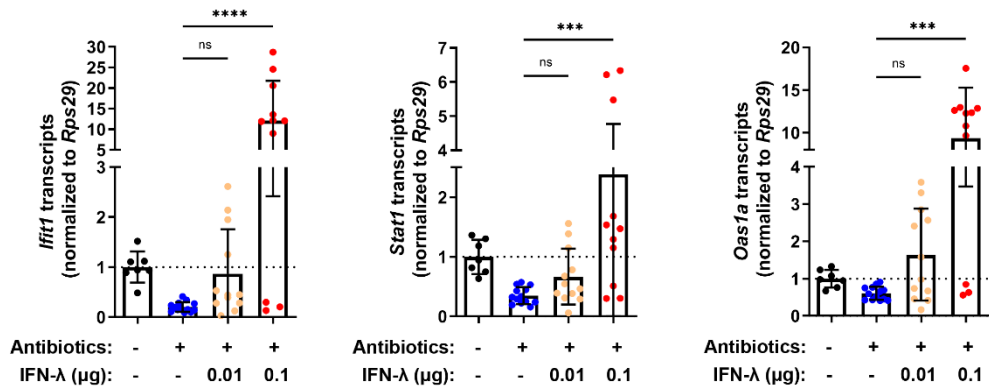


Figure 3.7. Treatment with antibiotics does not ablate responsiveness to IFN- λ . *Ifit1*, *Stat1*, and *Oas1a* expression was quantified in the ileum of WT mice treated with or without ABX and was normalized to untreated mice. Increasing quantities of IFN- λ were intraperitoneally injected into ABX-treated mice to rescue basal ISG expression. Data points represent individual mice and are pooled from 3 independent experiments. Statistical significance was determined by Kruskal-Wallis test with Dunn's multiple comparisons with *** = $p < 0.001$, and **** = $p < 0.0001$.

Homeostatic ISG expression is independent of type I IFN

To determine whether detection of enteric bacteria by TLRs stimulates homeostatic ISGs, we measured tissue ISG expression in mice that were deficient in TRIF or MYD88. Signaling through TRIF results in activation of interferon regulatory factors (IRFs), such as IRF3 and IRF7, that commonly contribute to IFN induction (164, 480, 481). Additionally, signaling through MYD88 can aid initiation of IFN expression, through nuclear factor kappa-light-chain-enhancer of activated B cells (NF- κ B) transcription factor family members (480) and IRF7 (482, 483). *Ifit1* expression in the ileum and colon of *Trif*^{-/-} mice was not significantly different than in WT mice, and *Ifit1* expression was reduced with ABX in *Trif*^{-/-} mice (**Figure 3A**). However, we found that mice lacking *Myd88* exhibited tissue-specific decreases in *Ifit1* expression, with significant decreases in the ileum, but not in the colon, relative to WT mice (**Figure 3A**). These data are consistent with a previous report (478) and suggest that signaling through MYD88, but not TRIF, is necessary for homeostatic ISG expression in the ileum, whereas other factors may dominate in the colon.

To expand these findings, we assessed the role of IRF3 and IRF7 transcription factors that are commonly activated downstream of MYD88 and TRIF. We did not observe significant decreases in *Ifit1* expression in the ileum or the colon of *Irf3*^{-/-} mice as compared to WT (**Figure 3.8B**), indicating that IRF3 is not required for homeostatic IFN- λ induction. However, we observed a modest (two-fold) decrease in *Ifit1* expression in both the ileum and colon of *Irf7*^{-/-} mice when compared to WT mice (**Figure 3.8B**). Although IRF7 is implicated by these data, it does not appear to be strictly required for homeostatic expression of *Ifit1* because expression is further reduced by ABX treatment (**Figure 3.8B**). These data suggest that IRF7 is not necessary for the homeostatic ISG response to the bacterial microbiota.

Type I and III IFNs stimulate overlapping ISG responses that are both dependent on STAT1. Therefore, to further investigate the contribution of type I IFN signaling to homeostatic ISG expression, we quantified *Ifit1* expression in ileum and colon tissue from *Ifnar1*^{-/-} or *Stat1*^{-/-} mice. *Ifit1* expression was not significantly different in either ileum or colon tissue of *Ifnar1*^{-/-} mice compared to WT (**Figure 3.8C**). However, *Ifit1* expression was significantly lower in ileum and colon tissue of *Stat1*^{-/-} mice compared to *Ifnar1*^{-/-} and WT mice. Importantly, treatment of *Stat1*^{-/-} mice with ABX did not further reduce *Ifit1* expression, emphasizing the necessity of STAT1 for this homeostatic ISG response.

Lastly, to determine whether type I IFN signaling plays a compensatory role in homeostatic ISG expression in the absence of *Ifnlr1*, we bred mice with heterozygous expression of both *Ifnlr1* and *Ifnar1* (*Ifnlr1*^{Het}/*Ifnar1*^{Het}) with mice that lack *Ifnlr1* and *Ifnar1* (*Ifnlr1*^{KO}/*Ifnar1*^{KO}). This breeding scheme produced littermate-matched mice that were *Ifnlr1*^{Het}/*Ifnar1*^{Het}, *Ifnlr1*^{KO}/*Ifnar1*^{KO}, and mice singly deficient in *Ifnlr1* (*Ifnlr1*^{KO}/*Ifnar1*^{Het}) or *Ifnar1* (*Ifnlr1*^{Het}/*Ifnar1*^{KO}). We found that *Ifit1* expression was not significantly different in *Ifnlr1*^{Het}/*Ifnar1*^{KO} relative to *Ifnlr1*^{Het}/*Ifnar1*^{Het} controls in ileal tissue (**Figure 3.8D**). *Ifit1* expression in *Ifnlr1*^{KO}/*Ifnar1*^{Het} was significantly lower compared to *Ifnlr1*^{Het}/*Ifnar1*^{Het} controls, but was not significantly different from *Ifnlr1*^{KO}/*Ifnar1*^{KO} mice (**Figure 3.8D**). Cumulatively, these data indicate that homeostatic ISG expression in the intestine is partly dependent on MYD88, and is independent of type I IFN signaling.

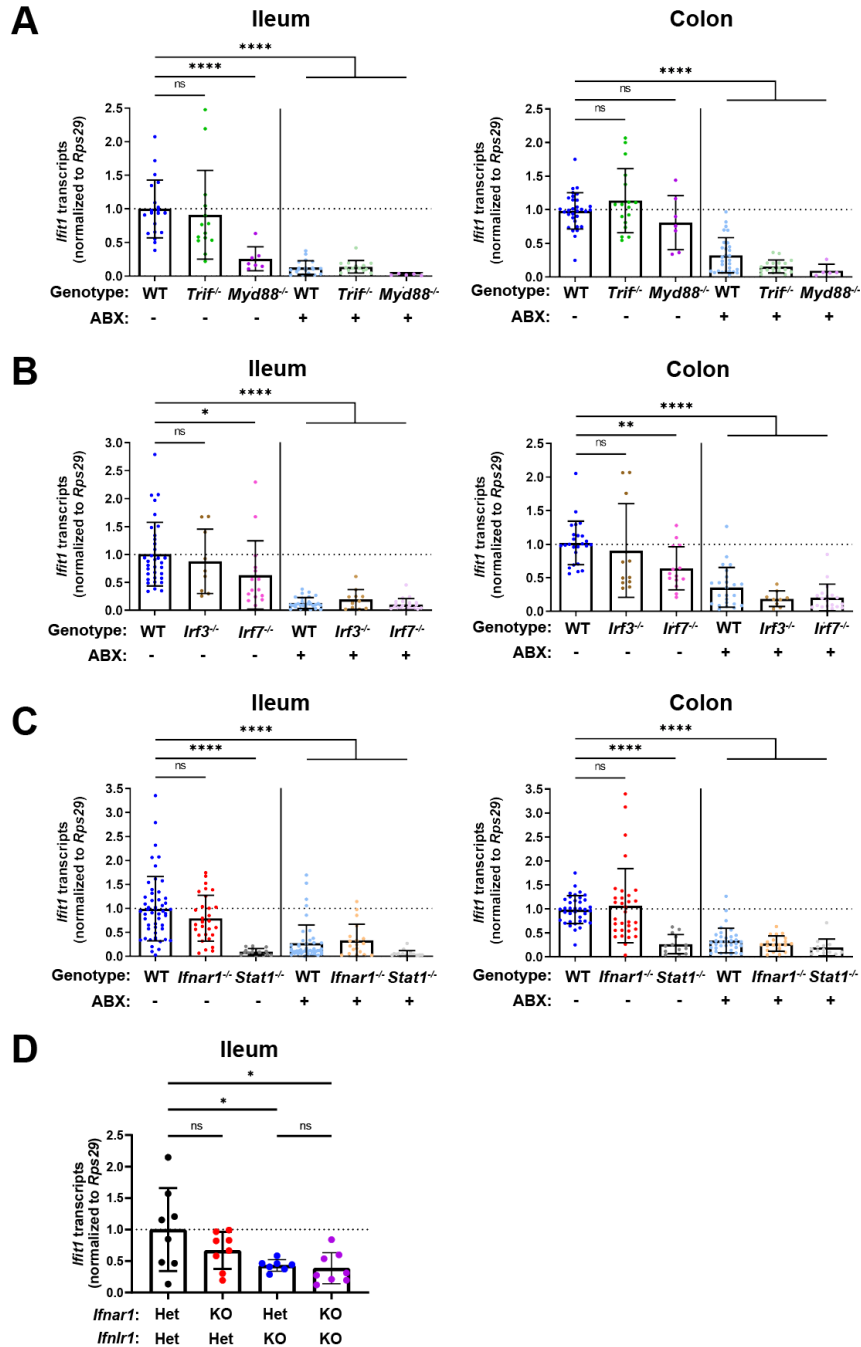


Figure 3.8. Homeostatic ISG expression is independent of type I IFN. *Ifit1* expression levels were assessed by qPCR from the ileum or colon of (A) *Trif*^{-/-} and *Myd88*^{-/-}, (B) *Irf3*^{-/-} and *Irf7*^{-/-}, or (C) *Ifnar1*^{-/-} and *Stat1*^{-/-} mice treated with or without ABX normalized to untreated, WT mice. Some WT controls are shared across experiments in (A-C). D. *Ifit1* expression was measured by qPCR in ileum tissue of indicated genotypes. Data points represent individual mice and are pooled from at least six independent experiments in (A-C) and two independent experiments in (D). Statistical significance was determined by one-way ANOVA with Dunnett's multiple comparisons in (A-C) and one-way ANOVA with Tukey's multiple comparisons in D, where * = $p < 0.05$, ** = $p < 0.01$, *** = $p < 0.001$, **** = $p < 0.0001$.

Homeostatic ISG expression in the intestine is restricted to epithelial cells

Given the primarily epithelial expression of *Ifnlr1*, we assessed which compartment of the ileum expresses homeostatic ISGs by isolating a stripped intestinal epithelial fraction and digesting the underlying lamina propria. We assessed ISG expression in these two fractions from WT and *Ifnlr1*^{-/-} mice treated with or without ABX. Treatment with ABX or loss of *Ifnlr1* reduced homeostatic ISGs in the IEC fraction, but the lamina propria had low expression of these ISGs relative to the epithelium of untreated WT mice, regardless of treatment or genotype (**Figure 3.9A**).

IECs express abundant *Ifnlr1*, but other intra-epithelial cell types do not (191, 194). To determine whether *Ifnlr1* expression by IECs was required for homeostatic ISG expression, we used mice with IECs that are conditionally deficient in *Ifnlr1* (*Ifnlr1*^{ΔIEC}) and littermates that retain normal *Ifnlr1* expression (*Ifnlr1*^{fllox/fllox}) (200). *Ifit1* and *Oas1a* expression in the ileum (**Figure 3.9B**) and colon (**Figure 3.9C**) of *Ifnlr1*^{fllox/fllox} mice was decreased upon treatment with ABX, consistent with the phenotype observed in WT mice. Conditional deletion of *Ifnlr1* in IECs reduced *Ifit1* and *Oas1a* to a similar extent as the reduction observed in *Ifnlr1*^{-/-} animals, above (**Figure 3.5A-B**). Together, these findings indicate that homeostatic ISGs are dependent on *Ifnlr1*-expression by IECs.

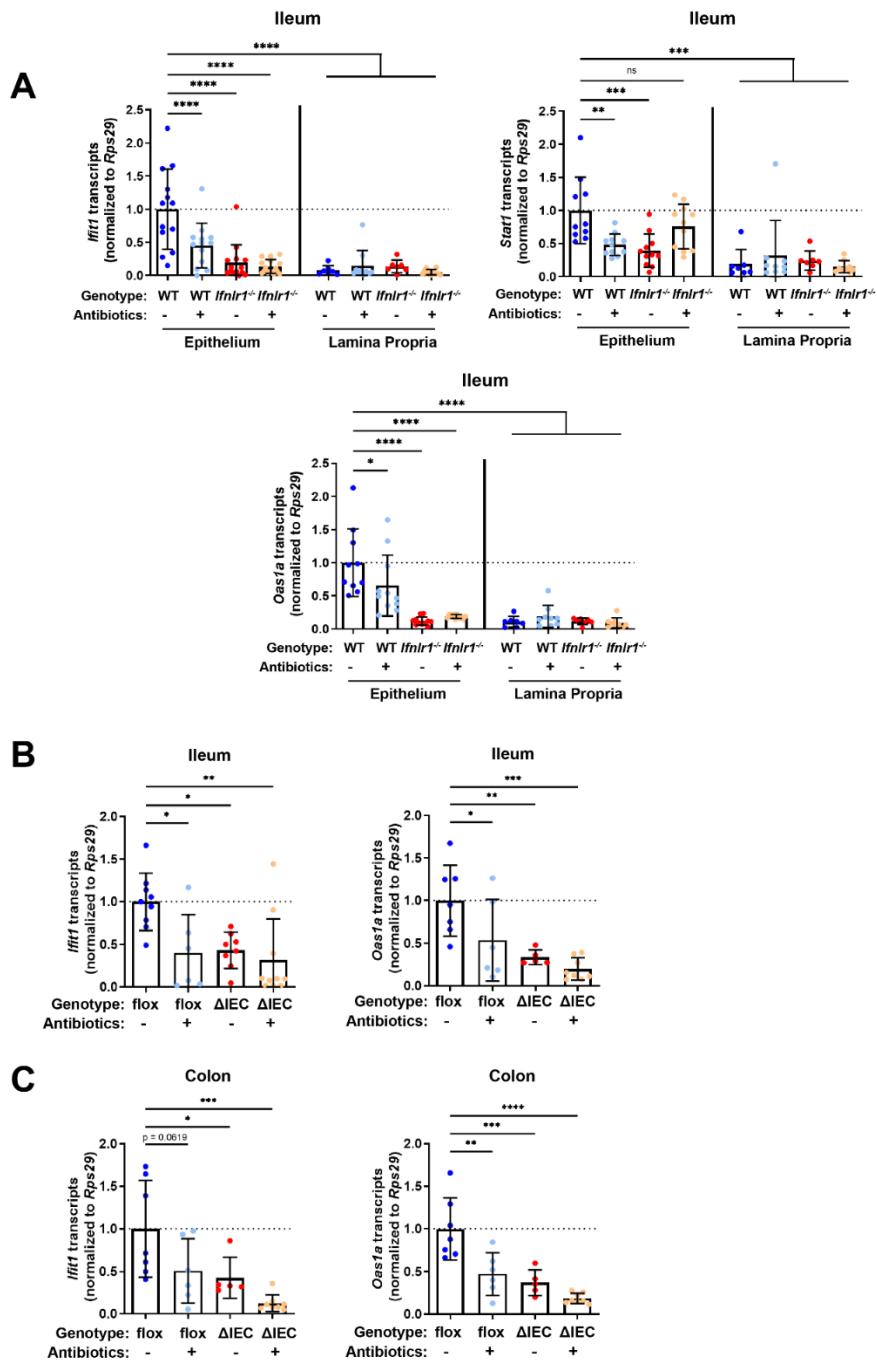


Figure 3.9. Homeostatic ISG expression in the intestine is restricted to epithelial cells. A. *Ifit1*, *Stat1*, and *Oas1a* expression was quantified in stripped epithelial cells or in the lamina propria cells of the ileum. Comparisons were performed between WT and *Ifnlr1*^{-/-} mice with or without ABX treatment, and ISG expression was normalized to WT values. **B-C.** *Ifit1* and *Oas1a* expression from the **(B)** ileum or **(C)** colon of mice with conditional presence (flox) or absence (Δ IEC) of *Ifnlr1* in intestinal epithelial cells. Data points represent individual mice and are pooled from three independent experiments in **(A)** and two independent experiments in **(B-C)**. Statistical significance was determined by one-way ANOVA with Dunnett's multiple comparisons. * = $p < 0.05$, ** = $p < 0.01$, *** = $p < 0.001$.

Bacterial microbiota stimulate expression of *Ifn12/3* by CD45-positive cells

A previous study (194) noted the presence of IFN- λ transcripts (*Ifn12/3*) at homeostasis in CD45+ cells within the stripped intestinal epithelium, but not in the lamina propria. To extend these findings and to determine whether CD45+ cells in the intestinal epithelium produce IFN- λ in response to bacterial microbiota at homeostasis, we enriched cell subsets from epithelial or lamina propria fractions of the ileum for quantification of *Ifn12/3* by qPCR. We treated WT mice with control, ABX, or stimulation with a synthetic dsRNA analogue (poly I:C). We then magnet-enriched EpCAM+ or CD45+ cells from stripped intestinal epithelium or digested lamina propria ileal tissue (**Figure 3.11**). We found that CD45+ cells from the intestinal epithelial and lamina propria fraction expressed detectable *Ifn12/3* at homeostasis, but EpCAM+ cells did not, which is consistent with Mahlaköiv et al. Furthermore, we found that expression of *Ifn12/3* in CD45+ cells from the epithelial fraction was significantly reduced with ABX-treatment, and CD45+ cells from lamina propria had a non-statistically-significant ($p = 0.0523$) reduction in *Ifn12/3* expression with ABX-treatment (**Figure 3.10A**). From these data, we conclude that epithelium-associated CD45+ leukocytes are the likely source of homeostatic IFN- λ in response to bacterial microbiota, but we do not rule out additional involvement of CD45+ cells in the lamina propria.

Similar to *Ifn12/3*, we found that CD45+ cells of the epithelial fraction modestly expressed IFN- β transcript (*Ifnb1*) at homeostasis. Additionally, CD45+ cells of the lamina propria robustly expressed *Ifnb1* at homeostasis. However, unlike *Ifn12/3*, *Ifnb1* was not decreased in mice treated with ABX (**Figure 3.10B**). These data indicate that *Ifnb1* expression by CD45+ cells in the intestine is less dependent on stimulation by bacterial

microbiota relative to *Ifn12/3*, consistent with the dominant role of IFN- λ responses in driving homeostatic ISG expression in the epithelium.

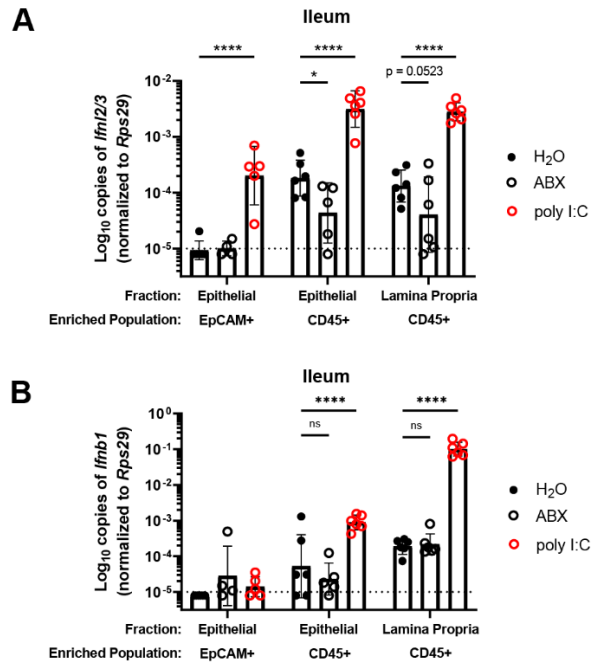


Figure 3.10. Bacterial microbiota stimulate expression of *IfnI2/3* by CD45-positive cells. A-B. Cellular suspensions from the ileal epithelium and lamina propria was harvested from WT mice treated with H₂O, ABX, or stimulated with poly I:C. Resulting cells were enriched for EpCAM-positive and CD45-positive cells by magnetic separation. *IfnI2/3* expression (**A**) and *Ifnb1* expression (**B**) was quantified from each enriched cellular fraction by qPCR. Data points represent individual mice and are pooled from 2 independent experiments. Statistical significance was determined by two-way ANOVA with Dunnett's multiple comparisons, where * = $p < 0.05$ and **** = $p < 0.0001$.

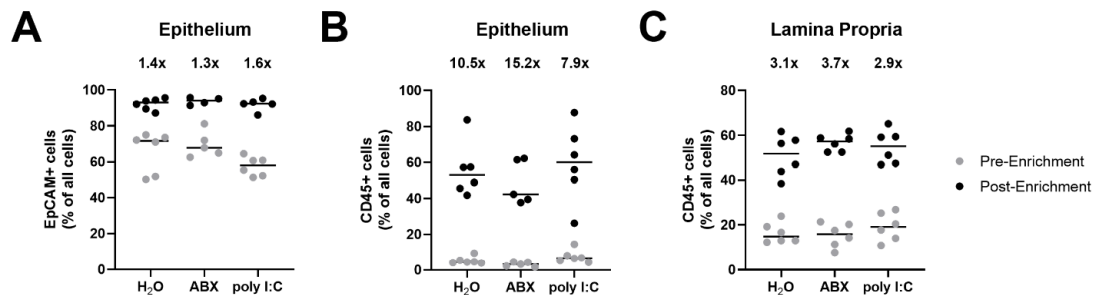


Figure 3.11. Enrichment of EpCAM+ and CD45+ cells from the intestinal epithelium and lamina propria. A-C. The ileal epithelium and lamina propria was harvested from WT mice treated with H₂O, ABX, or stimulated with poly I:C. Resulting cell suspensions were enriched for EpCAM-positive and CD45-positive cells and the purity of all live and dead cells pre- and post-enrichment were quantified by flow cytometry. The percentage of live and dead cell events with surface expression of (A) EpCAM or (B) CD45 prior to- and following- enrichment from stripped intestinal epithelium. C. The percentage of live and dead cell events with surface expression of CD45 prior to and following CD45 enrichment from isolated lamina propria. Mean fold enrichment for each condition is noted above each column. Data points represent individual mice and are pooled from 2 independent experiments.

Homeostatic ISG expression in the small intestine is highly localized

Homeostatic ISG expression in the ileum was of relatively low magnitude when compared to IFN- λ treatment (**Figures 3.1-3.5**). Therefore, we hypothesized that a low abundance of homeostatic ISG expression would be uniformly distributed between IECs of the intestinal epithelium, and we sought to assess the distribution of the homeostatic ISG, *Ifit1*, using *in situ* hybridization (RNAscope). Contrary to our hypothesis, RNAscope staining of the ileum from untreated WT mice revealed localized pockets of robust *Ifit1* expression in individual villi rather than ubiquitously low expression throughout the intestinal epithelium (**Figure 3.12A**). Additionally, *Ifit1* localization was skewed away from the crypt and towards the tips of individual villi within the ileum, and this localization was not specific to *Ifit1* because the distinct ISG *Usp18* co-localized with *Ifit1* (**Figure 3.12A**). These data indicate that homeostatic ISGs are sporadically expressed in individual villi and are primarily localized to mature enterocytes that are most distally located in villi. We determined that localized ISG expression within individual villi was not due to a localized ability to respond to IFN- λ because stimulation with exogenous IFN- λ resulted in *Ifit1* expression within all intestinal villi, but not intestinal crypts (**Figure 3.13**). The minimal expression of *Ifit1* within intestinal crypts following exogenous IFN- λ treatment suggests that homeostatic ISGs are localized to mature enterocytes because intestinal crypts do not exhibit robust responses to IFN- λ . Additionally, the non-uniform distribution of homeostatic *Ifit1* expression was ablated in the ileum of mice treated with ABX (**Figure 3.12B-D**), consistent with a dependency on bacterial microbiota. To determine whether localized *Ifit1* expression was dependent on IEC expression of *Ifnlr1*, we assessed the distribution of *Ifit1* expression in the ilea of littermate *Ifnlr1*^{flox/flox} and *Ifnlr1* Δ ^{IEC} mice. We found that the localized *Ifit1* expression observed in untreated WT mice was recapitulated

in *Ifnlr1*^{flox/flox} mice (**Figure 3.12E**), but these areas of ISG expression were ablated in *Ifnlr1*^{ΔIEC} mice (**Figure 3.12F-G**). Lastly, we found that this discrete localization of the homeostatic ISG response is not limited to the ileum, as localized *Ifit1* staining is also observed in the colonic epithelium (**Figure 3.14**). Together, our analyses indicated that homeostatic ISGs are expressed in a highly localized manner within the intestinal epithelium.

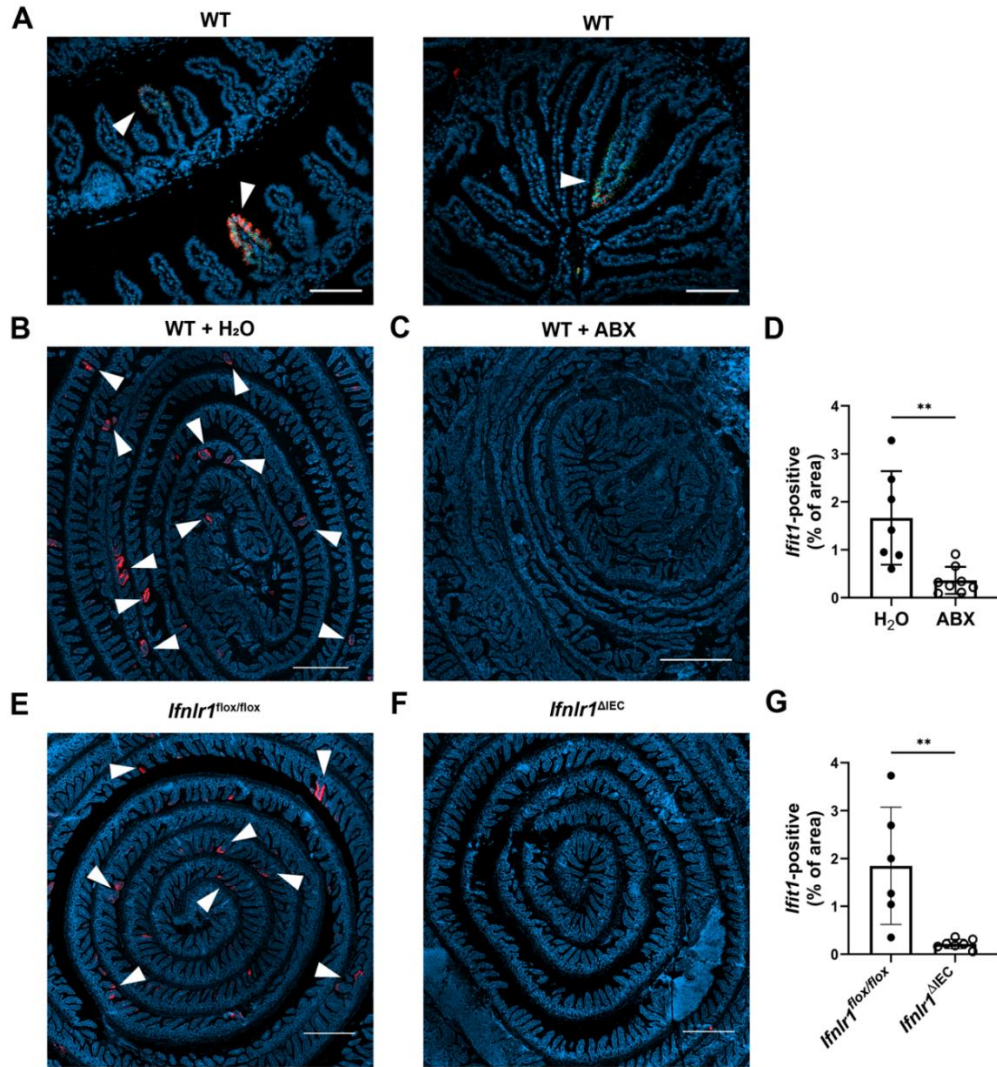


Figure 3.12. Homeostatic ISG expression in the small intestine is highly localized. The ilea of WT, *Ifnlr1^{flox/flox}*, or *Ifnlr1^{ΔIEC}* mice were harvested, processed into a Swiss rolls, and stained by *in situ* hybridization for the ISGs, *Ifit1* (red) and *Usp18* (green), with a DAPI (blue) counterstain. **A.** Representative high-magnification images of co-localized *Ifit1* (red) and *Usp18* (green) expression in the ileum of WT mice, see arrows. **B-D.** WT mice treated with H₂O control or ABX with quantification of *Ifit1* area relative to the total area of the section across replicate mice. **E-G.** *Ifnlr1^{flox/flox}* or *Ifnlr1^{ΔIEC}* mice at homeostasis with quantification of *Ifit1* area relative to the total area of the section across replicate mice. Scale bar = 100μm in **(A)** and 500μm in **(B-G)** and. Statistical significance was calculated by unpaired t-test where ** = p < 0.01. Each data point in **(D)** and **(G)** represents an individual mouse from 2 independent experiments.

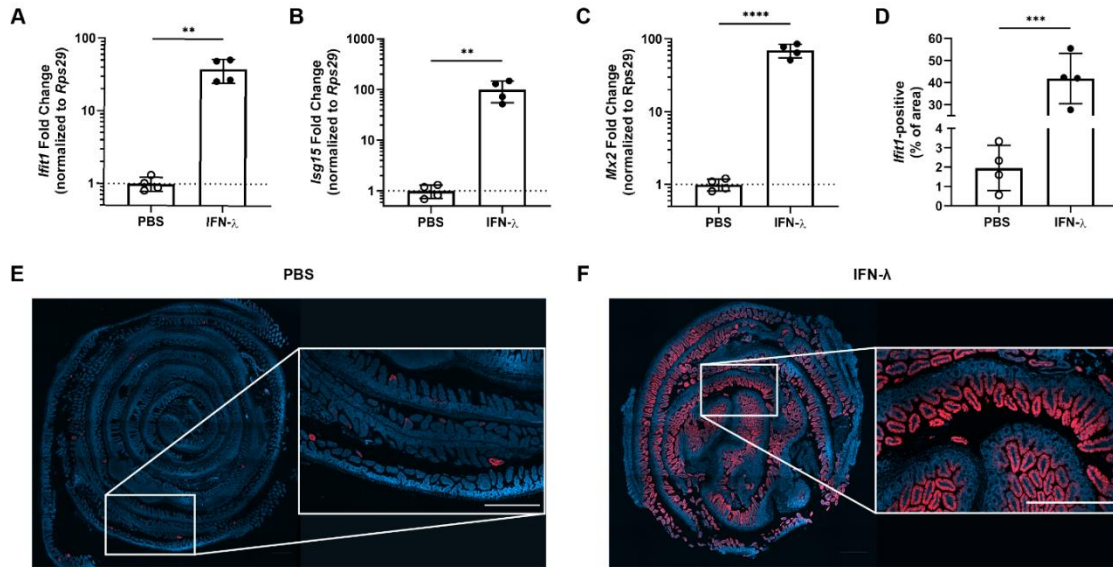


Figure 3.13. The entire intestinal epithelium is responsive to IFN-λ. Wild-type mice were injected with PBS or 3μg of pegylated IFN-λ3. The ileum was harvested after four hours and a small section was assessed for expression of the ISGs: *Ifit1* (A), *Isg15* (B), and *Mx2* (C) by qPCR. The remaining tissue was stained by RNAscope for the ISG, *Ifit1* (red), with a DAPI (blue) counterstain. D. Quantification of *Ifit1* area relative to the total area of the section across replicate mice. E-F. Representative images from the ileum of mice injected with PBS (E) or IFN-λ (F). Scale bar = 500μm in insets. Data points represent individual mice from a single experiment. Statistical significance was determined by unpaired t-test with ** = $p < 0.01$, *** = $p < 0.001$, and **** = $p < 0.0001$.

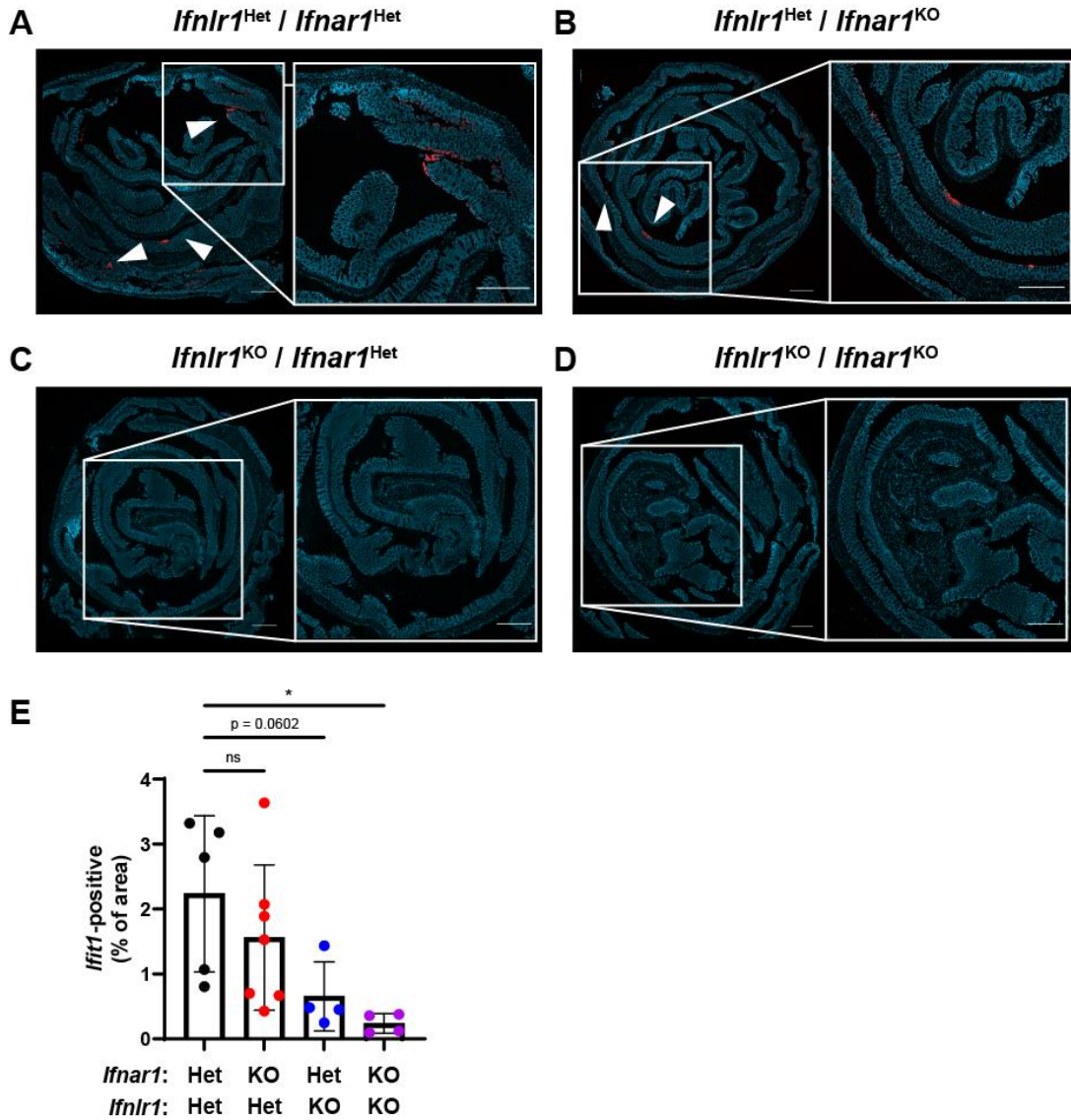


Figure 3.14. Homeostatic ISG expression is also highly localized in the colon. The colon of *Ifnlr1^{Het}/Ifnar1^{Het}*, *Ifnlr1^{Het}/Ifnar1^{KO}*, *Ifnlr1^{KO}/Ifnar1^{Het}*, and *Ifnlr1^{KO}/Ifnar1^{KO}* mice was harvested and stained by RNAscope for the ISG, *Ifit1* (red), with a DAPI (blue) counterstain. Representative images from (A) *Ifnlr1^{Het}/Ifnar1^{Het}*, (B) *Ifnlr1^{Het}/Ifnar1^{KO}*, (C) *Ifnlr1^{KO}/Ifnar1^{Het}*, and (D) *Ifnlr1^{KO}/Ifnar1^{KO}* mice with (E) quantification of *Ifit1* area from individual mice. Data are representative of two independent experiments. Scale bar = 500µm.

Mature enterocytes express homeostatic ISGs in public single-cell datasets from mouse and human

To determine the extent of conservation of homeostatic ISG expression by IECs, we performed orthogonal analyses of publicly available single-cell RNA-seq (scRNA-seq) datasets from mouse (42) and human (484) IECs. Recently, Haber et al. published a large single-cell RNA sequencing dataset that profiled sorted IECs from the small intestine of specific-pathogen-free mice and defined 15 distinct IEC subtypes (42). We analyzed IECs from this dataset, and found that of the 21 homeostatic ISGs identified in **Figure 3.1D**, 19 were present in the Haber et al. single-cell dataset. We determined the percentage of each epithelial cell subtype that expresses each individual homeostatic ISG, and generated a heatmap with hierarchical clustering to group IEC subtypes that have similar ISG expression patterns (**Figure 3.15A**). Homeostatic ISGs were predominantly expressed in mature enterocyte subtypes, which clustered separately from crypt-resident progenitor IECs such as transit amplifying (TA) cells and stem cells (**Figure 3.15A**). To compare homeostatic ISG expression between polar extremes of the crypt-villus axis, we grouped IEC subtypes that represented enterocytes (mature enterocyte cells) and crypt-associated cells (TA cells and stem cells) to compare the overall proportions of these cells with homeostatic ISG expression. We found that a significantly higher percentage of enterocytes express homeostatic ISGs than crypt-associated cells, but that these homeostatic ISGs were expressed in a relatively small proportion of enterocytes (< 20%) (**Figure 3.15B**). Notably, *Ifit1* (highlighted in red) was present in ~5% of enterocytes by scRNA-seq, which is consistent with our observation of 1-4% *Ifit1*-positive area by imaging the mouse small intestine (**Figure 3.12B-G**). Furthermore, the relative absence of ISG-positive crypt-associated cells in this scRNA-seq data is consistent with our observation that intestinal crypts lacked *Ifit1* and *Usp18* expression by imaging.

We expanded our investigation to a scRNA-seq dataset from the ileum of healthy, human, pediatric patients that was previously described (484). IECs from this dataset were previously clustered by Elmentaite et al and annotated as: enterocytes, early enterocytes, tuft cells, enteroendocrine cells, BEST4 enterocytes, goblet cells, TA cells, and crypt. For our analysis of homeostatic ISG expression, we excluded IEC sub-types with fewer than 20 constituent cells, which retained five annotated groups: enterocytes, early enterocytes, goblet cells, TA cells, and crypt. Of the 21 homeostatic ISGs identified in **Figure 3.1D**, 14 orthologous human genes were present in these data. Similar to analysis in **Figure 3.15A**, we determined the percentage of each group that expressed each individual homeostatic ISG and generated a heatmap of these data with hierarchical clustering to group IEC subtypes that have similar ISG expression patterns (**Figure 3.15C**). Enterocyte, early enterocyte, and goblet subtypes clustered separately from TA cells and crypt, with the highest proportion of homeostatic ISGs being present in the enterocyte subtype (**Figure 3.15C**). As with mouse IEC data, above, we grouped annotated cells that localize in the crypt (TA cells and crypt) and compared overall proportions of homeostatic ISG expression with the mature enterocyte subtype (**Figure 3.15D**). Similar to mice, homeostatic ISGs were present in significantly more enterocytes than crypt-associated cells, and most homeostatic ISGs in this human dataset were present in a relatively small proportion of cells (< 20%). These human data suggest that ISGs may be present in a small proportion of IECs from healthy, human ileal tissue at homeostasis and may share the localization observed in our murine analyses. Our analysis of a murine scRNA-seq dataset support our previous observations that homeostatic ISGs are not ubiquitously expressed throughout the intestinal epithelium; rather, they are expressed in a minority of IECs and skewed towards mature enterocytes along the crypt-villus axis. Our analysis of a human scRNA-seq dataset are consistent with observations in the murine model, though

future studies will be required to definitively address the existence of homeostatic ISGs in human tissue.

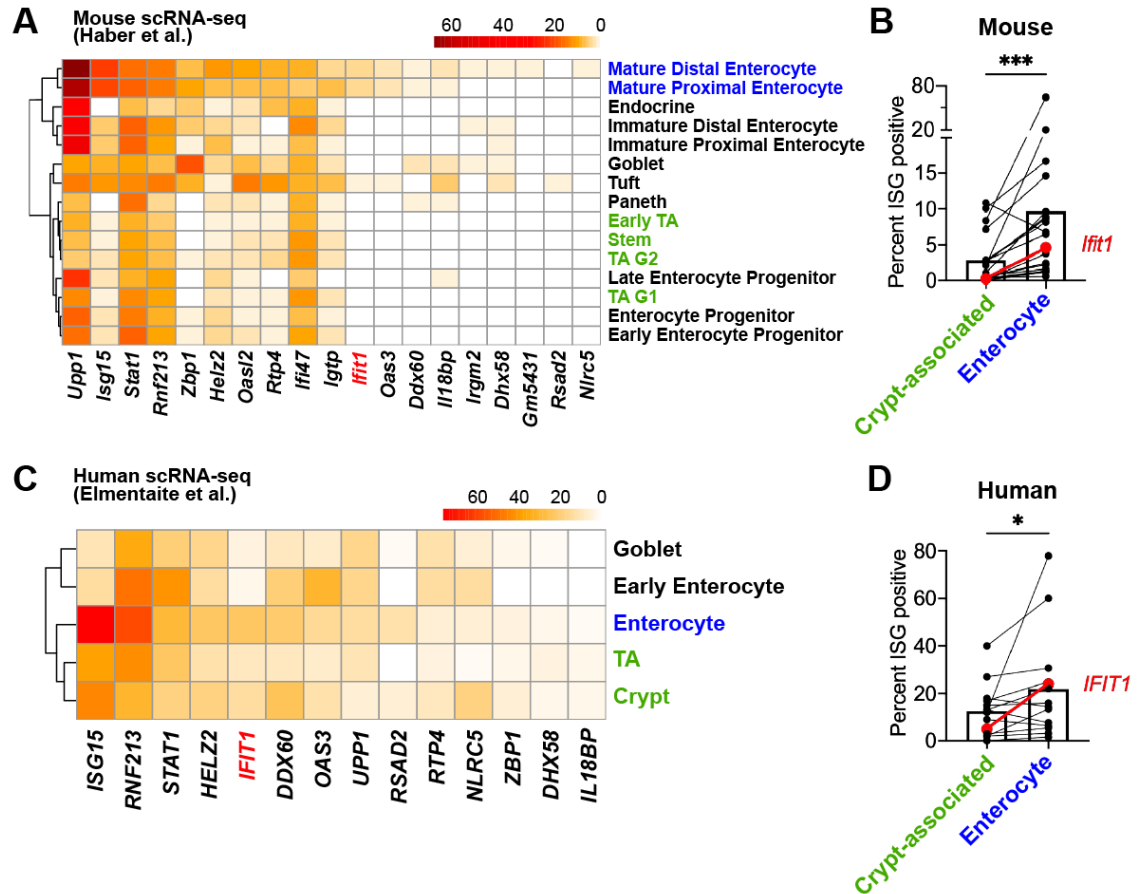


Figure 3.15. Mature enterocytes express homeostatic ISGs in public single-cell datasets from mouse and human. **A-B.** A mouse IEC single-cell transcriptional dataset (42) (GSE92332) was analyzed to determine the percentage of each epithelial cell subtypes that express homeostatic ISGs. **A.** Heatmap depicting the proportion of each epithelial cell type expressing nineteen of the twenty-one homeostatic ISGs identified in **Figure 3.1**. **B.** Enterocyte subtypes (blue text) and crypt-resident progenitor subtypes (green text) cells were grouped and the percentage of cells that express each homeostatic ISG was compared. **C-D.** A human IEC single-cell transcriptional dataset (484) (E-MTAB-8901) was analyzed for the percentage of epithelial cell subtypes that express homeostatic ISGs. **C.** A heatmap depicting the percentage of IEC subtypes that express human orthologs of murine homeostatic ISGs identified in **Figure 3.1**. **D.** The mature enterocyte subtype (blue text) and crypt-resident progenitor subtypes (green text) were grouped and the percentage of cells that express each homeostatic ISG was compared. Lines in **(B)** and **(D)** link paired ISGs in each IEC subset. Statistical significance in **(B)** and **(D)** was calculated by Wilcoxon test where * = $p < 0.05$, and *** = $p < 0.001$.

Assessing the effect of peroral bacterial products on localized homeostatic ISGs in ABX-treated mice

To further define the relationship between bacteria and homeostatic ISGs, we assessed whether oral administration of fecal contents or purified LPS (a bacterial MAMP and TLR4 agonist) could restore localized ISG expression in mice with depleted bacterial microbiota. Control groups of *Ifnlr1^{flox/flox}* mice with conventional microbiota (**Figure 3.16A**) retained a localized *Ifit1* expression pattern, whereas ABX-treated *Ifnlr1^{flox/flox}* mice (**Figure 3.16B**) and *Ifnlr1^{ΔIEC}* mice (**Figure 3.16C**) lacked *Ifit1* expression. Oral LPS administered to conventional *Ifnlr1^{flox/flox}* mice did not significantly alter the distribution or frequency of localized *Ifit1* expression (**Figure 3.16D**). However, localized *Ifit1* expression was visible in 4/12 ABX-treated *Ifnlr1^{flox/flox}* mice administered LPS (**Figure 3.16E, 3.16H-I**). In ABX-treated *Ifnlr1^{flox/flox}* mice treated with fecal transplant of conventional microbes, localized expression of *Ifit1* was visible in 4/8 mice (**Figure 3.16F, 3.16H-I**). Importantly, we did not observe localized *Ifit1* expression in *Ifnlr1^{ΔIEC}* mice following LPS administration (**Figure 3.16G**), indicating that LPS-stimulated *Ifit1* depends on IEC expression of *Ifnlr1*.

We noted that the visibility of localized *Ifit1* signal following LPS administration or fecal transplant appeared largely binary (i.e. present or absent) in our imaging data (**Figures 3.16E-F**, representative *Ifit1*-positive and *Ifit1*-negative images). Using quantification of *Ifit1* area (**Figure 3.16H**), we stratified mice into *Ifit1*-positive and *Ifit1*-negative groups (**Figure 3.16I-J**) based on a cut-off set at the maximal *Ifit1* area value of *Ifnlr1^{ΔIEC}* mice (dashed line in **Figure 3.16H**). Results of this unbiased stratification were consistent with visible *Ifit1* staining and indicated that 8/8 conventional *Ifnlr1^{flox/flox}* mice, 0/8 ABX-treated control mice, 4/12 LPS-treated mice, and 4/8 fecal transplant mice were *Ifit1*-positive (**Figure 3.16I-J**). Statistical analysis by Fisher's exact test indicated that LPS administration non-significantly increased ($p = 0.1022$) the proportion of mice that were

Ifit1-positive, whereas fecal reconstitution of ABX-treated mice significantly increased the likelihood of these mice being *Ifit1*-positive (**Figure 3.16J**). Importantly, mice that received fecal transplant had full restoration of 16S gene copies (**Figure 3.16K**) despite only 4/8 having homeostatic *Ifit1* expression. These findings suggest that reconstitution of the homeostatic ISG signal by fecal transfer has incomplete penetrance at this timepoint, underscoring the incomplete presence of localized *Ifit1* expression (4/12) in ABX-treated mice administered peroral LPS.

To corroborate and extend these findings, we performed orthogonal analyses of *Ifit1*, *Stat1*, and *Oas1a* expression in ileum tissue of WT mice treated with ABX followed by fecal transplant, LPS administration, administration of the TLR5 agonist: flagellin, or administration of TLR9 agonist: CpG DNA (**Figure 3.17**). Similar to imaging data, these qPCR data exhibited high variance. However, stratification of tissues into positive and negative for each ISG indicated that peroral administration of LPS to ABX-treated mice increased the proportion of ISG-positive tissues by 21-36% (*Ifit1*: $p=0.065$; *Stat1*, $p<0.05$; *Oas1a*, $p<0.05$). Additionally, peroral administration of flagellin significantly increased the proportion of ISG-positive mice by 25-44% (*Ifit1*: $p=0.052$; *Stat1*, $p<0.01$; *Oas1a*, $p<0.05$), whereas CpG DNA did not significantly increase the proportion of ISG-positive mice (**Figure 3.17**). Together, these data suggest that LPS and flagellin are sufficient to stimulate homeostatic ISG expression in a significant proportion of ABX-treated mice. The ability of multiple PRR ligands to stimulate homeostatic ISGs suggests that exposure to a variety of bacterial MAMPs is the basis for localized, homeostatic ISG expression.

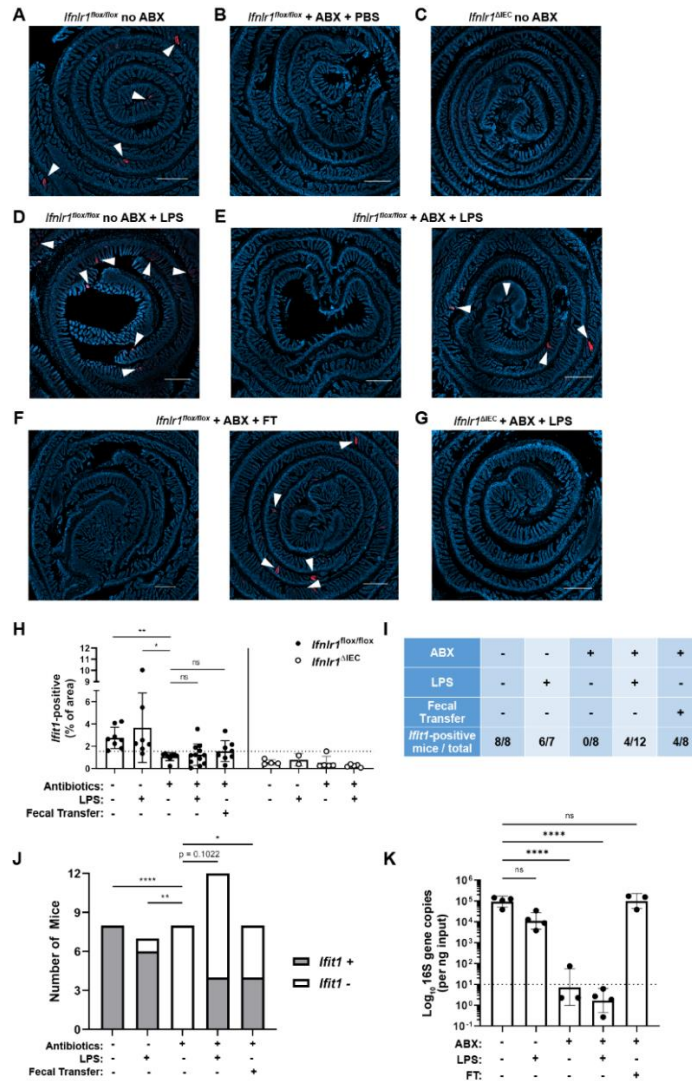


Figure 3.16. Assessing the effect of peroral bacterial products on localized homeostatic ISGs in ABX-treated mice. The ilea of treated WT, *Ifnlr1^{flox/flox}*, and *Ifnlr1^{ΔIEC}* mice were harvested, processed into Swiss rolls, and stained by *in situ* hybridization for the ISG, *Ifit1* (red), with a DAPI (blue) counterstain. **A-C.** Representative images from *Ifnlr1^{flox/flox}* mice treated with H₂O control followed by PBS stimulation (**A**), ABX followed by PBS stimulation (**B**), or from *Ifnlr1^{ΔIEC}* mice (**C**). **D.** Representative images of *Ifnlr1^{flox/flox}* mice treated with H₂O control followed by LPS stimulation. **E-F.** Two representative images of *Ifnlr1^{flox/flox}* mice treated with ABX followed by LPS stimulation (**E**) or ABX followed by fecal transplantation (**F**). **G.** A representative image of *Ifnlr1^{ΔIEC}* mice treated with ABX followed by LPS stimulation. **H.** Quantification of *Ifit1* area relative to the total area of each tissue section with a dashed line at the highest *Ifnlr1^{ΔIEC}* value. The proportion of *Ifit1*-positive mice (above dashed line) and *Ifit1*-negative mice (below dashed line) are tabulated (**I**) and graphed (**J**) for *Ifnlr1^{flox/flox}* mice of each condition. **K.** rDNA was isolated from the luminal contents of mice at endpoint harvest. 16S gene copies were assessed by qPCR and normalized to input. Limit of detection: dashed line. Where depicted, scale bar = 500μm. Data points represent individual mice and are pooled from 4 independent experiments in (**A-J**) and from 2 independent experiments in (**K**). Statistical significance was determined by Kruskal-Wallis with Dunn's multiple comparisons in (**H**), by one-way ANOVA with Dunn's multiple comparisons in (**K**), and by Fisher's exact tests in (**J**) where * = $p < 0.05$, ** = $p < 0.01$, and **** = $p < 0.0001$.

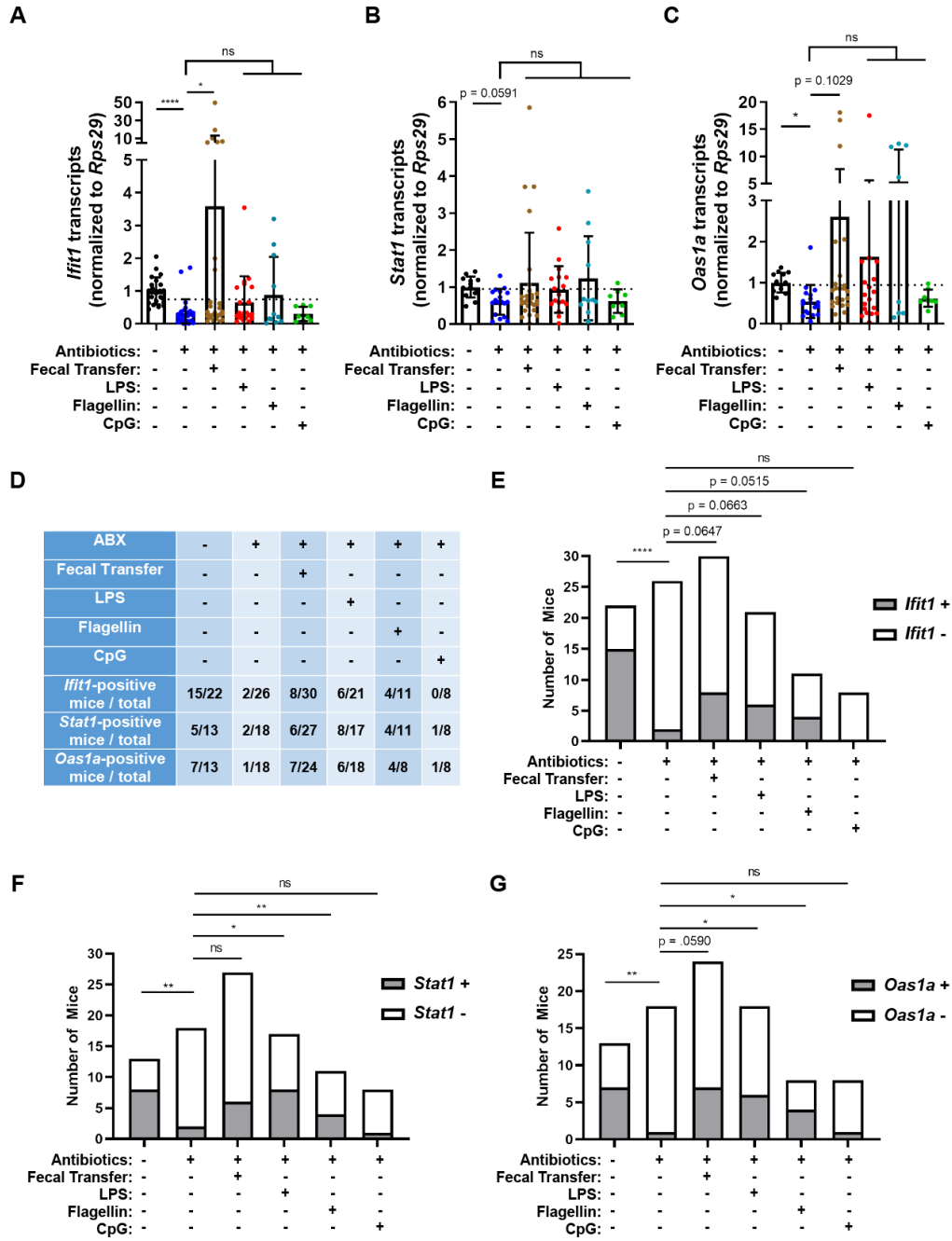


Figure 3.17. Assessing the effect of peroral bacterial products on homeostatic ISGs in ABX-treated mice. The ileum of treated WT, *Ifnlr1^{fllox/fllox}*, and *Ifnlr1^{ΔIEC}* mice was harvested and *Ifit1* (A), *Stat1* (B), and *Oas1a* (C) was quantified by qPCR. Delineation of positive ISG expression was conservatively selected as one standard deviation above the mean of ABX-treated mice (dashed line). Mice were binned into ISG-positive (above dashed line) or ISG-negative (below dashed line) groups and are tabulated for each condition in D. The proportion of mice with expression of *Ifit1* (E), *Stat1* (F), and *Oas1a* (G) are graphed for each condition. Data points represent individual mice and are pooled from 3-9 independent experiments. Statistical significance was determined by Kruskal-Wallis with Dunn's multiple comparisons (A-C) and by Fisher's exact test (E-G) where * = $p < 0.05$, ** = $p < 0.01$, and **** = $p < 0.0001$.

The homeostatic IFN- λ response preemptively protects IECs from murine rotavirus infection

To assess the capacity of homeostatic ISGs to protect IECs from viral infection, we utilized infection with murine rotavirus, an IEC-tropic pathogen. Prior studies of rotaviruses have identified viral immune evasion genes that block IFN induction through multiple mechanisms (241). However, we reasoned that pre-existing ISG expression stimulated by the bacterial microbiome at homeostasis may preemptively protect IECs from the infection before viral gene expression is initiated. To determine the role of an epithelial IFN- λ response over the course of murine rotavirus infection in adult mice, we monitored daily shedding of viral genomes in the stool of *Ifnlr1*^{flox/flox} mice and *Ifnlr1* ^{Δ IEC} littermates. We first detected murine rotavirus shedding in the stool on day two after inoculation and, at this early timepoint, *Ifnlr1* ^{Δ IEC} mice shed 20-fold more murine rotavirus genomes into their stool than *Ifnlr1*^{flox/flox} mice (**Figure 3.18A**). However, at the peak of viral shedding between days three and five, there were no significant differences between *Ifnlr1*^{flox/flox} and *Ifnlr1* ^{Δ IEC} littermates (**Figure 3.18A**). This similarity at peak of viral shedding was consistent with an ability of murine rotavirus to evade the host IFN response once infection is established. Together, these findings suggest that *Ifnlr1* ^{Δ IEC} mice have defects in protection against initiation of murine rotavirus infection and that the protective capacity of endogenous IFN- λ signaling against murine rotavirus is primarily prophylactic in nature.

To more stringently assess the capacity of *Ifnlr1* to protect IECs against the earliest stages of murine rotavirus infection, we inoculated mice with 5000 SD50 (50% shedding dose) to maximize the likelihood of uniform viral exposure throughout the intestine. At 24 hours post-inoculation, we quantified murine rotavirus genomes in the epithelial fraction and the proportion of infected IECs (live, EpCAM-positive, CD45-negative, and murine rotavirus -positive) by flow cytometry. At 24 hours post-inoculation, we found that *Ifnlr1* ^{Δ IEC}

mice had 20-fold more murine rotavirus genomes than *Ifnlr1*^{fllox/fllox} mice (**Figure 3.18B**). In addition, we found that a three-fold greater proportion of IECs were infected in *Ifnlr1*^{ΔIEC} mice than *Ifnlr1*^{fllox/fllox} mice at 24 hours post-infection (**Figure 3.18C-F**). However, the median fluorescence intensity (MFI) of murine rotavirus antigen was equivalent in infected IECs from *Ifnlr1*^{fllox/fllox} and *Ifnlr1*^{ΔIEC} mice (**Figure 3.18G**) and the MFI of murine rotavirus did not correlate ($r^2 = 0.0003$) with the percentage of infected IECs (**Figure 3.18H**). This equivalent antigen burden in infected cells from *Ifnlr1*^{fllox/fllox} and *Ifnlr1*^{ΔIEC} mice in combination with the lack of correlation between antigen burden and percentage of infected cells suggests that the protective role of *Ifnlr1* is to prevent infection of IECs rather than to limit replication within IECs after they are infected. We assessed an earlier timepoint at 12 hours post-inoculation and observed similar trends toward an increased proportion of IEC infection in *Ifnlr1*^{ΔIEC} relative to *Ifnlr1*^{fllox/fllox} littermates, but the extent of infection was 10-100 fold lower and near the limit of detection (**Figure 3.19**). Thus, the 12- and 24-hour timepoints capture the earliest detectable infection of IECs by murine rotavirus, and this early infection is significantly reduced by IFN-λ signaling.

To further contextualize the localization of ISGs and murine rotavirus infected cells over time, we performed *in situ* hybridization for murine rotavirus genomes and *Ifit1* in the ileum of WT mice at 12, 24, and 96 hours post-inoculation. Quantification of co-staining for *Ifit1* in infected cells indicated that a minority (~30%) were *Ifit1*⁺ at 12hr or 24hr post-inoculation, whereas a majority (~63%) of infected cells were *Ifit1*⁺ at 96hr post-inoculation (**Figure 3.18I-J, 3.20**). These co-staining data are consistent with early murine rotavirus evasion of IFN responses within infected IECs, at the same timepoints that we observed increased infection of *Ifnlr1*^{ΔIEC} mice (**Figures 3.18B-F, 3.19**). Furthermore, we found murine rotavirus inoculation did not increase the area of *Ifit1* expression in the intestine at 12-24 hours post-inoculation. However, at 96 hours post-inoculation, we found a

significant increase in epithelial *Ifit1* expression in the ileum that coincided with increased viral genomes and antigen (**Figure 3.21**), suggesting that *Ifit1* expression at 12 and 24 hours post-inoculation is primarily due to the preexisting homeostatic response rather than in response to murine rotavirus infection. Therefore, we propose that homeostatic ISGs stimulated by *Ifnlr1* expression on IECs plays an early protective role against viral infection that preempts viral IFN evasion mechanisms.

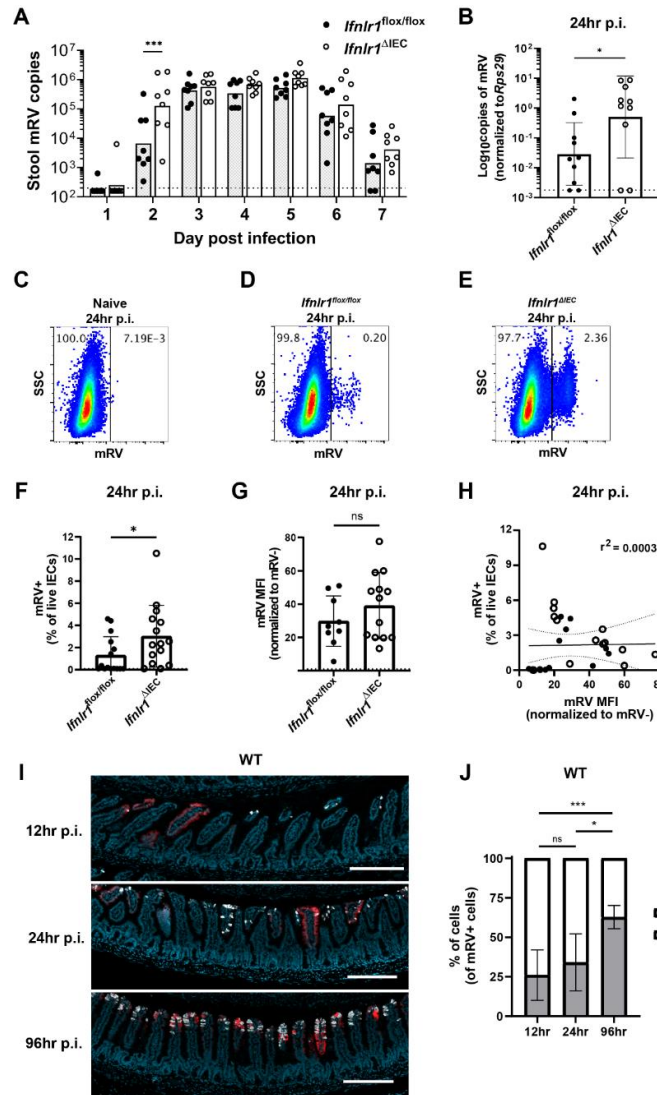


Figure 3.18. The homeostatic IFN- λ response preemptively protects IECs from murine rotavirus infection. *Ifnlr1*^{flox/flox} and *Ifnlr1* ^{Δ IEC} mice were infected with 100 SD50 (A) or 5000 SD50 (B-H) of murine rotavirus and stool (A) or stripped ileal intestinal epithelial cells (B-G) were assessed for murine rotavirus infection. A. Timecourse of genome copies detected in the stool of *Ifnlr1*^{flox/flox} and *Ifnlr1* ^{Δ IEC} mice by qPCR. B-G. Mechanically stripped intestinal epithelial cell fractions were analyzed by qPCR for genome copies (B) or flow cytometry for murine rotavirus antigen-positive IECs (C-G). Representative flow cytometry plots of naïve (C), *Ifnlr1*^{flox/flox} (D), and *Ifnlr1* ^{Δ IEC} (E) infected mice with quantification in (F). G. The MFI of murine rotavirus antigen in infected cells relative to uninfected cells. H. A linear correlation plot of murine rotavirus + cells and murine rotavirus MFI with 95% confidence intervals (dashed lines). I-J. WT mice were infected with 5000 SD50 of murine rotavirus and the ilea were processed into Swiss rolls and stained by *in situ* hybridization for the ISG, *Ifit1*, or murine rotavirus. The percentage of murine rotavirus infected cells that were *Ifit1*-positive and *Ifit1*-negative were determined. Additional representative images for (I-J) are depicted in Figure 3.20. Where designated in (A-G), dashed lines = LOD as set by naïve mice. Data points represent individual mice and are pooled from 2-3 independent experiments. Statistical significance was determined by two-way ANOVA with Sidak's multiple comparisons (A), by Mann Whitney (B, F), unpaired t-test (G), or Kruskal-Wallis with Dunn's multiple comparisons (J), where * = $p < 0.05$ and *** = $p < 0.001$.

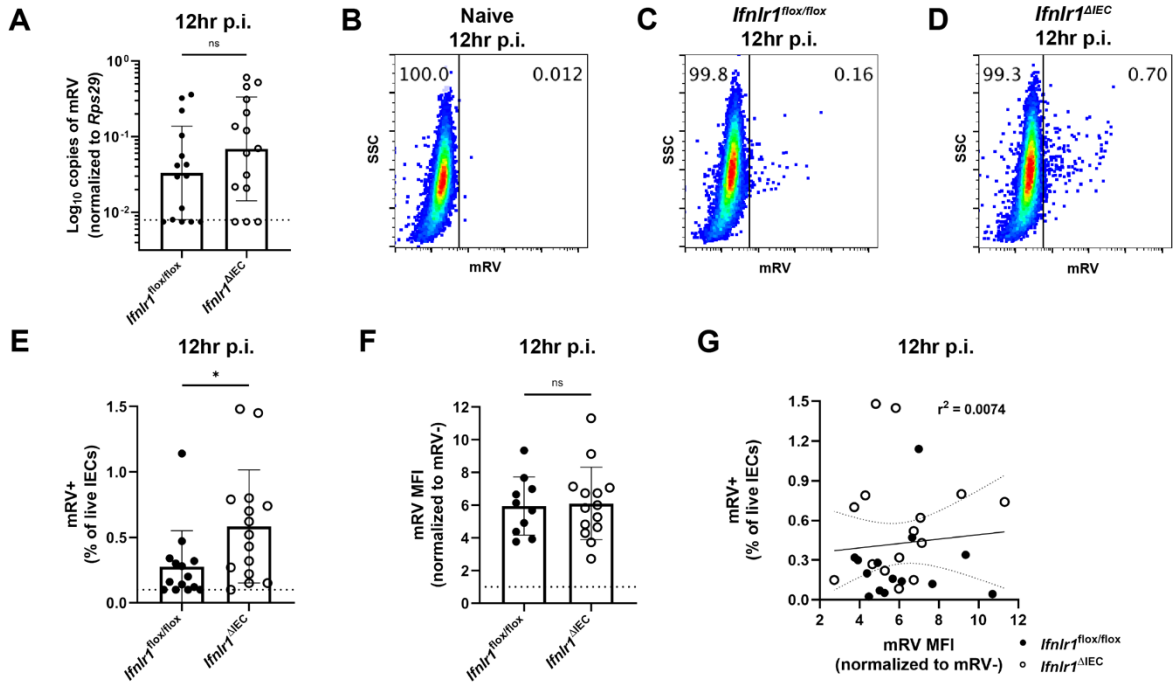


Figure 3.19. The homeostatic IFN- λ response preemptively protects IECs from murine rotavirus infection (12hr). *Ifnlr1^{flox/flox}* and *Ifnlr1 Δ IEC* mice were infected with 5000 SD50 of murine rotavirus by oral gavage and stripped ileal intestinal epithelial cell fractions were analyzed by qPCR for murine rotavirus genome copies (A) or flow cytometry for antigen-positive IECs (B-F). Representative flow cytometry plots of naïve (B), *Ifnlr1^{flox/flox}* (C), and *Ifnlr1 Δ IEC* (D) mice infected with murine rotavirus. E. The percentage of murine rotavirus + live IECs for each genotype. F. The MFI of antigen in infected cells relative to uninfected cells. G. A linear correlation plot of murine rotavirus + cells and murine rotavirus MFI with 95% confidence intervals (dashed lines). Where designated in (A, E-F), dashed lines = LOD as set by naïve mice. Data points represent individual mice and are pooled from 3 independent experiments. Statistical significance was calculated by Mann Whitney (A, E), or unpaired t-test (F) where * = $p < 0.05$.

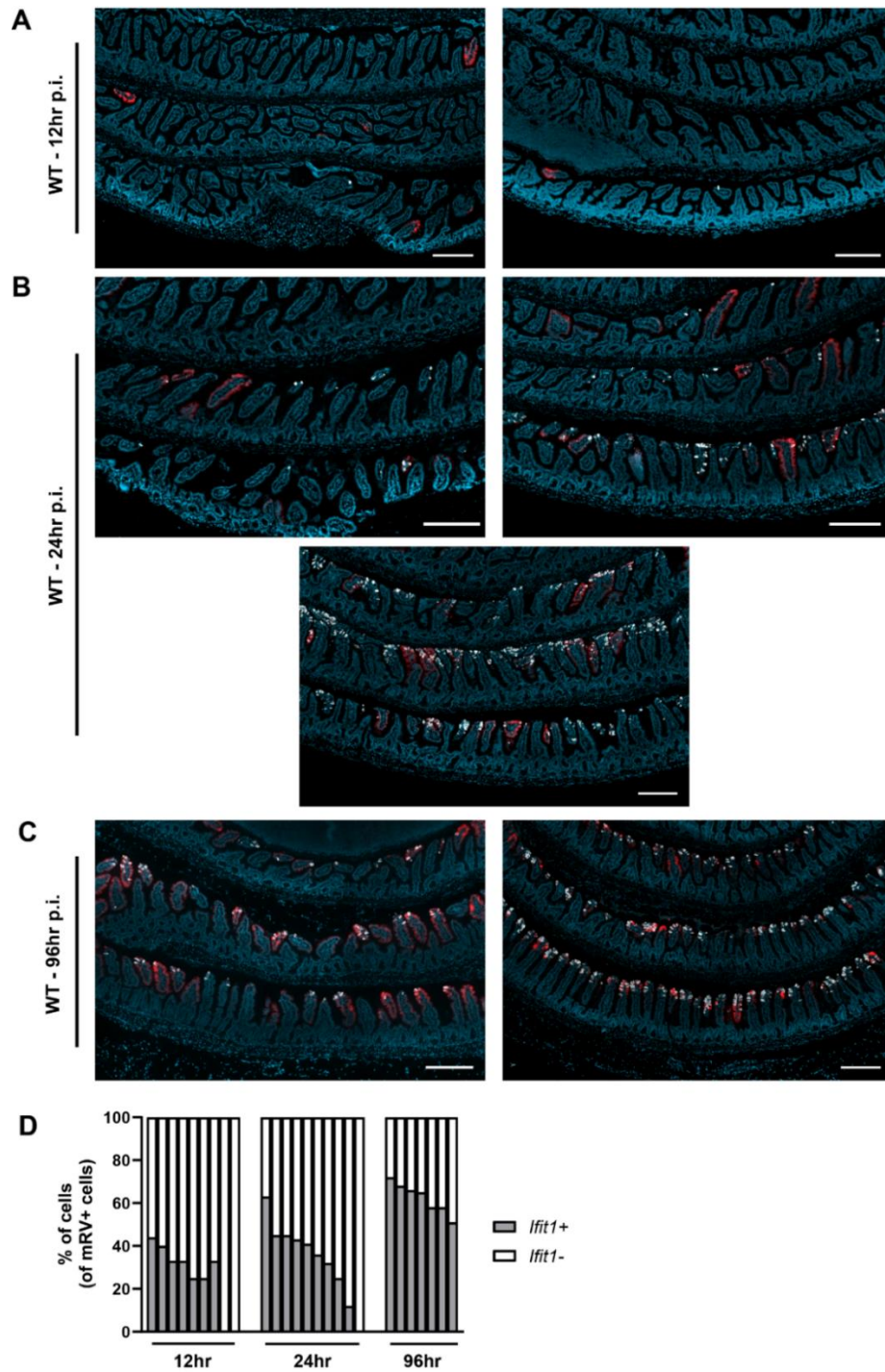


Figure 3.20. Murine rotavirus and *Ifit1* co-incidence. WT mice were infected with 5000 SD50 of murine rotavirus by oral gavage and the ilea were processed into Swiss rolls and stained by *in situ* hybridization for the ISG, *Ifit1* (red), and murine rotavirus RNA (white), with a DAPI (blue) counterstain. Representative images of ileum from (A) 12hr post-inoculation, (B) 24hr post-inoculation, and (C) 96hr post-inoculation, where each image represents an individual mouse. D. The percentage of infected cells that are *Ifit1*-positive and negative for each individual mouse. Where displayed, scale bar = 200 μ m.

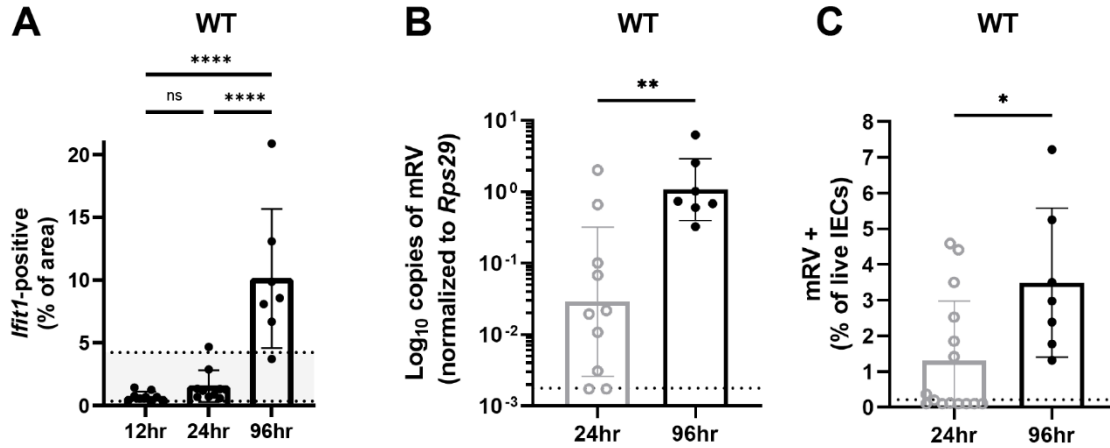


Figure 3.21. Murine rotavirus infection increases the distribution of *Ifit1* expression at late times post-inoculation. WT mice were infected with 5000 SD50 of murine rotavirus and the ilea were processed into Swiss rolls and stained by *in situ* hybridization for the ISG, *Ifit1* (red) with a DAPI (blue) counterstain. **A.** Quantification of *Ifit1* area relative to the total area of each tissue section with highlighted area representing historical range of *Ifit1* area in naïve WT mice. In parallel, stripped ileal intestinal epithelial cell fractions were analyzed by qPCR for murine rotavirus genome copies (**B**) or flow cytometry for antigen-positive IECs (**C**). For comparison in (**B-C**), 24hr data is historical and duplicated from *Ifnlr1*^{fllox/fllox} samples presented in **Figure 3.18**. Where displayed, scale bar = 500µm, and where designated, dashed lines = LOD as set by naïve mice. Data points represent individual mice and are pooled from 2 independent experiments. Statistical significance was calculated by one-way ANOVA with Tukey's multiple comparisons (**A**) and Mann Whitney (**B-C**), where ** = $p < 0.005$ and **** = $p < 0.0001$.

Discussion

Here, we report that bacterial microbiota induce an enteric IFN- λ response in IECs at homeostasis (**Figure 3.1-3.9**). Although there are previous reports of basal, non-receptor-dependent ISG expression in immortalized and primary cell lines (485), the homeostatic response that we report here is dependent on the IFN- λ receptor. Furthermore, we find this response is independent of type I IFN signaling (**Figure 3.8**), indicating that IFN- λ signaling plays a dominant and active role in the gastrointestinal epithelium. We also find minimal changes in ISG expression within the spleen and MLN after ABX treatment, suggesting that homeostatic ISGs are predominantly expressed in the intestine. These findings differ slightly from prior descriptions of systemic type I IFN responses that are dependent on bacterial microbiota (421, 423–426, 477). However, differences in the specific tissues and cell types analyzed make it difficult to draw direct comparisons across these studies. Therefore, we conclude that homeostatic ISGs are substantially present in IECs, but do not dispute the prior findings that relatively low homeostatic ISG expression induced by type I IFN plays an important role in extra-intestinal tissues and non-epithelial cell types.

A prior study by Mahlaköiv et al. noted the presence of *Ifnl2/3* transcripts in CD45+ cells within the stripped intestinal epithelium, but not the lamina propria, at homeostasis. We have confirmed these findings and have extended them to show that this homeostatic expression of *Ifnl2/3*, but not *Ifnb1*, is dependent on bacterial microbiota (**Figure 3.10**). However, we have been unable to detect IFN- λ transcripts by RNA scope *in situ* hybridization in mice at homeostasis, consistent with recently published data (486). This suggests that the production of IFN- λ is below the limit of detection by imaging or highly transient in nature. It is also unclear which CD45+ cell type produces homeostatic IFN- λ . Swamy et al. showed that T cell receptor stimulation led intraepithelial lymphocytes to

produce IFN- λ (351) and Mahlaköiv et al. suggested that the primary producers of IFN- λ at steady-state are intraepithelial lymphocytes due to the abundance of intraepithelial lymphocytes in the epithelial fraction. However, myeloid cells also reside near the intestinal epithelium and can sample luminal contents by various mechanisms (38, 401, 402). Although the cell type that produces homeostatic IFN- λ is unknown, enrichment for *Irf1/2/3* in CD45+ cells within the intestinal epithelial fraction suggests that proximity to bacterial stimuli may be a primary determinant in this response. We suggest that these cells may be actively surveying the intestinal epithelium to detect bacterial MAMPs. The specific CD45+ cell types responsible for producing homeostatic IFN- λ will be a topic of interest for future studies.

We initially anticipated that the distribution of homeostatic ISGs would be uniform among IECs. Instead, we found that this IFN- λ response is highly localized within enteric tissues. Homeostatic ISGs are observed in a minority of small intestinal villi and are primarily present in mature epithelium towards the villus tips (**Figure 3.12**). Likewise, homeostatic ISGs are present within patches of the mature epithelium in the colon (**Figure 3.14**). The surprising finding of localized ISGs in the ileum are supported by analysis of independently-generated scRNA-seq datasets from mouse and human small intestinal IECs that depict expression of homeostatic ISGs in a minority of cells with predominant expression in mature enterocytes (**Figure 3.15**).

The basis for localized ISG expression is unknown; however, it may reflect the distribution of cells capable of sensing bacterial microbiota, distinct microenvironments within the gastrointestinal tract, or qualitative differences in bacterial colonization. Given the results of our data in **Figure 3.16** and **Figure 3.17**, we suggest that LPS administration, flagellin administration, or fecal transplant can partially restore the expression of homeostatic ISGs in the small intestine. This interpretation supports the concept that

localized ISG-positive regions may be uniquely exposed or responsive to a variety of bacterial MAMPs. Indeed, we find that MYD88 is required for WT levels of homeostatic ISG expression in the small intestine (**Figure 3.8**). However, MYD88 is dispensable for homeostatic ISG expression in the colon, and TRIF is not required in either small intestine or colon (**Figure 3.8**). These data suggest that the bacterial microbiota broadly stimulates homeostatic IFN- λ through multiple, redundant PRRs. Furthermore, the presence of localized *Iffit1* expression in ABX-treated mice following LPS administration (**Figure 3.16**) suggests that localization is an intrinsic property of homeostatic ISG stimulation and is not likely to be due to qualitative differences in bacterial colonization.

ISG localization may be indicative of regional differences in access of luminal bacterial MAMPs to IFN- λ -producing cells. One host mechanism to limit bacterial interactions with the intestinal epithelium is the presence of mucus layers (487, 488). Intriguingly, the single mucus layer in the small intestine is much less adherent than the mucus layers present in the colon (487), which might allow occasional direct bacterial interactions with IECs or other cells near the intestinal epithelium. However, soluble components from enteric bacteria may also readily diffuse through mucus layers. In this case, there may be sporadic defects in tight junction proteins that are required to maintain the intestinal epithelium. Tight junction remodeling is essential to maintain intestinal integrity during apoptosis and extrusion of IECs that are regularly shed from the intestinal epithelium (489). Future studies will be necessary to determine whether defects in epithelial barrier integrity during extrusion events are linked to the local ISG responses that we observe and further delineation of the factors that render specific regions “responsive” will be of great interest for follow-up studies.

The preceding findings (**Figure 3.9**) suggested that the homeostatic ISG response in IECs would provide protection against IEC-tropic viruses, such as murine rotavirus.

Although bacterial-associated, IFN-independent mechanisms of murine rotavirus clearance have been reported (429, 430), we found that the signature of homeostatic ISGs in ileum tissue included well-characterized antiviral ISGs (**Figures 3.1 and 3.5**). To investigate whether these homeostatic ISGs protect against murine rotavirus, we used *Ifnlr1*^{ΔIEC} mice that lack homeostatic ISGs (**Figure 3.9 and 3.12**) rather than using ABX-treatment, which introduces pleiotropic effects on rotavirus infection (490) and dramatically increases transit time through the intestine (443). Using *Ifnlr1*^{ΔIEC} mice, we found increase in IEC infection at early stages of infection compared to *Ifnlr1*^{fllox/fllox} littermates (**Figure 3.18 and Figure 3.19**). However, the protection offered by IEC expression of *Ifnlr1* was lost by the middle and late stages of infection, consistent with the ability of murine rotavirus to antagonize induction of IFN responses once infection is established (241). Our observations during initiation of infection may provide important context to observations in other studies that report differing capacity for infection-induced IFN-λ to protect against murine rotavirus infection (195, 197). Ultimately, it is clear that prophylactic administration of exogenous IFN-λ protects against murine rotavirus infection (195, 197, 471), providing precedent that homeostatic IFN-λ would also be protective when induced by bacterial microbiota prior to infection.

Although we found that homeostatic ISGs provide protection during initiation of murine rotavirus infection, it remains unclear how these localized ISG pockets impart this protection. Given our findings in **Figure 3.16** and **Figure 3.17**, we suggest that these localized ISGs may be indicative of locations that are particularly vulnerable to viral infection if ISGs were not present at the time of viral exposure. However, alternative explanations for the protective effects that we observe are also plausible, such as: i) an inability to detect the full magnitude of ISG expression by imaging, or ii) an unknown temporal component to homeostatic ISG signaling that may be coincident with durable

ISG protein expression. Given the magnitude of signal amplification in RNAscope *in situ* hybridization and the similarity of *Ifit1* expression in our imaging data to *Ifit1* expression in public single-cell sequencing datasets, we find it unlikely that there is more widespread homeostatic ISG expression below the limit of our detection by imaging. However, we do think an uncharacterized temporal component of homeostatic ISG signaling is plausible, wherein individual villi may be rapidly and transiently expressing homeostatic ISGs in response to sensing of bacterial microbiota. This temporal model may also include a more durable ISG protein response that is not fully concordant with expression of ISG transcripts. In sum, these findings indicate that preexisting, homeostatic ISGs present in *Ifnlr1*-sufficient mice are protective during initiation of murine rotavirus infection, but that endogenous IFN- λ does not reduce murine rotavirus burden in infected cells. These data highlight the possibility that detection of bacterial microbiota in particularly exposed areas may preemptively activate homeostatic ISGs as a form of anticipatory immunity to protect the intestinal epithelium from enteric viruses.

CHAPTER 4: Conclusions, Implications, and Future Directions

Conclusions and Implications

The research performed in the preparation of this dissertation focused on defining the consequences and contexts surrounding IFN signaling in the intestinal epithelium. This work naturally evolved into two distinct lines of questioning:

- i) Why is IFN signaling in the intestine compartmentalized? And why do IECs preferentially respond to IFN- λ and lack responsiveness to IFN- α/β ?
- ii) Does the presence of the intestinal bacterial microbiota impact enteric IFN- λ signaling? Does the intestinal microbiota stimulate IFN- λ responses?

To answer these questions, I performed two studies that combined transcriptional profiling, fluorescent imaging, and flow cytometry on primary intestinal organoids and the tissues and cells isolated from wild-type and genetically-modified mice.

i) Selective IFN Responses of Intestinal Epithelial Cells

First, we found that IECs of neonatal mice are minimally responsive to IFN- α/β and that only IFN- λ provides significant protection against murine rotavirus to IECs. We then generated organoids from intestinal stem cells and stimulated them with IFN to determine whether the IFN- α/β hyporesponsiveness in IECs that we observed *in vivo* is an intrinsic quality. We found that organoids were dually responsive to IFN- β and IFN- λ , but that IFN- β stimulated ISGs to higher maximal expression levels than IFN- λ . We assessed the protective capacity of the organoid IFN response, and found that only IFN- β provided significant prophylactic protection against murine rotavirus to organoids. We continued by comprehensively comparing the ISG responses of *in vivo* IECs and organoid IECs by RNA sequencing. We performed differential expression analysis between IFN-stimulated

conditions and untreated controls to define sets of ISGs stimulated by IFN- β and IFN- λ in *in vivo* IECs and organoids. Comparison of these gene sets revealed that a large group of ISGs are specifically stimulated by IFN- β and not IFN- λ in organoids, but this group of IFN- β -specific ISGs was not robustly induced *in vivo*. Pathway analysis of revealed that apoptosis pathway genes were significantly enriched among these IFN- β -specific ISGs in organoids, but no prominent expression of apoptosis pathway genes was present *in vivo*. Using a model of TNF α triggered apoptosis, we found that pre-treatment with IFN- β , but not IFN- λ , potentiates apoptosis by TNF α by increasing the expression of apoptosis pathway genes at the time of challenge. To assess whether differences in promoter regulation are present in IFN- β -specific ISGs, we performed computational scoring of motifs in the promoters of IFN- β -specific ISGs and common ISGs stimulated by both IFN- β and IFN- λ . We found no evidence of novel motif usage by IFN- β -specific ISGs, but we did find that common ISGs have increased frequencies of ISRE motif sequences relative to IFN- β -specific ISGs. These findings suggest that more robust signaling is required for the induction of IFN- β -specific ISGs compared to common ISGs. Lastly, we confirmed that these IFN- β -specific ISGs and apoptosis pathway genes are dependent on STAT1 and show that IFN- β -specific ISGs are less likely to be associated with ISGF3 complex members upon reanalysis of a chromatin immunoprecipitation sequencing dataset.

Prior reports of IEC hyporesponsiveness to IFN- α/β responses *in vivo* have been made by several research groups. Previously, the physiological rationale for this lack of IFN- α/β response by IECs was hypothesized to be due to IFN- α/β ability to robustly elicit inflammatory cytokine expression, unlike IFN- λ . However, our studies in organoid IECs found no global increases in inflammatory cytokine expression in response to either IFN- α/β or IFN- λ stimulation. These findings suggest that inflammatory cytokine expression in response to observed to IFN- α/β may depend on cell-type, as IFN- α/β -stimulation of

inflammatory cytokine expression was previously assessed in myeloid cells. We also determined that IFN- β stimulation dramatically upregulates expression of apoptosis pathway genes in primary organoids that are dually responsive to IFN- λ and IFN- α/β . Analysis of public RNA-sequencing datasets indicate that these apoptosis pathway genes are also elicited in neutrophils, suggesting that potentiation of apoptotic processes by IFN- α/β may be broadly shared by many cell types. Since IEC proliferation and apoptosis is so critically balanced, there is strong physiological rationale to prevent apoptotic potentiation of IECs during inflammatory responses such as enteric infection. However, it remains to be seen whether dysregulation of IEC IFN- α/β responses occurs in the context of inflammation *in vivo*. Based on the findings of our studies, increased responsiveness of IECs to IFN- α/β could serve as a risk-factor in inflammatory diseases of the intestine. Increased susceptibility to inflammatory-induced apoptosis could readily undermine the integrity of the intestinal epithelium and incite a positive feedback loop of intestinal inflammation.

ii) The homeostatic interferon-lambda response to bacterial microbiota

We assessed whether ISGs are expressed at homeostasis in the ileum of mice by performing RNA-seq on ileum tissue with or without ABX-treatment in the presence and absence of *Ifnlr1*. We performed differential expression analysis between each condition and untreated controls to define a set of genes that decreases upon ABX-treatment, decreases in *Ifnlr1*^{-/-} mice, and are stimulated by IFN- λ *in vivo*. We find that this set of genes (homeostatic ISGs) are present at homeostasis in ileum and colon tissue of WT mice and depend on the presence of bacterial microbiota and *Ifnlr1* for their expression. We find no evidence of that homeostatic ISGs depend on microbiota or *Ifnlr1* in non-enteric tissues such as the MLN or spleen. To determine factors that facilitate homeostatic ISG signaling we screened a colony of genetically modified mice and determined that

homeostatic ISGs are independent of IFNAR1 signaling. Furthermore, expression of homeostatic ISGs are only modestly reliant on MyD88 and IRF7, primarily in ileal tissue. Given the preferential response to IFN- λ by IECs, we assessed the cellular location of homeostatic ISGs and find that their expression is restricted to IECs. Previous literature suggested that epithelial-associated CD45+ cells express *Ifnl2/3* at homeostasis. We validated these findings and extended them by showing that CD45+ cell expression of *Ifnl2/3* is dependent on the presence of intestinal microbiota. To assess the spatial distribution of these homeostatic ISGs within the intestinal epithelium, we performed *in situ* hybridization for ISGs in ileum and colonic tissues. This imaging revealed that homeostatic ISGs are not evenly expressed throughout the intestinal epithelium, but are highly localized to individual villi in the ileum and small epithelial patches in the colon. We corroborated our imaging analyses by analyzing public mouse and human single-cell RNA sequencing datasets wherein we determined that only a small fraction of IECs express homeostatic ISGs. To further define the relationship between bacteria and homeostatic ISGs, we assessed whether oral administration of bacterial products could restore ISG expression in ABX-treated mice. We find that restoration of homeostatic ISGs is incompletely penetrant, as only about half of mice have restored homeostatic ISG expression even among control mice that have reconstituted microbiota. Importantly, we find that these restored ISGs are localized in nature, suggesting that localization of ISG signal is an intrinsic feature of homeostatic ISG expression. Given the basal presence of homeostatic ISGs, we assessed whether these responses are protective against murine rotavirus infection. We find that homeostatic ISGs protect IECs during initiation of murine rotavirus infection, suggesting that the intestinal bacterial microbiota directly prime preemptive antiviral responses.

Although the intestinal bacterial microbiota was appreciated to induce homeostatic ISGs, it was previously restricted to non-IECs and was predominantly characterized in myeloid cells in systemic compartments. Furthermore, previous descriptions of homeostatic ISG responses centered on IFN- α/β responses. Our findings highlight homeostatic ISGs in the same tissue as the bacterial microbiota, in cells immediately adjacent to bacterial stimuli, and through IFN- λ signaling. Additionally, our study highlights the localized nature of the homeostatic IFN- λ response in IECs. The causes and consequences of these localized ISG responses remain unclear, but the results could have broad implications on the maintenance of the intestinal epithelium. In our study we found that these homeostatic ISGs are protective against viral infection, however it remains to be seen if homeostatic ISGs also have detrimental effects on the intestinal epithelium. Perhaps more widespread expression of homeostatic ISGs would impart increased protection against enteric viruses to the detriment of epithelial integrity or function. These localized responses suggest that homeostatic ISG responses in IECs may be balanced to only provide antiviral protection in regions of the epithelium that are most susceptible to enteric infection.

Future Directions

Determining the regulation of IFN- α/β hyporesponsiveness *in vivo*

In our study highlighted in Chapter 2, we found that IECs of neonatal mice are minimally responsive to IFN- α/β and are preferentially stimulated by IFN- λ . In contrast, we found that organoids were dually responsive to IFN- β and IFN- λ . However, it remains unclear how IFN- α/β signaling is regulated in IECs *in vivo* and with what developmental timing. We observe no differences in the expression of *Ifnar1*, *Ifnar2*, *Ifnlr1*, and *Il10rb* between neonatal IECs and organoid IECs (**Figure 4.1A**), suggesting that IFN- α/β signaling *in vivo* is not suppressed through a transcriptional regulation of IFN receptor components. However, we do find that organoid IECs have increased surface expression of both components of IFN- α/β receptor, IFNAR1 and IFNAR2, as compared with neonatal IECs (**Figure 4.1B**). These findings suggest that regulation of IFN- α/β hyporesponsiveness *in vivo* may be post-transcriptionally regulated. Intriguingly, we found that that expression of annotated IFN regulatory genes is decreased in organoids relative to neonatal IECs (**Figure 4.1C**). Among these IFN regulatory genes are TAM receptor kinases *Tyro3*, *Axl*, and *Mertk*; a TAM ligand, *Gas6*; and a gene downstream of TAM signaling, *Socs3*. TAM receptors are known to associate with IFNAR (among other stimulatory receptors) and function as a feedback inhibitor to antagonize ISG responses (491, 492). Much of TAM-mediated repression of IFN signaling can occur through suppressor of cytokine signaling 3 (SOCS3), as SOCS3 can drive degradation of TBK1 to block induction of IFNs and can inhibit JAK-STAT signaling to antagonize signaling through IFNAR (493).

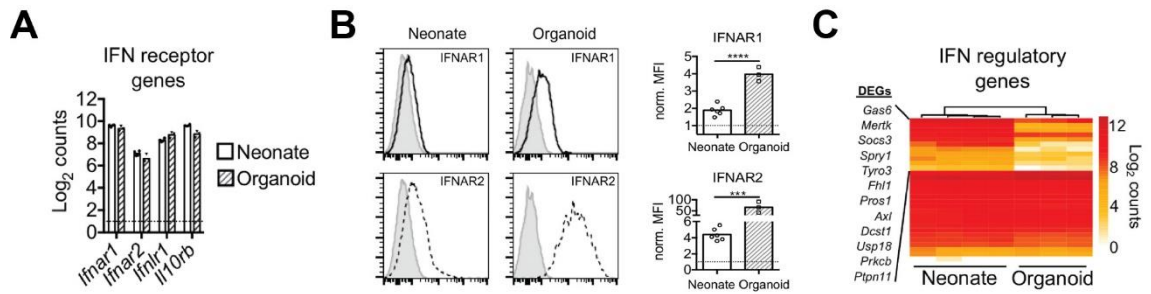


Figure 4.1. IFN regulatory genes are repressed in organoids relative to *in vivo* (from Figure 2.3). **A)** Log₂ normalized counts of the indicated IFN receptor genes from untreated neonate and organoid IECs. **B)** Flow cytometry staining of IFNAR1 and IFNAR2 on neonate IECs and organoid IECs. Gray histograms are control stains (no IFNAR antibody), and bar graphs show geometric mean fluorescence intensities (MFI) of IFNAR fluorescence normalized to the controls. **C)** A heat map of IFN regulatory gene expression from untreated neonate and organoid IECs. Differentially expressed genes (DEGs) listed in panel **C** are significantly different between neonate and organoid IECs. Data points represent results from replicate experiments. Significance was determined by a t test in **B**, where * = $P < 0.05$; ** = $P < 0.01$.

Although TAM genes are described as IFN regulatory genes, they have primarily been described in myeloid cells and lack characterization in IECs (458). Future research will determine if these TAM genes are necessary and sufficient for downregulation of the IFN- α/β response in IECs. To assess sufficiency, overexpression of TAM genes in murine organoid cultures can be performed followed by analysis of IFN receptor expression and responsiveness to each type of IFN. We hypothesize that overexpression of TAM genes will downregulate the IFN- α/β response *in vitro* and may provide insight into which TAM genes are of highest priority to assess *in vivo*. Extension of these results to genetic knockout mice would determine necessity in regulation of the response at steady-state. Deletion of all three TAM-family receptor kinases in mice has been performed, however it results in abundant lymphoproliferation and autoimmunity (494). It remains to be seen whether triple knockout TAM mice have increased surface level expression of IFNAR on IECs or increased sensitivity of IECs to IFN- α/β compared to genetically-intact control mice. Additionally, mice with single deletion of *Tyro3*, *Axl*, and *Mertk* are commercially available and do not exhibit pleiotropic effects on systemic immunity. These single-

deficient mice could also be assessed for increased surface level expression of IFNAR on IECs or increased sensitivity of IECs to IFN- α/β .

Profiling the Transcriptional Responses of Human Intestinal Tissues and Organoids

Using a model of TNF α triggered apoptosis, we found that pre-treatment with IFN- β , but not IFN- λ , potentiates apoptosis by TNF α by increasing the basal expression of apoptosis pathway genes (**Figure 2.5** and **Figure 2.6**). However, it remained unclear whether these findings in mice extend to humans and whether further investigation into the transcriptional responses of human tissues and organoids was warranted. To extend our findings of Chapter 2 to humans and determine whether concerted investigation in humans was warranted, we performed an extensive proof-of-concept experiment in human organoids derived from the ileum of three human subjects. This experiment was designed to determine if IFN stimulation exacerbates TNF α triggered apoptosis in human organoids similarly to murine organoids. To this end we treated human organoids with a saturating dose of all three types of IFN (IFN- β , IFN- γ , and IFN- λ). We then challenged IFN-treated and untreated organoids with TNF α . We found that treatment of human organoids with IFNs potentiated caspase-3 cleavage after TNF α challenge (**Figure 4.2A-B**), recapitulating the major findings in murine organoids. We extended these analyses by assessing the activity of caspase-3 and caspase-7 by flow cytometry using a fluorescent, caspase-3/7 cleavage-activated reporter (**Figure 4.2C-E**).

Just like our imaging analyses, treatment of human organoids with IFNs potentiated caspase-3/7 reporter cleavage after TNF α challenge in organoids derived from three separate subjects across multiple gastrointestinal sites. Together, these results indicate that combinatorial addition of IFNs do exacerbate TNF α triggered apoptosis in human organoids. Furthermore, full transcriptional profiling of human organoids following

IFN stimulation indicate that IFN- β and IFN- γ are the predominant drivers of potentiation in TNF α triggered apoptosis. These results also suggest a minimal role for IFN- λ in potentiation in TNF α triggered apoptosis, consistent with observations in murine organoids.

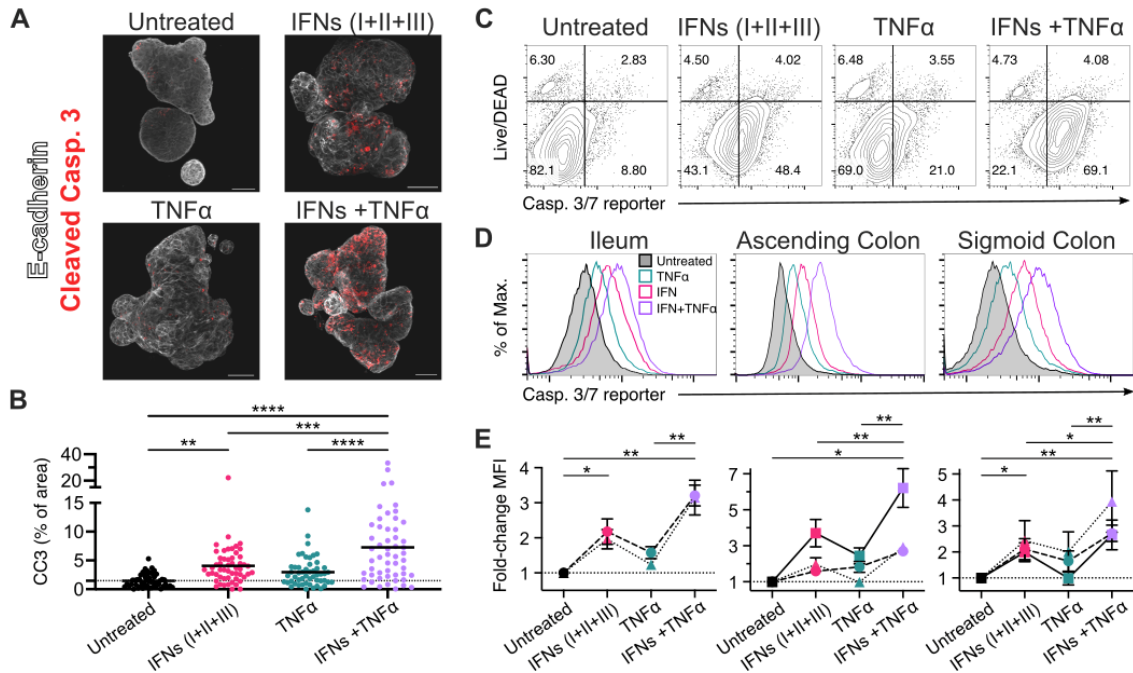


Figure 4.2. Combined IFN treatment potentiates TNF α cytotoxicity in human IEC organoids. IEC organoids were treated for 4 hours with PBS or pooled IFN types I, II, and III (1,000 U/mL each), followed by treatment with PBS or TNF α (100 ng/mL) for 20 hours. **A)** Representative images of IEC organoids after the indicated treatments, showing cleaved caspase 3 (red) and E-cadherin (white), scale bar = 50 μ m. **B)** The percent area positive for cleaved caspase 3 (CC3) relative to the E-cadherin positive area per field of view. Line indicates mean of untreated organoids. **C)** Representative flow cytometry plots of organoids subjected to the indicated treatments and stained with a caspase 3/7 reporter and “live/DEAD” cell permeability dye. **D)** Median fluorescence intensity (MFI) of caspase 3/7 reporter in live cells. **E)** Summary data of fold-change in caspase 3/7 reporter fluorescence relative to matched untreated control organoids from the ileum, ascending colon, and sigmoid colon, where each line style indicates a separate subject. Data in **(E)** represents three independent experiments. Statistical significance determined by one-way ANOVA **(B)** or two-way ANOVA **(E)** with Tukey’s multiple comparison test. * = $p < 0.05$; ** = $p < 0.01$; *** = $p < 0.001$; **** = $p < 0.0001$.

Future research will extend these findings into the context of IBD. Our findings suggest that both IFN- α/β and IFN- γ are capable of potentiating TNF α triggered apoptosis in human organoids. TNF α is one of the hallmark inflammatory cytokines that is increased

in IBD and has direct detrimental effects on the intestinal epithelium (495). Treatment with anti-TNF α is a frontline therapy for patients with IBD, highlighting its role in exacerbating the inflammatory environment in IBD. Likewise IFN signaling has been tied to IBD, as a higher basal presence of IFN stimulated genes in whole blood negatively correlates with patient response to anti-TNF therapy (496). Furthermore, a mouse model of Crohn's disease showed involvement of both STAT1 and STAT2 in mediating an inflammatory and cytotoxic state in the intestine (497). These findings suggests that increased IFN signaling in the intestinal epithelium may exacerbate TNF α -induced pathology beyond the control of anti-TNF therapy.

It remains unclear if patients with IBD have alterations in IFN signaling pathways in their IECs. To determine if surface expression of IFN receptors or transcriptional differences in IFN regulatory genes vary between patients with and without IBD, we will analyze human IECs for cell surface expression of IFN receptors and their basal transcriptional state. These studies will be performed on freshly isolated biopsies and paired organoid cell lines from inflamed and non-inflamed intestinal regions of patients with IBD. We will perform matched comparisons between sites of inflammation and to healthy control patients. Such studies will reveal whether there are basal differences in IFN pathways that could exacerbate IBD symptoms in patients.

Determining the cellular source of homeostatic IFN- λ

In our study highlighted in Chapter 2, we showed that epithelial-associated CD45+ cells express *Ifnl2/3*, but not *Ifnb1* at homeostasis. We also showed that CD45+ cell expression of *Ifnl2/3* is dependent on the presence of intestinal microbiota, as ABX-treatment reduced *Ifnl2/3* expression by these cells (**Figure 3.10**). However, many CD45+ cell types closely associate with IECs including IELs, macrophages, and dendritic cells.

To extend these analyses and determine the general identity of *Ifn12/3* expressing cells at homeostasis, we performed FACS and isolated distinct subsets of IEC-associated CD45+ cells. We isolated multiple cell types included T cells (CD45+/CD3+/MHC-II-) and five subsets of myeloid cells delineated by expression of CD11b, CD11c, CD103, and CX3CR1 (Figure 4.3A).

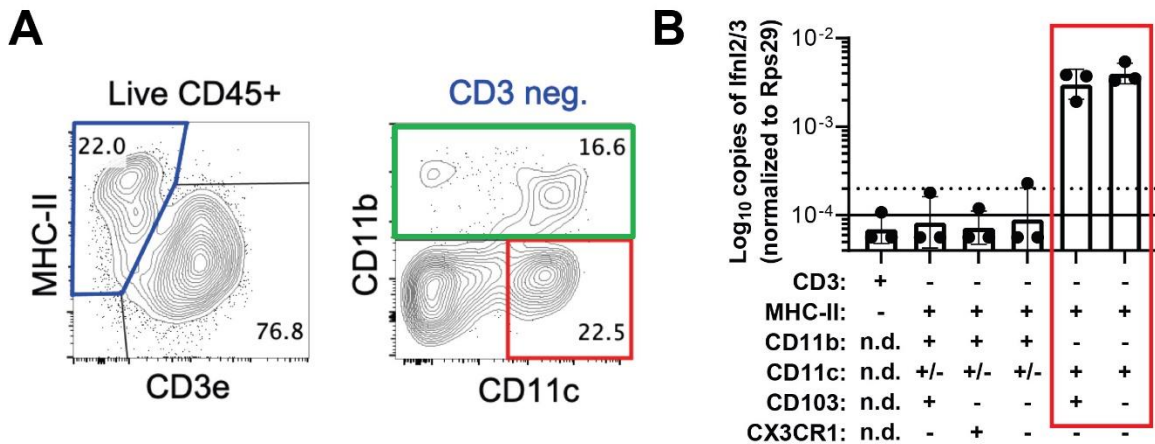


Figure 4.3. Epithelial-associated CD11c+/CD11b-/MHC-II+ myeloid cells produce *Ifn12/3* at homeostasis. Epithelial fractions were isolated from ileum of mice and CD45-positive leukocytes were enriched by magnet separation. **A.** Expression of indicated surface markers within the CD45-positive fraction. **B.** *Ifn12/3* quantified by qPCR from the indicated sorted cell subsets where n.d. = not determined. Solid line = limit of detection. Dashed line = expression level of bulk CD45+ cells. Red boxes indicate cells of interest.

We assessed the transcriptional abundance of *Ifn12/3* in each sorted cell-type and found that *Ifn12/3* was expressed by two myeloid populations that are CD11b-/CD11c+/MHC-II+ (Figure 4.3B). These two populations have differing expression of CD103, but both populations have expression of markers consistent with intestinal dendritic cells (332). Future research will be required to confirm identity of these IFN- λ expressing cells and their functional significance in the homeostatic ISG response. Confirming the identity of these cells is a significant priority and can be performed by combining two separate methods. First, more stringent sorting of myeloid cell subsets from mice will be performed to identify the specific cell type that expresses IFN- λ *in vivo*. From

our preliminary results, we hypothesize that multiple DC cell types may be responsible for production of IFN- λ at homeostasis. Additionally, we will perform selective deletion of multiple cell types in mice by crossing Cre recombinase inducible diphtheria toxin receptor (iDTR) mice with mice harboring cell-type specific expression of Cre followed by depletion of cells with administration of diphtheria toxin. For example, by crossing with Zbtb46-cre mice we will assess the role of canonical DCs, crossing with LysM-cre will allow investigation of monocytes and macrophages, and crossing with CD4-cre will provide a negative control. Following depletion we will assess the expression of homeostatic ISGs in the intestine and expect to find that DCs are required for homeostatic ISG expression.

Following identification of the cell type that produces IFN- λ at homeostasis, we will confirm the functional role of that cell type in localized homeostatic ISG responses. Furthermore, we will confirm that depleting these cells reduces protection against murine rotavirus infection. The elucidation of this cell type will also provide a means to more directly investigate the mechanism of microbiota sensing. For instance, we could determine the localization of these specific cell types within the intestinal epithelial layer and more directly assess whether localization of homeostatic ISGs is a function of the distribution of microbiota-sensing cells in the epithelium or whether it is a result of intrinsic epithelial processes that lead to localized sensing of bacterial microbiota.

Assessing the transcriptional profile of regions with localized homeostatic ISGs

Transcriptional profiling of whole ileum tissue revealed the presence of IFN stimulated genes at homeostasis (**Figure 3.1**). However, later we determined that homeostatic ISGs are highly localized and are not distributed evenly throughout the intestine (**Figure 3.12**). To extend our original transcriptional findings, we performed a

preliminary experiment to isolate ISG-positive and ISG-negative villi in the ileum and compare the transcriptional profile of these regions. To this end, we identified ISG-positive and neighboring ISG-negative villi in the ileum of WT mice using RNA scope (example **Figure 4.4A**). Following identification of target regions, we performed laser capture microdissection (LCM) to isolate multiple ISG-positive and ISG-negative regions from five mice. RNA sequencing and GSEA was performed on these samples to determine broad transcriptional signatures that differ between these regions. Consistent with expectations from the experimental design, we found that IFN response genes are dramatically enriched in ISG-positive villi compared to ISG-negative villi (**Figure 4.4B**). This results suggests that our LCM and RNA sequencing can accurately uncover transcriptional differences between these regions. Further analyses revealed enrichment of additional immune signatures in ISG-positive regions relative to ISG-negative regions. In particular, KEGG pathway genes associated with TLR signaling and hallmark inflammatory response genes are enriched in ISG-positive regions (**Figure 4.4C**). The enrichment of these responses suggests that sensing of bacterial microbiota may be increased in ISG-positive regions and that other localized inflammatory processes may be stimulated by bacterial microbiota. Lastly, we found decreases in cell cycle associated pathway genes and metabolic pathway genes in ISG-positive regions compared to ISG-negative regions (**Figure 4.4D**). These findings suggest that localized homeostatic ISGs correlate with intrinsic differences in responding villi.

It is unclear if alterations in these pathways contribute to the presence of homeostatic ISGs or whether they are a consequence of the homeostatic ISG response. However, decreases in cell cycle genes correlate with apoptotic processes in cells, suggesting that homeostatic ISGs may be stimulated in sites of normal intestinal epithelial turnover (498). Observations suggest that at any given time about 5% of villi are actively

shedding IECs (51). Coincidentally, this proportion is roughly equivalent with the proportion of intestinal epithelium expressing homeostatic ISGs (**Figure 3.12**). Future research will be required to confirm our observations of reduced cell cycle and metabolism genes in ISG-positive villi and to link these observations to localized turnover of IECs. Unfortunately, two-dimensional imaging approaches do not allow full coverage of intestinal villi and provide limited insight into the presence of apoptotic cells or shedding cells within villi. Ongoing work developing three-dimensional imaging approaches may offer the technical solution required to rigorously interrogate this line of research. It is also possible that decreases in cell cycle and metabolic pathways are the consequence of homeostatic ISG signaling, as IFN- λ can disrupt epithelial proliferation in the lung (499). If these decreases are confirmed to be consequences of homeostatic ISG expression, it would provide rationale for localized induction of ISG responses to bacterial stimuli. In this case, stimulation of highly-localized homeostatic ISG signaling could prevent widespread detrimental effects on the intestinal epithelium.

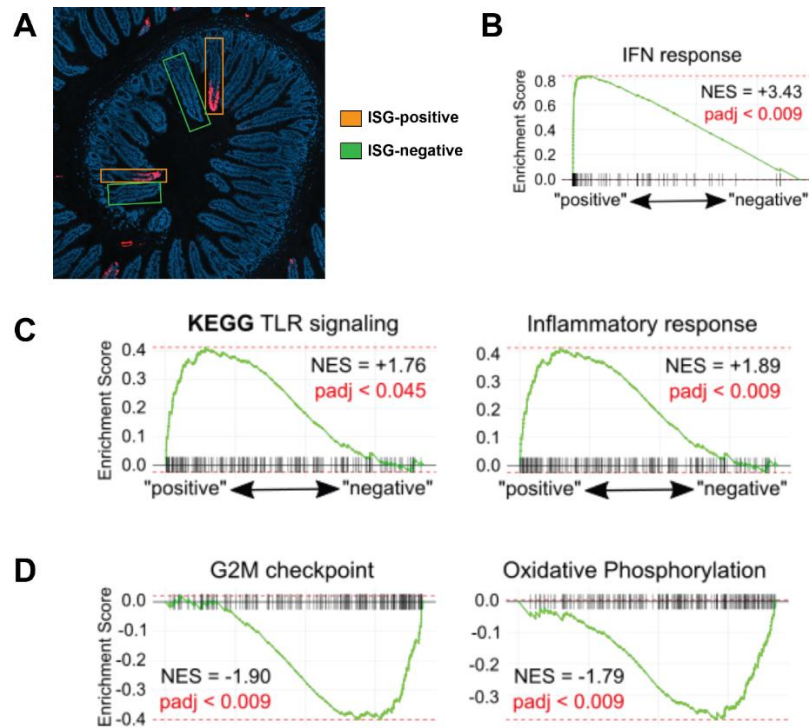


Figure 4.4. Pathway analysis of ISG-positive and ISG-negative regions of the ileum. Whole ileum was isolated and fixed for *in situ* hybridization and laser capture microdissection. **A)** RNA scope *in situ* hybridization was performed to identify ISG+ and ISG- regions of the ileum. **B-D)** Pathway analysis identified enrichment of IFN response pathway genes (**A**), TLR signaling pathway genes (**B**), and inflammatory response pathway genes (**C**) in ISG+ regions of ileum relative to ISG- regions. Pathway analysis identified depletion of cell cycle pathway genes and metabolism pathway genes in ISG+ regions of the ileum relative to ISG- regions. Normalized enrichment score (NES) and adjusted p-value are overlaid for each comparison.

Final Thoughts

IFN- λ is the most recently discovered and least characterized of the IFN types, and it has been incredibly exciting to study it! When combined with the wild world of enteric biology and immunology, it is hard to imagine a more enthralling topic to work on in graduate school. There is so much more to learn about IFN- λ and I am very interested to see all of the new discoveries and developments that will be made in the coming years. It has been a pleasure to document and share our observations and to have the privilege to provide a small contribution to this wonderful field of study.

Chapter 5: Materials and Methods

Mice

Mouse strains used include: C57BL/6J (stock # 000664), BALB/c (stock # 000651), *Stat1*^{-/-} (B6.129S(Cg)-*Stat1*^{tm1Dlv}/J), *Ifnlr1*^{-/-} and *Ifnlr1*^{fllox/fllox} (generated from *Ifnlr1*^{tm1a(EUCOMM)Wtsi} as published (200)), *Ifnar1*^{-/-} (B6.129.Ifnar1^{tm1}), *Trif*^{-/-} (JAX C57BL/6J-*Ticam1*^{Lps2}/J, stock #005037), *Myd88*^{-/-} (JAX B6.129P2(SJL)-*Myd88*^{tm1.1Defr}/J, stock #009088), *Irf3*^{-/-} (B6.129S/SvEv-Bcl2l12/Irf3^{tm1Ttg}), *Irf7*^{-/-} (B6.129P2-Irf7^{tm1Ttg}/TtgRbrc), *Stat1*^{-/-} (B6.129.-*Stat1*^{tm1Dlv}), and Villin-cre (B6.Cg-Tg(Vil1-cre)997Gum/J) mice. *Ifnlr1*^{-/-} and *Ifnar1*^{-/-} mice were bred to *Ifnlr1*^{Het}/*Ifnar1*^{Het} mice to generate littermate *Ifnlr1*^{Het}/*Ifnar1*^{Het}, *Ifnlr1*^{Het}/*Ifnar1*^{KO}, *Ifnlr1*^{KO}/*Ifnar1*^{Het}, *Ifnlr1*^{KO}/*Ifnar1*^{KO} offspring.

Mice were obtained from Jackson Laboratories and bred in specific-pathogen-free barrier facilities at Oregon Health & Science University. All mice were maintained in specific-pathogen-free facilities at Oregon Health & Science University (OHSU) and Washington University in St. Louis (WUSTL). Animal protocols were approved by the Institutional Animal Care and Use Committee at OHSU (protocol #IP00000228) and WUSTL (protocol #20190162) in accordance with standards provided in the *Animal Welfare Act*.

Mouse Treatments

For all experiments, mice were allocated into experimental groups based on genotype with equal representation of individual litters and equal sex ratios.

For neonatal IFN treatments, 200ng of IFN- β (PBL #12405-1) or IFN- λ 3 (PBL #12820-1) were administered to seven-day-old neonatal mice via sub-cutaneous injection; an equal volume of diluent (PBS) was administered to littermate control mice.

For ABX depletion of bacteria, mice were administered an *ad libitum* antibiotic cocktail consisting of: 1 g/L ampicillin, 1 g/L metronidazole, 1 g/L neomycin, and 0.5 g/L vancomycin (Sigma, St. Louis, MO) in autoclaved H₂O (OHSU) or in 20 mg/mL grape Kool-Aid (Kraft Foods, Northfield, IL) (WUSTL). Sterile H₂O (OHSU) or Kool-Aid (WUSTL) alone was used as a control. Mice were maintained on antibiotics or control for 2 weeks prior to harvest.

For IFN treatment of adult mice, recombinant IFN- λ was provided by Bristol-Myers Squibb (New York City, NY) as a monomeric conjugate comprised of 20kDa linear PEG attached to the amino-terminus of murine IFN- λ . Mice were injected intraperitoneally with the indicated amount of IFN- λ or an equal volume of PBS vehicle as indicated in figure legends at the indicated time prior to analysis.

As a positive control for stimulation of the IFN response, mice were administered 100 μ g of the synthetic dsRNA analogue, poly I:C (R&D, #4287) or PBS by intraperitoneal injection in a 200 μ L volume, 2 hours prior to harvest.

For enteric treatments with bacterial products, 25 μ g of lipopolysaccharide (Sigma #L4391), flagellin (Invivogen #tlrl-bsfla; from *Bacillus subtilis*) or CpG (Invivogen #tlrl-1585; Class A CpG oligonucleotide) were perorally administered to mice in 25 μ L of sterile PBS. Mice were treated on days 15 and 16 of antibiotic treatment or H₂O control prior to harvest on day 17.

For transplantation of fecal material, antibiotic treatment was stopped and mice were fed 25 μ L of fecal mixture by pipet for two consecutive days. Fecal mixture was prepared by collecting fecal samples from control mice; a single stool pellet was resuspended in 200 μ L of sterile PBS, stool was broken apart by pipetting, and large particulate was allowed to settle for several minutes prior to administration.

Rotavirus infection of mice

Mouse rotavirus (EC strain) was originally provided by Andrew Gewirtz (Georgia State University). Viral stocks were generated at OHSU by inoculating 4- to 6-day-old neonatal BALB/c mice and harvesting the entire gastrointestinal tract upon presentation of diarrheal symptoms 4 to 7 days later. Intestines were freeze-and-thawed, suspended in PBS, and homogenized in a bead beater using 1.0-mm zirconia-silica beads (BioSpec Products). These homogenates were clarified of debris, aliquoted, and stored at -70°C. The 50% shedding dose (SD50) was determined by inoculation of 10-fold serial dilutions in adult C57BL/6J mice.

For protection studies in neonatal mice, seven-day-old C57BL/6J mice were orally inoculated with 100x SD50 and intestines were isolated 20 hours later for quantitation of viral genomes by qPCR.

For stool time-course studies, mice were inoculated by peroral route with 100 SD50 and a single stool pellet was collected daily for viral quantitation by qPCR. For quantification of viral antigens and genomes from cells and tissues of adult mice, the mice were inoculated by intragastric gavage with 5000 SD50.

Organoid culture

Isolation and culture of primary mouse IEC organoids was performed essentially as described (74). Briefly, intestinal crypts were isolated by mechanical disruption, digestion with 2mg/mL collagenase type I, and centrifugation. Isolated crypts were resuspended in 15uL Matrigel (Corning #354234) per well and plated in 24-well plates.

Primary organoid culture media was Advanced DMEM/F12 (ThermoFisher #12634010) supplemented with 20% fetal bovine serum, 1X penicillin/streptomycin/L-

glutamine, and 10mM HEPES. Organoids were grown and maintained in 50% primary organoid culture media mixed with 50% conditioned media (CM) from L-WRN cells (ATCC cat#CRL-3276), which contained Wnt3a, R-spondin3, and Noggin. ROCK-inhibitor (Selleck Chemicals #S1049) and TGFbeta-inhibitor (Selleck Chemicals #S1067) were added to culture media to promote survival of dissociated cells. Media was replaced every two days. Every three days, or when organoids become dense, cells were disrupted with Trypsin/EDTA and re-plated at ~30,000 cells/well.

For IFN stimulations, IFN- β (PBL #12405-1), pegylated-IFN- λ 2 (Bristol Meyers-Squibb), IFN- λ 3 (PBL #12820-1), and TNF α (Peprotech #315-01A) were added to organoid cultures as indicated in the figure legends. For flow cytometry of organoid-derived IECs, organoids were first isolated from Matrigel by incubating in Cell Recovery Solution (Corning # 354253) at 4°C for 30 minutes, and IECs were then isolated from organoids by digestion with Accutase (Innovative Cell Technologies #AT-104) at 4°C for 30 minutes.

IEC organoid viability assays were adapted from Grabinger et al. (500). Organoids were seeded in 96 well plates at 500-1000 cells per 5 μ L matrigel per well. Following cytokine treatment as indicated in figure legend, MTT (Sigma #MM5655) was added to cell culture media at 0.5 mg/mL and incubated at 37 °C for 1 hour. Media was replaced with 100% DMSO and absorbance was measured at 570 nm on a BioTek plate reader. Background-subtracted OD values were normalized to untreated organoid wells (100% viability) for each independent experiment.

Rotavirus infection of organoids

Primary mouse IEC organoids were dissociated to the single-cell level with Trypsin/EDTA and were seeded at ~25,000 cells/well. Organoids were maintained in 50%

CM for two days followed by one day of culture in 5% CM – ROCK inhibitor and TGFbeta inhibitor were supplemented to maintain the concentrations present in 50% CM. Cells were treated for 8-hours with 10ng/mL IFN- β (PBL #12405-1), 10ng/mL IFN- λ 3 (PBL #12820-1), or PBS control. Organoids were inoculated with 500x SD50 murine rotavirus EC in 5% CM by overlaying inoculant, rocking at room-temperature for 30 minutes, and washing with PBS three times. Infected cells were incubated in 5% CM until the indicated timepoints. Cells were lysed in ZR Viral RNA Buffer (Zymoresearch) and viral genomes were detected by quantitative RT-PCR.

Organoid immunofluorescence

Following stimulation, organoids were removed from Matrigel by rocking at 4°C in cell recovery solution (Corning). Cells were stained by adapting previous protocols (501). In short, cells were fixed in 3.7% paraformaldehyde, permeabilized in ice-cold 100% methanol, and blocked in 5% normal goat serum, 5% bovine serum albumin, and 0.5% saponin in PBS. Cells were stained with mouse anti-Ecadherin (Becton Dickinson, #610182), rabbit anti-cleaved caspase 3 (Cell Signaling Technology, #9661S), secondary goat anti-mouse Alexa Fluor 555, and goat anti-rabbit Alexa Fluor 647 (ThermoFisher) in 1% normal goat serum, 1% bovine serum albumin, and 0.5% saponin in PBS. IEC organoids were counterstained with DAPI, mounted with ProLong Gold antifade reagent (ThermoFisher), and imaged using a Zeiss ApoTome2 on an Axio Imager, with a Zeiss AxioCam 506 (Zeiss). The CC3-positive area was measured and normalized to the total area of organoid surface using ImageJ.

RNAscope

Swiss rolls of intestinal tissue were fixed in 10% neutral-buffered formalin for 18-24hr and paraffin-embedded. Tissue sections (5 μ m) were cut and maintained at room

temperature with desiccant until staining. RNA *in situ* hybridization was performed using the RNAscope Multiplex Fluorescent v2 kit (Advanced Cell Diagnostics) per protocol guidelines. Staining with anti-sense probes for detection of *Lfit1* (ACD, #500071-C2), *Usp18* (ACD, #524651-C1) and murine rotavirus (ACD, #1030611-C1) was performed using ACDBio protocols and reagents. Murine rotavirus probes were designed to target 2-1683 of DQ391187 against NSP3, VP7, and NP4. Slides were stained with DAPI and mounted with ProLong Gold antifade reagent (ThermoFisher), and imaged using a Zeiss ApoTome2 on an Axio Imager, with a Zeiss AxioCam 506 (Zeiss).

Collected images were batch processed in Zeiss Zen 3.1 using unstained control slides to set background values and quantified using ImageJ. When applicable, the area of *Lfit1* was determined by positive *Lfit1* fluorescent area relative to the total fluorescent area of the tissue section. In infection studies, *Lfit1*+ murine rotavirus -infected cells were defined as murine rotavirus + particles with greater than 5 μ m area with a maximum *Lfit1* intensity greater than 10% above background. These *Lfit1*+ cells were then divided by the total number murine rotavirus + cells to determine the percentage of *Lfit1*+ murine rotavirus -infected cells.

Cell isolation from intestinal tissue

Epithelial fractions were prepared by non-enzymatic dissociation as previously described (502). Briefly, mouse ileum was opened longitudinally and agitated by shaking in stripping buffer (10% bovine calf serum, 15 mM HEPES, 5 mM EDTA, and 5 mM dithiothreitol [DTT] in PBS) for 20 min at 37°C. Lamina propria fractions were prepared by enzymatic digestion and dissociation with the Lamina Propria Dissociation Kit and GentleMacs Dissociator (Miltenyi Biotec). Dissociated cells were collected for use in qPCR analysis, flow cytometry, fluorescence-activated cells sorting, and magnet enrichment.

Flow Cytometry and Magnet Enrichment

Dissociated cells were collected and stained for flow cytometry or fluorescence-activated cell-sorting (FACS). Cells were stained with Zombie Aqua viability dye (BioLegend), Fc receptor-blocking antibody (CD16/CD32; BioLegend), anti-EpCAM (clone G8.8; BioLegend), and anti-CD45 (clone 30-F11; BioLegend). For analysis of IFNAR expression, cells were additionally stained with anti-IFNAR1 (clone MAR1; BioLegend) or anti-IFNAR2 (polyclonal goat IgG; R&D Systems). For analysis of murine rotavirus infection, cells were stained with anti-rotavirus (polyclonal; ThermoFisher, #PA1-7241) followed by goat anti-rabbit secondary (ThermoFisher). All data were analyzed using FlowJo software (BD Biosciences). Gates were set based on unstained and single-fluorophore stains. IECs were selected by gating on live, EpCAM-positive, CD45-negative cells. Gates for murine rotavirus infection were set based on naïve samples. For isolation of RNA, cells in the live gate were sorted as EpCAM-positive/CD45-negative IECs or EpCAM-negative/CD45-positive hematopoietic cells.

Where indicated, dissociated cells were enriched using MojoSort Mouse anti-APC Nanobeads (BioLegend, #480072). Cells were first stained for flow cytometry with anti-EpCAM or anti-CD45 antibodies with APC fluorophores. Following surface staining by flow cytometry, enrichment of cells was performed using MojoSort Mouse anti-APC Nanobeads by following manufacturer protocols.

Quantitative RT-PCR

RNA was isolated using RiboZol (Amresco), TRIzol (Life Technologies), or the ZR Viral RNA Kit (Zymoresearch). The larger of either 1µg of RNA or 5µL of RNA were used as a template for cDNA synthesis by the ImProm-II reverse transcriptase system (Promega) after DNA contamination was removed with the DNFree kit (Life Technologies). 16S bacterial rDNA was isolated from stool and intestinal contents with a

ZymoBIOMICS DNA kit (Zymo Research). Quantitative PCR was performed using PerfeCTa qPCR FastMix II (QuantaBio) and the absolute quantities of transcript were determined using standard curves composed of gBlocks (IDT) containing target sequences. Absolute copy numbers from tissue samples were normalized to the housekeeping gene, ribosomal protein S29 (*Rps29*), where samples with fewer than 1,000 copies of housekeeping gene were excluded. Taqman assays for selected genes were ordered from IDT: *Bid* (Mm.PT.58.8829163), *Bcl2l11* (Mm.PT.58.12605058), *Casp8* (Mm.PT.58.41467226), *Isg15* (Mm.PT.58.41476392.g), *Usp18* (Mm.PT.58.28965870), *Cxcl10* (Mm.PT.58.28790444), *Ifit1* (Mm.PT.58.32674307), *Oas1a* (Mm.PT.58.30459792), *Mx2* (Mm.PT.58.11386814), *Stat1* (Mm.PT.58.23792152), and *Rps29* (Mm.PT.58.21577577).

Taqman assays for *Ifnl2/3* and *Ifnb1* were designed previously (471) and consisted of the following primer-probe sequences: *Ifnl2/3* (Primer 1 – GTTCTCCCAGACCTTCAGG, Primer 2 – CCTGGGACCTGAAGCAG, Probe – CCTTGCAGGCTGAGGTGGC); *Ifnb1* (Primer 1 – CTCCAGCTCCAAGAAAGGAC, Primer 2 – GCCCTGTAGGTGAGGTTGAT, Probe – CAGGAGCTCCTGGAGCAGCTGA). Murine rotavirus was detected using Taqman primer-probe sets specific for 422-521 of GeneBank sequence DQ391187 as previously described (235) with the following sequences: Primer 1 – GTTCGTTGTGCCTCATTCG, Primer 2 – TCGGAACGTA CTTCTGGAC, Probe – AGGAATGCTTCAGCGCTG; and universal bacterial 16S rDNA was detected using Taqman primer-probe sets with previously designed sequences (503): Primer 1 – GGACTACCAGGGTATCTAATCCTGTT, Primer 2 – TCCTACGGGAGGCAGCAGT, Probe – CGTATTACCGCGGCTGCTGGCAC

RNA sequencing and expression analysis of neonatal epithelium and organoids

Quality of RNA samples were assessed using a TapeStation (Agilent) and mRNA sequencing libraries were prepared using the TruSeq RNA Library Prep Kit (Illumina). Barcoded triplicate samples from IEC organoids (9 total) and quadruplicate samples from neonates (12 total) were separately prepared and pooled. Single-read sequencing was performed using an Illumina HiSeq 2500 through the Massively Parallel Sequencing Shared Resource at OHSU.

Adaptor-trimmed reads were mapped to the mouse genome (GRCm38) using the STAR aligner (504), and mapping quality was evaluated using RSeQC (505), and MultiQC (506). All samples had between 15 and 30 million uniquely mapped reads with similar distribution across genomic features and uniform gene-body coverage. Read counts per gene were determined using the featureCounts program (507), and differential expression analysis was performed using DEseq2, as described (508). PCA analysis was performed on DEseq2 regularized logarithm (rlog) transformed data. Heatmaps were generated using log2-transformed data normalized to the mean of matched PBS control samples; heatmap clustering is based on Euclidean distance.

RNA sequencing and expression analysis of antibiotic- and IFN- λ -treated mice

Wild-type C57BL/6J or *Ifnlr1*^{-/-} mice were administered *ad libitum* Kool-aid or ABX for two weeks, or wild-type mice were administered 25 μ g recombinant IFN- λ for one day, then ileal segments lacking Peyer's patches were harvested and RNA sequencing was performed as prior (509). mRNA from ilea was purified with oligo-dT beads (Invitrogen, Carlsbad, CA) and cDNA was synthesized using a custom oligo-dT primer containing a barcode and adaptor-linker sequence, degradation of RNA-DNA hybrid following single-strand synthesis, and ligation of a second sequencing linker with T4 ligase (New England

Biolabs, Ipswich, MA). These reactions were cleaned up by solid phase reversible immobilization (SPRI), followed by enrichment by PCR and further SPRI to yield strand-specific RNA-seq libraries. Libraries were sequenced with an Illumina HiSeq 2500 with three to four mice were included in each group. Samples were demultiplexed with second mate, reads were aligned with STAR aligner and then counted with HT-Seq. Differentially expressed genes were identified using DESeq2 (508) based on cutoffs of 2-fold change, and an inclusive p-value < 0.5. Standard gene set enrichment analysis was performed to identify enrichments in IFN- λ response genes.

16S rRNA gene Illumina sequencing and analysis

For sequencing of the 16S rRNA gene, primer selection and PCRs were performed as described previously (510). Briefly, each sample was amplified in triplicate with Golay-barcoded primers specific for the V4 region (F515/R806), combined, and confirmed by gel electrophoresis. PCR reactions contained 18.8 μ L RNase/DNase-free water, 2.5 μ L of 10X High Fidelity PCR Buffer (Invitrogen, 11304-102), 0.5 μ L of 10 mM dNTPs, 1 μ L 50 mM MgSO₄, 0.5 μ L each of forward and reverse primers (10 μ M final concentration), 0.1 μ L of Platinum High Fidelity Taq (Invitrogen, 11304-102), and 1.0 μ L genomic DNA. Reactions were held at 94°C for 2 min to denature the DNA, with amplification proceeding for 26 cycles at 94°C for 15 s, 50°C for 30 s, and 68°C for 30 s; a final extension of 2 min at 68°C was added to ensure complete amplification. Amplicons were pooled and purified with 0.6x Agencourt AMPure XP beads (Beckman-Coulter, A63882) according to the manufacturer's instructions. The final pooled samples, along with aliquots of the three sequencing primers, were sent to the DNA Sequencing Innovation Lab (Washington University School of Medicine) for sequencing by the 2 X 250bp protocol with the Illumina MiSeq platform.

Read quality control and the resolution of amplicon sequence variants were

performed in R with DADA2 (511). Non-bacterial amplicon sequence variants were filtered out. The remaining reads were assigned taxonomy using the Ribosomal Database Project (RDP trainset 16/release 11.5) 16S rRNA gene sequence database (512). Ecological analyses, such as alpha-diversity (richness, Shannon diversity) and beta-diversity analyses (UniFrac distances), were performed using PhyloSeq and additional R packages (513). 16S sequencing data have been uploaded to the European Nucleotide Archive (accession #: PRJEB43446).

ChIP-seq analysis

Published ChIP-seq data from Platanitis et al. was downloaded from GEO (GSE115433) and narrowpeak files were analyzed using BEDOPS v.2.4.36 closest-features (514) to identify peaks within 500 bp of annotated transcription start sites associated with genes contained in the defined gene sets (common ISGs and IFN- β -specific ISGs). Genes were then classified as either having one or more ChIP-seq peaks associated with them, or zero associated peaks.

Single-cell RNA Sequencing Analyses

A mouse single-cell RNA sequencing dataset generated by Haber et al. was accessed from NCBI's Gene Expression Omnibus (GEO), accession #: GSE92332. A human pediatric single-cell RNA sequencing dataset generated by Elmentaite et al. was accessed in processed form from The Gut Cell Atlas, with raw data also available on EMBL-EBI Array Express, accession #: E-MTAB-8901. Files were analyzed in R using Seurat (v. 3.2.2)(515). For the Haber et al. dataset, UMI counts were normalized to counts per million, log₂ transformed, and homeostatic ISGs were selected for analysis. Data was collated by previously annotated cell-type and proportion of cells expressing each individual ISG was calculated. For Elmentaite et al, data was restricted to healthy controls

and then collated by previously annotated cell-type to determine the proportion of cells expressing individual ISGs.

Statistical Analyses

Sample size estimation was performed based on historical data. Data were analyzed with Prism software (GraphPad Prism Software), with specified tests as noted in the figure legends.

Data availability.

RNA sequencing data obtained in Chapter 2 have been deposited in the NCBI Gene Expression Omnibus under GEO Series accession number GSE142166. RNA sequencing data obtained in Chapter 3 have been deposited in the European Nucleotide Archive (accession #: PRJEB43446).

References

1. R. Bowcutt, R. Forman, M. Glymenaki, S. R. Carding, K. J. Else, S. M. Cruickshank, Heterogeneity across the murine small and large intestine. *World J. Gastroenterol.* **20**, 15216–15232 (2014).
2. K. D. Walton, D. Mishkind, M. R. Riddle, C. J. Tabin, D. L. Gumucio, Blueprint for an intestinal villus: Species-specific assembly required. *Wiley Interdiscip. Rev. Dev. Biol.* **7**, 1–19 (2018).
3. A. M. Mowat, W. W. Agace, Regional specialization within the intestinal immune system. *Nat. Rev. Immunol.* **14**, 667–685 (2014).
4. A. Ermund, A. Schütte, M. E. V Johansson, J. K. Gustafsson, G. C. Hansson, Studies of mucus in mouse stomach, small intestine, and colon. I. Gastrointestinal mucus layers have different properties depending on location as well as over the Peyer's patches. *Am. J. Physiol. - Gastrointest. Liver Physiol.* **305**, 341–347 (2013).
5. E. Marshman, C. Booth, C. S. Potten, The intestinal epithelial stem cell. *BioEssays.* **24**, 91–98 (2002).
6. T. K. Noah, B. Donahue, N. F. Shroyer, Intestinal development and differentiation. *Exp. Cell Res.* **317**, 2702–10 (2011).
7. N. Barker, Adult intestinal stem cells: critical drivers of epithelial homeostasis and regeneration. *Nat. Rev. Mol. Cell Biol.* **15**, 19–33 (2014).
8. H. Quastler, F. G. Sherman, Cell population kinetics in the intestinal epithelium of the mouse. *Exp. Cell Res.* **17**, 420–438 (1959).
9. B. E. Walker, C. P. Leblond, Sites of nucleic acid synthesis in the mouse visualized by radioautography after administration of C14-labelled adenine and thymidine. *Exp. Cell Res.* **14**, 510–531 (1958).
10. J. Guiu, E. Hannezo, S. Yui, S. Demharter, S. Ulyanchenko, M. Maimets, A. Jørgensen, S. Perlman, L. Lundvall, L. S. Mamsen, A. Larsen, R. H. Olesen, C. Y. Andersen, L. L. Thuesen, K. J. Hare, T. H. Pers, K. Khodosevich, B. D. Simons, K. B. Jensen, Tracing the origin of adult intestinal stem cells. *Nature.* **570**, 107–111 (2019).
11. N. Barker, J. H. Van Es, J. Kuipers, P. Kujala, M. Van Den Born, M. Cozijnsen, A. Haegebarth, J. Korving, H. Begthel, P. J. Peters, H. Clevers, Identification of stem cells in small intestine and colon by marker gene Lgr5. *Nature.* **449**, 1003–1007 (2007).
12. K. Kurokawa, Y. Hayakawa, K. Koike, Plasticity of intestinal epithelium: Stem cell niches and regulatory signals. *Int. J. Mol. Sci.* **22**, 1–13 (2021).
13. T. Sato, J. H. Van Es, H. J. Snippert, D. E. Stange, R. G. Vries, M. Van Den Born, N. Barker, N. F. Shroyer, M. Van De Wetering, H. Clevers, Paneth cells constitute the niche for Lgr5 stem cells in intestinal crypts. *Nature.* **469**, 415–418 (2011).
14. D. Pinto, A. Gregorieff, H. Begthel, H. Clevers, Canonical Wnt signals are essential for homeostasis of the intestinal epithelium. *Genes Dev.* **17**, 1709–1713 (2003).
15. F. Kuhnert, C. R. Davis, H. T. Wang, P. Chu, M. Lee, J. Yuan, R. Nusse, C. J. Kuo, Essential requirement for Wnt signaling in proliferation of adult small intestine and colon revealed by adenoviral expression of Dickkopf-1. *Proc. Natl. Acad. Sci.* **101**, 266–271 (2004).
16. D. Pinto, H. Clevers, Wnt control of stem cells and differentiation in the intestinal epithelium. *Exp. Cell Res.* **306**, 357–363 (2005).

17. S. Fre, M. Huyghe, P. Mourikis, S. Robine, D. Louvard, S. Artavanis-Tsakonas, Notch signals control the fate of immature progenitor cells in the intestine. *Nature*. **435**, 964–968 (2005).
18. Z. Kabiri, G. Greicius, B. Madan, S. Biechele, Z. Zhong, H. Zaribafzadeh, Edison, J. Aliyev, Y. Wu, R. Bunte, B. O. Williams, J. Rossant, D. M. Virshup, Stroma provides an intestinal stem cell niche in the absence of epithelial Wnts. *Development*. **141**, 2206–2215 (2014).
19. K. S. Yan, C. Y. Janda, J. Chang, G. X. Y. Zheng, K. A. Larkin, V. C. Luca, L. A. Chia, A. T. Mah, A. Han, J. M. Terry, A. Ootani, K. Roelf, M. Lee, J. Yuan, X. Li, C. R. Bolen, J. Wilhelmy, P. S. Davies, H. Ueno, R. J. Von Furstenberg, P. Belgrader, S. B. Ziraldo, H. Ordonez, S. J. Henning, M. H. Wong, M. P. Snyder, I. L. Weissman, A. J. Hsueh, T. S. Mikkelsen, K. C. Garcia, C. J. Kuo, Non-equivalence of Wnt and R-spondin ligands during Lgr5 + intestinal stem-cell self-renewal. *Nature*. **545**, 238–242 (2017).
20. M. E. Binnerts, K. A. Kim, J. M. Bright, S. M. Patel, K. Tran, M. Zhou, J. M. Leung, Y. Liu, W. E. Lomas, M. Dixon, S. A. Hazell, M. Wagle, W. S. Nie, N. Tomasevic, J. Williams, X. Zhan, M. D. Levy, W. D. Funk, A. Abo, R-Spondin1 regulates Wnt signaling by inhibiting internalization of LRP6. *Proc. Natl. Acad. Sci.* **104**, 14700–14705 (2007).
21. W. De Lau, N. Barker, T. Y. Low, B. K. Koo, V. S. W. Li, H. Teunissen, P. Kujala, A. Haegebarth, P. J. Peters, M. Van De Wetering, D. E. Stange, J. Van Es, D. Guardavaccaro, R. B. M. Schasfoort, Y. Mohri, K. Nishimori, S. Mohammed, A. J. R. Heck, H. Clevers, Lgr5 homologues associate with Wnt receptors and mediate R-spondin signalling. *Nature*. **476**, 293–297 (2011).
22. K. A. Kaphingst, S. Persky, C. Lachance, A reserve stem cell population in small intestine renders Lgr5-positive cells dispensable. *Nature*. **478**, 255–259 (2014).
23. E. Sangiorgi, M. R. Capecchi, Bmi1 is expressed in vivo in intestinal stem cells. *Nat. Genet.* **40**, 915–20 (2008).
24. K. S. Yan, O. Gevaert, G. X. Y. Zheng, B. Anchang, C. S. Probert, K. A. Larkin, P. S. Davies, Z. fen Cheng, J. S. Kaddis, A. Han, K. Roelf, R. I. Calderon, E. Cynn, X. Hu, K. Mandleywala, J. Wilhelmy, S. M. Grimes, D. C. Corney, S. C. Boutet, J. M. Terry, P. Belgrader, S. B. Ziraldo, T. S. Mikkelsen, F. Wang, R. J. von Furstenberg, N. R. Smith, P. Chandrakesan, R. May, M. A. S. Chrissy, R. Jain, C. A. Cartwright, J. C. Niland, Y. K. Hong, J. Carrington, D. T. Breault, J. Epstein, C. W. Houchen, J. P. Lynch, M. G. Martin, S. K. Plevritis, C. Curtis, H. P. Ji, L. Li, S. J. Henning, M. H. Wong, C. J. Kuo, Intestinal Enteroendocrine Lineage Cells Possess Homeostatic and Injury-Inducible Stem Cell Activity. *Cell Stem Cell*. **21**, 78-90.e6 (2017).
25. L. E. Sanman, I. W. Chen, J. M. Bieber, V. Steri, C. Trentesaux, B. Hann, O. D. Klein, L. F. Wu, S. J. Altschuler, Transit-Amplifying Cells Coordinate Changes in Intestinal Epithelial Cell-Type Composition. *Dev. Cell*. **56**, 356-365.e9 (2021).
26. Q. Yang, N. A. Bermingham, M. J. Finegold, H. Y. Zoghbi, Requirement of Math1 for secretory cell lineage commitment in the mouse intestine. *Science (80-)*. **294**, 2155–2158 (2001).
27. N. F. Shroyer, M. A. Helmrath, V. Y. C. Wang, B. Antalffy, S. J. Henning, H. Y. Zoghbi, Intestine-Specific Ablation of Mouse atonal homolog 1 (Math1) Reveals a Role in Cellular Homeostasis. *Gastroenterology*. **132**, 2478–2488 (2007).
28. K. L. VanDussen, L. C. Samuelson, Mouse atonal homolog 1 directs intestinal progenitors to secretory cell rather than absorptive cell fate. *Dev. Biol.* **346**, 215–223 (2010).

29. T. H. Kim, R. A. Shivdasani, Genetic evidence that intestinal Notch functions vary regionally and operate through a common mechanism of math1 repression. *J. Biol. Chem.* **286**, 11427–11433 (2011).
30. A. Kazanjian, T. Noah, D. Brown, J. Burkart, N. F. Shroyer, Atonal homolog 1 is required for growth and differentiation effects of Notch/ γ -secretase inhibitors on normal and cancerous intestinal epithelial cells. *Gastroenterology*. **139**, 918-928.e6 (2010).
31. J. H. Van Es, M. E. Van Gijn, O. Riccio, M. Van Den Born, M. Vooijs, H. Begthel, M. Cozijnsen, S. Robine, D. J. Winton, F. Radtke, H. Clevers, Notch/ γ -secretase inhibition turns proliferative cells in intestinal crypts and adenomas into goblet cells. *Nature*. **435**, 959–963 (2005).
32. C. L. Bevins, N. H. Salzman, Paneth cells, antimicrobial peptides and maintenance of intestinal homeostasis. *Nat. Rev. Microbiol.* **9**, 356–368 (2011).
33. M. E. Selsted, A. J. Ouellette, Mammalian defensins in the antimicrobial immune response. *Nat. Immunol.* **6**, 551–557 (2005).
34. X. Guo, J. Lv, R. Xi, The specification and function of enteroendocrine cells in Drosophila and mammals: a comparative review. *FEBS J.*, 1–24 (2021).
35. H. Melhem, D. Regan-Komito, J. H. Niess, Mucins dynamics in physiological and pathological conditions. *Int. J. Mol. Sci.* **22**, 1–16 (2021).
36. D. H. Kulkarni, J. K. Gustafsson, K. A. Knoop, K. G. McDonald, S. S. Bidani, J. E. Davis, A. N. Floyd, S. P. Hogan, C. Hsieh, R. D. Newberry, Goblet cell associated antigen passages support the induction and maintenance of oral tolerance. *Mucosal Immunol.* **13**, 271–282 (2020).
37. S. E. Howe, D. J. Lickteig, K. N. Plunkett, J. S. Ryerse, V. Konjufca, The uptake of soluble and particulate antigens by epithelial cells in the mouse small intestine. *PLoS One*. **9**, 1–11 (2014).
38. J. R. McDole, L. W. Wheeler, K. G. McDonald, B. Wang, V. Konjufca, K. A. Knoop, R. D. Newberry, M. J. Miller, Goblet cells deliver luminal antigen to CD103 + dendritic cells in the small intestine. *Nature*. **483**, 345–349 (2012).
39. F. Gerbe, J. H. Van Es, L. Makrini, B. Brulin, G. Mellitzer, S. Robine, B. Romagnolo, N. F. Shroyer, J. F. Bourgaux, C. Pignodel, H. Clevers, P. Jay, Distinct ATOH1 and Neurog3 requirements define tuft cells as a new secretory cell type in the intestinal epithelium. *J. Cell Biol.* **192**, 767–780 (2011).
40. C. Bezençon, A. Fürholz, F. Raymond, R. Mansourian, S. Métairon, J. Le Coutre, S. Damak, Murine intestinal cells expressing Trpm5 are mostly brush cells and express markers of neuronal and inflammatory cells. *J. Comp. Neurol.* **509**, 514–525 (2008).
41. H.-A. Ting, J. von Moltke, The Immune Function of Tuft Cells at Gut Mucosal Surfaces and Beyond. *J. Immunol.* **202**, 1321–1329 (2019).
42. A. L. Haber, M. Biton, N. Rogel, R. H. Herbst, K. Shekhar, C. Smillie, G. Burgin, T. M. Delorey, M. R. Howitt, Y. Katz, I. Tirosh, S. Beyaz, D. Dionne, M. Zhang, R. Raychowdhury, W. S. Garrett, O. Rozenblatt-Rosen, H. N. Shi, O. Yilmaz, R. J. Xavier, A. Regev, A single-cell survey of the small intestinal epithelium. *Nature*. **551**, 333–339 (2017).
43. S. A. Saenz, B. C. Taylor, D. Artis, Welcome to the neighborhood: Epithelial cell-derived cytokines license innate and adaptive immune responses at mucosal sites. *Immunol. Rev.* **226**, 172–190 (2008).
44. N. Miron, V. Cristea, Enterocytes: Active cells in tolerance to food and microbial antigens in the gut. *Clin. Exp. Immunol.* **167**, 405–412 (2012).
45. K. E. Carr, S. H. Smyth, M. T. McCullough, J. F. Morris, S. M. Moyes,

- Morphological aspects of interactions between microparticles and mammalian cells: Intestinal uptake and onward movement. *Prog. Histochem. Cytochem.* **46**, 185–252 (2012).
46. J. J. Reineke, D. Y. Cho, Y. T. Dingle, A. P. Morello, J. Jacob, C. G. Thanos, E. Mathiowitz, Unique insights into the intestinal absorption, transit, and subsequent biodistribution of polymer-derived microspheres. *Proc. Natl. Acad. Sci.* **110**, 13803–13808 (2013).
 47. J. L. Madara, Regulation of the movement of solutes across tight junctions. *Annu. Rev. Physiol.* **60**, 143–159 (1998).
 48. A. E. Moor, Y. Harnik, S. Ben-Moshe, E. E. Massasa, M. Rozenberg, R. Eilam, K. Bahar Halpern, S. Itzkovitz, Spatial Reconstruction of Single Enterocytes Uncovers Broad Zonation along the Intestinal Villus Axis. *Cell.* **175**, 1156-1167.e15 (2018).
 49. A. B. Thomson, M. Keelan, A. Thiesen, M. T. Clandinin, M. Ropeleski, G. E. Wild, Small bowel review: normal physiology part 1. *Dig. Dis. Sci.* **46**, 2567–87 (2001).
 50. P. Mehlen, A. Puisieux, Metastasis: A question of life or death. *Nat. Rev. Cancer.* **6**, 449–458 (2006).
 51. T. F. Bullen, S. Forrest, F. Campbell, A. R. Dodson, M. J. Hershman, D. M. Pritchard, J. R. Turner, M. H. Montrose, A. J. M. Watson, Characterization of epithelial cell shedding from human small intestine. *Lab. Invest.* **86**, 1052–1063 (2006).
 52. J. Rosenblatt, M. C. Raff, L. P. Cramer, An epithelial cell destined for apoptosis signals its neighbors to extrude it by an actin- and myosin-dependent mechanism. *Curr. Biol.* **11**, 1847–57 (2001).
 53. G. Slattum, K. M. McGee, J. Rosenblatt, P115 RhoGEF and microtubules decide the direction apoptotic cells extrude from an epithelium. *J. Cell Biol.* **186**, 693–702 (2009).
 54. D. Andrade, J. Rosenblatt, Apoptotic regulation of epithelial cellular extrusion. *Apoptosis.* **16**, 491–501 (2011).
 55. F. Ghazavi, J. Huysentruyt, J. De Coninck, S. Kourula, S. Martens, B. Hassannia, T. Wartewig, T. Divert, R. Roelandt, B. Popper, A. Hiergeist, P. Tougaard, T. Vanden Berghe, M. Joossens, G. Berx, N. Takahashi, A. Wahida, P. Vandenabeele, Executioner caspases 3 and 7 are dispensable for intestinal epithelium turnover and homeostasis at steady state. *Proc. Natl. Acad. Sci.* **119** (2022), doi:10.1073/pnas.2024508119.
 56. Y. Gu, T. Forostyan, R. Sabbadini, J. Rosenblatt, Epithelial cell extrusion requires the sphingosine-1-phosphate receptor 2 pathway. *J. Cell Biol.* **193**, 667–676 (2011).
 57. G. T. Eisenhoffer, P. D. Loftus, M. Yoshigi, H. Otsuna, C. Bin Chien, P. A. Morcos, J. Rosenblatt, Crowding induces live cell extrusion to maintain homeostatic cell numbers in epithelia. *Nature.* **484**, 546–549 (2012).
 58. D. R. Clayburgh, S. Rosen, E. D. Witkowski, F. Wang, S. Blair, S. Dudek, J. G. N. Garcia, J. C. Alverdy, J. R. Turner, A differentiation-dependent splice variant of myosin light chain kinase, MLCK1, regulates epithelial tight junction permeability. *J. Biol. Chem.* **279**, 55506–13 (2004).
 59. D. R. Clayburgh, T. A. Barrett, Y. Tang, J. B. Meddings, L. J. Van Eldik, D. M. Watterson, L. L. Clarke, R. J. Mrsny, J. R. Turner, Epithelial myosin light chain kinase-dependent barrier dysfunction mediates T cell activation-induced diarrhea in vivo. *J. Clin. Invest.* **115**, 2702–15 (2005).
 60. H. H. Uhlig, Monogenic diseases associated with intestinal inflammation:

Implications for the understanding of inflammatory bowel disease. *Gut*. **62**, 1795–1805 (2013).

61. L. Jostins, S. Ripke, R. K. Weersma, R. H. Duerr, D. P. McGovern, K. Y. Hui, J. C. Lee, L. Philip Schumm, Y. Sharma, C. A. Anderson, J. Essers, M. Mitrovic, K. Ning, I. Cleynen, E. Theatre, S. L. Spain, S. Raychaudhuri, P. Goyette, Z. Wei, C. Abraham, J. P. Achkar, T. Ahmad, L. Amininejad, A. N. Ananthakrishnan, V. Andersen, J. M. Andrews, L. Baidoo, T. Balschun, P. A. Bampton, A. Bitton, G. Boucher, S. Brand, C. Büning, A. Cohain, S. Cichon, M. D'Amato, D. De Jong, K. L. Devaney, M. Dubinsky, C. Edwards, D. Ellinghaus, L. R. Ferguson, D. Franchimont, K. Fransen, R. Geary, M. Georges, C. Gieger, J. Glas, T. Haritunians, A. Hart, C. Hawkey, M. Hedl, X. Hu, T. H. Karlsen, L. Kupcinskis, S. Kugathasan, A. Latiano, D. Laukens, I. C. Lawrance, C. W. Lees, E. Louis, G. Mahy, J. Mansfield, A. R. Morgan, C. Mowat, W. Newman, O. Palmieri, C. Y. Ponsioen, U. Potocnik, N. J. Prescott, M. Regueiro, J. I. Rotter, R. K. Russell, J. D. Sanderson, M. Sans, J. Satsangi, S. Schreiber, L. A. Simms, J. Sventoraityte, S. R. Targan, K. D. Taylor, M. Tremelling, H. W. Verspaget, M. De Vos, C. Wijmenga, D. C. Wilson, J. Winkelmann, R. J. Xavier, S. Zeissig, B. Zhang, C. K. Zhang, H. Zhao, M. S. Silverberg, V. Annese, H. Hakonarson, S. R. Brant, G. Radford-Smith, C. G. Mathew, J. D. Rioux, E. E. Schadt, M. J. Daly, A. Franke, M. Parkes, S. Vermeire, J. C. Barrett, J. H. Cho, M. Barclay, L. Peyrin-Biroulet, M. Chamailard, J. F. Colombel, M. Cottone, A. Croft, R. D'Inca, J. Halfvarson, K. Hanigan, P. Henderson, J. P. Hugot, A. Karban, N. A. Kennedy, M. Azam Khan, M. Lémann, A. Levine, D. Massey, M. Milla, G. W. Montgomery, S. M. Evelyn Ng, I. Oikonomou, H. Peeters, D. D. Proctor, J. F. Rahier, R. Roberts, P. Rutgeerts, F. Seibold, L. Stronati, K. M. Taylor, L. Törkvist, K. Ulick, J. Van Limbergen, A. Van Gossom, M. H. Vatn, H. Zhang, W. Zhang, J. M. Andrews, P. A. Bampton, M. Barclay, T. H. Florin, K. Krishnaprasad, K. Krishnaprasad, I. C. Lawrance, G. Mahy, G. W. Montgomery, G. Radford-Smith, R. L. Roberts, L. A. Simms, L. Amininejad, I. Cleynen, O. Dewit, D. Franchimont, M. Georges, D. Laukens, H. Peeters, J. F. Rahier, P. Rutgeerts, E. Theatre, A. Van Gossom, S. Vermeire, G. Aumais, L. Baidoo, A. M. Barrie, K. Beck, E. J. Bernard, D. G. Binion, A. Bitton, S. R. Brant, J. H. Cho, A. Cohen, K. Croitoru, M. J. Daly, L. W. Datta, C. Deslandres, R. H. Duerr, D. Dutridge, J. Ferguson, J. Fultz, P. Goyette, G. R. Greenberg, T. Haritunians, G. Jobin, S. Katz, R. G. Lahaie, D. P. McGovern, L. Nelson, S. M. Ng, K. Ning, I. Oikonomou, P. Paré, D. D. Proctor, M. D. Regueiro, J. D. Rioux, E. Ruggiero, L. Philip Schumm, M. Schwartz, R. Scott, Y. Sharma, M. S. Silverberg, D. Spears, A. Hillary Steinhart, J. M. Stempak, J. M. Swoger, C. Tsagarelis, W. Zhang, C. Zhang, H. Zhao, J. Aerts, T. Ahmad, H. Arbury, A. Attwood, A. Auton, S. G. Ball, A. J. Balmforth, C. Barnes, J. C. Barrett, I. Barroso, A. Barton, A. J. Bennett, S. Bhaskar, K. Blaszczyk, J. Bowes, O. J. Brand, P. S. Braund, F. Bredin, G. Breen, M. J. Brown, I. N. Bruce, J. Bull, O. S. Burren, J. Burton, J. Byrnes, S. Caesar, N. Cardin, C. M. Clee, A. J. Coffey, J. M. C. Connell, D. F. Conrad, J. D. Cooper, A. F. Dominiczak, K. Downes, H. E. Drummond, D. Dudakia, A. Dunham, B. Ebbs, D. Eccles, S. Edkins, C. Edwards, A. Elliot, P. Emery, D. M. Evans, G. Evans, S. Eyre, A. Farmer, I. Nicol Ferrier, E. Flynn, A. Forbes, L. Forty, J. A. Franklyn, T. M. Frayling, R. M. Freathy, E. Giannoulatou, P. Gibbs, P. Gilbert, K. Gordon-Smith, E. Gray, E. Green, C. J. Groves, D. Grozeva, R. Gwilliam, A. Hall, N. Hammond, M. Hardy, P. Harrison, N. Hassanali, H. Hebaishi, S. Hines, A. Hinks, G. A. Hitman, L. Hocking, C. Holmes, E. Howard, P. Howard, J. M. M. Howson, D. Hughes, S. Hunt, J. D. Isaacs, M. Jain, D. P. Jewell,

- T. Johnson, J. D. Jolley, I. R. Jones, L. A. Jones, G. Kirov, C. F. Langford, H. Lango-Allen, G. Mark Lathrop, J. Lee, K. L. Lee, C. Lees, K. Lewis, C. M. Lindgren, M. Maisuria-Armer, J. Maller, J. Mansfield, J. L. Marchini, P. Martin, D. C. O. Massey, W. L. McArdle, P. McGuffin, K. E. McLay, G. McVean, A. Mentzer, M. L. Mimmack, A. E. Morgan, A. P. Morris, C. Mowat, P. B. Munroe, S. Myers, W. Newman, E. R. Nimmo, M. C. O'Donovan, A. Onipinla, N. R. Ovington, M. J. Owen, K. Palin, A. Palotie, K. Parnell, R. Pearson, D. Pernet, J. R. B. Perry, A. Phillips, V. Plagnol, N. J. Prescott, I. Prokopenko, M. A. Quail, S. Rafelt, N. W. Rayner, D. M. Reid, A. Renwick, S. M. Ring, N. Robertson, S. Robson, E. Russell, D. St Clair, J. G. Sambrook, J. D. Sanderson, S. J. Sawcer, H. Schuilenburg, C. E. Scott, R. Scott, S. Seal, S. Shaw-Hawkins, B. M. Shields, M. J. Simmonds, D. J. Smyth, E. Somaskantharajah, K. Spanova, S. Steer, J. Stephens, H. E. Stevens, K. Stirrups, M. A. Stone, D. P. Strachan, Z. Su, D. P. M. Symmons, J. R. Thompson, W. Thomson, M. D. Tobin, M. E. Travers, C. Turnbull, D. Vukcevic, L. V. Wain, M. Walker, N. M. Walker, C. Wallace, M. Warren-Perry, N. A. Watkins, J. Webster, M. N. Weedon, A. G. Wilson, M. Woodburn, B. Paul Wordsworth, C. Yau, A. H. Young, E. Zeggini, M. A. Brown, P. R. Burton, M. J. Caulfield, A. Compston, M. Farrall, S. C. L. Gough, A. S. Hall, A. T. Hattersley, A. V. S. Hill, C. G. Mathew, M. Pembrey, J. Satsangi, M. R. Stratton, J. Worthington, M. E. Hurles, A. Duncanson, W. H. Ouwehand, M. Parkes, N. Rahman, J. A. Todd, N. J. Samani, D. P. Kwiatkowski, M. I. McCarthy, N. Craddock, P. Deloukas, P. Donnelly, J. M. Blackwell, E. Bramon, J. P. Casas, A. Corvin, J. Jankowski, H. S. Markus, C. N. A. Palmer, R. Plomin, A. Rautanen, R. C. Trembath, A. C. Viswanathan, N. W. Wood, C. C. A. Spencer, G. Band, C. Bellenguez, C. Freeman, G. Hellenthal, E. Giannoulatou, M. Pirinen, R. Pearson, A. Strange, H. Blackburn, S. J. Bumpstead, S. Dronov, M. Gillman, A. Jayakumar, O. T. McCann, J. Liddle, S. C. Potter, R. Ravindrarajah, M. Ricketts, M. Waller, P. Weston, S. Widaa, P. Whittaker, Host-microbe interactions have shaped the genetic architecture of inflammatory bowel disease. *Nature*. **491**, 119–124 (2012).
62. D. Kontoyiannis, M. Pasparakis, T. T. Pizarro, F. Cominelli, G. Kollias, Impaired on/off regulation of TNF biosynthesis in mice lacking TNF AU- rich elements: Implications for joint and gut-associated immunopathologies. *Immunity*. **10**, 387–398 (1999).
63. M. Leppkes, M. Roulis, M. F. Neurath, G. Kollias, C. Becker, Pleiotropic functions of TNF- α in the regulation of the intestinal epithelial response to inflammation. *Int. Immunol.* **26**, 509–515 (2014).
64. E. Mizoguchi, A. Mizoguchi, H. Takedatsu, E. Cario, Y. P. de Jong, C. J. Ooi, R. J. Xavier, C. Terhorst, D. K. Podolsky, A. K. Bhan, Role of tumor necrosis factor receptor 2 (TNFR2) in colonic epithelial hyperplasia and chronic intestinal inflammation in mice. *Gastroenterology*. **122**, 134–44 (2002).
65. D. A. Flusberg, P. K. Sorger, Surviving apoptosis: Life-death signaling in single cells. *Trends Cell Biol.* **25**, 446–458 (2015).
66. R. Kiesslich, M. Goetz, E. M. Angus, Q. Hu, Y. Guan, C. Potten, T. Allen, M. F. Neurath, N. F. Shroyer, M. H. Montrose, A. J. M. Watson, Identification of Epithelial Gaps in Human Small and Large Intestine by Confocal Endomicroscopy. *Gastroenterology*. **133**, 1769–1778 (2007).
67. P. F. Piguet, C. Vesin, J. Guo, Y. Donati, C. Barazzone, TNF-induced enterocyte apoptosis in mice is mediated by the TNF receptor 1 and does not require p53. *Eur. J. Immunol.* **28**, 3499–3505 (1998).
68. S. He, L. Wang, L. Miao, T. Wang, F. Du, L. Zhao, X. Wang, Receptor Interacting

- Protein Kinase-3 Determines Cellular Necrotic Response to TNF- α . *Cell*. **137**, 1100–1111 (2009).
69. Y. Lin, S. Choksi, H. M. Shen, Q. F. Yang, G. M. Hur, Y. S. Kim, J. H. Tran, S. A. Nedospasov, Z. G. Liu, Tumor Necrosis Factor-induced Nonapoptotic Cell Death Requires Receptor-interacting Protein-mediated Cellular Reactive Oxygen Species Accumulation. *J. Biol. Chem.* **279**, 10822–10828 (2004).
 70. S. Grootjans, T. Vanden Berghe, P. Vandenabeele, Initiation and execution mechanisms of necroptosis: An overview. *Cell Death Differ.* **24**, 1184–1195 (2017).
 71. T. Sato, R. G. Vries, H. J. Snippert, M. Van De Wetering, N. Barker, D. E. Stange, J. H. Van Es, A. Abo, P. Kujala, P. J. Peters, H. Clevers, Single Lgr5 stem cells build crypt-villus structures in vitro without a mesenchymal niche. *Nature*. **459**, 262–265 (2009).
 72. M. Beaumont, F. Blanc, C. Cherbuy, G. Egidy, E. Giuffra, S. Lacroix-Lamandé, A. Wiedemann, Intestinal organoids in farm animals. *Vet. Res.* **52**, 33 (2021).
 73. G. Schwank, H. Clevers, CRISPR/Cas9-Mediated Genome Editing of Mouse Small Intestinal Organoids. *Methods Mol. Biol.* **1422**, 3–11 (2016).
 74. H. Miyoshi, T. S. Stappenbeck, In vitro expansion and genetic modification of gastrointestinal stem cells in spheroid culture. *Nat. Protoc.* **8**, 2471–2482 (2013).
 75. K. L. VanDussen, N. M. Sonnek, T. S. Stappenbeck, L-WRN conditioned medium for gastrointestinal epithelial stem cell culture shows replicable batch-to-batch activity levels across multiple research teams. *Stem Cell Res.* **37**, 101430 (2019).
 76. J. Y. Co, M. Margalef-Català, X. Li, A. T. Mah, C. J. Kuo, D. M. Monack, M. R. Amieva, Controlling Epithelial Polarity: A Human Enteroid Model for Host-Pathogen Interactions. *Cell Rep.* **26**, 2509–2520 (2019).
 77. D. Serra, U. Mayr, A. Boni, I. Lukonin, M. Rempfler, L. Challet Meylan, M. B. Stadler, P. Strnad, P. Papasaikas, D. Vischi, A. Waldt, G. Roma, P. Liberali, Self-organization and symmetry breaking in intestinal organoid development. *Nature*. **569**, 66–72 (2019).
 78. M. Stelzner, M. Helmrath, J. C. Y. Dunn, S. J. Henning, C. W. Houchen, C. Kuo, J. Lynch, L. Li, S. T. Magness, M. G. Martin, M. H. Wong, J. Yu, A nomenclature for intestinal in vitro cultures. *Am. J. Physiol. - Gastrointest. Liver Physiol.* **302**, 1359–1363 (2012).
 79. S. Middendorp, K. Schneeberger, C. L. Wiegerinck, M. Mokry, R. D. L. Akkerman, S. van Wijngaarden, H. Clevers, E. E. S. Nieuwenhuis, Adult stem cells in the small intestine are intrinsically programmed with their location-specific function. *Stem Cells*. **32**, 1083–91 (2014).
 80. B. van der Hee, O. Madsen, J. Vervoort, H. Smidt, J. M. Wells, Congruence of Transcription Programs in Adult Stem Cell-Derived Jejunum Organoids and Original Tissue During Long-Term Culture. *Front. Cell Dev. Biol.* **8** (2020), doi:10.3389/fcell.2020.00375.
 81. C. Aguilar, M. Alves da Silva, M. Saraiva, M. Neyazi, I. A. S. Olsson, S. Bartfeld, Organoids as host models for infection biology – a review of methods. *Exp. Mol. Med.* **53**, 1471–1482 (2021).
 82. Y. Yin, M. Bijvelds, W. Dang, L. Xu, A. A. van der Eijk, K. Knipping, N. Tuysuz, J. F. Dekkers, Y. Wang, J. de Jonge, D. Sprengers, L. J. W. van der Laan, J. M. Beekman, D. Ten Berge, H. J. Metselaar, H. de Jonge, M. P. G. Koopmans, M. P. Peppelenbosch, Q. Pan, Modeling rotavirus infection and antiviral therapy using primary intestinal organoids. *Antiviral Res.* **123**, 120–31 (2015).
 83. S. R. Finkbeiner, X. L. Zeng, B. Utama, R. L. Atmar, N. F. Shroyer, M. K. Estesa,

- Stem cell-derived human intestinal organoids as an infection model for rotaviruses. *MBio*. **3**, 1–6 (2012).
84. K. Saxena, S. E. Blutt, K. Ettayebi, X. Zeng, J. R. Broughman, S. E. Crawford, U. C. Karandikar, N. P. Sastri, M. E. Conner, A. R. Opekun, D. Y. Graham, W. Qureshi, V. Sherman, J. Foulke-abel, J. In, O. Kovbasnjuk, N. C. Zachos, M. Donowitz, K. Estes, Human Intestinal Enteroids: a New Model To Study Human Rotavirus Infection, Host Restriction, and Pathophysiology. *J. Virol.* **90**, 43–56 (2016).
 85. C. G. Drummond, A. M. Bolock, C. Ma, C. J. Luke, M. Good, C. B. Coyne, Enteroviruses infect human enteroids and induce antiviral signaling in a cell lineage-specific manner. *Proc. Natl. Acad. Sci.* **114**, 1672–1677 (2017).
 86. S. Zhu, S. Ding, P. Wang, Z. Wei, W. Pan, N. W. Palm, Y. Yang, H. Yu, H. Li, G. Wang, X. Lei, M. R. de Zoete, J. Zhao, Y. Zheng, H. Chen, Y. Zhao, K. A. Jurado, N. Feng, L. Shan, Y. Kluger, J. Lu, C. Abraham, E. Fikrig, H. B. Greenberg, R. A. Flavell, Nlrp9b inflammasome restricts rotavirus infection in intestinal epithelial cells. *Nature*. **546**, 667–670 (2017).
 87. J. Krüger, R. Groß, C. Conzelmann, J. A. Müller, L. Koepke, K. M. J. Sparrer, T. Weil, D. Schütz, T. Seufferlein, T. F. E. Barth, S. Stenger, S. Heller, J. Münch, A. Kleger, Drug Inhibition of SARS-CoV-2 Replication in Human Pluripotent Stem Cell-Derived Intestinal Organoids. *Cmgh*. **11**, 935–948 (2021).
 88. A. Mithal, A. J. Hume, J. Lindstrom-Vautrin, C. Villacorta-Martin, J. Olejnik, E. Bullitt, A. Hinds, E. Mühlberger, G. Mostoslavsky, Human Pluripotent Stem Cell-Derived Intestinal Organoids Model SARS-CoV-2 Infection Revealing a Common Epithelial Inflammatory Response. *Stem Cell Reports*. **16**, 940–953 (2021).
 89. M. M. Lamers, J. Beumer, J. Van Der Vaart, K. Knoops, J. Puschhof, T. I. Breugem, R. B. G. Ravelli, J. P. Van Schayck, A. Z. Mykytyn, H. Q. Duimel, E. Van Donselaar, S. Riesebosch, H. J. H. Kuijpers, D. Schipper, W. J. V. De Wetering, M. De Graaf, M. Koopmans, E. Cuppen, P. J. Peters, B. L. Haagmans, H. Clevers, SARS-CoV-2 productively infects human gut enterocytes. *Science* (80-.). **369**, 50–54 (2020).
 90. J. Puschhof, C. Pleguezuelos-Manzano, A. Martinez-Silgado, N. Akkerman, A. Saftien, C. Boot, A. de Waal, J. Beumer, D. Dutta, I. Heo, H. Clevers, Intestinal organoid cocultures with microbes. *Nat. Protoc.* **16**, 4633–4649 (2021).
 91. S. Bartfeld, T. Bayram, M. Van De Wetering, M. Huch, H. Begthel, P. Kujala, R. Vries, P. J. Peters, H. Clevers, In vitro expansion of human gastric epithelial stem cells and their responses to bacterial infection. *Gastroenterology*. **148**, 126-136.e6 (2015).
 92. Y. G. Zhang, S. Wu, Y. Xia, J. Sun, Salmonella-infected crypt-derived intestinal organoid culture system for host–bacterial interactions. *Physiol. Rep.* **2**, 1–11 (2014).
 93. E. A. Lees, J. L. Forbester, S. Forrest, L. Kane, D. Goulding, G. Dougan, Using human induced pluripotent stem cell-derived intestinal organoids to study and modify epithelial cell protection against Salmonella and other pathogens. *J. Vis. Exp.* **2019**, 1–9 (2019).
 94. J. L. Leslie, S. Huang, J. S. Opp, M. S. Nagy, M. Kobayashi, V. B. Young, J. R. Spence, Persistence and toxin production by *Clostridium difficile* within human intestinal organoids result in disruption of epithelial paracellular barrier function. *Infect. Immun.* **83**, 138–145 (2015).
 95. I. Heo, D. Dutta, D. A. Schaefer, N. Iakobachvili, B. Artegiani, N. Sachs, K. E. Boonekamp, G. Bowden, A. P. A. Hendrickx, R. J. L. Willems, P. J. Peters, M. W.

- Riggs, R. O'Connor, H. Clevers, Modelling Cryptosporidium infection in human small intestinal and lung organoids. *Nat. Microbiol.* **3**, 814–823 (2018).
96. G. Noel, N. W. Baetz, J. F. Staab, M. Donowitz, O. Kovbasnjuk, M. F. Pasetti, N. C. Zachos, A primary human macrophage- enteroid co-culture model to investigate mucosal gut physiology and host-pathogen interactions. *Sci. Rep.* **7**, 45270 (2017).
 97. C. M. Cattaneo, K. K. Dijkstra, L. F. Fanchi, S. Kelderman, S. Kaing, N. van Rooij, S. van den Brink, T. N. Schumacher, E. E. Voest, Tumor organoid–T-cell coculture systems. *Nat. Protoc.* **15**, 15–39 (2020).
 98. R. R. C. E. Schreurs, M. E. Baumdick, A. Drewniak, M. J. Bunders, In vitro co-culture of human intestinal organoids and lamina propria-derived CD4+ T cells. *STAR Protoc.* **2** (2021), doi:10.1016/j.xpro.2021.100519.
 99. A. J. Sadler, B. R. G. Williams, Interferon-inducible antiviral effectors. *Nat. Rev. Immunol.* **8**, 559–68 (2008).
 100. J. W. Schoggins, C. M. Rice, Interferon-stimulated genes and their antiviral effector functions. *Curr. Opin. Virol.* **1**, 519–25 (2011).
 101. S. F. Li, M. J. Gong, F. R. Zhao, J. J. Shao, Y. L. Xie, Y. G. Zhang, H. Y. Chang, Type I interferons: Distinct biological activities and current applications for viral infection. *Cell. Physiol. Biochem.* **51**, 2377–2396 (2018).
 102. E. V. Mesev, R. A. LeDesma, A. Ploss, Decoding type I and III interferon signalling during viral infection. *Nat. Microbiol.* (2019), doi:10.1038/s41564-019-0421-x.
 103. H. M. Lazear, T. J. Nice, M. S. Diamond, Interferon- λ : immune functions at barrier surfaces and beyond. *Immunity.* **43**, 15–28 (2015).
 104. S. H. Kim, B. Cohen, D. Novick, M. Rubinstein, Mammalian type I interferon receptors consists of two subunits: IFN α R1 and IFN α R2. *Gene.* **196**, 279–286 (1997).
 105. M. A. Farrar, R. D. Schreiber, The molecular cell biology of interferon- γ and its receptor. *Annu. Rev. Immunol.* **11**, 571–611 (1993).
 106. S. V. Kotenko, G. Gallagher, V. V. V. Baurin, A. Lewis-Antes, M. Shen, N. K. Shah, J. A. Langer, F. Sheikh, H. Dickensheets, R. P. Donnelly, IFN- λ s mediate antiviral protection through a distinct class II cytokine receptor complex. *Nat. Immunol.* **4**, 69–77 (2003).
 107. P. Sheppard, W. Kindsvogel, W. Xu, K. Henderson, S. Schlutsmeyer, T. E. Whitmore, R. Kuestner, U. Garrigues, C. Birks, J. Roraback, C. Ostrander, D. Dong, J. Shin, S. Presnell, B. Fox, B. Haldeman, E. Cooper, D. Taft, T. Gilbert, F. J. Grant, M. Tackett, W. Krivan, G. McKnight, C. Clegg, D. Foster, K. M. Klucher, IL-28, IL-29 and their class II cytokine receptor IL-28R. *Nat. Immunol.* **4**, 63–68 (2003).
 108. H. H. Gad, C. Dellgren, O. J. Hamming, S. Vends, S. R. Paludan, R. Hartmann, Interferon- λ is functionally an interferon but structurally related to the interleukin-10 family. *J. Biol. Chem.* **284**, 20869–75 (2009).
 109. J. L. Mendoza, W. M. Schneider, H.-H. H. Hoffmann, K. Vercauteren, K. M. Jude, A. Xiong, I. Moraga, T. M. Horton, J. S. Glenn, Y. P. de Jong, C. M. Rice, K. C. Garcia, The IFN- λ -IFN- λ R1-IL-10R β Complex Reveals Structural Features Underlying Type III IFN Functional Plasticity. *Immunity.* **46**, 379–392 (2017).
 110. W. M. Schneider, M. D. Chevillotte, C. M. Rice, Interferon-stimulated genes: a complex web of host defenses. *Annu. Rev. Immunol.* **32**, 513–45 (2014).
 111. C. Schindler, C. Plumlee, Interferons pen the JAK-STAT pathway. *Semin. Cell Dev. Biol.* **19**, 311–318 (2008).

112. H. Harada, M. Matsumoto, M. Sato, Y. Kashiwazaki, T. Kimura, M. Kitagawa, T. Yokochi, R. S. P. Tan, T. Takasugi, Y. Kadokawa, C. Schindler, R. D. Schreiber, S. Noguchi, T. Taniguchi, Regulation of IFN- α/β genes: Evidence for a dual function of the transcription factor complex ISGF3 in the production and action of IFN- α/β . *Genes to Cells*. **1**, 995–1005 (1996).
113. A. Kohli, X. Zhang, J. Yang, R. S. Russell, R. P. Donnelly, F. Sheikh, A. Sherman, H. Young, T. Imamichi, R. A. Lempicki, H. Masur, S. Kottlilil, Distinct and overlapping genomic profiles and antiviral effects of Interferon- λ and - α On HCV-infected and noninfected hepatoma cells. *J. Viral Hepat.* **19**, 843–853 (2012).
114. T. Marcello, A. Grakoui, G. Barba-Spaeth, E. S. Machlin, S. V Kotenko, M. R. MacDonald, C. M. Rice, Interferons alpha and lambda inhibit hepatitis C virus replication with distinct signal transduction and gene regulation kinetics. *Gastroenterology*. **131**, 1887–98 (2006).
115. S. E. Doyle, H. Schreckhise, K. Khuu-Duong, K. Henderson, R. Rosler, H. Storey, L. Yao, H. Liu, F. Barahmand-Pour, P. Sivakumar, C. Chan, C. Birks, D. Foster, C. H. Clegg, P. Wietzke-Braun, S. Mihm, K. M. Klucher, Interleukin-29 uses a type 1 interferon-like program to promote antiviral responses in human hepatocytes. *Hepatology*. **44**, 896–906 (2006).
116. J. W. Schoggins, Interferon-Stimulated Genes: What Do They All Do? *Annu. Rev. Virol.* **6**, 567–584 (2019).
117. C. C. Bailey, G. Zhong, I. C. Huang, M. Farzan, IFITM-family proteins: The cell's first line of antiviral defense. *Annu. Rev. Virol.* **1**, 261–283 (2014).
118. A. A. Anafu, C. H. Bowen, C. R. Chin, A. L. Brass, G. H. Holm, Interferon-inducible transmembrane protein 3 (IFITM3) restricts reovirus cell entry. *J. Biol. Chem.* **288**, 17261–17271 (2013).
119. O. Haller, P. Staeheli, M. Schwemmler, G. Kochs, Mx GTPases: Dynamin-like antiviral machines of innate immunity. *Trends Microbiol.* **23**, 154–163 (2015).
120. H. Kristiansen, H. H. Gad, S. Eskildsen-Larsen, P. Despres, R. Hartmann, The oligoadenylate synthetase family: An ancient protein family with multiple antiviral activities. *J. Interf. Cytokine Res.* **31**, 41–47 (2011).
121. J. V. Dzimianski, F. E. M. Scholte, É. Bergeron, S. D. Pegan, ISG15: It's Complicated. *J. Mol. Biol.* **431**, 4203–4216 (2019).
122. M. Van Gent, K. M. J. Sparrer, M. U. Gack, TRIM proteins and their roles in antiviral host defenses. *Annu. Rev. Virol.* **5**, 385–405 (2018).
123. C. J. Hattlmann, J. N. Kelly, S. D. Barr, TRIM22: A Diverse and Dynamic Antiviral Protein. *Mol. Biol. Int.* **2012**, 1–10 (2012).
124. G. I. Vladimer, M. W. Górna, G. Superti-Furga, IFITs: Emerging roles as key antiviral proteins. *Front. Immunol.* **5**, 1–6 (2014).
125. M. S. Diamond, M. Farzan, The broad-spectrum antiviral functions of IFIT and IFITM proteins. *Nat. Rev. Immunol.* **13**, 46–57 (2013).
126. N. Au-Yeung, R. Mandhana, C. M. Horvath, Transcriptional regulation by STAT1 and STAT2 in the interferon JAK-STAT pathway. *JAK-STAT.* **2**, e23931 (2013).
127. A. H. H. van Boxel-Dezaire, M. R. S. Rani, G. R. Stark, Complex Modulation of Cell Type-Specific Signaling in Response to Type I Interferons. *Immunity*. **25**, 361–372 (2006).
128. C. Mazewski, R. E. Perez, E. N. Fish, L. C. Platanius, Type I Interferon (IFN)-Regulated Activation of Canonical and Non-Canonical Signaling Pathways. *Front. Immunol.* **11**, 1–13 (2020).
129. A. Majoros, E. Platanius, E. Kernbauer-Hölzl, F. Rosebrock, M. Müller, T. Decker, Canonical and non-canonical aspects of JAK-STAT signaling: Lessons from

- interferons for cytokine responses. *Front. Immunol.* **8** (2017), doi:10.3389/fimmu.2017.00029.
130. H. Cheon, E. G. Holvey-Bates, J. W. Schoggins, S. Forster, P. Hertzog, N. Imanaka, C. M. Rice, M. W. Jackson, D. J. Junk, G. R. Stark, IFN β -dependent increases in STAT1, STAT2, and IRF9 mediate resistance to viruses and DNA damage. *EMBO J.* **32**, 2751–2763 (2013).
 131. W. Wang, Y. Yin, L. Xu, J. Su, F. Huang, Y. Wang, P. P. C. Boor, K. Chen, W. Wang, W. Cao, X. Zhou, P. Liu, L. J. W. van der Laan, J. Kwekkeboom, M. P. Peppelenbosch, Q. Pan, Unphosphorylated ISGF3 drives constitutive expression of interferon-stimulated genes to protect against viral infections. *Sci. Signal.* **10**, eaah4248 (2017).
 132. Y. J. Lou, X. R. Pan, P. M. Jia, D. Li, S. Xiao, Z. L. Zhang, S. J. Chen, Z. Chen, J. H. Tong, Irf-9/stat2 functional interaction drives Retinoic acid-induced gene expression independently of stat1. *Cancer Res.* **69**, 3673–3680 (2009).
 133. P. T. N. Sarkis, S. Ying, R. Xu, X.-F. Yu, STAT1-Independent Cell Type-Specific Regulation of Antiviral APOBEC3G by IFN- α . *J. Immunol.* **177**, 4530–4540 (2006).
 134. H. A. R. Bluysen, D. E. Levy, Stat2 is a transcriptional activator that requires sequence-specific contacts provided by Stat1 and p48 for stable interaction with DNA. *J. Biol. Chem.* **272**, 4600–4605 (1997).
 135. S. T. Perry, M. D. Buck, S. M. Lada, C. Schindler, S. Shresta, STAT2 mediates innate immunity to dengue virus in the absence of STAT1 via the type I interferon receptor. *PLoS Pathog.* **7** (2011), doi:10.1371/journal.ppat.1001297.
 136. S. Majumder, L. Z. Zhou, P. Chaturvedi, G. Babcock, S. Aras, R. M. Ransohoff, p48/STAT-1 α -containing complexes play a predominant role in induction of IFN- γ -inducible protein, 10 kDa (IP-10) by IFN- γ alone or in synergy with TNF- α . *J. Immunol.* **161**, 4736–44 (1998).
 137. I. Rauch, F. Rosebrock, E. Hainzl, S. Heider, A. Majoros, S. Wienerroither, B. Strobl, S. Stockinger, L. Kenner, M. Müller, T. Decker, Noncanonical Effects of IRF9 in Intestinal Inflammation: More than Type I and Type III Interferons. *Mol. Cell. Biol.* **35**, 2332–2343 (2015).
 138. A. Zimmermann, M. Trilling, M. Wagner, M. Wilborn, I. Bubic, S. Jonjic, U. Koszinowski, H. Hengel, A cytomegaloviral protein reveals a dual role for STAT2 in IFN- γ signaling and antiviral responses. *J. Exp. Med.* **201**, 1543–1553 (2005).
 139. A. N. Morrow, H. Schmeisser, T. Tsuno, K. C. Zoon, A Novel Role for IFN-Stimulated Gene Factor 3 II in IFN- γ Signaling and Induction of Antiviral Activity in Human Cells. *J. Immunol.* **186**, 1685–1693 (2011).
 140. C. R. Bolen, S. Ding, M. D. Robek, S. H. Kleinstein, Dynamic expression profiling of type I and type III interferon-stimulated hepatocytes reveals a stable hierarchy of gene expression. *Hepatology.* **59**, 1262–1272 (2014).
 141. N. Jilg, W. Lin, J. Hong, E. A. Schaefer, D. Wolski, J. Meixong, K. Goto, C. Brisac, P. Chusri, D. N. Fusco, S. Chevaliez, J. Luther, K. Kumthip, T. J. Urban, L. F. Peng, G. M. Lauer, R. T. Chung, Kinetic differences in the induction of interferon stimulated genes by interferon- α and interleukin 28B are altered by infection with hepatitis C virus. *Hepatology.* **59**, 1250–1261 (2014).
 142. K. Pervolaraki, S. Rastgou Talemi, D. Albrecht, C. Bamford, J. Mendoza, C. Garcia, T. Höfer, M. L. Stanifer, S. Boulant, Differential induction of interferon stimulated genes between type I and 2 type III interferons is independent of interferon receptor abundance. *PLoS Pathog.* **14**, e1007420 (2018).
 143. K. Pervolaraki, M. L. Stanifer, S. Münchau, L. A. Renn, D. Albrecht, S. Kurzhals, E. Senís, D. Grimm, J. Schröder-Braunstein, R. L. Rabin, S. Boulant, S. Munchau,

- L. A. Renn, D. Albrecht, S. Kurzhals, E. Senis, D. Grimm, J. Schroder-Braunstein, R. L. Rabin, S. Boulant, Type I and Type III Interferons Display Different Dependency on Mitogen-Activated Protein Kinases to Mount an Antiviral State in the Human Gut. *Front. Immunol.* **8**, 1–16 (2017).
144. Z. Zhou, O. J. Hamming, N. Ank, S. R. Paludan, A. L. Nielsen, R. Hartmann, Type III Interferon (IFN) Induces a Type I IFN-Like Response in a Restricted Subset of Cells through Signaling Pathways Involving both the Jak-STAT Pathway and the Mitogen-Activated Protein Kinases. *J. Virol.* **81**, 7749–7758 (2007).
145. A. Broggi, Y. Tan, F. Granucci, I. Zanoni, IFN- λ suppresses intestinal inflammation by non-translational regulation of neutrophil function. *Nat. Immunol.* **18**, 1084–1093 (2017).
146. S. Davidson, T. M. McCabe, S. Crotta, H. H. Gad, E. M. Hessel, S. Beinke, R. Hartmann, A. Wack, IFN λ is a potent anti-influenza therapeutic without the inflammatory side effects of IFN α treatment. *EMBO Mol. Med.* **8**, 1099–1112 (2016).
147. I. E. Galani, V. Triantafyllia, E.-E. E. Eleminiadou, O. Koltsida, A. Stavropoulos, M. Manioudaki, D. Thanos, S. E. Doyle, S. V. Kotenko, K. Thanopoulou, E. Andreakos, Interferon- λ Mediates Non-redundant Front-Line Antiviral Protection against Influenza Virus Infection without Compromising Host Fitness. *Immunity.* **46**, 875-890.e6 (2017).
148. A. Forero, S. Ozarkar, H. Li, C. H. Lee, E. A. Hemann, M. S. Nadjombati, M. R. Hendricks, L. So, R. Green, C. N. Roy, S. N. Sarkar, J. von Moltke, S. K. Anderson, M. Gale, R. Savan, Differential Activation of the Transcription Factor IRF1 Underlies the Distinct Immune Responses Elicited by Type I and Type III Interferons. *Immunity.* **51**, 451-464.e6 (2019).
149. K.-H. Lim, L. M. Staudt, Toll-like receptor signaling. *Cold Spring Harb. Perspect. Biol.* **5**, a011247 (2013).
150. M. R. Thompson, J. J. Kaminski, E. A. Kurt-Jones, K. A. Fitzgerald, Pattern recognition receptors and the innate immune response to viral infection. *Viruses.* **3**, 920–40 (2011).
151. R. K. Durbin, S. V. Kotenko, J. E. Durbin, Interferon induction and function at the mucosal surface. *Immunol. Rev.* **255**, 25–39 (2013).
152. V. A. K. Rathinam, K. A. Fitzgerald, Cytosolic surveillance and antiviral immunity. *Curr. Opin. Virol.* **1**, 455–462 (2011).
153. H. Ishikawa, G. N. Barber, STING is an endoplasmic reticulum adaptor that facilitates innate immune signalling. *Nature.* **455**, 674–678 (2008).
154. L. Sun, J. Wu, F. Du, X. Chen, Z. J. Chen, Cyclic GMP-AMP synthase is a cytosolic DNA sensor that activates the type I interferon pathway. *Science (80-.).* **339**, 786–91 (2013).
155. M. Yoneyama, M. Kikuchi, T. Natsukawa, N. Shinobu, T. Imaizumi, M. Miyagishi, K. Taira, S. Akira, T. Fujita, The RNA helicase RIG-I has an essential function in double-stranded RNA-induced innate antiviral responses. *Nat. Immunol.* **5**, 730–737 (2004).
156. R. Sumpter, Y.-M. Loo, E. Foy, K. Li, M. Yoneyama, T. Fujita, S. M. Lemon, M. Gale, Regulating Intracellular Antiviral Defense and Permissiveness to Hepatitis C Virus RNA Replication through a Cellular RNA Helicase, RIG-I. *J. Virol.* **79**, 2689–2699 (2005).
157. R. B. Seth, L. Sun, C. K. Ea, Z. J. Chen, Identification and characterization of MAVS, a mitochondrial antiviral signaling protein that activates NF- κ B and IRF3. *Cell.* **122**, 669–682 (2005).

158. K. Takeda, S. Akira, Toll-like receptors in innate immunity. *Int. Immunol.* **17**, 1–14 (2005).
159. K. Takeda, T. Kaisho, S. Akira, Toll-like receptors. *Annu. Rev. Immunol.* **21**, 335–376 (2003).
160. J. C. Kagan, T. Su, T. Horng, A. Chow, S. Akira, R. Medzhitov, TRAM couples endocytosis of Toll-like receptor 4 to the induction of interferon- β . *Nat. Immunol.* **9**, 361–368 (2008).
161. W. C. Au, P. A. Moore, D. W. LaFleur, B. Tombal, P. M. Pitha, Characterization of the interferon regulatory factor-7 and its potential role in the transcription activation of interferon A genes. *J. Biol. Chem.* **273**, 29210–29217 (1998).
162. M. Sato, H. Suemori, N. Hata, M. Asagiri, K. Ogasawara, K. Nakao, T. Nakaya, M. Katsuki, S. Noguchi, N. Tanaka, T. Taniguchi, Distinct and essential roles of transcription factors IRF-3 and IRF-7 in response to viruses for IFN- α/β gene induction. *Immunity.* **13**, 539–48 (2000).
163. M. Sato, N. Hata, M. Asagiri, T. Nakaya, T. Taniguchi, N. Tanaka, Positive feedback regulation of type I IFN genes by the IFN-inducible transcription factor IRF-7. *FEBS Lett.* **441**, 106–110 (1998).
164. K. Honda, H. Yanai, H. Negishi, M. Asagiri, M. Sato, T. Mizutani, N. Shimada, Y. Ohba, A. Takaoka, N. Yoshida, T. Taniguchi, IRF-7 is the master regulator of type-I interferon-dependent immune responses. *Nature.* **434**, 772–7 (2005).
165. M. Yoneyama, W. Suhara, Y. Fukuhara, M. Sato, K. Ozato, T. Fujita, Autocrine amplification of type I interferon gene expression mediated by interferon stimulated gene factor 3 (ISGF3). *J. Biochem.* **120**, 160–169 (1996).
166. I. Marie, J. E. Durbin, D. E. Levy, Differential viral induction of distinct interferon-alpha genes by positive feedback through interferon regulatory factor-7. *EMBO J.* **17**, 6660–6669 (1998).
167. K. Honda, H. Yanai, T. Mizutani, H. Negishi, N. Shimada, N. Suzuki, Y. Ohba, A. Takaoka, W. C. Yeh, T. Taniguchi, Role of a transductional-transcriptional processor complex involving MyD88 and IRF-7 in Toll-like receptor signaling. *Proc. Natl. Acad. Sci.* **101**, 15416–15421 (2004).
168. T. Kawai, S. Sato, K. J. Ishii, C. Coban, H. Hemmi, M. Yamamoto, K. Terai, M. Matsuda, J. I. Inoue, S. Uematsu, O. Takeuchi, S. Akira, Interferon- α induction through Toll-like receptors involves a direct interaction of IRF7 with MyD88 and TRAF6. *Nat. Immunol.* **5**, 1061–1068 (2004).
169. A. Izaguirre, B. J. Barnes, S. Amrute, W.-S. Yeow, N. Megjugorac, J. Dai, D. Feng, E. Chung, P. M. Pitha, P. Fitzgerald-Bocarsly, Comparative analysis of IRF and IFN-alpha expression in human plasmacytoid and monocyte-derived dendritic cells. *J. Leukoc. Biol.* **74**, 1125–1138 (2003).
170. M. B. Iversen, S. R. Paludan, Mechanisms of type III interferon expression. *J. Interf. Cytokine Res.* **30**, 573–8 (2010).
171. S. L. Schafer, R. Lin, P. A. Moore, J. Hiscott, P. M. Pitha, Regulation of type I interferon gene expression by interferon regulatory factor-3. *J. Biol. Chem.* **273**, 2714–2720 (1998).
172. M. Sato, N. Tanaka, N. Hata, E. Oda, T. Taniguchi, Involvement of the IRF family transcription factor IRF-3 in virus-induced activation of the IFN- β gene. *FEBS Lett.* **425**, 112–116 (1998).
173. K. Onoguchi, M. Yoneyama, A. Takemura, S. Akira, T. Taniguchi, H. Namiki, T. Fujita, Viral Infections Activate Types I and III Interferon Genes through a Common Mechanism. *J. Biol. Chem.* **282**, 7576–7581 (2007).
174. P. I. Osterlund, T. E. Pietilä, V. Veckman, S. V. Kotenko, I. Julkunen, IFN

- regulatory factor family members differentially regulate the expression of type III IFN (IFN- λ) genes. *J. Immunol.* **179**, 3434–42 (2007).
175. M. B. Iversen, N. Ank, J. Melchjorsen, S. R. Paludan, Expression of type III interferon (IFN) in the vaginal mucosa is mediated primarily by dendritic cells and displays stronger dependence on NF-kappaB than type I IFNs. *J. Virol.* **84**, 4579–86 (2010).
 176. K. M. Monroe, S. M. McWhirter, R. E. Vance, Induction of type I interferons by bacteria. *Cell. Microbiol.* **12**, 881–90 (2010).
 177. A. Sing, T. Merlin, H. P. Knopf, P. J. Nielsen, H. Loppnow, C. Galanos, M. A. Freudenberg, Bacterial induction of beta interferon in mice is a function of the lipopolysaccharide component. *Infect. Immun.* **68**, 1600–1607 (2000).
 178. W. Kang, A. Park, J. W. Huh, G. You, D. J. Jung, M. Song, H. K. Lee, Y. M. Kim, Flagellin-stimulated production of interferon- β promotes anti-flagellin IgG2c and IgA responses. *Mol. Cells.* **43**, 251–263 (2020).
 179. C. Aubry, S. C. Corr, S. Wienerroither, C. Goulard, R. Jones, A. M. Jamieson, T. Decker, L. A. J. O’Neill, O. Dussurget, P. Cossart, Both TLR2 and TRIF contribute to interferon- β production during listeria infection. *PLoS One.* **7**, 1–9 (2012).
 180. E. N. B. Ghanem, D. S. McElroy, S. E. F. D’Orazio, Multiple mechanisms contribute to the robust rapid gamma interferon response by CD8 + T cells during *Listeria monocytogenes* infection. *Infect. Immun.* **77**, 1492–1501 (2009).
 181. G. Mancuso, M. Gambuzza, A. Midiri, C. Biondo, S. Papasergi, S. Akira, G. Teti, C. Beninati, Bacterial recognition by TLR7 in the lysosomes of conventional dendritic cells. *Nat. Immunol.* **10**, 587–594 (2009).
 182. T. Kawashima, A. Kosaka, H. Yan, Z. Guo, R. Uchiyama, R. Fukui, D. Kaneko, Y. Kumagai, D. J. You, J. Carreras, S. Uematsu, M. H. Jang, O. Takeuchi, T. Kaisho, S. Akira, K. Miyake, H. Tsutsui, T. Saito, I. Nishimura, N. M. Tsuji, Double-Stranded RNA of Intestinal Commensal but Not Pathogenic Bacteria Triggers Production of Protective Interferon- β . *Immunity.* **38**, 1187–1197 (2013).
 183. S. A. Tursi, E. Y. Lee, N. J. Medeiros, M. H. Lee, L. K. Nicastro, B. Buttaro, S. Gallucci, R. P. Wilson, G. C. L. Wong, Ç. Tükel, Bacterial amyloid curli acts as a carrier for DNA to elicit an autoimmune response via TLR2 and TLR9. *PLoS Pathog.* **13**, 1–25 (2017).
 184. A. R. Jang, J. H. Choi, S. J. Shin, J. H. Park, Mycobacterium tuberculosis ESAT6 induces IFN- β gene expression in Macrophages via TLRs-mediated signaling. *Cytokine.* **104**, 104–109 (2018).
 185. A. K. Pandey, Y. Yang, Z. Jiang, S. M. Fortune, F. Coulombe, M. A. Behr, K. A. Fitzgerald, C. M. Sasseti, M. A. Kelliher, Nod2, Rip2 and Irf5 play a critical role in the type I interferon response to Mycobacterium tuberculosis. *PLoS Pathog.* **5** (2009).
 186. A. Mishra, G. C. Lai, L. J. Yao, T. T. Aung, N. Shental, A. Rotter-Maskowitz, E. Shepherdson, G. S. N. Singh, R. Pai, A. Shanti, R. M. M. Wong, A. Lee, C. Khyriem, C. A. Dutertre, S. Chakarov, K. G. Srinivasan, N. B. Shadan, X.-M. Zhang, S. Khalilnezhad, F. Cottier, A. S. M. Tan, G. Low, P. Chen, Y. Fan, P. X. Hor, A. K. M. Lee, M. Choolani, D. Vermijlen, A. Sharma, G. Fuks, R. Straussman, N. Pavelka, B. Malleret, N. McGovern, S. Albani, J. K. Y. Chan, F. Ginhoux, Microbial exposure during early human development primes fetal immune cells. *Cell.* **184**, 3394-3409.e20 (2021).
 187. R. L. Kinsella, D. X. Zhu, G. A. Harrison, A. E. Mayer Bridwell, J. Prusa, S. M. Chavez, C. L. Stallings, Perspectives and Advances in the Understanding of Tuberculosis. *Annu. Rev. Pathol. Mech. Dis.* **16**, 377–408 (2021).

188. O. Dussurget, H. Bierne, P. Cossart, The bacterial pathogen *Listeria monocytogenes* and the interferon family: Type I, type II and type III interferons. *Front. Cell. Infect. Microbiol.* **4**, 1–12 (2014).
189. F. Pontiroli, O. Dussurget, I. Zanoni, M. Urbano, O. Beretta, F. Granucci, P. Ricciardi-Castagnoli, P. Cossart, M. Foti, The timing of IFN β production affects early innate responses to *Listeria monocytogenes* and determines the overall outcome of lethal infection. *PLoS One.* **7**, 1–13 (2012).
190. E. Kernbauer, V. Maier, I. Rauch, M. Müller, T. Decker, Route of Infection Determines the Impact of Type I Interferons on Innate Immunity to *Listeria monocytogenes*. *PLoS One.* **8** (2013), doi:10.1371/journal.pone.0065007.
191. C. Sommereyns, S. Paul, P. Staeheli, T. Michiels, IFN- λ (IFN- λ) is expressed in a tissue-dependent fashion and primarily acts on epithelial cells in vivo. *PLoS Pathog.* **4**, e1000017 (2008).
192. J. Linden, D. Schnepf, M. Wischnewski, L. Ye, J. Gawron, A. Ohnemus, C. Friedrich, G. Gasteiger, P. Staeheli, Interferon- λ Receptor Expression: Novel Reporter Mouse Reveals Within-and Cross-Tissue Heterogeneity. *J. Interf. Cytokine Res.* **40**, 292–300 (2020).
193. L. Ye, D. Schnepf, P. Staeheli, Interferon- λ orchestrates innate and adaptive mucosal immune responses. *Nat. Rev. Immunol.* **19**, 614–625 (2019).
194. T. Mahlaköiv, P. Hernandez, K. Gronke, A. Diefenbach, P. Staeheli, Leukocyte-derived IFN- α/β and epithelial IFN- λ constitute a compartmentalized mucosal defense system that restricts enteric virus infections. *PLoS Pathog.* **11**, e1004782 (2015).
195. J. Pott, T. Mahlaköiv, M. Mordstein, C. U. Duerr, T. Michiels, S. Stockinger, P. Staeheli, M. W. Hornef, IFN- λ determines the intestinal epithelial antiviral host defense. *Proc. Natl. Acad. Sci.* **108**, 7944–7949 (2011).
196. M. Mordstein, E. Neugebauer, V. Ditt, B. Jessen, T. Rieger, V. Falcone, F. Sorgeloos, S. Ehl, D. Mayer, G. Kochs, M. Schwemmler, C. Drosten, T. Michiels, P. Staeheli, Lambda Interferon Renders Epithelial Cells of the Respiratory and Gastrointestinal Tracts Resistant to Viral Infections. *J. Virol.* **84**, 5670–5677 (2010).
197. J.-D. Lin, N. Feng, A. Sen, M. Balan, H.-C. Tseng, C. McElrath, S. V. Smirnov, J. Peng, L. L. Yasukawa, R. K. Durbin, J. E. Durbin, H. B. Greenberg, S. V. Kotenko, Distinct Roles of Type I and Type III Interferons in Intestinal Immunity to Homologous and Heterologous Rotavirus Infections. *PLoS Pathog.* **12**, e1005600 (2016).
198. Y. V. Katlinskaya, K. V. Katlinski, A. Lasri, N. Li, D. P. Beiting, A. C. Durham, T. Yang, E. Pikarsky, C. J. Lengner, F. B. Johnson, Y. Ben-Neriah, S. Y. Fuchs, Type I Interferons Control Proliferation and Function of the Intestinal Epithelium. *Mol. Cell. Biol.* **36**, 1124–1135 (2016).
199. T. J. Nice, M. T. Baldrige, B. T. McCune, J. M. Norman, H. M. Lazear, M. Artyomov, M. S. Diamond, H. W. Virgin, Interferon- λ cures persistent murine norovirus infection in the absence of adaptive immunity. *Science (80-)*. **347**, 269–73 (2015).
200. M. T. Baldrige, S. Lee, J. J. Brown, N. McAllister, K. Urbanek, T. S. Dermody, T. J. Nice, H. W. Virgin, Expression of Ifnlr1 on Intestinal Epithelial Cells Is Critical to the Antiviral Effects of Interferon Lambda against Norovirus and Reovirus. *J. Virol.* **91** (2017), doi:10.1128/jvi.02079-16.
201. S. Davidson, T. M. McCabe, S. Crotta, H. H. Gad, E. M. Hessel, S. Beinke, R. Hartmann, A. Wack, IFN λ is a potent anti-influenza therapeutic without the

- inflammatory side effects of IFN α treatment. *EMBO Mol. Med.* **8**, 1099–1112 (2016).
202. E. A. Caine, S. M. Scheaffer, N. Arora, K. Zaitsev, M. N. Artyomov, C. B. Coyne, K. H. Moley, M. S. Diamond, Interferon lambda protects the female reproductive tract against Zika virus infection. *Nat. Commun.* **10** (2019), doi:10.1038/s41467-018-07993-2.
 203. A. Bayer, N. J. Lennemann, Y. Ouyang, J. C. Bramley, S. Morosky, E. T. D. A. Marques, S. Cherry, Y. Sadovsky, C. B. Coyne, Type III Interferons Produced by Human Placental Trophoblasts Confer Protection against Zika Virus Infection. *Cell Host Microbe.* **19**, 705–712 (2016).
 204. L. J. Yockey, K. A. Jurado, N. Arora, A. Millet, T. Rakib, K. M. Milano, A. K. Hastings, E. Fikrig, Y. Kong, T. L. Horvath, S. Weatherbee, H. J. Kliman, C. B. Coyne, A. Iwasaki, Type I interferons instigate fetal demise after Zika virus infection. *Sci. Immunol.* **3** (2018), doi:10.1126/sciimmunol.aao1680.
 205. S. Bhushal, M. Wolfsmüller, T. A. Selvakumar, L. Kemper, D. Wirth, M. W. Hornef, H. Hauser, M. Köster, Cell polarization and epigenetic status shape the heterogeneous response to type III interferons in intestinal epithelial cells. *Front. Immunol.* **8** (2017), doi:10.3389/fimmu.2017.00671.
 206. K. Saxena, L. M. Simon, X.-L. Zeng, S. E. Blutt, S. E. Crawford, N. P. Sastri, U. C. Karandikar, N. J. Ajami, N. C. Zachos, O. Kovbasnjuk, M. Donowitz, M. E. Conner, C. A. Shaw, M. K. Estes, A paradox of transcriptional and functional innate interferon responses of human intestinal enteroids to enteric virus infection. *Proc. Natl. Acad. Sci.* **114**, E570–E579 (2017).
 207. A. O. Kolawole, C. Mirabelli, D. R. Hill, S. A. Svoboda, A. B. Janowski, K. D. Passalacqua, B. N. Rodriguez, M. K. Dame, P. Freiden, R. P. Berger, D. Vu, M. Hosmillo, M. X. D. O’Riordan, S. Schultz-Cherry, S. Guix, J. R. Spence, D. Wang, C. E. Wobus, Astrovirus replication in human intestinal enteroids reveals multi-cellular tropism and an intricate host innate immune landscape. *PLOS Pathog.* **15**, e1008057 (2019).
 208. E. Knipe, M. David, M. Peter, M. K. Estes, A. Z. Kapikian, Rotaviruses, 1–107 (2007).
 209. GBD 2015 Mortality and Causes of Death Collaborators, Global, regional, and national life expectancy, all-cause mortality, and cause-specific mortality for 249 causes of death, 1980-2015: a systematic analysis for the Global Burden of Disease Study 2015. *Lancet.* **388**, 1459–1544 (2016).
 210. T. Vesikari, D. O. Matson, P. Dennehy, P. Van Damme, M. Santosham, Z. Rodriguez, M. J. Dallas, J. F. Heyse, M. G. Goveia, S. B. Black, H. R. Shinefield, C. D. C. Christie, S. Ylitalo, R. F. Itzler, M. L. Coia, M. T. Onorato, B. A. Adeyi, G. S. Marshall, L. Gothefors, D. Campens, A. Karvonen, J. P. Watt, K. L. O’Brien, M. J. DiNubile, H. F. Clark, J. W. Boslego, P. A. Offit, P. M. Heaton, Safety and Efficacy of a Pentavalent Human–Bovine (WC3) Reassortant Rotavirus Vaccine. *N. Engl. J. Med.* **354**, 23–33 (2006).
 211. G. M. Ruiz-Palacios, I. Pérez-Schael, F. R. Velázquez, H. Abate, T. Breuer, S. C. Clemens, B. Cheuvart, F. Espinoza, P. Gillard, B. L. Innis, Y. Cervantes, A. C. Linhares, P. López, M. Macías-Parra, E. Ortega-Barría, V. Richardson, D. M. Rivera-Medina, L. Rivera, B. Salinas, N. Pavía-Ruz, J. Salmerón, R. Rüttimann, J. C. Tinoco, P. Rubio, E. Nuñez, M. L. Guerrero, J. P. Yarzabal, S. Damaso, N. Tornieporth, X. Sáez-Llorens, R. F. Vergara, T. Vesikari, A. Bouckenooghe, R. Clemens, B. De Vos, M. O’Ryan, Human Rotavirus Vaccine Study Group, Safety and efficacy of an attenuated vaccine against severe rotavirus gastroenteritis. *N.*

- Engl. J. Med.* **354**, 11–22 (2006).
212. J. E. Tate, A. H. Burton, C. Boschi-Pinto, U. D. Parashar, World Health Organization–Coordinated Global Rotavirus Surveillance Network, Global, Regional, and National Estimates of Rotavirus Mortality in Children <5 Years of Age, 2000–2013. *Clin. Infect. Dis.* **62**, S96–S105 (2016).
 213. M. D. Esona, R. Gautam, Rotavirus. *Clin. Lab. Med.* **35**, 363–391 (2015).
 214. U. Desselberger, Rotaviruses. *Virus Res.* **190**, 75–96 (2014).
 215. R. H. Yolken, R. Willoughby, S. B. Wee, R. Miskuff, S. Vonderfecht, Sialic acid glycoproteins inhibit in vitro and in vivo replication of rotaviruses. *J. Clin. Invest.* **79**, 148–154 (1987).
 216. J. E. Stencel-Baerenwald, K. Reiss, D. M. Reiter, T. Stehle, T. S. Dermody, The sweet spot: Defining virus-sialic acid interactions. *Nat. Rev. Microbiol.* **12**, 739–749 (2014).
 217. Y. Liu, P. Huang, B. Jiang, M. Tan, A. L. Morrow, X. Jiang, Poly-LacNAc as an age-specific ligand for rotavirus P[11] in neonates and infants. *PLoS One.* **8**, 1–10 (2013).
 218. D. Silva-Ayala, T. López, M. Gutiérrez, N. Perrimon, S. López, C. F. Arias, M. K. Estes, Genome-wide RNAi screen reveals a role for the ESCRT complex in rotavirus cell entry. *Proc. Natl. Acad. Sci.* **110**, 10270–10275 (2013).
 219. M. A. Diaz-Salinas, D. Silva-Ayala, S. Lopez, C. F. Arias, Rotaviruses Reach Late Endosomes and Require the Cation-Dependent Mannose-6-Phosphate Receptor and the Activity of Cathepsin Proteases To Enter the Cell. *J. Virol.* **88**, 4389–4402 (2014).
 220. A. Gardet, M. Breton, P. Fontanges, G. Trugnan, S. Chwetzoff, Rotavirus Spike Protein VP4 Binds to and Remodels Actin Bundles of the Epithelial Brush Border into Actin Bodies. *J. Virol.* **80**, 3947–3956 (2006).
 221. M. S. McNulty, W. L. Curran, J. B. McFerran, The morphogenesis of a cytopathic bovine rotavirus in Madin Darby bovine kidney cells. *J. Gen. Virol.* **33**, 503–508 (1976).
 222. H. B. Greenberg, P. T. Vo, R. Jones, Cultivation and characterization of three strains of murine rotavirus. *J. Virol.* **57**, 585–590 (1986).
 223. R. G. Wyatt, W. D. James, E. H. Bohl, K. W. Theil, L. J. Saif, A. R. Kalica, H. B. Greenberg, A. Z. Kapikian, R. M. Chanock, Human rotavirus type 2: cultivation in vitro. *Science (80-)*. **207**, 189–91 (1980).
 224. Y. Hoshino, R. G. Wyatt, H. B. Greenberg, J. Flores, A. Z. Kapikian, Serotypic similarity and diversity of rotaviruses of mammalian and avian origin as studied by plaque-reduction neutralization. *J. Infect. Dis.* **149**, 694–702 (1984).
 225. N. Feng, J. W. Burns, L. Bracy, H. B. Greenberg, Comparison of Mucosal and Systemic Humoral Immune Responses and Subsequent Protection in Mice Orally Inoculated with a Homologous or a Heterologous Rotavirus. *J. Virol.* **68**, 7766–7773 (1994).
 226. S. J. Dunn, J. W. Burns, T. L. Cross, P. T. Vo, R. L. Ward, M. Bremont, H. B. Greenberg, Comparison of VP4 and VP7 of Five Murine Rotavirus Strains. *Virology.* **203** (1994), pp. 250–259.
 227. J. W. Burns, A. A. Krishnaney, P. T. Vo, R. V. Rouse, L. J. Anderson, H. B. Greenberg, Analyses of homologous rotavirus infection in the mouse model. *Virology.* **207**, 143–53 (1995).
 228. M. A. Franco, H. B. Greenberg, Immunity to Rotavirus in T Cell Deficient Mice. *Virology.* **179**, 169–179 (1997).
 229. J. L. VanCott, M. M. McNeal, J. Flint, S. A. Bailey, A. H. C. Choi, R. L. Ward, Role

- for T cell-independent B cell activity in the resolution of primary rotavirus infection in mice. *Eur. J. Immunol.* **31**, 3380–3387 (2001).
230. S. Kordasti, C. Istrate, M. Banasaz, M. Rottenberg, H. Sjövall, O. Lundgren, L. Svensson, Rotavirus infection is not associated with small intestinal fluid secretion in the adult mouse. *J. Virol.* **80**, 11355–61 (2006).
 231. Y. Dong, C. Q. Y. Zeng, J. M. Ball, M. K. Estes, A. P. Morris, The rotavirus enterotoxin NSP4 mobilizes intracellular calcium in human intestinal cells by stimulating phospholipase C-mediated inositol 1,4,5-trisphosphate production. *Proc. Natl. Acad. Sci.* **94**, 3960–3965 (1997).
 232. J. M. Ball, P. Tian, C. Q. Zeng, A. P. Morris, M. K. Estes, Age-dependent diarrhea induced by a rotaviral nonstructural glycoprotein. *Science (80-)*. **272**, 101–4 (1996).
 233. C. Istrate, M. Hagbom, E. Vikström, K. Magnusson, Rotavirus Infection Increases Intestinal Motility but Not Permeability at the Onset of Diarrhea. *J. Virol.* **88**, 3161–3169 (2014).
 234. J. Pott, S. Stockinger, N. Torow, A. Smoczek, C. Lindner, G. McInerney, F. Bäckhed, U. Baumann, O. Pabst, A. Bleich, M. W. Hornef, Age-dependent TLR3 expression of the intestinal epithelium contributes to rotavirus susceptibility. *PLoS Pathog.* **8** (2012), doi:10.1371/journal.ppat.1002670.
 235. M. Fenaux, M. A. Cuadras, N. Feng, M. Jaimes, H. B. Greenberg, Extraintestinal spread and replication of a homologous EC rotavirus strain and a heterologous rhesus rotavirus in BALB/c mice. *J. Virol.* **80**, 5219–32 (2006).
 236. N. Feng, B. Kim, M. Fenaux, H. Nguyen, P. Vo, M. B. Omary, H. B. Greenberg, Role of interferon in homologous and heterologous rotavirus infection in the intestines and extraintestinal organs of suckling mice. *J. Virol.* **82**, 7578–90 (2008).
 237. E. E. Rollo, K. P. Kumar, N. C. Reich, J. Angel, H. B. Greenberg, R. Sheth, J. Anderson, B. Oh, S. J. Hempson, R. Erich, R. D. Shaw, E. E. Rollo, K. P. Kumar, N. C. Reich, J. Cohen, J. Angel, H. B. Greenberg, R. Sheth, J. Anderson, B. Oh, S. J. Hempson, E. R. Mackow, R. D. Shaw, The Epithelial Cell Response to Rotavirus Infection. *J. Immunol.* **163**, 4442–4452 (1999).
 238. J. A. Boshuizen, J. H. J. Reimerink, A. M. Korteland-van Male, V. J. J. van Ham, M. P. G. Koopmans, H. A. Büller, J. Dekker, A. W. C. Einerhand, Changes in small intestinal homeostasis, morphology, and gene expression during rotavirus infection of infant mice. *J. Virol.* **77**, 13005–16 (2003).
 239. M. P. Osborne, S. J. Haddon, A. J. Spencer, J. Collins, W. G. Starkey, T. S. Wallis, G. J. Clarke, K. J. Worton, D. C. Candy, J. Stephen, An electron microscopic investigation of time-related changes in the intestine of neonatal mice infected with murine rotavirus. *J. Pediatr. Gastroenterol. Nutr.* **7**, 236–48 (1988).
 240. C. Bomidi, M. Robertson, C. Coarfa, M. K. Estes, S. E. Blutt, Single-cell sequencing of rotavirus-infected intestinal epithelium reveals cell-type specific epithelial repair and tuft cell infection. *Proc. Natl. Acad. Sci.* **118** (2021), doi:10.1073/pnas.2112814118.
 241. M. M. Arnold, A. Sen, H. B. Greenberg, J. T. Patton, The battle between rotavirus and its host for control of the interferon signaling pathway. *PLoS Pathog.* **9**, e1003064 (2013).
 242. M. M. Arnold, M. Barro, J. T. Patton, Rotavirus NSP1 Mediates Degradation of Interferon Regulatory Factors through Targeting of the Dimerization Domain. *J. Virol.* **87**, 9813–9821 (2013).
 243. M. M. Arnold, J. T. Patton, Diversity of Interferon Antagonist Activities Mediated by

- NSP1 Proteins of Different Rotavirus Strains. *J. Virol.* **85**, 1970–1979 (2011).
244. G. Holloway, T. T. Truong, B. S. Coulson, Rotavirus Antagonizes Cellular Antiviral Responses by Inhibiting the Nuclear Accumulation of STAT1 , STAT2 , and NF- κ B. *J. Virol.* **83**, 4942–4951 (2009).
 245. A. Sen, L. Rott, N. Phan, G. Mukherjee, H. B. Greenberg, Rotavirus NSP1 Protein Inhibits Interferon-Mediated STAT1 Activation. *J. Virol.* **88**, 41–53 (2014).
 246. A. Sen, A. Sharma, H. B. Greenberg, Rotavirus Degrades Multiple Interferon (IFN) Type Receptors To Inhibit IFN Signaling and Protects against Mortality from Endotoxin in Suckling Mice. *J. Virol.* **92**, e01394-17 (2018).
 247. A. Sen, M. E. Rothenberg, G. Mukherjee, N. Feng, T. Kalisky, N. Nair, I. M. Johnstone, M. F. Clarke, H. B. Greenberg, Innate immune response to homologous rotavirus infection in the small intestinal villous epithelium at single-cell resolution. *Proc. Natl. Acad. Sci.* **109**, 20667–20672 (2012).
 248. S. Ding, S. Zhu, L. Ren, N. Feng, Y. Song, X. Ge, B. Li, R. A. Flavell, H. B. Greenberg, Rotavirus VP3 targets MAVS for degradation to inhibit type III interferon expression in intestinal epithelial cells. *Elife.* **7** (2018), doi:10.7554/eLife.39494.
 249. N. Feng, L. L. Yasukawa, A. Sen, H. B. Greenberg, Permissive Replication of Homologous Murine Rotavirus in the Mouse Intestine Is Primarily Regulated by VP4 and NSP1. *J. Virol.* **87**, 8307–8316 (2013).
 250. J. L. Vancott, M. M. McNeal, A. H. C. Choi, R. L. Ward, The role of interferons in rotavirus infections and protection. *J. Interf. Cytokine Res.* **23**, 163–170 (2003).
 251. P. P. Hernández, T. Mahlaköiv, I. Yang, V. Schwierzeck, N. Nguyen, F. Guendel, K. Gronke, B. Ryffel, C. Hölscher, L. Dumoutier, J.-C. C. Renaud, S. Suerbaum, P. Staeheli, A. Diefenbach, Interferon- λ and interleukin 22 act synergistically for the induction of interferon-stimulated genes and control of rotavirus infection. *Nat. Immunol.* **16**, 698–707 (2015).
 252. P. B. Eckburg, E. M. Bik, C. N. Bernstein, E. Purdom, L. Dethlefsen, M. Sargent, S. R. Gill, K. E. Nelson, D. A. Relman, Diversity of the human intestinal microbial flora. *Science (80-.)*. **308**, 1635–1638 (2005).
 253. R. Sender, S. Fuchs, R. Milo, Revised Estimates for the Number of Human and Bacteria Cells in the Body. *PLoS Biol.* **14**, e1002533 (2016).
 254. J. Walter, R. Ley, The human gut microbiome: Ecology and recent evolutionary changes. *Annu. Rev. Microbiol.* **65**, 411–429 (2011).
 255. M. Begley, C. G. M. Gahan, C. Hill, The interaction between bacteria and bile. *FEMS Microbiol. Rev.* **29**, 625–651 (2005).
 256. J. Tap, S. Mondot, F. Levenez, E. Pelletier, C. Caron, J. P. Furet, E. Ugarte, R. Muñoz-Tamayo, D. L. E. Paslier, R. Nalin, J. Dore, M. Leclerc, Towards the human intestinal microbiota phylogenetic core. *Environ. Microbiol.* **11**, 2574–2584 (2009).
 257. E. K. Costello, C. L. Lauber, M. Hamady, N. Fierer, J. I. Gordon, R. Knight, Bacterial community variation in human body habitats across space and time. *Science (80-.)*. **326**, 1694–7 (2009).
 258. M. Wang, S. Ahrné, B. Jeppsson, G. Molin, Comparison of bacterial diversity along the human intestinal tract by direct cloning and sequencing of 16S rRNA genes. *FEMS Microbiol. Ecol.* **54**, 219–231 (2005).
 259. X. Wang, S. P. Heazlewood, D. O. Krause, T. H. J. Florin, Molecular characterization of the microbial species that colonize human ileal and colonic mucosa by using 16S rDNA sequence analysis. *J. Appl. Microbiol.* **95**, 508–520 (2003).

260. M. Tanaka, J. Nakayama, Development of the gut microbiota in infancy and its impact on health in later life. *Allergol. Int.* **66**, 515–522 (2017).
261. E. S. Lim, C. Rodriguez, L. R. Holtz, Amniotic fluid from healthy term pregnancies does not harbor a detectable microbial community. *Microbiome.* **7**, 22 (2019).
262. M. G. Dominguez-Bello, E. K. Costello, M. Contreras, M. Magris, G. Hidalgo, N. Fierer, R. Knight, Delivery mode shapes the acquisition and structure of the initial microbiota across multiple body habitats in newborns. *Proc. Natl. Acad. Sci.* **107**, 11971–11975 (2010).
263. Y. Vallès, A. Artacho, A. Pascual-García, M. L. Ferrús, M. J. Gosalbes, J. J. Abellán, M. P. Francino, Microbial Succession in the Gut: Directional Trends of Taxonomic and Functional Change in a Birth Cohort of Spanish Infants. *PLoS Genet.* **10** (2014), doi:10.1371/journal.pgen.1004406.
264. M. Fallani, S. Amarri, A. Uusijarvi, R. Adam, S. Khanna, M. Aguilera, A. Gil, J. M. Vieites, E. Norin, D. Young, J. A. Scott, J. Doré, C. A. Edwards, Determinants of the human infant intestinal microbiota after the introduction of first complementary foods in infant samples from five European centres. *Microbiology.* **157**, 1385–1392 (2011).
265. Q. Yang, X. Huang, P. Wang, Z. Yan, W. Sun, S. Zhao, S. Gun, Longitudinal development of the gut microbiota in healthy and diarrheic piglets induced by age-related dietary changes. *Microbiologyopen.* **8**, 1–17 (2019).
266. R. E. Ley, M. Hamady, C. Lozupone, P. J. Turnbaugh, R. R. Ramey, J. S. Bircher, M. L. Schlegel, T. A. Tucker, M. D. Schrenzel, R. Knight, J. I. Gordon, Evolution of mammals and their gut microbes. *Science (80-)*. **320**, 1647–1651 (2008).
267. K. D. Parker, S. E. Albeke, J. P. Gigley, A. M. Goldstein, N. L. Ward, Microbiome composition in both wild-type and disease model mice is heavily influenced by mouse facility. *Front. Microbiol.* **9**, 1–13 (2018).
268. I. I. Ivanov, K. Atarashi, N. Manel, E. L. Brodie, U. Karaoz, D. Wei, K. C. Goldfarb, C. A. Santee, V. Lynch, T. Tanoue, A. Imaoka, K. Itoh, K. Takeda, D. R. Littman, C. Li, C. Yang, G. Hather, R. Liu, H. Zhao, Induction of intestinal Th17 cells by segmented filamentous bacteria. *Cell.* **139**, 485–498 (2009).
269. G. Singh, A. Brass, S. M. Cruickshank, C. G. Knight, Cage and maternal effects on the bacterial communities of the murine gut. *Sci. Rep.* **11**, 1–12 (2021).
270. T. S. Stappenbeck, H. W. Virgin, Accounting for reciprocal host-microbiome interactions in experimental science. *Nature.* **534**, 191–199 (2016).
271. J. R. Pleasants, Rearing germfree cesarean-born rats, mice, and rabbits through weaning. *Ann. N. Y. Acad. Sci.* **78**, 116–26 (1959).
272. M. Basic, A. Bleich, Gnotobiotics: Past, present and future. *Lab. Anim.* **53**, 232–243 (2019).
273. S. Rakoff-Nahoum, J. Paglino, F. Eslami-Varzaneh, S. Edberg, R. Medzhitov, Recognition of commensal microflora by toll-like receptors is required for intestinal homeostasis. *Cell.* **118**, 229–241 (2004).
274. A. C. Ericsson, C. L. Franklin, Manipulating the gut microbiota: Methods and challenges. *ILAR J.* **56**, 205–217 (2015).
275. D. A. Hill, C. Hoffmann, M. C. Abt, Y. Du, D. Kobuley, T. J. Kirn, F. D. Bushman, D. Artis, Metagenomic analyses reveal antibiotic-induced temporal and spatial changes in intestinal microbiota with associated alterations in immune cell homeostasis. *Mucosal Immunol.* **3**, 148–158 (2010).
276. D. H. Reikvam, A. Erofeev, A. Sandvik, V. Grcic, F. L. Jahnsen, P. Gaustad, K. D. McCoy, A. J. Macpherson, L. A. Meza-Zepeda, F. E. Johansen, Depletion of murine intestinal microbiota: Effects on gut mucosa and epithelial gene

- expression. *PLoS One*. **6**, 1–13 (2011).
277. D. A. Antonopoulos, S. M. Huse, H. G. Morrison, T. M. Schmidt, M. L. Sogin, V. B. Young, Reproducible community dynamics of the gastrointestinal microbiota following antibiotic perturbation. *Infect. Immun.* **77**, 2367–2375 (2009).
 278. C. J. Robinson, V. B. Young, Antibiotic administration alters the community structure of the gastrointestinal microbiota. *Gut Microbes*. **1**, 279–284 (2010).
 279. K. Bush, P. A. Bradford, β -Lactams and β -Lactamase Inhibitors: An Overview. *Cold Spring Harb. Perspect. Med.* **6** (2016), doi:10.1101/cshperspect.a025247.
 280. P. J. Stogios, A. Savchenko, Molecular mechanisms of vancomycin resistance. *Protein Sci.* **29**, 654–669 (2020).
 281. B. Becker, M. A. Cooper, Aminoglycoside antibiotics in the 21st century. *ACS Chem. Biol.* **8**, 105–115 (2013).
 282. L. P. Kotra, J. Haddad, S. Mobashery, Aminoglycosides: Perspectives on mechanisms of action and resistance and strategies to counter resistance. *Antimicrob. Agents Chemother.* **44**, 3249–3256 (2000).
 283. K. M. Krause, A. W. Serio, T. R. Kane, L. E. Connolly, Aminoglycosides: An Overview. *Cold Spring Harb. Perspect. Med.* **6** (2016), doi:10.1101/cshperspect.a027029.
 284. S. A. Dingsdag, N. Hunter, Metronidazole: An update on metabolism, structure-cytotoxicity and resistance mechanisms. *J. Antimicrob. Chemother.* **73**, 265–279 (2018).
 285. D. R. Goulding, P. H. Myers, A. B. Dickerson, M. M. Comins, R. A. Wiltshire, T. L. Blankenship-Paris, Comparative Efficacy of Two Types of Antibiotic Mixtures in Gut Flora Depletion in Female C57BL/6 Mice. *Comp. Med.* **71**, 203–209 (2021).
 286. V. Gaboriau-Routhiau, S. Rakotobe, E. Lécuyer, I. Mulder, A. Lan, C. Bridonneau, V. Rochet, A. Pisi, M. De Paepe, G. Brandi, G. Eberl, J. Snel, D. Kelly, N. Cerf-Bensussan, The Key Role of Segmented Filamentous Bacteria in the Coordinated Maturation of Gut Helper T Cell Responses. *Immunity*. **31**, 677–689 (2009).
 287. S. K. Mazmanian, H. L. Cui, A. O. Tzianabos, D. L. Kasper, An immunomodulatory molecule of symbiotic bacteria directs maturation of the host immune system. *Cell*. **122**, 107–118 (2005).
 288. J. L. Round, S. M. Lee, J. Li, G. Tran, B. Jabri, T. A. Chatila, S. K. Mazmanian, The toll-like receptor 2 pathway establishes colonization by a commensal of the human microbiota. *Science (80-)*. **332**, 974–977 (2011).
 289. S. Hapfelmeier, M. a E. Lawson, E. Slack, J. K. Kirundi, M. Stoel, M. Heikenwalder, J. Cahenzli, Y. Velykoredko, L. Maria, K. Endt, M. B. Geuking, R. Curtiss, K. D. McCoy, A. J. Macpherson, Reversible microbial colonization of germ-free mice reveals the dynamics of IgA immune responses. *Science (80-)*. **328**, 1705–1709 (2010).
 290. F. E. Dewhirst, C. C. Chien, B. J. Paster, R. L. Ericson, R. P. Orcutt, D. B. Schauer, J. G. Fox, Phylogeny of the defined murine microbiota: Altered Schaedler flora. *Appl. Environ. Microbiol.* **65**, 3287–3292 (1999).
 291. R. B. Sarma-Rupavtarm, Z. Ge, D. B. Schauer, J. G. Fox, M. F. Polz, Spatial distribution and stability of the eight microbial species of the altered Schaedler flora in the mouse gastrointestinal tract. *Appl. Environ. Microbiol.* **70**, 2791–2800 (2004).
 292. M. W. Brand, M. J. Wannemuehler, G. J. Phillips, A. Proctor, A. M. Overstreet, A. E. Jergens, R. P. Orcutt, J. G. Fox, The altered schaedler flora: Continued applications of a defined murine microbial community. *ILAR J.* **56**, 169–178 (2015).

293. M. Schoeler, R. Caesar, Dietary lipids, gut microbiota and lipid metabolism. *Rev. Endocr. Metab. Disord.* **20**, 461–472 (2019).
294. V. R. Velagapudi, R. Hezaveh, C. S. Reigstad, P. Gopalacharyulu, L. Yetukuri, S. Islam, J. Felin, R. Perkins, J. Borén, M. Orešič, F. Bäckhed, The gut microbiota modulates host energy and lipid metabolism in mice. *J. Lipid Res.* **51**, 1101–1112 (2010).
295. B. S. Wostmann, The germfree animal in nutritional studies. *Annu. Rev. Nutr.* **1**, 257–79 (1981).
296. Z. Wang, E. Klipfell, B. J. Bennett, R. Koeth, B. S. Levison, B. Dugar, A. E. Feldstein, E. B. Britt, X. Fu, Y. M. Chung, Y. Wu, P. Schauer, J. D. Smith, H. Allayee, W. H. W. Tang, J. A. Didonato, A. J. Lusis, S. L. Hazen, Gut flora metabolism of phosphatidylcholine promotes cardiovascular disease. *Nature.* **472**, 57–65 (2011).
297. F. Bäckhed, J. K. Manchester, C. F. Semenkovich, J. I. Gordon, Mechanisms underlying the resistance to diet-induced obesity in germ-free mice. *Proc. Natl. Acad. Sci.* **104**, 979–984 (2007).
298. M. V. Chakravarthy, I. J. Lodhi, L. Yin, R. R. V. Malapaka, H. E. Xu, J. Turk, C. F. Semenkovich, Identification of a Physiologically Relevant Endogenous Ligand for PPAR α in Liver. *Cell.* **138**, 476–488 (2009).
299. J. K. Reddy, T. Hashimoto, Peroxisomal beta-oxidation and peroxisome proliferator-activated receptor alpha: an adaptive metabolic system. *Annu. Rev. Nutr.* **21**, 193–230 (2001).
300. M. G. Rooks, W. S. Garrett, Gut microbiota, metabolites and host immunity. *Nat. Rev. Immunol.* **16**, 341–352 (2016).
301. J. G. LeBlanc, F. Chain, R. Martín, L. G. Bermúdez-Humarán, S. Courau, P. Langella, Beneficial effects on host energy metabolism of short-chain fatty acids and vitamins produced by commensal and probiotic bacteria. *Microb. Cell Fact.* **16**, 1–10 (2017).
302. H. J. Binder, Role of colonic short-chain fatty acid transport in diarrhea. *Annu. Rev. Physiol.* **72**, 297–313 (2009).
303. E. N. Bergman, Energy contributions of volatile fatty acids from the gastrointestinal tract in various species. *Physiol. Rev.* **70**, 567–590 (1990).
304. A. J. Brown, S. M. Goldsworthy, A. A. Barnes, M. M. Eilert, L. Tcheang, D. Daniels, A. I. Muir, M. J. Wigglesworth, I. Kinghorn, N. J. Fraser, N. B. Pike, J. C. Strum, K. M. Steplewski, P. R. Murdock, J. C. Holder, F. H. Marshall, P. G. Szekeres, S. Wilson, D. M. Ignar, S. M. Foord, A. Wise, S. J. Dowell, The orphan G protein-coupled receptors GPR41 and GPR43 are activated by propionate and other short chain carboxylic acids. *J. Biol. Chem.* **278**, 11312–11319 (2003).
305. S. I. Karaki, R. Mitsui, H. Hayashi, I. Kato, H. Sugiyama, T. Iwanaga, J. B. Furness, A. Kuwahara, Short-chain fatty acid receptor, GPR43, is expressed by enteroendocrine cells and mucosal mast cells in rat intestine. *Cell Tissue Res.* **324**, 353–360 (2006).
306. B. S. Samuel, A. Shaito, T. Motoike, F. E. Rey, F. Backhed, J. K. Manchester, R. E. Hammer, S. C. Williams, J. Crowley, M. Yanagisawa, J. I. Gordon, Effects of the gut microbiota on host adiposity are modulated by the short-chain fatty-acid binding G protein-coupled receptor, Gpr41. *Proc. Natl. Acad. Sci.* **105**, 16767–16772 (2008).
307. D. Inoue, G. Tsujimoto, I. Kimura, Regulation of energy homeostasis by GPR41. *Front. Endocrinol. (Lausanne).* **5**, 5–7 (2014).
308. I. Kimura, D. Inoue, K. Hirano, G. Tsujimoto, The SCFA receptor GPR43 and

- energy metabolism. *Front. Endocrinol. (Lausanne)*. **5**, 3–5 (2014).
309. J. Park, T. Kotani, T. Konno, J. Setiawan, Y. Kitamura, S. Imada, Y. Usui, N. Hatano, M. Shinohara, Y. Saito, Y. Murata, T. Matozaki, Promotion of Intestinal Epithelial Cell Turnover by Commensal Bacteria: Role of Short-Chain Fatty Acids. *PLoS One*. **11**, e0156334 (2016).
 310. M. K. Nøhr, K. L. Egerod, S. H. Christiansen, A. Gille, S. Offermanns, T. W. Schwartz, M. Møller, Expression of the short chain fatty acid receptor GPR41/FFAR3 in autonomic and somatic sensory ganglia. *Neuroscience*. **290**, 126–137 (2015).
 311. P. A. Muller, M. Schneeberger, F. Matheis, P. Wang, Z. Kerner, A. Ilanges, K. Pellegrino, J. del Mármol, T. B. R. Castro, M. Furuichi, M. Perkins, W. Han, A. Rao, A. J. Picard, J. R. Cross, K. Honda, I. de Araujo, D. Mucida, Microbiota modulate sympathetic neurons via a gut–brain circuit. *Nature*. **583**, 441–446 (2020).
 312. K. M. Maslowski, A. T. Vieira, A. Ng, J. Kranich, F. Sierro, Di Yu, H. C. Schilter, M. S. Rolph, F. MacKay, D. Artis, R. J. Xavier, M. M. Teixeira, C. R. MacKay, Regulation of inflammatory responses by gut microbiota and chemoattractant receptor GPR43. *Nature*. **461**, 1282–1286 (2009).
 313. H. Fujiwara, M. D. Docampo, M. Riwes, D. Peltier, T. Toubai, I. Henig, S. J. Wu, S. Kim, A. Taylor, S. Brabbs, C. Liu, C. Zajac, K. Oravecz-Wilson, Y. Sun, G. Núñez, J. E. Levine, M. R. M. van den Brink, J. L. M. Ferrara, P. Reddy, Microbial metabolite sensor GPR43 controls severity of experimental GVHD. *Nat. Commun.* **9** (2018), doi:10.1038/s41467-018-06048-w.
 314. J. Cai, L. Sun, F. J. Gonzalez, Gut microbiota-derived bile acids in intestinal immunity, inflammation, and tumorigenesis. *Cell Host Microbe*. **30**, 289–300 (2022).
 315. F. J. Gonzalez, Nuclear receptor control of enterohepatic circulation. *Compr. Physiol.* **2**, 2811–28 (2012).
 316. M. Funabashi, T. L. Grove, M. Wang, Y. Varma, M. E. McFadden, L. C. Brown, C. Guo, S. Higginbottom, S. C. Almo, M. A. Fischbach, A metabolic pathway for bile acid dehydroxylation by the gut microbiome. *Nature*. **582**, 566–570 (2020).
 317. L. Jiang, H. Zhang, D. Xiao, H. Wei, Y. Chen, Farnesoid X receptor (FXR): Structures and ligands. *Comput. Struct. Biotechnol. J.* **19**, 2148–2159 (2021).
 318. K. M. Anderson, C. P. Gayer, The Pathophysiology of Farnesoid X Receptor (FXR) in the GI Tract: Inflammation, Barrier Function and Innate Immunity. *Cells*. **10**, 1–15 (2021).
 319. J. G. LeBlanc, C. Milani, G. S. de Giori, F. Sesma, D. van Sinderen, M. Ventura, Bacteria as vitamin suppliers to their host: A gut microbiota perspective. *Curr. Opin. Biotechnol.* **24**, 160–168 (2013).
 320. M. J. Hill, Intestinal flora and endogenous vitamin synthesis. *Eur. J. Cancer Prev.*, S43-5 (1997).
 321. J. H. Martens, H. Barg, M. Warren, D. Jahn, Microbial production of vitamin B12. *Appl. Microbiol. Biotechnol.* **58**, 275–285 (2002).
 322. S. Kim, A. Covington, E. G. Pamer, The intestinal microbiota: Antibiotics, colonization resistance, and enteric pathogens. *Immunol. Rev.* **279**, 90–105 (2017).
 323. I. Sekirov, N. M. Tam, M. Jogova, M. L. Robertson, Y. Li, C. Lupp, B. B. Finlay, Antibiotic-induced perturbations of the intestinal microbiota alter host susceptibility to enteric infection. *Infect. Immun.* **76**, 4726–4736 (2008).
 324. S. Becattini, E. R. Littmann, R. A. Carter, S. G. Kim, S. M. Morjaria, L. Ling, Y.

- Gyaltshen, E. Fontana, Y. Taur, I. M. Leiner, E. G. Pamer, Commensal microbes provide first line defense against *Listeria monocytogenes* infection. *J. Exp. Med.* **214**, 1973–1989 (2017).
325. S. Caballero, S. Kim, R. A. Carter, I. M. Leiner, B. Sušac, L. Miller, G. J. Kim, L. Ling, E. G. Pamer, Cooperating Commensals Restore Colonization Resistance to Vancomycin-Resistant *Enterococcus faecium*. *Cell Host Microbe.* **21**, 592-602.e4 (2017).
326. C. G. Buffie, V. Bucci, R. R. Stein, P. T. McKenney, L. Ling, A. Gobourne, D. No, H. Liu, M. Kinnebrew, A. Viale, E. Littmann, M. R. M. Van Den Brink, R. R. Jenq, Y. Taur, C. Sander, J. R. Cross, N. C. Toussaint, J. B. Xavier, E. G. Pamer, Precision microbiome reconstitution restores bile acid mediated resistance to *Clostridium difficile*. *Nature.* **517**, 205–208 (2015).
327. L. V. Hooper, M. H. Wong, A. Thelin, L. Hansson, P. G. Falk, J. I. Gordon, Molecular analysis of commensal host-microbial relationships in the intestine. *Science (80-).* **291**, 881–884 (2001).
328. M. E. V. Johansson, H. E. Jakobsson, J. Holmén-Larsson, A. Schütte, A. Ermund, A. M. Rodríguez-Piñero, L. Arike, C. Wising, F. Svensson, F. Bäckhed, G. C. Hansson, Normalization of host intestinal mucus layers requires long-term microbial colonization. *Cell Host Microbe.* **18**, 582–592 (2015).
329. S. Ahmadi, S. Wang, R. Nagpal, B. Wang, S. Jain, A. Razazan, S. P. Mishra, X. Zhu, Z. Wang, K. Kavanagh, H. Yadav, A human-origin probiotic cocktail ameliorates aging-related leaky gut and inflammation via modulating the microbiota/taurine/tight junction axis. *JCI Insight.* **5** (2020), doi:10.1172/jci.insight.132055.
330. Y. Feng, Y. Huang, Y. Wang, P. Wang, H. Song, F. Wang, Antibiotics induced intestinal tight junction barrier dysfunction is associated with microbiota dysbiosis, activated NLRP3 inflammasome and autophagy. *PLoS One.* **14**, 1–19 (2019).
331. B. Allam-Ndoul, S. Castonguay-Paradis, A. Veilleux, Gut microbiota and intestinal trans-epithelial permeability. *Int. J. Mol. Sci.* **21**, 1–14 (2020).
332. V. Cerovic, C. C. Bain, A. M. Mowat, S. W. F. Milling, Intestinal macrophages and dendritic cells: What's the difference? *Trends Immunol.* **35**, 270–277 (2014).
333. G. Eberl, M. Lochner, The development of intestinal lymphoid tissues at the interface of self and microbiota. *Mucosal Immunol.* **2**, 478–485 (2009).
334. K. W. Beagley, K. Fujihashi, A. S. Lagoo, S. Lagoo-Deenadaylan, C. A. Black, A. M. Murray, A. T. Sharmanov, M. Yamamoto, J. R. McGhee, C. O. Elson, Differences in intraepithelial lymphocyte T cell subsets isolated from murine small versus large intestine. *J. Immunol.* **154**, 5611–9 (1995).
335. H. Cheroutre, F. Lambolez, D. Mucida, The light and dark sides of intestinal intraepithelial lymphocytes. *Nat. Rev. Immunol.* **11**, 445–56 (2011).
336. B. S. Sheridan, L. Lefrançois, Intraepithelial lymphocytes: to serve and protect. *Curr. Gastroenterol. Rep.* **12**, 513–21 (2010).
337. K. L. Cepek, S. K. Shaw, C. M. Parker, G. J. Russell, J. S. Morrow, D. L. Rimm, M. B. Brenner, Adhesion between epithelial cells and T lymphocytes mediated by E-cadherin and the alpha E beta 7 integrin. *Nature.* **372**, 190–3 (1994).
338. H. Cheroutre, Starting at the beginning: New perspectives on the biology of mucosal T cells. *Annu. Rev. Immunol.* **22**, 217–246 (2004).
339. N. Xiong, D. H. Raulet, Development and selection of $\gamma\delta$ T cells. *Immunol. Rev.* **215**, 15–31 (2007).
340. L. Jia, K. L. Edelblum, Intravital Imaging of Intraepithelial Lymphocytes in Murine Small Intestine. *J. Vis. Exp.* **176**, 139–148 (2019).

341. M. A. Fischer, N. B. Golovchenko, K. L. Edelblum, $\gamma\delta$ T cell migration: Separating trafficking from surveillance behaviors at barrier surfaces. *Immunol. Rev.* **298**, 165–180 (2020).
342. J. Shires, E. Theodoridis, A. C. Hayday, Biological insights into TCR $\gamma\delta$ + and TCR $\alpha\beta$ + intraepithelial lymphocytes provided by serial analysis of gene expression (SAGE). *Immunity.* **15**, 419–434 (2001).
343. A. S. Ismail, K. M. Severson, S. Vaishnava, C. L. Behrendt, X. Yu, J. L. Benjamin, K. A. Ruhn, B. Hou, A. L. DeFranco, F. Yarovinsky, L. V. Hooper, $\gamma\delta$ Intraepithelial Lymphocytes Are Essential Mediators of Host-Microbial Homeostasis At the Intestinal Mucosal Surface. *Proc. Natl. Acad. Sci.* **108**, 8743–8748 (2011).
344. A. A. Kühl, N. N. Pawlowski, K. Grollich, C. Loddenkemper, M. Zeitz, J. C. Hoffmann, Aggravation of intestinal inflammation by depletion/deficiency of $\gamma\delta$ T cells in different types of IBD animal models. *J. Leukoc. Biol.* **81**, 168–175 (2007).
345. K. Inagaki-Ohara, T. Chinen, G. Matsuzaki, A. Sasaki, Y. Sakamoto, K. Hiromatsu, F. Nakamura-Uchiyama, Y. Nawa, A. Yoshimura, Mucosal T Cells Bearing TCR $\gamma\delta$ Play a Protective Role in Intestinal Inflammation. *J. Immunol.* **173**, 1390–1398 (2004).
346. K. L. Edelblum, G. Singh, M. A. Odenwald, A. Lingaraju, K. El Bissati, R. McLeod, A. I. Sperling, J. R. Turner, $\gamma\delta$ Intraepithelial Lymphocyte Migration Limits Transepithelial Pathogen Invasion and Systemic Disease in Mice. *Gastroenterology.* **148**, 1417–1426 (2015).
347. S. S. Kanwar, N. K. Ganguly, B. N. S. Walia, R. C. Mahajan, Direct and antibody dependent cell mediated cytotoxicity against Giardia lamblia by splenic and intestinal lymphoid cells in mice. *Gut.* **27**, 73–77 (1986).
348. S. Müller, M. Bühler-Jungo, C. Mueller, Intestinal Intraepithelial Lymphocytes Exert Potent Protective Cytotoxic Activity During an Acute Virus Infection. *J. Immunol.* **164**, 1986–1994 (2000).
349. T. Dharakul, M. Labbe, J. Cohen, A. R. Bellamy, J. E. Street, E. R. Mackow, L. Fiore, L. Rott, H. B. Greenberg, Immunization with baculovirus-expressed recombinant rotavirus proteins VP1, VP4, VP6, and VP7 induces CD8+ T lymphocytes that mediate clearance of chronic rotavirus infection in SCID mice. *J. Virol.* **65**, 5928–5932 (1991).
350. A. C. Lepage, D. Buzoni-Gatel, D. T. Bout, L. H. Kasper, Gut-derived intraepithelial lymphocytes induce long term immunity against Toxoplasma gondii. *J. Immunol.* **161**, 4902–8 (1998).
351. M. Swamy, L. Abeler-Dörner, J. Chettle, T. Mahlaköiv, D. Goubau, P. Chakravarty, G. Ramsay, C. Reis e Sousa, P. Staeheli, B. A. Blacklaws, J. L. Heeney, A. C. Hayday, Intestinal intraepithelial lymphocyte activation promotes innate antiviral resistance. *Nat. Commun.* **6**, 7090 (2015).
352. H. Hamada, T. Hiroi, Y. Nishiyama, H. Takahashi, Y. Masunaga, S. Hachimura, S. Kaminogawa, H. Takahashi-Iwanaga, T. Iwanaga, H. Kiyono, H. Yamamoto, H. Ishikawa, Identification of Multiple Isolated Lymphoid Follicles on the Antimesenteric Wall of the Mouse Small Intestine. *J. Immunol.* **168**, 57–64 (2002).
353. K. Masahata, E. Umemoto, H. Kayama, M. Kotani, S. Nakamura, T. Kurakawa, J. Kikuta, K. Gotoh, D. Motooka, S. Sato, T. Higuchi, Y. Baba, T. Kurosaki, M. Kinoshita, Y. Shimada, T. Kimura, R. Okumura, A. Takeda, M. Tajima, O. Yoshie, M. Fukuzawa, H. Kiyono, S. Fagarasan, T. Iida, M. Ishii, K. Takeda, Generation of colonic IgA-secreting cells in the caecal patch. *Nat. Commun.* **5**, 1–13 (2014).
354. A. Cerutti, The regulation of IgA class switching. *Nat. Rev. Immunol.* **8**, 421–34 (2008).

355. P. Brandtzaeg, F. E. Johansen, Mucosal B cells: Phenotypic characteristics, transcriptional regulation, and homing properties. *Immunol. Rev.* **206**, 32–63 (2005).
356. O. Pabst, E. Slack, IgA and the intestinal microbiota: the importance of being specific. *Mucosal Immunol.* **13**, 12–21 (2020).
357. H. Wei, J. Y. Wang, Role of polymeric immunoglobulin receptor in iga and igm transcytosis. *Int. J. Mol. Sci.* **22**, 1–20 (2021).
358. H. Spits, D. Artis, M. Colonna, A. Diefenbach, J. P. Di Santo, G. Eberl, S. Koyasu, R. M. Locksley, A. N. J. McKenzie, R. E. Mebius, F. Powrie, E. Vivier, Innate lymphoid cells—a proposal for uniform nomenclature. *Nat. Rev. Immunol.* **13**, 145–149 (2013).
359. N. Powell, A. W. Walker, E. Stolarczyk, J. B. Canavan, M. R. Gökmen, E. Marks, I. Jackson, A. Hashim, M. A. Curtis, R. G. Jenner, J. K. Howard, J. Parkhill, T. T. MacDonald, G. M. Lord, The Transcription Factor T-bet Regulates Intestinal Inflammation Mediated by Interleukin-7 Receptor+ Innate Lymphoid Cells. *Immunity.* **37**, 674–684 (2012).
360. T. Hoyler, C. S. N. Klose, A. Souabni, A. Turqueti-Neves, D. Pfeifer, E. L. Rawlins, D. Voehringer, M. Busslinger, A. Diefenbach, The Transcription Factor GATA-3 Controls Cell Fate and Maintenance of Type 2 Innate Lymphoid Cells. *Immunity.* **37**, 634–648 (2012).
361. C. Luci, A. Reynders, I. I. Ivanov, C. Cogne, L. Chiche, L. Chasson, J. Hardwigsen, E. Anguiano, J. Banchereau, D. Chaussabel, M. Dalod, D. R. Littman, E. Vivier, E. Tomasello, Influence of the transcription factor ROR γ t on the development of NKp46+ cell populations in gut and skin. *Nat. Immunol.* **10**, 75–82 (2009).
362. C. Cairo, T. J. Webb, Effective Barriers: The Role of NKT Cells and Innate Lymphoid Cells in the Gut. *J. Immunol.* **208**, 235–246 (2022).
363. O. El Weizman, N. M. Adams, I. S. Schuster, C. Krishna, Y. Pritykin, C. Lau, M. A. Degli-Esposti, C. S. Leslie, J. C. Sun, T. E. O’Sullivan, ILC1 Confer Early Host Protection at Initial Sites of Viral Infection. *Cell.* **171**, 795-808.e12 (2017).
364. J. K. Bando, S. Gilfillan, B. Di Luccia, J. L. Fachi, J. L. Fachi, C. Sécca, M. Cella, M. Colonna, ILC2s are the predominant source of intestinal ILC-derived IL-10. *J. Exp. Med.* **217** (2020), doi:10.1084/jem_20191520.
365. H. Takatori, Y. Kanno, W. T. Watford, C. M. Tato, G. Weiss, I. I. Ivanov, D. R. Littman, J. J. O’Shea, Lymphoid tissue inducer-like cells are an innate source of IL-17 and IL-22. *J. Exp. Med.* **206**, 35–41 (2009).
366. S. Sawa, M. Lochner, N. Satoh-Takayama, S. Dulauroy, M. Bérard, M. Kleinschek, D. Cua, J. P. Di Santo, G. Eberl, ROR γ t+ innate lymphoid cells regulate intestinal homeostasis by integrating negative signals from the symbiotic microbiota. *Nat. Immunol.* **12**, 320–328 (2011).
367. Y. Takada, T. Hisamatsu, N. Kamada, M. T. Kitazume, H. Honda, Y. Oshima, R. Saito, T. Takayama, T. Kobayashi, H. Chinen, Y. Mikami, T. Kanai, S. Okamoto, T. Hibi, Monocyte Chemoattractant Protein-1 Contributes to Gut Homeostasis and Intestinal Inflammation by Composition of IL-10–Producing Regulatory Macrophage Subset. *J. Immunol.* **184**, 2671–2676 (2010).
368. M. M. Meredith, K. Liu, G. Darrasse-Jeze, A. O. Kamphorst, H. A. Schreiber, P. Guermonprez, J. Idoyaga, C. Cheong, K. H. Yao, R. E. Niec, M. C. Nussenzweig, Expression of the zinc finger transcription factor zDC (Zbtb46, Btd4) defines the classical dendritic cell lineage. *J. Exp. Med.* **209**, 1153–1165 (2012).
369. B. M. Bradford, D. P. Sester, D. A. Hume, N. A. Mabbott, Defining the anatomical

- localisation of subsets of the murine mononuclear phagocyte system using integrin alpha X (Itgax, CD11c) and colony stimulating factor 1 receptor (Csf1r, CD115) expression fails to discriminate dendritic cells from macrophages. *Immunobiology*. **216**, 1228–1237 (2011).
370. A. Rivollier, J. He, A. Kole, V. Valatas, B. L. Kelsall, Inflammation switches the differentiation program of Ly6chi monocytes from antiinflammatory macrophages to inflammatory dendritic cells in the colon. *J. Exp. Med.* **209**, 139–155 (2012).
371. P. Pavli, C. E. Woodhams, W. F. Doe, D. A. Hume, Isolation and characterization of antigen-presenting dendritic cells from the mouse intestinal lamina propria. *Immunology*. **70**, 40–7 (1990).
372. E. Zigmund, C. Varol, J. Farache, E. Elmaliah, A. T. Satpathy, G. Friedlander, M. Mack, N. Shpigel, I. G. Boneca, K. M. Murphy, G. Shakhar, Z. Halpern, S. Jung, Ly6Chi Monocytes in the Inflamed Colon Give Rise to Proinflammatory Effector Cells and Migratory Antigen-Presenting Cells. *Immunity*. **37**, 1076–1090 (2012).
373. S. Tamoutounour, S. Henri, H. Lelouard, B. de Bovis, C. de Haar, C. J. van der Woude, A. M. Woltman, Y. Reyat, D. Bonnet, D. Sichien, C. C. Bain, A. M. Mowat, C. Reis e Sousa, L. F. Poulin, B. Malissen, M. Guilliams, CD64 distinguishes macrophages from dendritic cells in the gut and reveals the Th1-inducing role of mesenteric lymph node macrophages during colitis. *Eur. J. Immunol.* **42**, 3150–3166 (2012).
374. R. J. Cummings, G. Barbet, G. Bongers, B. M. Hartmann, K. Gettler, L. Muniz, G. C. Furtado, J. Cho, S. A. Lira, J. M. Blander, Different tissue phagocytes sample apoptotic cells to direct distinct homeostasis programs. *Nature*. **539**, 565–569 (2016).
375. L. E. Smythies, M. Sellers, R. H. Clements, M. Mosteller-Barnum, G. Meng, W. H. Benjamin, J. M. Orenstein, P. D. Smith, Human intestinal macrophages display profound inflammatory anergy despite avid phagocytic and bacteriocidal activity. *J. Clin. Invest.* **115**, 66–75 (2005).
376. C. C. Bain, C. L. Scott, H. Uronen-Hansson, S. Gudjonsson, O. Jansson, O. Grip, M. Guilliams, B. Malissen, W. W. Agace, A. M. I. Mowat, Resident and pro-inflammatory macrophages in the colon represent alternative context-dependent fates of the same Ly6Chi monocyte precursors. *Mucosal Immunol.* **6**, 498–510 (2013).
377. J. L. Coombes, K. R. R. Siddiqui, C. V. Arancibia-Cárcamo, J. Hall, C. M. Sun, Y. Belkaid, F. Powrie, A functionally specialized population of mucosal CD103+ DCs induces Foxp3+ regulatory T cells via a TGF- β -and retinoic acid-dependent mechanism. *J. Exp. Med.* **204**, 1757–1764 (2007).
378. C. M. Sun, J. A. Hall, R. B. Blank, N. Bouladoux, M. Oukka, J. R. Mora, Y. Belkaid, Small intestine lamina propria dendritic cells promote de novo generation of Foxp3 T reg cells via retinoic acid. *J. Exp. Med.* **204**, 1775–1785 (2007).
379. S. Uematsu, K. Fujimoto, M. H. Jang, B. G. Yang, Y. J. Jung, M. Nishiyama, S. Sato, T. Tsujimura, M. Yamamoto, Y. Yokota, H. Kiyono, M. Miyasaka, K. J. Ishii, S. Akira, Regulation of humoral and cellular gut immunity by lamina propria dendritic cells expressing Toll-like receptor 5. *Nat. Immunol.* **9**, 769–776 (2008).
380. V. Cerovic, C. D. Jenkins, A. G. C. Barnes, S. W. F. Milling, G. G. MacPherson, L. S. Klavinskis, Hyporesponsiveness of Intestinal Dendritic Cells to TLR Stimulation Is Limited to TLR4. *J. Immunol.* **182**, 2405–2415 (2009).
381. H. Chung, S. J. Pamp, J. A. Hill, N. K. Surana, S. M. Edelman, E. B. Troy, N. C. Reading, E. J. Villablanca, S. Wang, J. R. Mora, Y. Umesaki, D. Mathis, C. Benoist, D. A. Relman, D. L. Kasper, Gut immune maturation depends on

- colonization with a host-specific microbiota. *Cell*. **149**, 1578–1593 (2012).
382. E. M. Brown, M. Sadarangani, B. B. Finlay, The role of the immune system in governing host-microbe interactions in the intestine. *Nat. Immunol.* **14**, 660–667 (2013).
 383. E. Larsson, V. Tremaroli, Y. S. Lee, O. Koren, I. Nookaew, A. Fricker, J. Nielsen, R. E. Ley, F. Bäckhed, Analysis of gut microbial regulation of host gene expression along the length of the gut and regulation of gut microbial ecology through MyD88. *Gut*. **61**, 1124–1131 (2012).
 384. K. Honda, D. R. Littman, The microbiota in adaptive immune homeostasis and disease. *Nature*. **535**, 75–84 (2016).
 385. I. I. Ivanov, D. R. Littman, Modulation of immune homeostasis by commensal bacteria. *Curr. Opin. Microbiol.* **14**, 106–114 (2011).
 386. L. V Hooper, D. R. Littman, A. J. Macpherson, Interactions between the microbiota and the immune system. *Science (80-.)*. **336**, 1268–73 (2012).
 387. J. F. Burgueño, M. T. Abreu, Epithelial Toll-like receptors and their role in gut homeostasis and disease. *Nat. Rev. Gastroenterol. Hepatol.* **17**, 263–278 (2020).
 388. A. E. Price, K. Shamardani, K. A. Lugo, J. Deguine, A. W. Roberts, B. L. Lee, G. M. Barton, A Map of Toll-like Receptor Expression in the Intestinal Epithelium Reveals Distinct Spatial, Cell Type-Specific, and Temporal Patterns. *Immunity*. **49**, 560–575 (2018).
 389. N. Hörmann, I. Brandão, S. Jäckel, N. Ens, M. Lillich, U. Walter, C. Reinhardt, Gut microbial colonization orchestrates TLR2 expression, signaling and epithelial proliferation in the small intestinal mucosa. *PLoS One*. **9**, 2–12 (2014).
 390. H. Sheng, J. Shao, C. M. Townsend, B. M. Evers, Phosphatidylinositol 3-kinase mediates proliferative signals in intestinal epithelial cells. *Gut*. **52**, 1472–1478 (2003).
 391. H. L. Cash, C. V. Whitham, C. L. Behrendt, L. V. Hooper, Symbiotic bacteria direct expression of an intestinal bactericidal lectin. *Science (80-.)*. **313**, 1126–1130 (2006).
 392. S. Vaishnava, C. L. Behrendt, A. S. Ismail, L. Eckmann, L. V. Hooper, Paneth cells directly sense gut commensals and maintain homeostasis at the intestinal host-microbial interface. *Proc. Natl. Acad. Sci.* **105**, 20858–20863 (2008).
 393. K. Brandl, G. Plitas, C. N. Mihu, C. Ubeda, T. Jia, M. Fleisher, B. Schnabl, R. P. DeMatteo, E. G. Pamer, Vancomycin-resistant enterococci exploit antibiotic-induced innate immune deficits. *Nature*. **455**, 804–807 (2008).
 394. A. L. Frantz, E. W. Rogier, C. R. Weber, L. Shen, D. A. Cohen, L. A. Fenton, M. E. C. Bruno, C. S. Kaetzel, Targeted deletion of MyD88 in intestinal epithelial cells results in compromised antibacterial immunity associated with downregulation of polymeric immunoglobulin receptor, mucin-2, and antibacterial peptides. *Mucosal Immunol.* **5**, 501–512 (2012).
 395. K. Brandl, G. Plitas, B. Schnabl, R. P. DeMatteo, E. G. Pamer, MyD88-mediated signals induce the bactericidal lectin RegIIIγ and protect mice against intestinal *Listeria monocytogenes* infection. *J. Exp. Med.* **204**, 1891–1900 (2007).
 396. G. M. H. Birchenough, E. E. L. Nystrom, M. E. V. Johansson, G. C. Hansson, A sentinel goblet cell guards the colonic crypt by triggering Nlrp6-dependent Muc2 secretion. *Science (80-.)*. **352**, 1535–1542 (2016).
 397. A. Mukherji, A. Kobiita, T. Ye, P. Chambon, Homeostasis in intestinal epithelium is orchestrated by the circadian clock and microbiota cues transduced by TLRs. *Cell*. **153**, 812–827 (2013).
 398. J. F. Brooks, C. L. Behrendt, K. A. Ruhn, S. Lee, P. Raj, J. S. Takahashi, L. V.

- Hooper, The microbiota coordinates diurnal rhythms in innate immunity with the circadian clock. *Cell*. **184**, 4154-4167.e12 (2021).
399. A. Dillon, D. D. Lo, M Cells: Intelligent Engineering of Mucosal Immune Surveillance. *Front. Immunol.* **10**, 1499 (2019).
 400. O. S. Sakhony, B. Rossy, V. Gusti, A. J. Pham, K. Vu, D. D. Lo, M cell-derived vesicles suggest a unique pathway for trans-epithelial antigen delivery. *Tissue Barriers*. **3** (2015), doi:10.1080/21688370.2015.1004975.
 401. J. H. Niess, S. Brand, X. Gu, L. Landsman, S. Jung, B. A. McCormick, J. M. Vyas, M. Boes, H. L. Ploegh, J. G. Fox, D. R. Littman, H.-C. Reinecker, CX3CR1-mediated dendritic cell access to the intestinal lumen and bacterial clearance. *Science (80-.)*. **307**, 254–8 (2005).
 402. M. Chieppa, M. Rescigno, A. Y. C. Huang, R. N. Germain, Dynamic imaging of dendritic cell extension into the small bowel lumen in response to epithelial cell TLR engagement. *J. Exp. Med.* **203**, 2841–52 (2006).
 403. K. A. Knoop, K. G. McDonald, S. McCrate, J. R. McDole, R. D. Newberry, Microbial sensing by goblet cells controls immune surveillance of luminal antigens in the colon. *Mucosal Immunol.* **8**, 198–210 (2015).
 404. J. K. Gustafsson, J. E. Davis, T. Rappai, K. G. McDonald, D. H. Kulkarni, K. A. Knoop, S. P. Hogan, J. A. J. Fitzpatrick, W. I. Lencer, R. D. Newberry, Intestinal goblet cells sample and deliver luminal antigens by regulated endocytic uptake and transcytosis. *Elife*. **10**, 1–29 (2021).
 405. J. Farache, I. Koren, I. Milo, I. Gurevich, K. W. Kim, E. Zigmond, G. C. Furtado, S. A. Lira, G. Shakhar, Luminal Bacteria Recruit CD103+ Dendritic Cells into the Intestinal Epithelium to Sample Bacterial Antigens for Presentation. *Immunity*. **38**, 581–595 (2013).
 406. B. Koscsó, S. Kurapati, R. R. Rodrigues, J. Nedjic, K. Gowda, C. Shin, C. Soni, A. Z. Ashraf, I. Purushothaman, M. Palisoc, S. Xu, H. Sun, S. B. Chodiseti, E. Lin, M. Mack, Y. I. Kawasawa, P. He, Z. S. M. Rahman, I. Aifantis, N. Shulzhenko, A. Morgun, M. Bogunovic, Gut-resident CX3CR1hi macrophages induce tertiary lymphoid structures and IgA response in situ. *Sci. Immunol.* **5** (2020), doi:10.1126/sciimmunol.aax0062.
 407. M. C. Gold, D. M. Lewinsohn, Co-dependents: MR1-restricted MAIT cells and their antimicrobial function. *Nat. Rev. Microbiol.* **11**, 14–19 (2013).
 408. E. W. Meermeier, M. J. Harriff, E. Karamooz, D. M. Lewinsohn, MAIT cells and microbial immunity. *Immunol. Cell Biol.* **96**, 607–617 (2018).
 409. P. Riegert, V. Wanner, S. Bahram, Genomics, isoforms, expression, and phylogeny of the MHC class I-related MR1 gene. *J. Immunol.* **161**, 4066–77 (1998).
 410. L. Kjer-Nielsen, O. Patel, A. J. Corbett, J. Le Nours, B. Meehan, L. Liu, M. Bhati, Z. Chen, L. Kostenko, R. Reantragoon, N. A. Williamson, A. W. Purcell, N. L. Dudek, M. J. McConville, R. A. J. O’Hair, G. N. Khairallah, D. I. Godfrey, D. P. Fairlie, J. Rossjohn, J. McCluskey, MR1 presents microbial vitamin B metabolites to MAIT cells. *Nature*. **491**, 717–723 (2012).
 411. A. J. Corbett, S. B. G. Eckle, R. W. Birkinshaw, L. Liu, O. Patel, J. Mahony, Z. Chen, R. Reantragoon, B. Meehan, H. Cao, N. A. Williamson, R. A. Strugnell, D. Van Sinderen, J. Y. W. Mak, D. P. Fairlie, L. Kjer-Nielsen, J. Rossjohn, J. McCluskey, T-cell activation by transitory neo-antigens derived from distinct microbial pathways. *Nature*. **509**, 361–365 (2014).
 412. M. G. Constantinides, V. M. Link, S. Tamoutounour, A. C. Wong, P. J. Perez-Chaparro, S. J. Han, Y. E. Chen, K. Li, S. Farhat, A. Weckel, S. R. Krishnamurthy,

- I. Vujkovic-Cvijin, J. L. Linehan, N. Bouladoux, E. D. Merrill, S. Roy, D. J. Cua, E. J. Adams, A. Bhandoola, T. C. Scharschmidt, J. Aubé, M. A. Fischbach, Y. Belkaid, MAIT cells are imprinted by the microbiota in early life and promote tissue repair. *Science (80-.)*. **366** (2019), doi:10.1126/science.aax6624.
413. F. Tilloy, E. Treiner, S. H. Park, C. Garcia, F. Lemonnier, H. De La Salle, A. Bendelac, M. Bonneville, O. Lantz, An invariant T cell receptor α chain defines a novel TAP-independent major histocompatibility complex class Ib-restricted α/β T cell subpopulation in mammals. *J. Exp. Med.* **189**, 1907–1921 (1999).
414. M. A. Woods Acevedo, J. K. Pfeiffer, Microbiota-immune system interactions and enteric virus infection. *Curr. Opin. Virol.* **46**, 15–19 (2021).
415. C. M. Robinson, Enteric viruses exploit the microbiota to promote infection. *Curr. Opin. Virol.* **37**, 58–62 (2019).
416. K. O. Chang, S. V. Sosnovtsev, G. Belliot, Y. Kim, L. J. Saif, K. Y. Green, Bile acids are essential for porcine enteric calicivirus replication in association with down-regulation of signal transducer and activator of transcription 1. *Proc. Natl. Acad. Sci.* **101**, 8733–8738 (2004).
417. K.-O. Chang, D. W. George, Bile Acids Promote the Expression of Hepatitis C Virus in Replicon-Harboring Cells. *J. Virol.* **81**, 9633–9640 (2007).
418. K. R. Grau, S. Zhu, S. T. Peterson, E. W. Helm, D. Philip, M. Phillips, A. Hernandez, H. Turula, P. Frasse, V. R. Graziano, C. B. Wilen, C. E. Wobus, M. T. Baldrige, S. M. Karst, The intestinal regionalization of acute norovirus infection is regulated by the microbiota via bile acid-mediated priming of type III interferon. *Nat. Microbiol.* **5**, 84–92 (2020).
419. Y. Kim, K. Chang, Inhibitory effects of bile acids and synthetic farnesoid X receptor agonists on rotavirus replication. *J. Virol.* **85**, 12570–7 (2011).
420. N. Honke, N. Shaabani, C. Hardt, C. Krings, D. Häussinger, P. A. Lang, V. Keitel, K. S. Lang, Farnesoid X receptor in mice prevents severe liver immunopathology during lymphocytic choriomeningitis virus infection. *Cell. Physiol. Biochem.* **41**, 323–338 (2017).
421. E. S. Winkler, S. Shrihari, B. L. Hykes, S. A. Handley, P. S. Andhey, Y.-J. J. S. J. S. Huang, A. Swain, L. Droit, K. K. Chebrolu, M. Mack, D. L. Vanlandingham, L. B. Thackray, M. Cella, M. Colonna, M. N. Artyomov, T. S. Stappenbeck, M. S. Diamond, The Intestinal Microbiome Restricts Alphavirus Infection and Dissemination through a Bile Acid-Type I IFN Signaling Axis. *Cell.* **182**, 901-918.e18 (2020).
422. L. Schaupp, S. Muth, L. Rogell, M. Kofoed-Branzk, F. Melchior, S. Lienenklaus, S. C. Ganal-Vonarburg, M. Klein, F. Guendel, T. Hain, K. Schütze, U. Grundmann, V. Schmitt, M. Dorsch, J. Spanier, P.-K. Larsen, T. Schwanz, S. Jäckel, C. Reinhardt, T. Bopp, S. Danckwardt, K. Mahnke, G. A. Heinz, M.-F. Mashreghi, P. Durek, U. Kalinke, O. Kretz, T. B. Huber, S. Weiss, C. Wilhelm, A. J. Macpherson, H. Schild, A. Diefenbach, H. C. Probst, Microbiota-Induced Type I Interferons Instruct a Poised Basal State of Dendritic Cells. *Cell.* **181**, 1080-1096.e19 (2020).
423. K. C. Bradley, K. Finsterbusch, D. Schnepf, S. Crotta, M. Llorian, S. Davidson, S. Y. Fuchs, P. Staeheli, A. Wack, Microbiota-Driven Tonic Interferon Signals in Lung Stromal Cells Protect from Influenza Virus Infection. *Cell Rep.* **28**, 245-256.e4 (2019).
424. A. L. Steed, G. P. Christophi, G. E. Kaiko, L. Sun, V. M. Goodwin, U. Jain, E. Esaulova, M. N. Artyomov, D. J. Morales, M. J. Holtzman, A. C. M. M. Boon, D. J. Lenschow, T. S. Stappenbeck, The microbial metabolite desaminotyrosine protects from influenza through type I interferon. *Science (80-.)*. **357**, 498–502

- (2017).
425. M. C. Abt, L. C. Osborne, L. A. Monticelli, T. A. Doering, T. Alenghat, G. F. Sonnenberg, M. A. Paley, M. Antenus, K. L. Williams, J. Erikson, E. J. Wherry, D. Artis, Commensal bacteria calibrate the activation threshold of innate antiviral immunity. *Immunity*. **37**, 158–70 (2012).
 426. K. L. Stefan, M. V Kim, A. Iwasaki, D. L. Kasper, K. L. Stefan, M. V Kim, A. Iwasaki, D. L. Kasper, Commensal Microbiota Modulation of Natural Resistance to Virus Infection. *Cell*. **183**, 1–13 (2020).
 427. X. L. Yang, G. Wang, J. Y. Xie, H. Li, S. X. Chen, W. Liu, S. J. Zhu, The intestinal microbiome primes host innate immunity against enteric virus systemic infection through type I interferon. *MBio*. **12** (2021), doi:10.1128/mBio.00366-21.
 428. D. Schnepf, P. Hernandez, T. Mahlaköiv, S. Crotta, M. E. Sullender, S. T. Peterson, A. Ohnemus, C. Michiels, I. Gentle, L. Dumoutier, C. A. Reis, A. Diefenbach, A. Wack, M. T. Baldrige, P. Staeheli, Rotavirus susceptibility of antibiotic-treated mice ascribed to diminished expression of interleukin-22. *PLoS One*. **16**, 1–16 (2021).
 429. B. Zhang, B. Chassaing, Z. Shi, R. Uchiyama, Z. Zhang, T. L. Denning, S. E. Crawford, A. J. Pruijssers, J. A. Iskarpatyoti, M. K. Estes, T. S. Dermody, W. Ouyang, I. R. Williams, M. Vijay-Kumar, A. T. Gewirtz, Viral infection. Prevention and cure of rotavirus infection via TLR5/NLRC4-mediated production of IL-22 and IL-18. *Science (80-.)*. **346**, 861–5 (2014).
 430. Z. Shi, J. Zou, Z. Zhang, X. Zhao, J. Noriega, B. Zhang, C. Zhao, H. Ingle, K. Bittinger, L. M. Mattei, A. J. Pruijssers, R. K. Plemper, T. J. Nice, M. T. Baldrige, T. S. Dermody, B. Chassaing, A. T. Gewirtz, Segmented Filamentous Bacteria Prevent and Cure Rotavirus Infection. *Cell*. **179**, 644-658.e13 (2019).
 431. M. Kane, L. K. Case, K. Kopaskie, A. Kozlova, C. Macdearmid, A. V Chervonsky, T. V Golovkina, Successful Transmission of a Retrovirus Depends on the Commensal Microbiota. *Science (80-.)*. **334**, 245–249 (2011).
 432. B. A. Jude, Y. Pobezhinskaya, J. Bishop, S. Parke, R. M. Medzhitov, A. V. Chervonsky, T. V. Golovkina, Subversion of the innate immune system by a retrovirus. *Nat. Immunol.* **4**, 573–578 (2003).
 433. L. B. Thackray, S. A. Handley, M. J. Gorman, S. Poddar, P. Bagadia, C. G. Briseño, D. J. Theisen, Q. Tan, B. L. Hykes, H. Lin, T. M. Lucas, C. Desai, J. I. Gordon, K. M. Murphy, H. W. Virgin, M. S. Diamond, Oral Antibiotic Treatment of Mice Exacerbates the Disease Severity of Multiple Flavivirus Infections. *Cell Rep*. **22**, 3440-3453.e6 (2018).
 434. S. K. Kuss, G. T. Best, C. A. Etheredge, A. J. Pruijssers, J. M. Frierson, L. V. Hooper, T. S. Dermody, J. K. Pfeiffer, Intestinal microbiota promote enteric virus replication and systemic pathogenesis. *Science (80-.)*. **334**, 249–252 (2011).
 435. T. H. Wideman, A. J. Zautra, R. R. Edwards, Bacterial lipopolysaccharide binding enhances virion stability and promotes environmental fitness of an enteric virus. *Cell Host Microbe*. **15**, 36–46 (2014).
 436. A. K. Berger, H. Yi, D. B. Kearns, B. A. Mainou, Bacteria and bacterial envelope components enhance mammalian reovirus thermostability. *PLoS Pathog*. **13**, 1–30 (2017).
 437. C. M. Robinson, M. A. Woods Acevedo, B. T. McCune, J. K. Pfeiffer, Related Enteric Viruses Have Different Requirements for Host Microbiota in Mice. *J. Virol*. **93**, 1–10 (2019).
 438. E. R. Aguilera, Y. Nguyen, J. Sasaki, J. K. Pfeiffer, Bacterial Stabilization of a Panel of Picornaviruses. *mSphere*. **4**, 1–10 (2019).

439. C. A. Nelson, C. B. Wilen, Y. Dai, R. C. Orchard, A. S. Kim, R. A. Stegeman, L. L. Hsieh, T. J. Smith, H. W. Virgin, D. H. Fremont, Structural basis for murine norovirus engagement of bile acids and the CD300lf receptor. *Proc. Natl. Acad. Sci.* **115**, E9201–E9210 (2018).
440. R. C. Orchard, C. B. Wilen, J. G. Doench, M. T. Baldrige, B. T. McCune, Y. C. J. Lee, S. Lee, S. M. Pruett-Miller, C. A. Nelson, D. H. Fremont, H. W. Virgin, Discovery of a proteinaceous cellular receptor for a norovirus. *Science (80-)*. **353**, 933–936 (2016).
441. K. Ettayebi, S. E. Crawford, K. Murakami, J. R. Broughman, U. Karandikar, V. R. Tenge, F. H. Neill, S. E. Blutt, X.-L. Zeng, L. Qu, B. Kou, A. R. Opekun, D. Burrin, D. Y. Graham, S. Ramani, R. L. Atmar, M. K. Estes, Replication of human noroviruses in stem cell-derived human enteroids. *Science (80-)*. **353**, 1387–1393 (2016).
442. T. Kilic, A. Koromyslova, G. S. Hansman, Structural Basis for Human Norovirus Capsid Binding to Bile Acids. *J. Virol.* **93**, 1–17 (2019).
443. M. T. Baldrige, T. J. Nice, B. T. McCune, C. C. Yokoyama, A. Kambal, M. Wheadon, M. S. Diamond, Y. Ivanova, M. Artyomov, H. W. Virgin, Commensal microbes and interferon- λ determine persistence of enteric murine norovirus infection. *Science (80-)*. **347**, 266–9 (2015).
444. C. B. Wilen, S. Lee, L. L. Hsieh, R. C. Orchard, C. Desai, B. L. Hykes, M. R. McAllaster, D. R. Balce, T. Feehley, J. R. Brestoff, C. A. Hickey, C. C. Yokoyama, Y.-T. Wang, D. A. MacDuff, D. Kreamalmayer, M. R. Howitt, J. A. Neil, K. Cadwell, P. M. Allen, S. A. Handley, M. van Lookeren Campagne, M. T. Baldrige, H. W. Virgin, Tropism for tuft cells determines immune promotion of norovirus pathogenesis. *Science (80-)*. **360**, 204–208 (2018).
445. M. A. Woods Acevedo, A. K. Erickson, J. K. Pfeiffer, The Antibiotic Neomycin Enhances Coxsackievirus Plaque Formation. *mSphere*. **4**, e00632-18 (2019).
446. A. Katsnelson, Minding the microbiome of your mice. *Lab Anim. (NY)*. **48**, 313–315 (2019).
447. L. K. Beura, S. E. Hamilton, K. Bi, J. M. Schenkel, O. A. Odumade, K. A. Casey, E. A. Thompson, K. A. Fraser, P. C. Rosato, A. Filali-Mouhim, R. P. Sekaly, M. K. Jenkins, V. Vezys, W. Nicholas Haining, S. C. Jameson, D. Masopust, Normalizing the environment recapitulates adult human immune traits in laboratory mice. *Nature*. **532**, 512–516 (2016).
448. S. P. Rosshart, B. G. Vassallo, D. Angeletti, D. S. Hutchinson, A. P. Morgan, K. Takeda, H. D. Hickman, J. A. McCulloch, J. H. Badger, N. J. Ajami, G. Trinchieri, F. Pardo-Manuel de Villena, J. W. Yewdell, B. Rehmann, Wild Mouse Gut Microbiota Promotes Host Fitness and Improves Disease Resistance. *Cell*. **171**, 1015-1028.e13 (2017).
449. S. P. Rosshart, J. Herz, B. G. Vassallo, A. Hunter, M. K. Wall, J. H. Badger, J. A. McCulloch, D. G. Anastasakis, A. A. Sarshad, I. Leonardi, N. Collins, J. A. Blatter, S. J. Han, S. Tamoutounour, S. Potapova, M. B. Foster St Claire, W. Yuan, S. K. Sen, M. S. Dreier, B. Hild, M. Hafner, D. Wang, I. D. Iliev, Y. Belkaid, G. Trinchieri, B. Rehmann, Laboratory mice born to wild mice have natural microbiota and model human immune responses. *Science (80-)*. **365** (2019), doi:10.1126/science.aaw4361.
450. J. M. Leung, S. A. Budischak, H. Chung The, C. Hansen, R. Bowcutt, R. Neill, M. Shellman, P. Loke, A. L. Graham, Rapid environmental effects on gut nematode susceptibility in rewilded mice. *PLoS Biol.* **16**, e2004108 (2018).
451. E. J. Fay, K. M. Balla, S. N. Roach, F. K. Shepherd, D. S. Putri, T. D. Wiggen, S.

- A. Goldstein, M. J. Pierson, M. T. Ferris, C. E. Thefaine, A. Tucker, M. Salnikov, V. Cortez, S. R. Compton, S. V. Kotenko, R. C. Hunter, D. Masopust, N. C. Elde, R. A. Langlois, Natural rodent model of viral transmission reveals biological features of virus population dynamics. *J. Exp. Med.* **219** (2022), doi:10.1084/jem.20211220.
452. T. J. Nice, B. A. Robinson, J. A. Van Winkle, The Role of Interferon in Persistent Viral Infection: Insights from Murine Norovirus. *Trends Microbiol.* **26**, 510–524 (2018).
453. L. B. Ivashkiv, L. T. Donlin, Regulation of type I interferon responses. *Nat. Rev. Immunol.* **14**, 36–49 (2013).
454. T. A. Selvakumar, S. Bhushal, U. Kalinke, D. Wirth, H. Hauser, M. Köster, M. W. Hornef, Identification of a Predominantly Interferon- λ -Induced Transcriptional Profile in Murine Intestinal Epithelial Cells. *Front. Immunol.* **8**, 1302 (2017).
455. C. Good, A. I. Wells, C. B. Coyne, Type III interferon signaling restricts enterovirus 71 infection of goblet cells. *Sci. Adv.* **5**, eaau4255 (2019).
456. K. I. Arimoto, S. Miyauchi, S. A. Stoner, J. B. Fan, D. E. Zhang, Negative regulation of type I IFN signaling. *J. Leukoc. Biol.* **103**, 1099–1116 (2018).
457. K. Chen, J. Liu, X. Cao, Regulation of type I interferon signaling in immunity and inflammation: A comprehensive review. *J. Autoimmun.* **83**, 1–11 (2017).
458. C. V. Rothlin, E. A. Carrera-Silva, L. Bosurgi, S. Ghosh, TAM Receptor Signaling in Immune Homeostasis. *Annu. Rev. Immunol.* **33**, 355–391 (2015).
459. U. Raudvere, L. Kolberg, I. Kuzmin, T. Arak, P. Adler, H. Peterson, J. Vilo, g:Profiler: a web server for functional enrichment analysis and conversions of gene lists (2019 update). *Nucleic Acids Res.* **47**, W191–W198 (2019).
460. A. Ashkenazi, V. M. Dixit, Apoptosis control by death and decoy receptors. *Curr. Opin. Cell Biol.* **11**, 255–260 (1999).
461. S. Heinz, C. Benner, N. Spann, E. Bertolino, Y. C. Lin, P. Laslo, J. X. Cheng, C. Murre, H. Singh, C. K. Glass, Simple combinations of lineage-determining transcription factors prime cis-regulatory elements required for macrophage and B cell identities. *Mol. Cell.* **38**, 576–89 (2010).
462. E. Platanitis, D. Demiroz, A. Schneller, K. Fischer, C. Capelle, M. Hartl, T. Gossenreiter, M. Müller, M. Novatchkova, T. Decker, A molecular switch from STAT2-IRF9 to ISGF3 underlies interferon-induced gene transcription. *Nat. Commun.* **10**, 2921 (2019).
463. J. A. Neil, Y. Matsuzawa-Ishimoto, E. Kernbauer-Hölzl, S. L. Schuster, S. Sota, M. Venzon, S. Dallari, A. Galvao Neto, A. Hine, D. Hudesman, P. Loke, T. J. Nice, K. Cadwell, IFN-I and IL-22 mediate protective effects of intestinal viral infection. *Nat. Microbiol.* **4**, 1737–1749 (2019).
464. E. Kernbauer, Y. Ding, K. Cadwell, An enteric virus can replace the beneficial function of commensal bacteria. *Nature.* **516**, 94–98 (2014).
465. J. W. Schoggins, C. M. Rice, Interferon-stimulated genes and their antiviral effector functions. *Curr. Opin. Virol.* **1**, 519–25 (2011).
466. H. Ingle, S. T. Peterson, M. T. Baldridge, Distinct Effects of Type I and III Interferons on Enteric Viruses. *Viruses.* **10** (2018), doi:10.3390/v10010046.
467. J. M. Rojas, A. Alejo, V. Martín, N. Sevilla, Viral pathogen-induced mechanisms to antagonize mammalian interferon (IFN) signaling pathway. *Cell. Mol. Life Sci.* **78**, 1423–1444 (2021).
468. K. E. Taylor, K. L. Mossman, Recent advances in understanding viral evasion of type I interferon. *Immunology.* **138**, 190–7 (2013).
469. D. E. Levy, A. García-Sastre, The virus battles: IFN induction of the antiviral state

- and mechanisms of viral evasion. *Cytokine Growth Factor Rev.* **12** (2001), pp. 143–156.
470. S. V Kotenko, J. E. Durbin, Contribution of type III interferons to antiviral immunity: Location, Location, Location. *J. Biol. Chem.* **292**, 7295–7303 (2017).
 471. J. A. Van Winkle, D. A. Constant, L. Li, T. J. Nice, Selective Interferon Responses of Intestinal Epithelial Cells Minimize Tumor Necrosis Factor Alpha Cytotoxicity. *J. Virol.* **94**, e00603-20 (2020).
 472. P. P. Hernández, T. Mahlakoiv, I. Yang, V. Schwierzeck, F. Guendel, K. Gronke, B. Ryffel, L. Dumoutier, J. Renauld, S. Suerbaum, N. Nguyen, F. Guendel, K. Gronke, B. Ryffel, C. Hoelscher, L. Dumoutier, J. Renauld, S. Suerbaum, P. Staeheli, A. Diefenbach, Interferon- λ and interleukin-22 cooperate for the induction of interferon-stimulated genes and control of rotavirus infection. *Nat. Immunol.* **16**, 698–707 (2015).
 473. R. Krajmalnik-Brown, Z. E. Ilhan, D. W. Kang, J. K. DiBaise, Effects of gut microbes on nutrient absorption and energy regulation. *Nutr. Clin. Pract.* **27**, 201–214 (2012).
 474. H. Chu, S. K. Mazmanian, Innate immune recognition of the microbiota promotes host-microbial symbiosis. *Nat. Immunol.* **14**, 668–75 (2013).
 475. A. Iwasaki, R. Medzhitov, Control of adaptive immunity by the innate immune system. *Nat. Immunol.* **16**, 343–53 (2015).
 476. C. Odendall, A. A. Voak, J. C. Kagan, Type III IFNs Are Commonly Induced by Bacteria-Sensing TLRs and Reinforce Epithelial Barriers during Infection. *J. Immunol.* **199**, 3270–3279 (2017).
 477. S. C. Ganal, S. L. Sanos, C. Kallfass, K. Oberle, C. Johner, C. Kirschning, S. Lienenklaus, S. Weiss, P. Staeheli, P. Aichele, A. Diefenbach, Priming of natural killer cells by nonmucosal mononuclear phagocytes requires instructive signals from commensal microbiota. *Immunity.* **37**, 171–86 (2012).
 478. S. Stockinger, C. U. Duerr, M. Fulde, T. Dolowschiak, J. Pott, I. Yang, D. Eibach, F. Bäckhed, S. Akira, S. Suerbaum, M. Brugman, M. W. Hornef, TRIF signaling drives homeostatic intestinal epithelial antimicrobial peptide expression. *J. Immunol.* **193**, 4223–34 (2014).
 479. A. Liberzon, C. Birger, H. Thorvaldsdóttir, M. Ghandi, J. P. Mesirov, P. Tamayo, The Molecular Signatures Database (MSigDB) hallmark gene set collection. *Cell Syst.* **1**, 417–425 (2016).
 480. P. I. Osterlund, T. E. Pietilä, V. Veckman, S. V Kotenko, I. Julkunen, IFN regulatory factor family members differentially regulate the expression of type III IFN (IFN- λ) genes. *J. Immunol.* **179**, 3434–42 (2007).
 481. S. Schmid, M. Mordstein, G. Kochs, A. García-Sastre, B. R. TenOever, Transcription factor redundancy ensures induction of the antiviral state. *J. Biol. Chem.* **285**, 42013–42022 (2010).
 482. E. Tomasello, K. Naciri, R. Chelbi, G. Bessou, A. Fries, E. Gressier, A. Abbas, E. Pollet, P. Pierre, T. Lawrence, T. Vu Manh, M. Dalod, Molecular dissection of plasmacytoid dendritic cell activation in vivo during a viral infection. *EMBO J.* **37**, 1–19 (2018).
 483. K. Honda, Y. Ohba, H. Yanai, H. Negishi, T. Mizutani, A. Takaoka, C. Taya, T. Taniguchi, Spatiotemporal regulation of MyD88-IRF-7 signalling for robust type-I interferon induction. *Nature.* **434**, 1035–40 (2005).
 484. R. Elmentaite, A. D. B. Ross, K. Roberts, K. R. James, D. Ortmann, T. Gomes, K. Nayak, L. Tuck, S. Pritchard, O. A. Bayraktar, R. Heuschkel, L. Vallier, S. A. Teichmann, M. Zilbauer, Single-Cell Sequencing of Developing Human Gut

- Reveals Transcriptional Links to Childhood Crohn's Disease. *Dev. Cell.* **55**, 771-783.e5 (2020).
485. M. S. Hakim, S. Chen, S. Ding, Y. Yin, A. Ikram, X. X. Ma, W. Wang, M. P. Peppelenbosch, Q. Pan, Basal interferon signaling and therapeutic use of interferons in controlling rotavirus infection in human intestinal cells and organoids. *Sci. Rep.* **8**, 1–13 (2018).
 486. H. Ingle, E. Hassan, J. Gawron, B. Mihi, Y. Li, E. A. Kennedy, G. Kalugotla, H. Makimaa, S. Lee, P. Desai, K. G. McDonald, M. S. Diamond, R. D. Newberry, M. Good, M. T. Baldrige, Murine astrovirus tropism for goblet cells and enterocytes facilitates an IFN- λ response in vivo and in enteroid cultures. *Mucosal Immunol.* **14**, 751–761 (2021).
 487. M. E. V. Johansson, J. M. H. Larsson, G. C. Hansson, The two mucus layers of colon are organized by the MUC2 mucin, whereas the outer layer is a legislator of host-microbial interactions. *Proc. Natl. Acad. Sci.* **108**, 4659–65 (2011).
 488. C. Atuma, V. Strugala, A. Allen, L. Holm, The adherent gastrointestinal mucus gel layer: thickness and physical state in vivo. *Am. J. Physiol. Gastrointest. Liver Physiol.* **280**, G922-9 (2001).
 489. J. M. Williams, C. A. Duckworth, M. D. Burkitt, A. J. M. Watson, B. J. Campbell, D. M. Pritchard, Epithelial cell shedding and barrier function: a matter of life and death at the small intestinal villus tip. *Vet. Pathol.* **52**, 445–55 (2015).
 490. R. Uchiyama, B. Chassaing, B. Zhang, A. T. Gewirtz, Antibiotic treatment suppresses rotavirus infection and enhances specific humoral immunity. *J. Infect. Dis.* **210**, 171–182 (2014).
 491. G. Lemke, C. V Rothlin, Immunobiology of the TAM receptors. *Nat. Rev. Immunol.* **8**, 327–36 (2008).
 492. C. V. Rothlin, S. Ghosh, E. I. Zuniga, M. B. A. Oldstone, G. Lemke, TAM Receptors Are Pleiotropic Inhibitors of the Innate Immune Response. *Cell.* **131**, 1124–1136 (2007).
 493. D. Liu, C. Sheng, S. Gao, C. Yao, J. Li, W. Jiang, H. Chen, J. Wu, C. Pan, S. Chen, W. Huang, SOCS3 Drives Proteasomal Degradation of TBK1 and Negatively Regulates Antiviral Innate Immunity. *Mol. Cell. Biol.* **35**, 2400–2413 (2015).
 494. Q. Lu, G. Lemke, Homeostatic regulation of the immune system by receptor tyrosine kinases of the Tyro 3 family. *Science (80-)*. **293**, 306–311 (2001).
 495. M. Friedrich, M. Pohin, F. Powrie, Cytokine Networks in the Pathophysiology of Inflammatory Bowel Disease. *Immunity.* **50**, 992–1006 (2019).
 496. C. P. Mavragani, A. Nezos, N. Dovrolis, N. P. Andreou, E. Legaki, L. A. Sechi, G. Bamias, M. Gazouli, Type i and ii interferon signatures can predict the response to anti-Tnf agents in inflammatory bowel disease patients: Involvement of the microbiota. *Inflamm. Bowel Dis.* **26**, 1543–1553 (2020).
 497. I. Stolzer, A. Dressel, M. T. Chiriach, M. F. Neurath, C. Günther, An IFN-STAT Axis Augments Tissue Damage and Inflammation in a Mouse Model of Crohn's Disease. *Front. Med.* **8**, 1–11 (2021).
 498. M. Blank, Y. Shiloh, Programs for cell death: Apoptosis is only one way to go. *Cell Cycle.* **6**, 686–695 (2007).
 499. J. Major, S. Crotta, M. Llorian, T. M. McCabe, H. H. Gad, S. L. Priestnall, R. Hartmann, A. Wack, Type I and III interferons disrupt lung epithelial repair during recovery from viral infection. *Science (80-)*. **369**, 712–717 (2020).
 500. T. Grabinger, L. Luks, F. Kostadinova, C. Zimmerlin, J. P. Medema, M. Leist, T. Brunner, Ex vivo culture of intestinal crypt organoids as a model system for

- assessing cell death induction in intestinal epithelial cells and enteropathy. *Cell Death Dis.* **5**, e1228 (2014).
501. J. Pott, A. M. Kabat, K. J. Maloy, Intestinal Epithelial Cell Autophagy Is Required to Protect against TNF-Induced Apoptosis during Chronic Colitis in Mice. *Cell Host Microbe.* **23**, 191-202.e4 (2018).
 502. T. J. Nice, L. C. Osborne, V. T. Tomov, D. Artis, E. J. J. Wherry, H. W. Virgin, Type I Interferon Receptor Deficiency in Dendritic Cells Facilitates Systemic Murine Norovirus Persistence Despite Enhanced Adaptive Immunity. *PLoS Pathog.* **12**, e1005684 (2016).
 503. M. Nadkarni, F. E. Martin, N. A. Jacques, N. Hunter, Determination of bacterial load by real-time PCR using a broad range (universal) probe and primer set. *Microbiology.* **148**, 257–266 (2002).
 504. A. Dobin, C. A. Davis, F. Schlesinger, J. Drenkow, C. Zaleski, S. Jha, P. Batut, M. Chaisson, T. R. Gingeras, STAR: Ultrafast universal RNA-seq aligner. *Bioinformatics.* **29**, 15–21 (2013).
 505. L. Wang, S. Wang, W. Li, RSeQC: Quality control of RNA-seq experiments. *Bioinformatics.* **28**, 2184–2185 (2012).
 506. P. Ewels, M. Magnusson, S. Lundin, M. Källér, MultiQC: Summarize analysis results for multiple tools and samples in a single report. *Bioinformatics.* **32**, 3047–3048 (2016).
 507. Y. Liao, G. K. Smyth, W. Shi, featureCounts: an efficient general purpose program for assigning sequence reads to genomic features. *Bioinformatics.* **30**, 923–930 (2014).
 508. M. I. Love, W. Huber, S. Anders, Moderated estimation of fold change and dispersion for RNA-seq data with DESeq2. *Genome Biol.* **15**, 550 (2014).
 509. S. Park, M. D. Buck, C. Desai, X. Zhang, E. Loginicheva, J. Martinez, M. L. Freeman, T. Saitoh, S. Akira, J. L. Guan, Y. W. He, M. A. Blackman, S. A. Handley, B. Levine, D. R. Green, T. A. Reese, M. N. Artyomov, H. W. Virgin, Autophagy Genes Enhance Murine Gammaherpesvirus 68 Reactivation from Latency by Preventing Virus-Induced Systemic Inflammation. *Cell Host Microbe.* **19**, 91–101 (2016).
 510. J. G. Caporaso, C. L. Lauber, W. A. Walters, D. Berg-Lyons, C. A. Lozupone, P. J. Turnbaugh, N. Fierer, R. Knight, Global patterns of 16S rRNA diversity at a depth of millions of sequences per sample. *Proc. Natl. Acad. Sci.* **108**, 4516–22 (2011).
 511. B. J. Callahan, P. J. McMurdie, M. J. Rosen, A. W. Han, A. J. A. Johnson, S. P. Holmes, DADA2: High-resolution sample inference from Illumina amplicon data. *Nat. Methods.* **13**, 581–3 (2016).
 512. J. R. Cole, Q. Wang, J. A. Fish, B. Chai, D. M. McGarrell, Y. Sun, C. T. Brown, A. Porras-Alfaro, C. R. Kuske, J. M. Tiedje, Ribosomal Database Project: data and tools for high throughput rRNA analysis. *Nucleic Acids Res.* **42**, D633-42 (2014).
 513. P. J. McMurdie, S. Holmes, phyloseq: an R package for reproducible interactive analysis and graphics of microbiome census data. *PLoS One.* **8**, e61217 (2013).
 514. S. Neph, M. S. Kuehn, A. P. Reynolds, E. Haugen, R. E. Thurman, A. K. Johnson, E. Rynes, M. T. Maurano, J. Vierstra, S. Thomas, R. Sandstrom, R. Humbert, J. A. Stamatoyannopoulos, BEDOPS: high-performance genomic feature operations. *Bioinformatics.* **28**, 1919–1920 (2012).
 515. T. Stuart, A. Butler, P. Hoffman, C. Hafemeister, E. Papalexi, W. M. Mauck, Y. Hao, M. Stoeckius, P. Smibert, R. Satija, Comprehensive Integration of Single-Cell Data. *Cell.* **177**, 1888-1902.e21 (2019).

Addendum

CURRICULUM VITAE JACOB A. VAN WINKLE

Department of Molecular Microbiology & Immunology
Oregon Health and Science University
3181 SW Sam Jackson Park Road
L220
Portland OR 97239
vanwijac@ohsu.edu

Current Position:

September 2016 – Present

PhD Candidate, Department of Microbiology & Immunology
Oregon Health and Science University, Portland OR
Advisor: Timothy J. Nice, PhD

Education:

2016 – Present

Ph.D, Molecular Microbiology and Immunology
Oregon Health and Science University, Portland OR

2012 – 2016

Bachelor of Science with Honors, Biochemistry, Seattle Pacific
University, Seattle WA

Previous Positions/Employment:

2015 – 2016

Laboratory Assistant, Department of Chemistry, Seattle Pacific
University, Seattle WA. Prepared reagents for all chemistry lab
courses.

2014 – 2016

Chemistry Tutor, Center for Learning, Seattle Pacific University,
Seattle WA

2015

Summer Research Intern, College of Pharmacy, California
Northstate University, Elk Grove CA. Screening therapeutic
compounds in an *in vitro* IBD model.

2014

Summer Research Intern, College of Pharmacy, California
Northstate University, Elk Grove CA. Studying alpha-galactose-
1,3-galactose red meat allergy and sensitivity.

2014

Laboratory Teaching Assistant, Department of Chemistry,
Seattle Pacific University, Seattle WA.

Honors and Awards:

2021

**American Association of Immunologists Lefrancois-Biolegend
Memorial Award**

2021

Nominee – OHSU's Graduate Student Organization Exemplary
Future Scientist

2020 **American Association of Immunologists (AAI) Trainee Abstract Award**, conference cancelled due to Covid-19
2012-2016 **Seattle Pacific University President's Scholar Award**
2015 **Seattle Pacific University's David T. & Christina L. Wong Scholarship**

Professional Societies and Organizations

2019 – Present **Member**, American Association of Immunologists
2014 – 2016 **President**, Meditrack Tutoring Club, Seattle Pacific University

Oral Presentations

1. American Association of Immunologists Annual Meeting, virtual, 10-15 May, 2021
2. OHSU Research Week, Portland OR, virtual, 3-6 May, 2021
3. OHSU Program in Biomedical Sciences Recruitment, virtual, 9 February, 2021
4. American Association of Immunologists Annual Meeting, Honolulu HI, 8-12 May, 2020, cancelled due to Covid-19
5. Molecular Microbiology and Immunology Departmental Retreat, Silverton OR, 20-22 September, 2019
6. Wellcome Genome Trust Advanced Course, Hinxton UK, 19-28 June, 2019
7. American Society for Microbiology Northwest Branch Meeting, Portland OR, 5-6 October, 2018
8. Fred Hutchinson Graduate Student Symposium, Seattle WA, 29-30 August, 2018
9. OHSU Research Week, Portland OR, 30 April-2 May, 2018

Poster Presentations

1. American Association of Immunologists Annual Meeting, virtual, 10-15 May, 2021
2. American Association of Immunologists Annual Meeting, Honolulu HI, 8-12 May, 2020, cancelled due to Covid-19
3. Midwinter Conference of Immunologists, Asilomar CA, 25-28 January, 2020
4. Program in Molecular and Cellular Biosciences Retreat, Troutdale OR, 16-17 September, 2019
5. Program in Molecular and Cellular Biosciences Retreat, Troutdale OR, 17-18 September, 2018
6. Keystone Symposia, Cells vs. Pathogens, Monterrey CA, 23-26 March, 2018

Completed Research Support

T32 #AI007472 9/1/2018 – 8/31/2020
Role: Trainee
Interactions at the Microbe-Host Interface

T32 #GM071338 9/1/2017 – 8/31/2018
Role: Trainee
Program in Enhanced Research Training

Manuscripts in Preparation:

1. Constant DA, **Van Winkle JA**, VanderHoek E, Dekker S, Sofia MA, Regner E, Modiano N, Tsikitis VL, and Nice TJ. Transcriptional and Cytotoxic Responses of Human Intestinal Organoids to Interferon Type I, II, and III. *Submitted.*

Peer Reviewed Publications:

1. **Van Winkle JA**, Peterson ST, Kennedy EA, Wheadon MJ, Ingle H, Desai C, Rodgers R, Constant DA, Wright AP, Li L, Artyomov M, Lee S, Baldrige MT, and Nice TJ. A homeostatic interferon-lambda response to bacterial microbiota stimulates preemptive antiviral defense within discrete pockets of intestinal epithelium. *eLife* 2022; 11:e74072
PMID: 35137688
2. **Van Winkle JA**, Constant DA, Li L, and Nice TJ. Selective interferon responses of intestinal epithelial cells minimize TNF α cytotoxicity. *Journal of Virology* 2020; 94(21): e00603-20
PMID: 32847859
3. Robinson BA, **Van Winkle JA**, McCune BT, Peters AM, and Nice TJ. Caspase-mediated cleavage of murine norovirus NS1/2 potentiates apoptosis and is required for persistent infection of intestinal epithelial cells. *PLOS Pathogens* 2019; 15(7): e1007940
PMID: 31329638
4. **Van Winkle JA**, Robinson BA, Peters AM, Li L, Nouboussi RV, Mack M, and Nice TJ. Persistence of Systemic Murine Norovirus Is Maintained by Inflammatory Recruitment of Susceptible Myeloid Cells. *Cell Host & Microbe* 2018; 24(5): 665-676
PMID: 30392829
5. Nice TJ, Robinson BA, **Van Winkle JA**. The Role of Interferon in Persistent Viral Infection: Insights from Murine Norovirus. *Trends in Microbiology* 2018; 26(6): P510-524
PMID: 29157967